

WL-TR-93-2007

AD-A265 842



DTIC  
ELECTE  
JUN 16 1993  
S C D



2

**ADVANCED THERMALLY STABLE COAL-DERIVED JET FUELS;  
ANNUAL REPORT**

**COMPOSITIONAL FACTORS AFFECTING THERMAL DEGRADATION OF JET  
FUELS**

C. Song, S. Eser, H.H. Schobert, P.G. Hatcher, M.M. Coleman, Y. Peng,  
L. Selvaraj, W.-C. Lai, M. Parzynski, C. Burgess, E. Yoon, K. Gergova,  
J.-L. Faulon, J. Bortiatynski, D. Parfitt, P.M. Walsh, K. Wenzel, R. Arumugam,  
M. Sobkowiak, Y. Liu, L. Hou, R.M. Copenhaver

Fuel Science Program  
Department of Materials Science & Engineering  
The Pennsylvania State University  
209 Academic Projects Building  
University Park, PA 16802

December 1992

Final Report for 08/01/91-07/31/92

**APPROVED FOR PUBLIC RELEASE; DISTRIBUTION IS UNLIMITED.**

AERO PROPULSION AND POWER DIRECTORATE  
WRIGHT LABORATORY  
AIR FORCE MATERIEL COMMAND  
WRIGHT PATTERSON AFB OH 45433-7650

Reproduced From  
Best Available Copy

93 6 15 192

93-13501



## NOTICE

When government drawings, specifications or other data are used for any purpose other than in connection with a definitely government-related procurement, the United States Government incurs no responsibility or any obligation whatsoever. The fact that the government may have formulated or in any way supplied the said drawings, specifications, or other data is not to be regarded by implication, or otherwise in any manner construed, as licensing the holder or any other person or corporation; or as conveying any rights or permission to manufacture, use or sell any patented invention that may in any way be related thereto.

This report is releasable to the National Technical Information Service (NTIS). At NTIS, it will be available to the general public, including foreign nations.

This technical report has been reviewed and is approved for publication.



DONN M. STORCH, Major, USAF  
Program Manager  
Fuels & Lubrication Division



LEO S. HAROOTYAN, JR.  
Chief, Fuels & Lubrication Division  
Aero Propulsion & Power Directorate

If your address has changed, if you wish to be removed from our mailing list, or if the addressee is no longer employed by your organization, please notify WL/POS BLDG 490, 1790 LOOP RD N, WRIGHT-PATTERSON AFB OH 45433-7103, to help us maintain a current mailing list.

Copies of this report should not be returned unless return is required by security considerations, contractual obligations or notice on a specific document.

REPORT DOCUMENTATION PAGE			Form Approved OMB No. 0704-0188	
Public reporting burden for this collection of information is estimated to average 1 hour per response, including the time for reviewing instructions, searching existing data sources, gathering and maintaining the data needed, and completing and reviewing the collection of information. Send comments regarding this burden estimate or any other aspect of this collection of information, including suggestions for reducing this burden, to Washington Headquarters Services, Directorate for Information Operations and Reports, 1215 Jefferson Davis Highway, Suite 1204, Arlington, VA 22202-4302, and to the Office of Management and Budget, Paperwork Reduction Project (0704-0188), Washington, DC 20503.				
1. AGENCY USE ONLY (Leave blank)		2. REPORT DATE DECEMBER 1992		3. REPORT TYPE AND DATES COVERED FINAL - Aug 91 - JUL 92
4. TITLE AND SUBTITLE ADVANCED THERMALLY STABLE COAL-DERIVED JET FUELS ANNUAL REPORT; COMPOSITIONAL FACTORS AFFECTING THERMAL DEGRADATION OF JET FUELS			5. FUNDING NUMBERS C: MIPR FY1455-91N-0638 PE: 62203F PR: 3048 TA: 05 WO: 87	
6. AUTHOR(S) C. Song, S. Eber, H.H. Schubert, P.G. Hatcher, M.M. Coleman, Y. Peng, L. Selvaraj, W.-C. Lai, M. Parzynski, C. Burgess, E. Yoon, K. Gargava, J.-L. Paulon, J. Bortiatynski, D. Parfitt, P.M. Walsh, K. Wenzel, R. Aramngan, M. Sobkowick, Y. Liu, L. Hoa, R.M. Copenhagen				
7. PERFORMING ORGANIZATION NAME(S) AND ADDRESS(ES) Fuel Science Program Department of Materials Science & Engineering The Pennsylvania State University 209 Academic Projects Building University Park, PA 16802			8. PERFORMING ORGANIZATION REPORT NUMBER	
9. SPONSORING/MONITORING AGENCY NAME(S) AND ADDRESS(ES) WL/POS Attn: Donn Storch, 513-255-2722 Aero Propulsion and Power Directorate Wright Laboratory Air Force Materiel Command Wright Patterson AFB OH 45433-7103			10. SPONSORING/MONITORING AGENCY REPORT NUMBER  WL-TR-93-2007	
11. SUPPLEMENTARY NOTES				
12a. DISTRIBUTION / AVAILABILITY STATEMENT  Approved for public release; distribution is unlimited.			12b. DISTRIBUTION CODE	
13. ABSTRACT (Maximum 200 words) This report is a summary of recent progress in a continuing long-term program at Penn State University to develop thermally stable jet fuels for high performance aircraft, which was initiated in FY89 by the U.S. Air Force working jointly with the Department of Energy, Pittsburgh Energy Technology Center.  This project focuses on the compositional factors affecting high temperature thermal stability of coal-derived and petroleum-based jet fuels in pyrolytic regime. Thermal stability refers to the resistance of fuel to chemical decomposition at high temperatures to cause the solid deposition and liquid depletion. There are four broad objectives in this project, and the research work is divided into four tasks. The first task clarifies the chemistry of fuel degradation and mechanisms of solid formation, and identifying thermally stable classes of hydrocarbon compounds, and providing information for enhancing intrinsic stability of jet fuels. The second task involves characterization of the solids including deposits, sediments and gums produced from fuels and model compounds at high temperatures. The third task is to explore the means to enhance the thermal stability of fuels by examining the effects of various additives. The fourth task is a newly initiated exploratory study on conversion of coals to thermally stable jet fuels.				
14. SUBJECT TERMS  jet fuel; deposition; coal liquefaction			15. NUMBER OF PAGES 175	
			16. PRICE CODE	
17. SECURITY CLASSIFICATION OF REPORT UNCLASSIFIED	18. SECURITY CLASSIFICATION OF THIS PAGE UNCLASSIFIED	19. SECURITY CLASSIFICATION OF ABSTRACT UNCLASSIFIED	20. LIMITATION OF ABSTRACT UL	

## DISCLAIMER

This report was prepared as an account of work sponsored by the United States Government. Neither the United States Government nor any agency thereof, nor any of their employees, makes any warranty express or implied, or assumes any legal liability or responsibility for the accuracy, completeness, or usefulness of any information, apparatus, product, or process disclosed, or represents that its use would not infringe privately owned rights. Reference herein to any specific commercial product, process or service by trade name, mark manufacturer, or otherwise, does not necessarily constitute or imply its endorsement, recommendation, or favoring by the United States Government or any agency thereof. The views and opinions of authors expressed herein do not necessarily state or reflect those of the United States Government or any agency thereof.

## ACKNOWLEDGEMENTS

This project was jointly supported by the U.S. Department of Energy, Pittsburgh Energy Technology Center (DOE PETC), and the Air Force Wright Laboratory/Aero Propulsion and Power Directorate, Wright-Patterson AFB. Funding was provided through Sandia National Laboratories under contract DE-AC04-76DP00789. We are pleased to thank Mr. W.E. Harrison III, Dr. D.M. Storch and Mr. S.D. Anderson of Wright Laboratory for providing technical advice, support and jet fuel samples, Dr. E. Klavetter of SNL and Dr. S. Rogers of PETC for their support and helpful discussions, and Drs. G. Stigel and R. Hickey of PETC and Dr. P. Zhou of Burns & Roe Service Co. for the WI-MD and FT-MD samples. The authors would also like to thank Dr. A. Davis and Mr. D. Glick of PSU for providing coal sample and data from the DOE/Penn State Coal Sample Bank. Finally, C. Song wishes to thank Ms. K. Copenhagen for her skillful editorial assistance in preparing the final report.

Accession For	
NTIS CRA&I	<input checked="checked" type="checkbox"/>
DTIC TAB	<input type="checkbox"/>
Unannounced	<input type="checkbox"/>
Justification	
By	
Distribution /	
Availability Codes	
Dist	Avail and/or Special
A-1	



## TABLE OF CONTENTS

<b>ACKNOWLEDGEMENTS</b> .....	iii
<b>EXECUTIVE SUMMARY</b> .....	1
<b>TECHNICAL PROGRESS</b> .....	5
<b>TASK 1.</b> Investigation of the Quantitative Degradation Chemistry of Fuels .....	5
Activity 1. Pyrolytic Degradation of Coal- and Petroleum-Derived Aviation Jet Fuels and Middle Distillates .....	5
Activity 2. Two-Dimensional (2D) NMR Analysis of Coal- and Petroleum-Derived Jet Fuels .....	18
Activity 3. Thermal Degradation of Long-Chain Paraffins .....	22
Activity 4. Mechanisms for PAH and Solid Formation During Thermal Degradation of Jet Fuels .....	43
Activity 5. Thermal Degradation of Alkylbenzenes .....	55
Activity 6. Hydrogen-Transferring Pyrolysis of Hydrocarbons. Enhancing High Temperature Thermal Stability of Aviation Jet Fuels by H-Donors .....	69
<b>TASK 2.</b> Characterization of Solid Gums, Sediments, and Carbonaceous Deposits .....	88
Activity 1. Characterization of Solid Deposits from Thermal Stressing of Jet Fuels and Related Compounds by Polarized-Light Microscopy .....	888
Activity 2. Formation of Solid Deposits from Jet Fuels in the Presence of Different Solid Carbons .....	96
<b>TASK 3.</b> Coal-Based Fuel Stabilization Studies .....	111
Activity 1. Stabilizers for Jet Fuels at High Temperatures .....	111
Activity 2. Analysis of Stressed Jet Fuels with Stabilizers by NMR .....	128
<b>TASK 4.</b> Exploratory Conversion of Coal to High Thermal Stability Jet Fuel .....	136
Activity 1. Computer-Assisted Structural Elucidation of Vitrinite from High Volatile Bituminous Coals .....	136
Activity 2. Liquefaction of Coals to Produce Jet Fuels .....	145
Activity 3. Bimetallic Dispersed Catalysts for Coal Liquefaction .....	156
<b>Appendix</b> List of Relevant Papers on Coal- and Petroleum-Derived Jet Fuels and on Coal Structure and Liquefaction from Penn State Team .....	163

## LIST OF FIGURES

	<u>Page</u>
1.1 Total and specific ion chromatograms (ions of m/z 57, 83, 91, 105, and 142) of JP-8P2 from GC-MS analysis .....	8
1.2 Specific ion chromatograms (ion of m/z 57) of six paraffinic fuels .....	10
1.3 Total ion chromatograms of the neat sample of, and the liquid products from FT-MD after thermal stressing at 450°C for 1-8 hours .....	12
1.4 Paraffins distribution of liquids from FT-MD .....	13
1.5 Yields of H <sub>2</sub> and C <sub>1</sub> -C <sub>4</sub> gases from JP-8P at 450°C .....	14
1.6 Yields of gases at 450°C .....	15
1.7 Yields of solid deposits at 450°C .....	16
1.8 Total ion chromatograms of the neat sample of, and the liquid products from, Wi-MD after thermal stressing at 450°C for 1-8 hours .....	17
1.9 The heterocorrelated multiple quantum coherence (HMQC) spectrum of JP-8C (a) the aliphatic region (b) the aromatic region .....	20
1.10 The heterocorrelated multiple quantum coherence (HMQC) spectrum of JP-8P (a) the aliphatic region (b) the aromatic region .....	21
1.11 A schematic diagram of the 25-ml microautoclave (tubing bomb) reactor .....	25
1.12 Rate of solid deposition for C <sub>8</sub> , C <sub>12</sub> , C <sub>13</sub> , C <sub>14</sub> at various thermal stressing conditions .....	28
1.13 Solid State CPMAS <sup>13</sup> C NMR spectrum of the solids produced from tetradecane at 450°C for 8 hours.....	29
1.14 Solid State CPMAS <sup>13</sup> C NMR spectrum of the solids produced from tetradecane at 475°C for 24 hours.....	31
1.15 GC-MS chromatogram of dodecane stressed at 425°C for 6 hours illustrating the production of smaller and larger molecular weight n-alkanes .....	33
1.16 GC-MS chromatogram of dodecane stressed at 450°C for 6 hours illustrating the production of alkylbenzenes, naphthalene, alkyl naphthalenes .....	34
1.17 GC-MS chromatogram of tetradecane stressed at 450°C for 24 hours illustrating the production of multicyclic 3-4 ring compounds .....	35
1.18 GC-MS chromatogram of tridecane stressed at 475°C for 6 hours illustrating the large proportion of alkylbenzenes produced .....	36
1.19 Comparison of the rate of solid deposition for C <sub>10</sub> to the model compounds at various thermal stressing conditions .....	39
1.20 Progression of degradation in the liquid products .....	40
1.21 Comparison of chromatograms octane for 450°C for 2 hours (A), dodecane 400°C for 48 hours (B), and tetradecane 425°C for 12 hours (C).....	41
1.22 Decomposition of model compounds and jet fuels at 450°C for 4 hours in N <sub>2</sub> ...	44
1.23 Solid formation from n-BB, JP-8P and JP-8C at 450°C .....	46
1.24 Relation between solid deposition and liquid aromaticity during JP-8P stressing .....	47

1.25	Cross-polarization magic angle spinning $^{13}\text{C}$ NMR of solid deposits from n-decane (top, 450°C-6 hours) and from n-butylbenzene (bottom, 450°C-4 hours) .....	49
1.26	Possible mechanisms for solid formation from jet fuels .....	50
1.27	GC-MS total ion chromatogram of liquid products from n-butylbenzene stressed at 450°C for 4 hours.....	51
1.28	Possible mechanisms for the formation of PAHs .....	52
1.29	General reaction scheme of paraffins .....	57
1.30	Schematic experimental design of the research work .....	58
1.31	The disappearance of the substrate compounds at 450°C .....	61
1.32	Formation of solid products at 450°C from the pyrolysis of butylbenzenes .....	61
1.33	Selectivities of benzene in the pyrolysis of butylbenzenes .....	65
1.34	Selectivities of toluene in the pyrolysis of butylbenzenes .....	65
1.35	Selectivities of ethylbenzene in the pyrolysis of butylbenzenes .....	66
1.36	Selectivities of naphthalene in the pyrolysis of butylbenzenes .....	67
1.37	System t-p profiles for pyrolysis of model compounds .....	71
1.38	Conversion of model compounds during pyrolysis at 450°C under 0.69 MPa (cold) $\text{N}_2$ .....	72
1.39	Product distribution for pyrolysis of n-butylcyclohexane (n-BCH) as a function of residence time at 450°C .....	73
1.40	Product distribution for pyrolysis of n-butylcyclohexane (n-BCH) as a function of molar conversion of n-BCH at 450°C .....	74
1.41	Possible mechanisms for pyrolysis of n-butylcyclohexane .....	75
1.42	Product distribution for pyrolysis of ethylcyclohexane (ECH) .....	76
1.43	Compositional change during decalin pyrolysis .....	78
1.44	Conversion and isomerization during pyrolysis of pure cis-decalin and pure trans-decalin at 450°C .....	79
1.45	Isomerization of cis-decalin to trans-decalin .....	80
1.46	Possible mechanisms for pyrolysis of n-alkanes $\text{C}_m\text{H}_{2m+2}$ .....	80
1.47	Inhibiting effect of tetralin on solid deposit formation from JP-8P fuel, n- $\text{C}_{14}$ , and n-BB .....	82
1.48	Radical stabilization via H-transfer from tetralin and decalin .....	84
1.49	Isomerization of tetralin to 1-methylindan .....	85
1.50	Products formed from tetralin in pyrolysis & H-transferring pyrolysis .....	85
2.1	Polarized-light micrographs of the burner solids (BR) .....	91
2.2	Scanning electron micrographs of the burner solids (BR) .....	92
2.3	Polarized-light micrographs of the solids produced from JP-8P (a) and JP-8C (B) by thermal stressing at 450°C for 16 hours in nitrogen.....	94
2.4	Gas chromatograms for head space gases obtained from JP-8 with and without the added activated carbon-1 at 450°C for 5 hours.....	100

2.5	Specific ion chromatograms for mass 71 for the liquids obtained from JP-8 alone and JP-8 with activated carbon-1 stressed at 450°C for 5 hours.....	103
2.6	Specific ion chromatograms for mass 91 for the liquids obtained from JP-8 alone and JP-8 with activated carbon-1 stressed at 450°C for 5 hours.....	104
2.7	Specific ion chromatograms for masses 141 and 142 for the liquids obtained from JP-8 alone and JP-8 with activated carbon-1 stressed at 450°C for 5 hours..	105
2.8	Gas chromatograms for dodecane products obtained at 450°C with and without added activated carbon-1 .....	106
3.1	Oxygenated species formed by reaction between n-dodecane and air; A + K + HP = alcohols + ketones + hydroperoxides .....	115
3.2	Distribution of n-alkanes and 1-olefins at three temperatures .....	115
3.3	FTIR spectra of dodecane stressed under 100 psi air at 425°C .....	118
3.4	Deoxygenated fuel at 100 psi (0.1 ppm of O <sub>2</sub> ) .....	122
3.5	Relative rate for deposit formation at 121°C of various 10/90 aromatic or naphthene in n-decane binary blends compared to pure n-decane, plotted against number of benzylic hydrogen atoms present in aromatic or naphthene ...	124
3.6	<sup>1</sup> H NMR spectra of neat Jet A-1 fuel thermally stressed for the times indicated over air at 425°C .....	131
3.7	Scale expanded <sup>1</sup> H NMR spectra in the olefinic region of neat Jet A-1 fuel thermally stressed for the times indicated over air at 425°C .....	132
3.8	<sup>1</sup> H NMR spectra of Jet A-1 fuel containing 5% benzyl alcohol thermally stressed for the times indicated over air at 425°C .....	134
3.9	Scale expanded <sup>1</sup> H NMR spectra in the olefinic region of Jet A-1 fuel containing 5% benzyl alcohol thermally stressed for the times indicated over air at 425°C ...	135
4.1	Solid-state <sup>13</sup> C NMR data for the high volatile C bituminous coalified wood obtained by the CPMAS and Bloch decay methods .....	138
4.2	The pyrolysis/gc/ms trace of total ion current for the sample Hv bituminous coalified wood .....	140
4.3	The two-dimensional display of the three-dimensional structural model for high volatile bituminous coalified wood .....	144
4.4	A reaction model for coal liquefaction .....	152

## LIST OF TABLES

	<u>Page</u>
1.1 Coal- and petroleum-derived jet fuels and middle distillates .....	6
1.2 Approximate compositions of paraffinic fuels .....	9
1.3 Tentative assignments of $^1\text{H}$ NMR and $^{13}\text{C}$ NMR spectra of jet fuels .....	22
1.4 Summary of deposits produced at specific reaction temperatures and times .....	27
1.5 Aromaticity as a function of rank .....	32
1.6 Gas products identified from the thermal stressing of model compounds $\text{C}_8$ , $\text{C}_{12}$ , $\text{C}_{13}$ , and $\text{C}_{14}$ .....	40
1.7 Composition of gaseous products from sec- and iso-butylbenzenes at $450^\circ\text{C}$ ....	64
1.8 Deposit formation and liquid depletion during H-transferring pyrolysis of hydrocarbons and JP-8P jet fuel .....	83
2.1 Yields of liquids and solids products and pressure build-up from thermal stressing experiments on jet fuel and dodecane .....	999
2.2 Head space gas composition determined by GC using a FID detector .....	101
2.3 Head space gas yields from JP-98 with and without added carbons .....	102
2.4 Yields of paraffins from dodecane stressed at $450^\circ\text{C}$ for 5 hours with and without the activated carbon-1 .....	108
2.5 Yields of aromatics from dodecane stressed at $450^\circ\text{C}$ for 5 hours with and without the activated carbon .....	108
2.6 Specific area measurements on added carbons before and after thermal stressing .....	110
3.1 General features for oxygen-dodecane reactions .....	116
3.2 The effect of individual nitrogen compounds on total deposit formation in a deoxygenated jet fuel .....	121
3.3 The effect of individual oxygen compounds on total deposit formation in a deoxygenated jet fuel .....	121
4.1 Solid-state $^{13}\text{C}$ NMR data for coalified wood samples .....	139
4.2 Flash pyrolysis data for Hv C bituminous coalified wood .....	141
4.3 Data for coal samples .....	148
4.4 Data for solvent swelling, aromaticity, and liquefaction conversion for single stage reactions .....	151
4.5 Liquefaction of Montana subbituminous coal at $400^\circ\text{C}$ .....	159
4.6 Liquefaction of Montana subbituminous coat at $425^\circ\text{C}$ .....	159
4.7 Liquefaction of Pittsburgh #8 bituminous coal at $400^\circ\text{C}$ .....	160
4.8 Liquefaction of Pittsburgh #8 bituminous coal at $425^\circ\text{C}$ .....	160

## EXECUTIVE SUMMARY

This report is a summary of recent progress in a continuing long-term program at Penn State University to develop thermally stable jet fuels for high performance aircraft, which was initiated in FY89 by the U.S. Air Force, working jointly with the Department of Energy, Pittsburgh Energy Technology Center.

In Task 1 of this report, we examined the high temperature (400-475°C) degradation behavior of several coal- and petroleum-derived jet fuels and middle distillates; two-dimensional NMR of coal- and petroleum-derived JP-8 fuels; pyrolytic degradation of a number of model compounds including long-chain paraffins, cycloalkanes, alkylbenzenes, and hydroaromatic compounds; mechanisms of formation of solid deposits and polyaromatic hydrocarbons from jet fuels; and hydrogen-transferring pyrolysis to suppress solid formation from jet fuels.

Thermal stressing of jet fuels and middle distillates has been studied in tubing bomb reactors at 450°C for a heating period of 0-8 hours under 0.69 MPa UHP-N<sub>2</sub>. The fuel samples examined are three coal-derived fuels including JP-8C jet fuel, middle distillates from direct coal liquefaction (WI-MD and HRI-MD) and middle distillates from Fischer-Tropsch (FT-MD) synthesis (which is the so-called indirect coal liquefaction); six petroleum-derived jet fuels including two JP-8 (JP-8P and JP-8P2), one thermally stable jet fuel JPTS, one special fuel JP-7 and two commercial fuels Jet A and Jet A-1. The thermal stability of the fuels is significantly affected by their chemical composition. The fuels with higher contents of 1-3 ring cycloalkanes and/or hydroaromatics are more stable than those with higher contents of long-chain paraffins. The former includes JP-8C, HRI-MD and WI-MD, and the latter covers the remaining seven fuels including six petroleum-derived fuels and one fuel from indirect coal liquefaction. Among the paraffinic fuels, higher stability was observed for those fuels having narrower distribution of paraffins with relatively shorter chain, e.g., JP-7 and Jet A-1. Overall, coal-derived JP-8C and HRI-MD exhibit the best thermal stability among the ten fuels studied in terms of less solid deposition and gas formation.

A series of straight-chain alkanes including n-octane, n-dodecane, n-tridecane, and n-tetradecane, were thermally stressed at 400-475°C for 1-72 hours in a nitrogen atmosphere in order to determine the stability of a suite of model compounds. Deposit formation not only increased with increasing temperature and time, but also increased with increasing carbon content, thus indicating that the stability decreases with increasing chain length. Selected samples of the degraded liquid products of all four compounds for various reaction times at each temperature have been analyzed by GC and GC-MS. The results show a steady and continuous trend for all compounds. At low temperature and short times, where no solid deposit is observed, the main reactions occurring are cracking and recombination to form linear and cycloalkanes. At more severe stressings, where moderate solid deposit formation is observed, alkylbenzenes and

naphthalenes are found in the stressed liquid. At very high temperatures and long stress periods, where large amounts of deposits are noted, alkylated naphthalenes, fluorenes, anthracenes, and pyrenes are all found in the liquid. It has also been observed that when the largest compound present is naphthalene, very small amounts of deposits have been obtained, indicating that naphthalene may be a precursor to solid formation.

For testing on alkylbenzenes, four isomers of butylbenzenes (n-, iso-, sec-, and tert-butylbenzene) were used as model compounds (450°C, 0.69 MPa N<sub>2</sub>). Detailed temporal variation and analysis of the product distribution indicates that there are significant differences in the reaction pathways of the four compounds. The results showed that the degree of branching in the side-chain significantly affects the reactivity of alkylbenzenes. The order of reactivity (conversion of substrate) was found to be: n- >> sec- > iso- > tert-butylbenzene. Due to the variations in reactivity, the tendencies for them to form carbonaceous solids are different. The data also show that the trends for the conversion of the substrate compounds do not necessarily parallel to those for the formation of solid products. This can be attributed to the formation of different "active" intermediate products from the four isomers during the pyrolysis.

The mechanistic driving forces that govern the formation of high molecular weight compounds and solids from jet fuels at high temperatures are also discussed. The degradation of jet fuels at high temperatures is accompanied by the depletion and darkening of the liquid fuels and the formation of gas and solid materials. GC-MS analysis of liquid products indicated the gradual decomposition and the increased formation of cyclic hydrocarbons and PAHs with increasing severity. Spectroscopic characterization indicated that the solids are highly aromatic in nature, suggesting the path for solid formation from PAHs. From these results, the overall reaction sequence for solid formation from petroleum-derived paraffinic jet fuels is considered to be as follows: long-chain paraffins → cyclic alkanes/alkenes → alkylbenzenes → polyaromatics → solids. Some alkylaromatics formed from decomposition, cyclization and dehydrogenation of paraffins, seem to play an important role in the formation of the precursors to the solids. Such precursors may include some of the two- to four-ring PAHs formed in the liquids during pyrolytic degradation of jet fuels. The mechanisms for the formation of a number of PAHs, which have been detected in thermally stressed jet fuels and model compounds, are proposed.

Hydrogen-transferring pyrolysis was studied, with the goal of clarifying the effects of hydrogen-donors on the pyrolytic degradation and solid-forming tendencies of jet fuel components. The H-transferring pyrolysis of petroleum-derived JP-8 jet fuel, n-tetradecane (n-C<sub>14</sub>) and n-butylbenzene (n-BB) was conducted at 450°C under 0.69 MPa UHP-N<sub>2</sub> in the presence of 0-100 vol% tetralin, cis- and trans-decalin and their mixture. The product distribution patterns for H-transferring pyrolysis are different from those for conventional pyrolysis: adding H-donors such as tetralin or decalin to the conventional jet fuel significantly reduced or even eliminated the formation of carbonaceous deposits at 450°C and decreased the extents of fuel decomposition and gas formation,

which lead to substantial increase in the fuel stability. For runs at 450°C for 4 hours, adding 10 vol% tetralin to JP-8, n-C<sub>14</sub> and n-BB reduced the formation of deposits by 94% (from 3.1 to 0.2 wt%), 77% (from 3.0 to 0.7 wt%) and 54% (from 5.6 to 2.6 wt%), respectively. The enhanced stability can be attributed to the stabilization of the reactive radicals via hydrogen-abstraction from tetralin or decalin type compounds, which contributes mainly to inhibiting the secondary radical reactions and suppressing solid formation. These results clearly demonstrate that by means of hydrogen-transferring pyrolysis, hydrocarbon jet fuels can be used at high operating temperatures with little or no solid deposition.

In Task 2, polarized light microscopy and scanning electron microscopy were used to examine the microstructure of solid deposits including the deposit samples from an actual fuel line in an aircraft engine, from laboratory stressing of jet fuels and some model compounds in microautoclaves, as well as those produced from stressing a JP-8 Neat fuel with and without an added activated carbon. Actual fuel system deposits showed distinctly different microstructures which were produced by both gas-phase and liquid-phase reactions, involving pyrolytic carbon formation and carbonaceous mesophase development, respectively. Samples of petroleum- and coal-derived JP-8 jet fuel samples also produced gas-phase and liquid-phase solids (with somewhat different microstructures) upon stressing in batch reactors at 450°C. It is inferred that the formation of solids in both gas-phase and liquid-phase reactions involves the formation of polyaromatic compounds.

The presence of solid carbons, especially of activated carbons, during thermal stressing of a JP-8 jet fuel and a model compound dodecane causes substantial changes in the prevailing reaction mechanisms clearly shown by the changes in the gas yields and composition. The activated carbon surfaces appear to be effective in stabilizing the free radicals or catalyzing recombination reactions to form more gases and to preserve constitute paraffins in the fuel at 450°C. A notable effect of adding activated carbons is the prevention of solid deposition on the metallic surfaces even after severe thermal stressing of JP-8 fuel at 450°C for 5 hours. This observation suggests that the surface of the initial solid deposits provides a more attractive area for further solid deposition than the relatively inert bare metal surface. Different microstructures of the deposits observed on the added solid carbons mostly after stressing at 475°C indicate that the deposition mechanisms are also affected by the presence of different carbon surfaces during thermal stressing of the fuel.

Task 3 includes testing of various additives to enhance the thermal stability of jet fuels. Classic antioxidants such as hindered phenols, amines, mercaptans and various organometallic compounds that have been successfully employed to stabilize the degradation of polymers such as poly(vinyl chloride) and poly(vinyl alcohol) do not retard degradation of the jet fuel at high temperatures. We also tested some aliphatic alcohols, including methanol, ethanol, 2-propanol, pentanol and heptanol, and aromatic alcohols including benzyl alcohol and 1,4-benzenedimethanol



as stabilizers. The principal reaction pathways that lead to the formation of carbonaceous solids have been studied by using FT-IR and NMR spectroscopy. Among the aliphatic alcohols studied only ethanol appeared to retard the degradation of and "additive free" Jet A-1 significantly. Among all the additives tested, benzyl alcohol and benzenedimethanol showed best inhibiting effects. Therefore, these two aromatic alcohols and similar molecules offer considerable potential as additives that retard the formation of carbonaceous solid in hydrocarbon fuels, lubricants and the like, that are subjected to thermal stresses at high temperatures.

Task 4 is the newly initiated exploratory study on conversion of coals to thermally stable jet fuels. As first step, a series of coal samples including a resin-rich coal were characterized by using solid state CPMAS and DDMAS  $^{13}\text{C}$  NMR, pyrolysis-GC-MS and by computer-assisted modelling of their structures. The method for computer-assisted structural elucidation, and the results from computer modelling of coal structure using a vitrinite sample from a high volatile bituminous coal are described in this report. The model is constructed from elemental, solid-state  $^{13}\text{C}$  NMR, and flash pyrolysis-GC-MS data. Also reported are the preliminary data for catalytic liquefaction of two Pennsylvania bituminous coals, one Montana and one Wyoming subbituminous coal, and one Indiana bituminous coal, using dispersed metal sulfide catalysts.

To develop new dispersed catalysts, several bimetallic compounds were synthesized and tested for liquefaction of a Pennsylvania bituminous coal and a Montana subbituminous coal. The bimetallic organometallic compounds,  $\text{Mo}_2\text{Co}_2\text{S}_4(\text{Cp})_2(\text{CO})_2$  ( $\text{Cp}$  = cyclopentadiene),  $\text{Mo}_2\text{Co}_2\text{S}_4(\text{Cp}')_2(\text{CO})_2$  ( $\text{Cp}'$  = 1,2,3,4,5-pentamethylcyclopentadiene), and  $\text{Mo}_2\text{Co}_2(\text{S}_2\text{CNEt}_2)_2(\text{CH}_3\text{CN})_2(\text{CO})_2$  have been tested as catalytic precursors for direct coal liquefaction. The catalytic effects of these three bimetallic thiocubanes on the liquefaction of coal with respect to ligand effects, temperature, reaction conditions, and coal rank are discussed in this report.

## TECHNICAL PROGRESS

### TASK 1. INVESTIGATION OF THE QUANTITATIVE DEGRADATION CHEMISTRY OF FUELS

The objectives of this task are to study the chemistry of thermal degradation of jet fuels and the mechanisms for solid formation from jet fuels, and to provide information to support enhancing the intrinsic stability of jet fuels. The experimental work of this task includes thermal stressing of coal- and petroleum-derived jet fuels and middle distillates, and various model compounds (as jet fuel components) including long-chain paraffins, cycloalkanes, alkylaromatics and hydroaromatics.

#### *Activity 1. Pyrolytic Degradation of Coal- and Petroleum-Derived Aviation Jet Fuels and Middle Distillates*

##### Introduction

The high temperature thermal stability of jet fuels plays an important role in the design and development of future hypersonic aircraft. It was reported that the fuel in these new hypersonic aircraft may reach temperatures higher than 500°C. The temperatures are much higher than the current maximum operating temperature for the conventional aviation jet fuels. When the fuels are exposed to such high temperatures, serious pyrolytic degradation of the fuels will occur and will result in the formation of solid deposits on critical aircraft systems such as fuel pipeline, filter, and engine parts.<sup>1</sup> This means that advanced jet fuels are required for hypersonic aircraft. The development of such fuels warrants detailed study of pyrolytic degradation of hydrocarbon fuels.

The ultimate goal of our research project is to develop advanced jet fuels that are thermally stable at high temperatures. The objectives of this work are to rank the thermal stability of current fuels, to identify thermally stable compounds in fuels, to clarify the chemistry of pyrolytic degradation and mechanisms of solid formation, and to enhance the intrinsic stability of jet fuels by optimizing fuel composition. The future fuels might derive not only from petroleum, but also from hydrocarbon resources such as coal, tar sands, and oil shale. The scope of this report will concentrate on the thermal stability study of ten fuels including four coal-derived fuels and six petroleum-derived military and commercial jet fuels. The results concerning the effects of hydrogen-donors on the fuel stability are presented elsewhere.<sup>2</sup> In this study, the relative thermal stabilities of the fuels have been elucidated by their chemical composition.

## Experimental

### Samples

Ten fuel samples including jet fuels and middle distillates were studied. Four coal-derived fuels include JP-8C from hydrotreating of liquids produced from the Great Plains Gasification plant, and middle distillates derived either from direct coal liquefaction (WI-MD from Wilsonville plant and HRI-MD from HRI) or from indirect coal liquefaction (FT-MD from Fischer-Tropsch synthesis). Six petroleum-derived military and commercial jet fuels include JPTS (thermally stable jet fuel), JP7, JP-8P, JP-8P2, Jet A, and Jet A-1. The basic information of these fuels is presented in Table 1.1, and the properties of the samples are discussed in the following section.

**Table 1.1.** Coal- and petroleum-derived jet fuels and middle distillates

Fuel	Description	Received	Supplier/Source	Sample No.
<b>Coal-Derived Fuels</b>				
1) JP-8C	Hydrotreated JP-8	5-30-89	WPAFB	89-POSF-2685 ?
2) WI-MD	Middle distillates from coal liquefaction at Wilsonville	4-20-90	DOE PETC	259E MD
3) FT-MD	Middle distillates from Fischer-Tropsch Synthesis	8-16-91	DOE PETC	PETC F-T
4) HRI-MD	Middle distillates from coal liquefaction at HRI	11-26-91	WPAFB	83 POSF-0849
<b>Petroleum-Derived Jet Fuels</b>				
5) JP-8P	Petroleum-Derived JP-8	5-30-89	WPAFB	
6) JP-8P2	Petroleum-Derived JP-8	5-31-90	WPAFB/Tank S-15	
7) JP-7	Petroleum-Derived JP-7	5-31-90	WPAFB/Tank S-16	
8) Jet A-1	Commercial jet fuel	8-16-91	WPAFB/Tank S-7	90-POSF-2747
9) JPTS	Thermally stable jet fuel	8-16-91	WPAFB	91-POSF-2799
10) Jet A	Commercial jet fuel	8-16-91	WPAFB	90-POSF-2827

### Apparatus and Procedures

Thermal stressing of the jet fuels and middle distillates were studied in tubing bomb reactors at 450°C for a heating period of 0-8 hours under 0.69 MPa UHP-N<sub>2</sub>. The tubing bomb reactors were described in detail elsewhere elsewhere.<sup>3</sup> A 5 ml sample was confined in a leak-tested reactor. The sample was deoxygenated through repetitive (6 times) pressurization to 6.9 MPa with UHP-N<sub>2</sub> and purging to remove oxygen/air in the reactor or dissolved in the sample. The reactor was pressurized to the desired starting pressure of 0.69 MPa with UHP-N<sub>2</sub> before being immersed into a fluidized sand bath which has been preheated to 450°C. After the experiment was started, the reaction pressure was closely monitored. The experiment was ended after the desired stressing time by removing the reactor from the fluidized sand bath and

immediately quenching in a cool water bath. The headspace gas was collected in a gas sampling bag.

### **Product Chemical Analysis**

The gas samples were analyzed for their compositions and quantities by using a Perkin-Elmer Autosystem gas chromatograph (GC). Two detectors, a thermal conductivity detector (TCD) and a flame ionization detector (FID), were used to analyze the gas composition. The TCD was used to determine  $\text{CH}_4$ ,  $\text{C}_2\text{H}_2$ ,  $\text{C}_2\text{H}_4$ , and  $\text{C}_2\text{H}_6$  as well as non-hydrocarbon gases such as  $\text{H}_2$ ,  $\text{CO}$ , and  $\text{CO}_2$ . The FID was used to detect hydrocarbon gases from  $\text{C}_1$  to  $\text{C}_6$ . The GC columns used were a 10-foot long, 1/8-inch-diameter stainless steel column packed with 100/120 Carbosieve SII (Supelco) for TCD and a 6-foot long, 1/8-inch-diameter stainless steel column packed with 80/100 Chemipack C 18 for FID. There are two liquid samples collected from each experiment: one is the liquid residue directly collected from the reactor and the other is washed from the reactor wall with pentane. The compounds in the liquid products were identified by a HP 5890 Series II GC coupled with HP 5971A Mass Selective Detector (MSD) and quantified by a Perkin-Elmer GC 8500. The column used was a 30 m, 0.25 mm i.d., DB-17 Fused Silica Capillary Column (50% phenyl, 50% methyl silicone) with a film thickness of 0.25 mm. The solid deposits are operationally defined as the materials which are not soluble in the resulting liquid co-products and pentane (washing solvent). The solid deposits are to be analyzed by Fourier transform infra-red spectroscopy and NMR spectroscopy.

## **Results and Discussion**

### **Properties of Samples**

The fuel densities range from  $0.76 \text{ g/cm}^3$  (FT-MD) to  $0.96 \text{ g/cm}^3$  (WI-MD) with most falling in a smaller range of  $0.79$  to  $0.81 \text{ g/cm}^3$  (JPTS, JP-7, JP-8P, Jet A, Jet A-1, and JP-8P2). The densities of JP-8C and HRI-MD are  $0.84$  and  $0.92 \text{ g/cm}^3$ , respectively. All the fuels were analyzed by GC and GC-MS before and after thermal stressing, and they are all complex mixtures of hundreds of compounds. Because of the large number of compounds in the fuels, one way to visualize their compositions is employing the total ion chromatograms (TIC) and specific ion chromatograms (SIC) of GC-MS analysis. Figure 1.1 presents the TIC and SIC (ions of  $m/z$  57, 83, 91, 105, and 142) of JP-8P2. The fragment ions of  $m/z$  57, 83, and 142 are characteristics of long-chain paraffins, alkylcyclohexanes, and alkylnaphthalenes, respectively. The ions of 91 and 105 imply the presence of alkylbenzenes. From the resemblance between TIC and SIC of  $m/z$  57, we can find that the dominant constituents in JP-8P2 are the long-chain paraffins with carbon-number ranging from  $\text{C}_8$  to  $\text{C}_{17}$  with most falling between  $\text{C}_{10}$  to  $\text{C}_{15}$ . The alkylbenzenes ( $\text{C}_2$ - $\text{C}_6$ -, mainly  $\text{C}_3$ - $\text{C}_5$ -) content is about 20 percent. JP-8P2 also includes 5% alkylcyclohexanes ( $\text{C}_3$ - $\text{C}_8$ -) and low concentrations of tetralin, alkylindan, and alkylnaphthalenes.

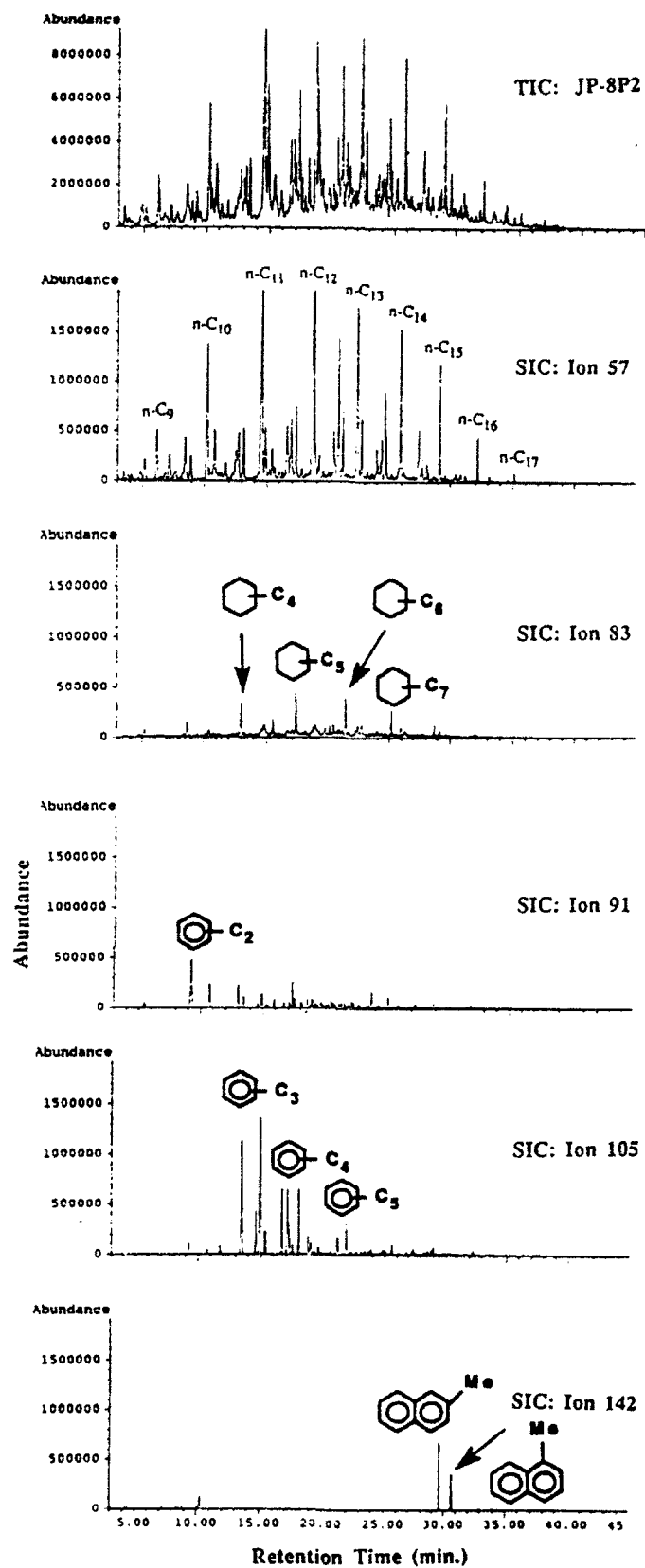


**Figure 1.1.** Total and specific ion chromatograms (ions of m/z 57, 83, 91, 105, and 142) of JP-8P2 from GC-MS analysis.

JP-8P, Jet A, JP-7, FT-MD, JPTS, and Jet A-1 are also paraffinic fuels derived from petroleum with long-chain paraffins as the dominant constituents, but the overall compositions and paraffins distributions are somewhat different. Figure 1.2 shows the SIC ( $m/z$  57) for six of the seven paraffinic fuels. We can see that JP-8P and Jet A are quite similar to JP-8P2 in terms of the long-chain paraffins distributions. Jet A-1 has a narrower band from C<sub>10</sub> to C<sub>14</sub> with most falling between C<sub>11</sub> and C<sub>12</sub>. JPTS has a band from C<sub>9</sub> to C<sub>15</sub>. JP-7 has a band from C<sub>11</sub> to C<sub>16</sub> with an average carbon number of 12. FT-MD is also a paraffinic fuel, although derived from coal, having almost exclusively paraffins (C<sub>9</sub> ~ C<sub>21</sub>) with very low concentration of cycloparaffins. Table 1.2 summarizes the approximate compositions of the seven paraffinic fuels based on the three major hydrocarbon types found in fuels (paraffins, alkylbenzenes, alkylcyclohexanes) and others (such as alkylnaphthalenes, alkylindans, etc).

**Table 1.2.** Approximate compositions of paraffinic fuels

Fuel	Weight %		
	Paraffins (%)	Alkylbenzenes (%)	Alkylcyclohexanes (%)
JP-8P2	~ 70	~ 20 (C <sub>2</sub> - ~ C <sub>6</sub> -)	~ 5 (C <sub>3</sub> - ~ C <sub>8</sub> -)
JP-8P	~ 75	~ 12 (C <sub>2</sub> - ~ C <sub>4</sub> -)	~ 8 (C <sub>3</sub> - ~ C <sub>7</sub> -)
Jet A	~ 80	~ 10 (C <sub>2</sub> - ~ C <sub>4</sub> -)	~ 6 (C <sub>1</sub> - ~ C <sub>6</sub> -)
JP-7	~ 90	very low	~ 10 (C <sub>5</sub> - ~ C <sub>8</sub> -)
FT-MD	~ 100		low
JPTS	~ 70	~ 8 (C <sub>2</sub> - ~ C <sub>4</sub> -)	~ 13 (C <sub>1</sub> - ~ C <sub>7</sub> -)
Jet A-1	~ 65	~ 26 (C <sub>3</sub> - ~ C <sub>5</sub> -)	~ 6 (C <sub>4</sub> - ~ C <sub>5</sub> -)

JP-8C, WI-MD, and HRI-MD are all coal-derived fuels, but their compositions are quite different from petroleum-derived paraffinic fuels. JP-8C is composed mainly of monocyclic and bicyclic alkanes, and two-ring hydroaromatic compounds. The major components are alkyl-substituted cyclohexanes (about 45%), decalin (6.3%), C<sub>1</sub>-decalin (4%), and tetralin (3.9%). There are also about 10% alkylbenzenes. HRI-MD is a heavy fuel, i.e., with many high molecular-weight components compared with the paraffinic fuels and JP-8C. HRI-MD consists of (alkyl) bicyclic alkanes, alkyl two-ring aromatic compounds and some alkylbenzenes. There are about 15% alkyl-substituted (mainly, C<sub>0</sub>- ~ C<sub>3</sub>-) cyclohexanes and only 8% long-chain paraffins. There are also some (C<sub>0</sub>- ~ C<sub>2</sub>-) 3-ring or 4-ring aromatics. Regarding WI-MD, it is heavier (with

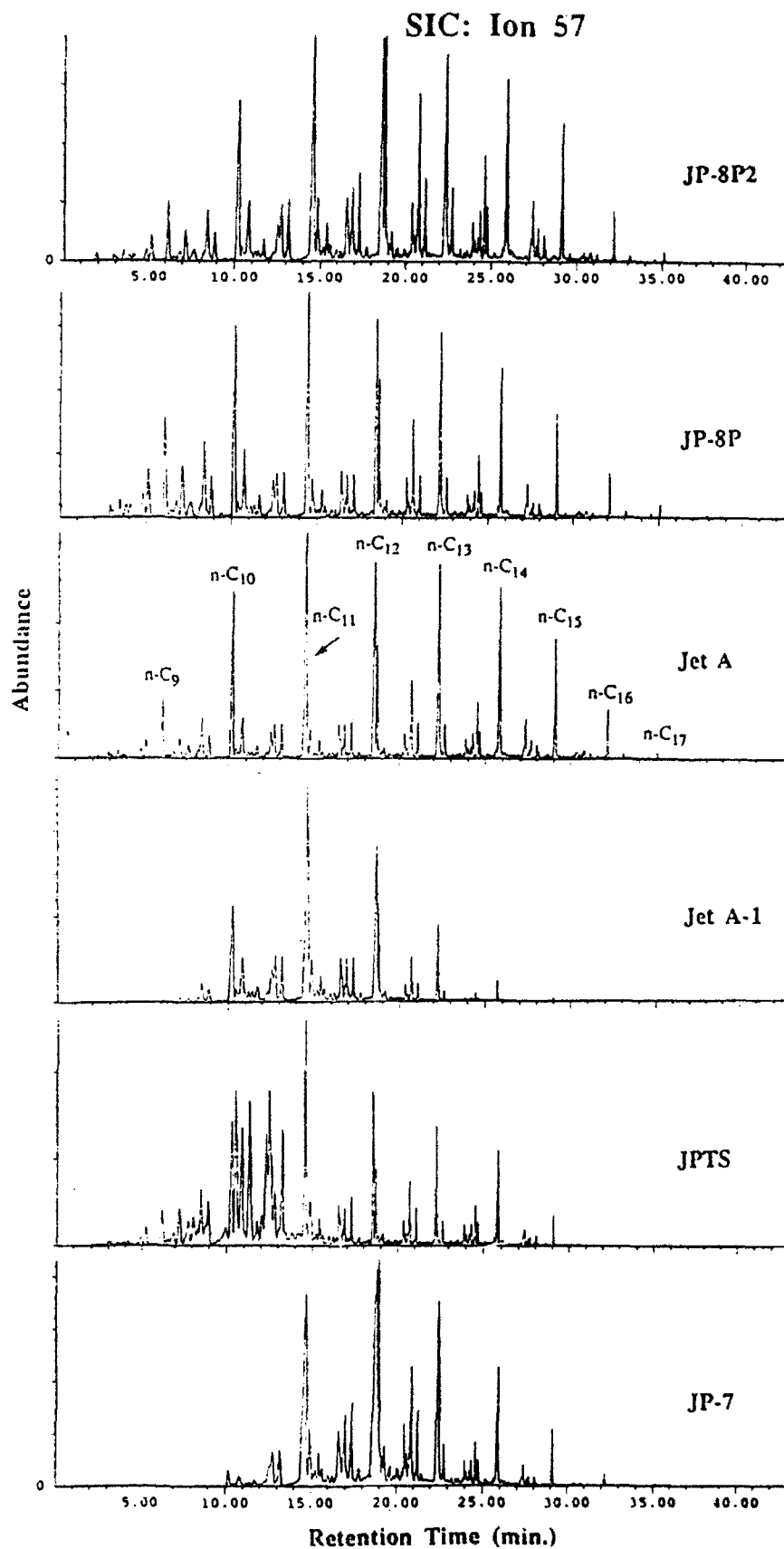


**Figure 1.2.** Specific ion chromatograms (ion of  $m/z$  57) of six paraffinic fuels.

carbon number  $\geq 12$ ) than the other nine fuels with few light molecular weight compounds. It has very high content of aromatics (with ring size not less than 2). The most abundant peaks are pyrene (4%) and multi-hydropyrenes (total about 8%), and less than 10% paraffins ( $C_{14} \sim C_{25}$ ).

#### **Degradation Product Distributions and Stability Comparison**

The relative thermal stabilities of hydrocarbons in fuels as well as the whole fuels themselves were identified based on the overall reaction products (gas, liquid, and solid) distributions and GC/GC-MS analysis of the liquid products. For the hydrocarbons in fuels, it was found that at  $450^{\circ}\text{C}$  long-chain n- and iso-paraffins ( $\geq C_{11}$ ), and n-alkylbenzenes ( $\text{alkyl} \geq C_3$ ) are some of the unstable compounds. Some compounds that are relatively more stable compounds include long-chain paraffins ( $\leq C_8$ ), long-chain paraffins ( $C_9$  and  $C_{10}$ , up to 4 hours),  $C_0$ - to  $C_3$ -cycloalkanes, and  $C_0$ - to  $C_2$ -benzenes. One example is shown in Figure 1.3, which presents the total ion chromatograms of the neat sample of, and the liquid products from, FT-MD after thermal stressing at  $450^{\circ}\text{C}$  for 1-8 hours. Recall that FT-MD is a paraffinic fuel which has paraffins ranging from  $C_9$  to  $C_{21}$ . We can clearly find that long-chain paraffins of  $C_{11}$  through  $C_{21}$  decompose quickly; the decomposition rate increases with increasing chain size. Quantitative results from GC and qualitative results from GC-MS indicate that the main reactions occurring in the first 2.5 hours include cracking of the paraffins into lower alkanes and olefins, and cyclization to form alkylcyclic alkanes and olefins. The alkylcyclic compounds were then subjected to dehydrogenation to form alkylbenzenes. This observation is consistent with the mechanisms proposed by elsewhere.<sup>4</sup> A quantitative presentation of how the paraffins content changes with time is shown in Figure 1.4 for the same sample. The paraffins were divided into 12 groups based on the carbon numbers; each group consists of straight and branched alkanes with the same carbon number. Figure 1.4 shows that at  $450^{\circ}\text{C}$  long-chain paraffins with carbon number no less than 11 (i.e.,  $C_n$ ,  $n \geq 11$ ) are unstable.  $C_{15}$  through  $C_{21}$  decompose completely by 2.5 hours. Notice that the content of  $C_9$  increases from the initial 0.5% to 5.7% at 1 hour and then decreases to 3.1% after 2.5 hours. The initial increase is contributed from cracking yield from longer chain paraffins, and the  $C_9$  later decomposes and results in the  $C_9$  fraction decreasing with increasing time.

The yields of the gas components from JP-8P thermally stressed at  $450^{\circ}\text{C}$  for 1-8 hours are presented in Figure 1.5. Methane is always the most abundant gaseous product (in mmole) followed by ethane and propane over the stressing range; this is also true for all other nine fuels studied. Another common characteristic for the fuels is that the paraffinic gases ( $\text{CH}_4$ ,  $\text{C}_2\text{H}_6$ ,  $\text{C}_3\text{H}_8$ , and  $\text{C}_4\text{H}_{10}$ ) increase with increasing time but the olefinic gases ( $\text{C}_2\text{H}_4$ ,  $\text{C}_3\text{H}_6$ ,  $\text{C}_4\text{H}_8$ ) increase initially then decrease with increasing time. Continuous cracking accounts for the progressive increase of paraffinic gases and the initial increase of olefinic gases. Olefins are known to be less stable and highly reactive because of unsaturation; this results in the later decrease of olefinic gases.



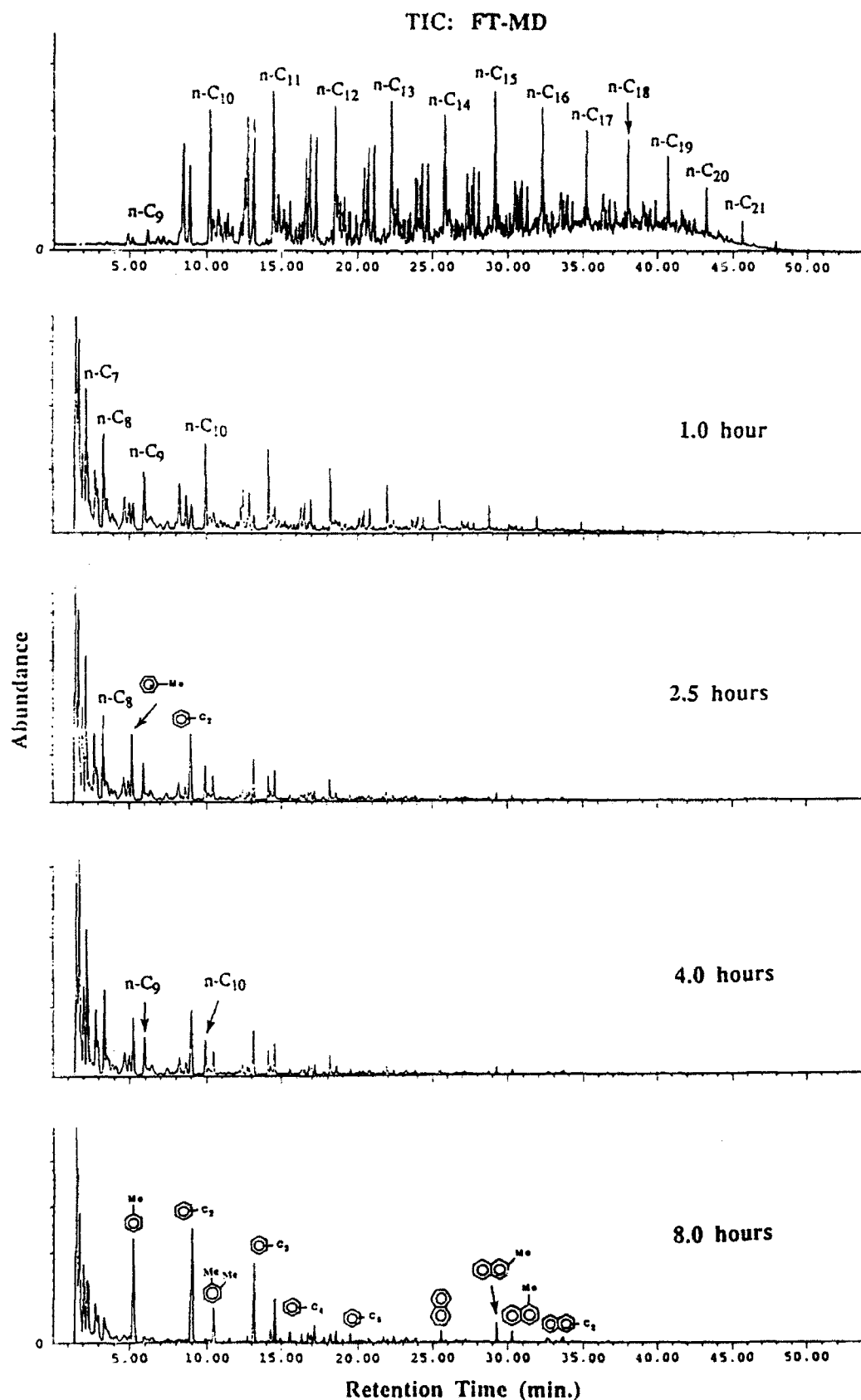


**Figure 1.3.** Total ion chromatograms of the neat sample of, and the liquid products from FT-MD after thermal stressing at 450°C for 1-8 hours.

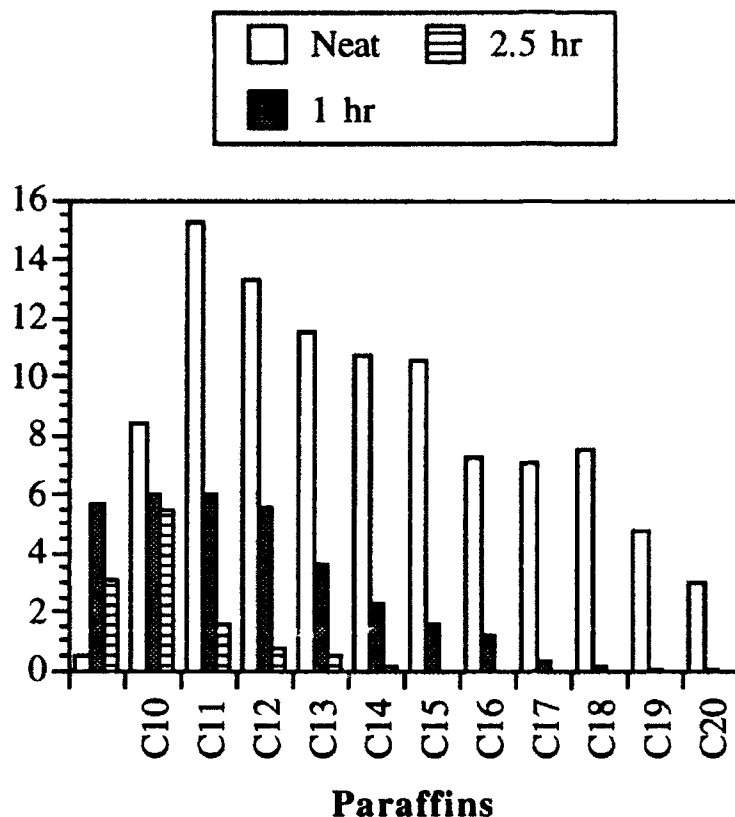


**Figure 1.4.** Paraffins distribution of liquids from FT-MD.

The decomposition extents of the 10 fuels are significantly affected by their compositions. Figure 1.6 shows the gas yields from the 10 fuels stressed for 1-8 hours. The figure indicates that the three coal-derived non-paraffinic fuels, i.e., JP-8C, HRI-MD, and WI-MD, are more stable than the other seven paraffinic fuels in terms of less gas formation. The difference in stability in terms of the gas formation is attributed to the composition difference. Paraffinic fuels produce more gases because the major reaction for long-chain paraffins is cracking into lighter gases of alkanes and olefins. On the other hand, the compositions of the three coal-derived non-paraffinic fuels are quite different from the paraffinic fuels; they have low fraction of paraffins but are rich in cyclic alkanes and hydroaromatics. Thus the major reaction for them is dehydrogenation to form alkylbenzenes (liquid yields) instead of the formation of low molecular-weight gases. It can be seen that HRI-MD and FT-MD produce the gas the least and the most, respectively. For example, the gas yields for HRI-MD and FT-MD are respectively 3.3% and 17% at 1 hour, 10% and 33% at 4 hours, and 16% and 52% at 8 hours. The six petroleum-derived paraffinic fuels (JP-8P, Jet A, JP-7, FT-MD, JPTS, and Jet A-1) have similar gas yields (ranging from 37% to 40%) for 8-hour stressing. However, for 1- ~ 4-hour stressing, Jet A-1 has the lowest or second to the lowest gas

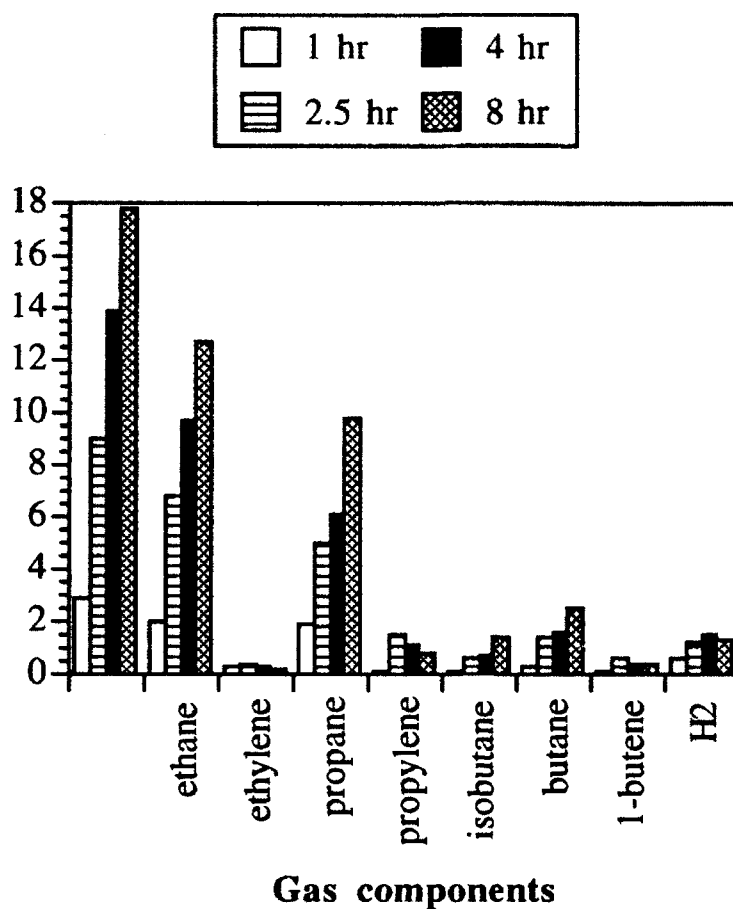


**Figure 1.5.** Yields of H<sub>2</sub> and C<sub>1</sub>-C<sub>4</sub> gases from JP-8P at 450°C.

yields; this is consistent with the fact that among the paraffinic fuels, Jet A-1 has the lowest paraffin content and the narrowest paraffin band (from C<sub>10</sub> to C<sub>14</sub>, with most falling between C<sub>11</sub> and C<sub>12</sub>).

The solid yields from the ten fuels stressed for 1-8 hours are presented in Figure 1.7. The figure shows that there is no solid formed after 1-hour stressing for all the 10 fuels, and the solid starts to form between 1 and 2.5 hours. The induction time, which is the time period needed for the formation of solid precursors (such as polyaromatics) from reactive intermediates, differs for each fuel. It was found that fuels rich in hydrogen-donors (such as cyclic alkanes) have longer induction period and tend to have better stability. The hydrogen abstracted from hydrogen-donors stabilizes the reactive radicals; this in consequence inhibits the secondary radical reactions and suppresses solid formation.<sup>2</sup> Two of the three coal-derived non-paraffinic fuels, JP-8C and HRI-MD, have much better stability than other fuels in terms of much less solid formation. This is again attributed to the composition difference and the fact that JP-8C and HRI-MD have high concentration of hydrogen donors. Figure 1.7 also shows that JP-7 and JPTS have higher

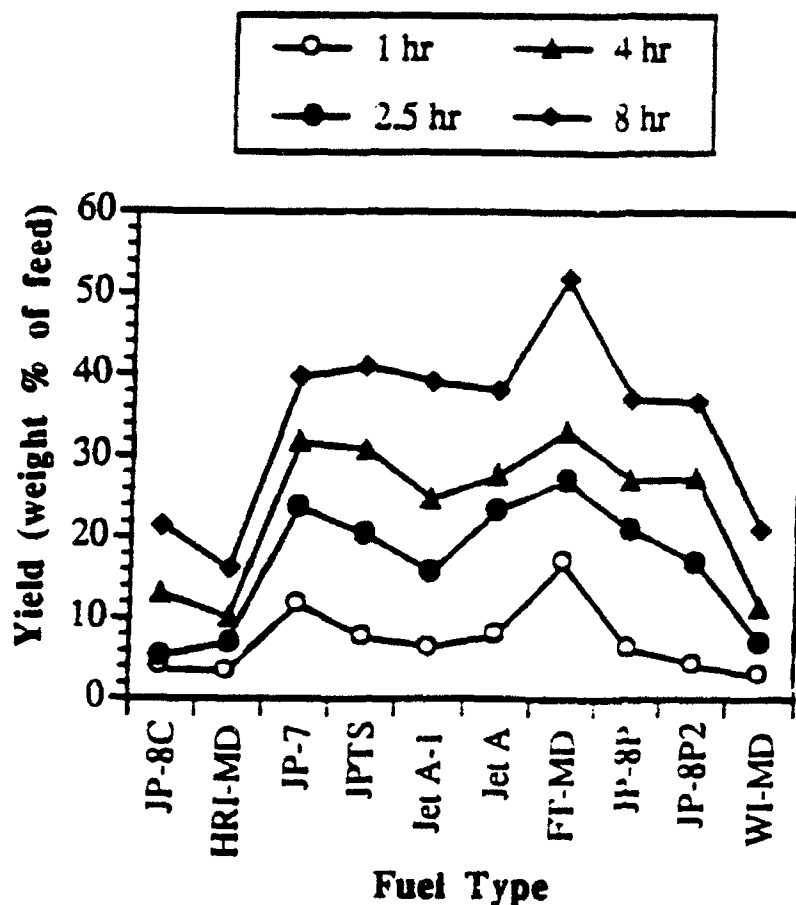


**Figure 1.6.** Yields of gases at 450°C.

stability among the seven paraffinic fuels in terms of less solid formation. This is also attributed to their lower aromatics content and higher hydrogen-donor compounds (alkylcyclohexanes).

WI-MD, on the other hand, does not have good stability in the long run, judging from its high solid formation at 8-hour stressing. Figure 1.8 presents the total ion chromatograms of the neat sample of, and the liquid products from, WI-MD after thermal stressing at 450°C for 1-8 hours. It can be seen that WI-MD has very high content of aromatics and hydroaromatics. The hydroaromatics decomposed quickly to form saturated aromatics through dehydrogenation, and these aromatic compounds subsequently form more polycyclic aromatic hydrocarbons and solid deposits. WI-MD seems to be stable in terms of low gas formation; however, GC-MS analysis of the liquid products shows that in fact WI-MD is quite unstable and decomposes quickly to form aromatics and precursors to solid. In short, WI-MD tends to form more solid than other fuels due to its high aromatic content nature, and it cannot be a good jet fuel.

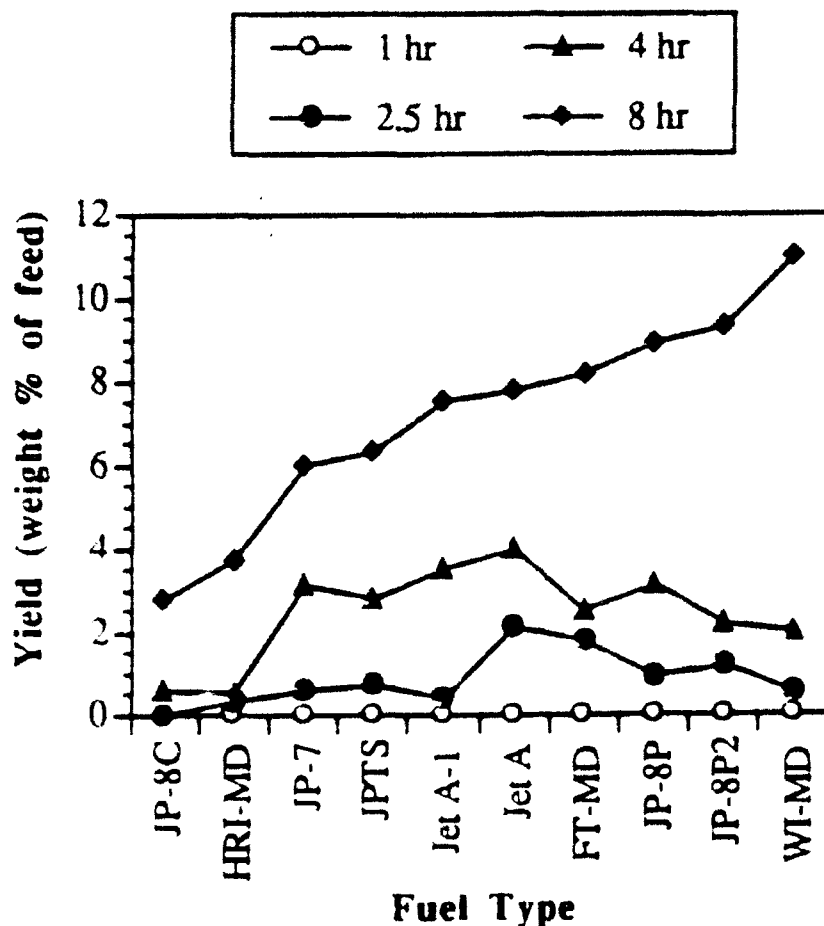


**Figure 1.7.** Yields of solid deposits at 450°C

### Conclusions

The thermal stability of the fuels is significantly affected by their chemical composition. Pyrolysis of 10 jet fuels and middle distillates has been studied in a tubing bomb reactor. The compositions of the stressed as well as neat fuels were all qualitatively and quantitatively characterized by GC and GC-MS. This information is useful in explaining and evaluating the thermal stability of fuels. The relative thermal stabilities of hydrocarbons in fuels as well as the whole fuels themselves were identified. The fuels with higher contents of 1-3 ring cycloalkanes and/or hydroaromatics are more stable than those with higher contents of long-chain paraffins in terms of less gas formation. The former includes JP-8C, HRI-MD and WI-MD, and the latter covers the remaining seven fuels including six petroleum-derived paraffinic fuels and one paraffinic fuel from indirect coal liquefaction. Among the paraffinic fuels, higher stability in terms of less gas formation was observed for those fuels having narrower distribution of paraffins with relatively shorter chain, e.g., Jet A-1; those with lower aromatics content and higher hydrogen-donor compounds exhibits less solid formation. Overall, coal-derived JP-8C and HRI-MD have the best thermal stability among the ten fuels studied either in terms of less gas or solid formation.

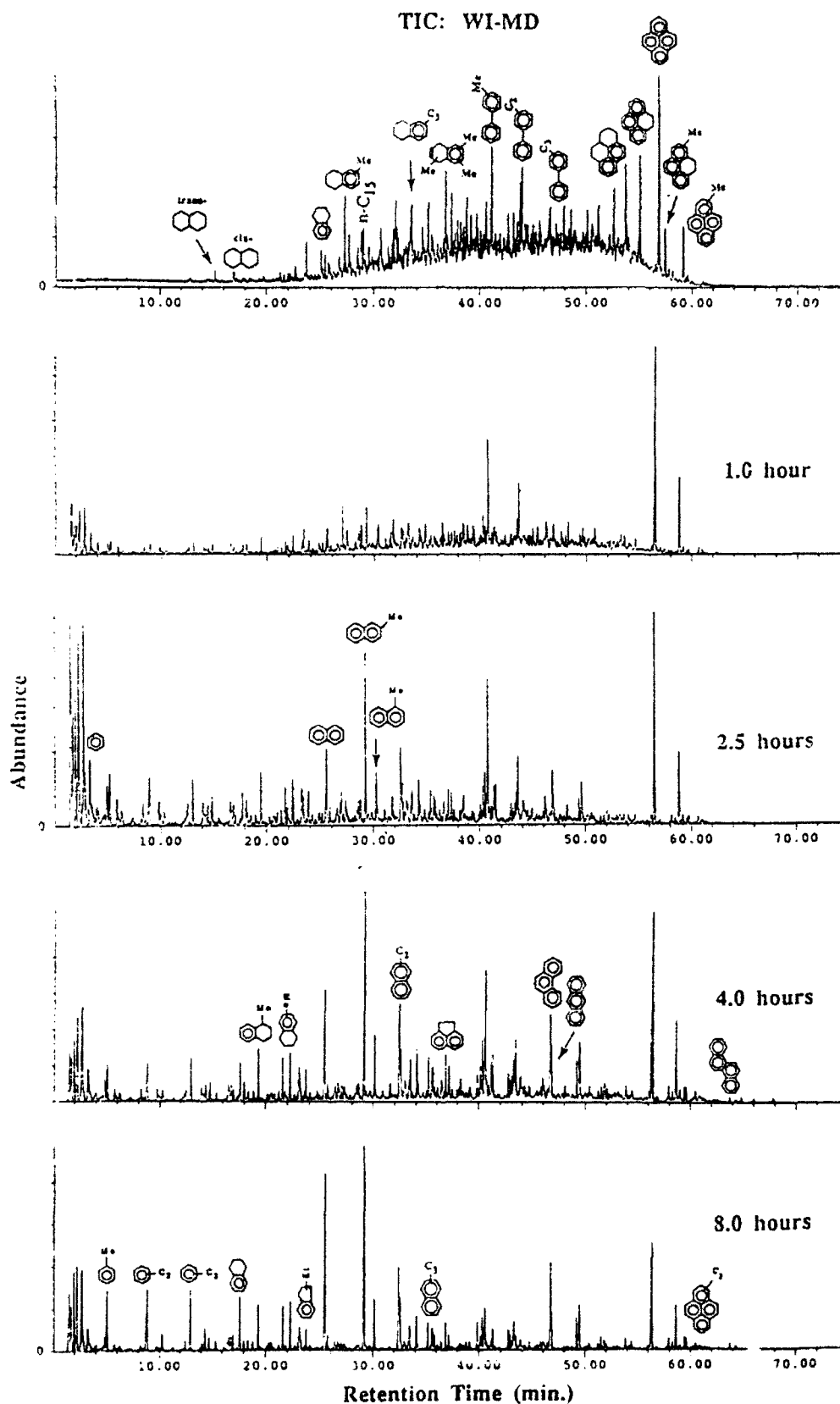


**Figure 1.8.** Total ion chromatograms of the neat sample of, and the liquid products from, WI-MD after thermal stressing at 450°C for 1-8 hours.

## References

1. Roquermore, W. M., Pearce, J. A., Harrison III, W. E., Krazinski, J. L., and Vanka, S. P., *Preprints, American Chemical Society, Division of Petroleum Chemistry*, **34(4)**, 1989, 841.
2. Song, C., Lai, W.-C., and Schobert, H. H., "Hydrogen-Transferring Pyrolysis of Cyclic and Straight-Chain Hydrocarbons. Enhancing High Temperature Thermal Stability of Aviation Jet Fuels by Hydrogen-Donors," *Preprints, American Chemical Society, Division of Fuel Chemistry*, **37(4)**, pp 1655-1633, 1992.
3. Eser, S., Song, C., Schobert, H. H., Hatcher, P. G. et al., "Advanced Thermally Stable Jet Fuels Development Program Annual Report", Volume II, Interim Report for period July 1989 to June 1990, WRDC-TR-90-2079, Vol. II, September 1990.
4. Song, C., Peng, Y., Jiang, H., and Schobert, H. H., "On the Mechanisms of PAH and Solid Formation during Thermal Degradation of Jet Fuels", *Preprints, American Chemical Society, Division of Petroleum Chemistry*, **37(2)**, 1992a, 484-492.

### **Activity 2. Two-Dimensional (2D) NMR Analysis of Coal- and Petroleum-Jet Fuels**

In the previous annual report,  $^1\text{H}$  NMR data were included for the coal and petroleum derived jet fuels as well as their thermally stressed counterparts. The NMR spectra were used as a means of structurally identifying the basic functional groups present which in turn could be linked to the individual components possessing these functionalities. Once identified the next task was to quantitate the presence of the various components in the fuel mixtures as a means of following thermal degradation in these systems. As a prelude to this work, further NMR studies were needed to confirm the tentative structural assignments that were made for the  $^1\text{H}$  NMR spectra.

$^{13}\text{C}$  NMR provides a larger chemical shift range in which to assign functional groups of complex mixtures. 2D heterocorrelated NMR spectroscopy provides a means of correlating  $^{13}\text{C}$  and  $^1\text{H}$  chemical shifts of carbons with their directly attached protons. One particularly useful 2D technique is the heterocorrelated multiple quantum coherence (HMQC) experiment. The HMQC experiment offers the added advantage of significantly increased sensitivity, because unlike the normal heterocorrelated experiment (Hetero COSY), HMQC utilizes  $^1\text{H}$  detection. The increased sensitivity over  $^{13}\text{C}$  detected heterocorrelated spectroscopy can be quantified by calculating  $(\gamma_{1\text{H}} / \gamma_{13\text{C}})^{5/2}$  where  $\gamma_{13\text{C}} = 1/4 \gamma_{1\text{H}}$ . In this case direct  $^{13}\text{C}$ - $^1\text{H}$  correlation information was

obtained by using a modified HMQC experiment in which a BIRD sequence was used to facilitate suppression of protons not coupled to  $^{13}\text{C}$ . In addition, GARP decoupling was applied during acquisition. The HMQC spectra obtained for JP-8C and JP-8P are shown in Figures 1.9 and 1.10, respectively.

The complexity of the fuel mixtures prohibits the assignment of each crosspeak to specific carbons in a chemical structure, but the majority of the signals can be assigned to specific types of carbons previously identified in the mixture. Table 1.3 lists various types of carbon species and their  $^{13}\text{C}$  and  $^1\text{H}$  chemical shift ranges. The spectra in Figures 1.9 and 1.10 display plots of the aliphatic and aromatic regions *a* and *b*, respectively. Each plot was analyzed for the presence of carbon functional groups that have been identified by GC-MS data. From this data, it was found that JP-8C is predominantly comprised of cyclic aliphatic and aromatic hydrocarbons. The region labeled A in Figure 1.9a of the spectrum can be assigned to the terminal methyl groups of hydrocarbon sidechains. Region B contains broad signals which reflects the numerous types of methylene carbons found in aliphatic cyclic hydrocarbons and sidechains. The regions labeled C and D have been assigned to methyl and methylene groups, respectively, that are directly attached to aromatic ring structures. Figure 1.9b contains one broad set of signals that have been assigned to the carbons of alkylated benzenes.

A similar examination of the HMQC spectrum for JP-8P shown in Figure 1.10 was also carried out. The aliphatic portion (a) of the spectrum contains three main regions. Regions A and B are representative of the domination by straight-chain aliphatics in this mixture. Region A has been assigned to the carbons of the terminal methyl groups and region B has been assigned to the methylene carbons contained in the long chain hydrocarbons. Region C has been assigned to the methyl carbons of the substituted naphthalene and benzene species that are also predominantly found in JP-8P. The assignment of the aromatic region coincides with the assignment of region C, since regions D and E have been assigned to the carbons of the substituted benzene and naphthalene species.

The 2D spectra do indeed provide additional chemical shift information for the assignment of the functional groups of the various components contained in the jet fuel mixtures. If structural features of specific components in the mixture are to be examined by NMR following thermal stressing, then a more complete assignment of  $^{13}\text{C}$  and heterocorrelated spectra is needed. However, it is important to note that some structural entities are sufficiently resolved (e.g., Figure 1a, regions C and D) to allow tracking of their behavior over the course of thermal stressing. Future work will focus on applying the above 2D NMR techniques to thermally stressed jet fuel samples.



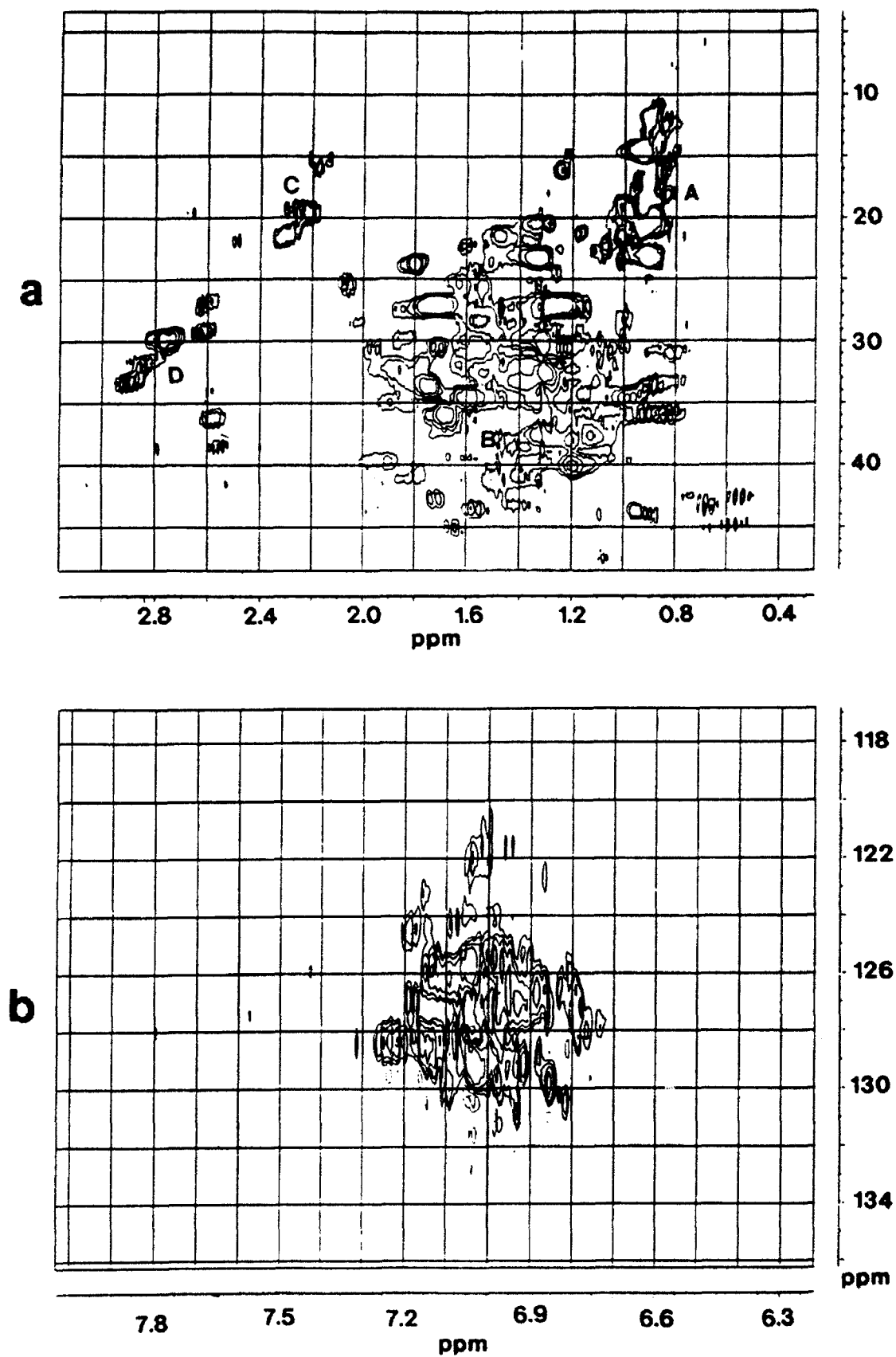


**Figure 1-9.** The heterocorrelated multiple quantum coherence (HMQC) spectrum of JP-8C (a) the aliphatic region (b) the aromatic region.

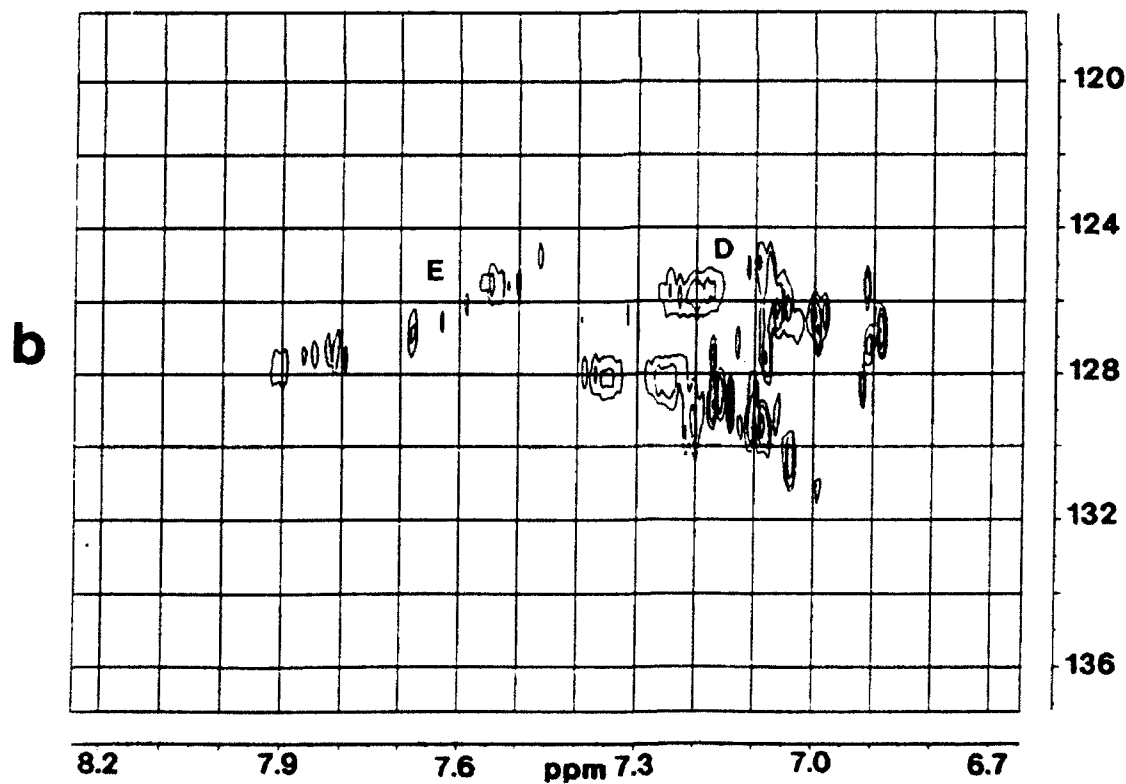
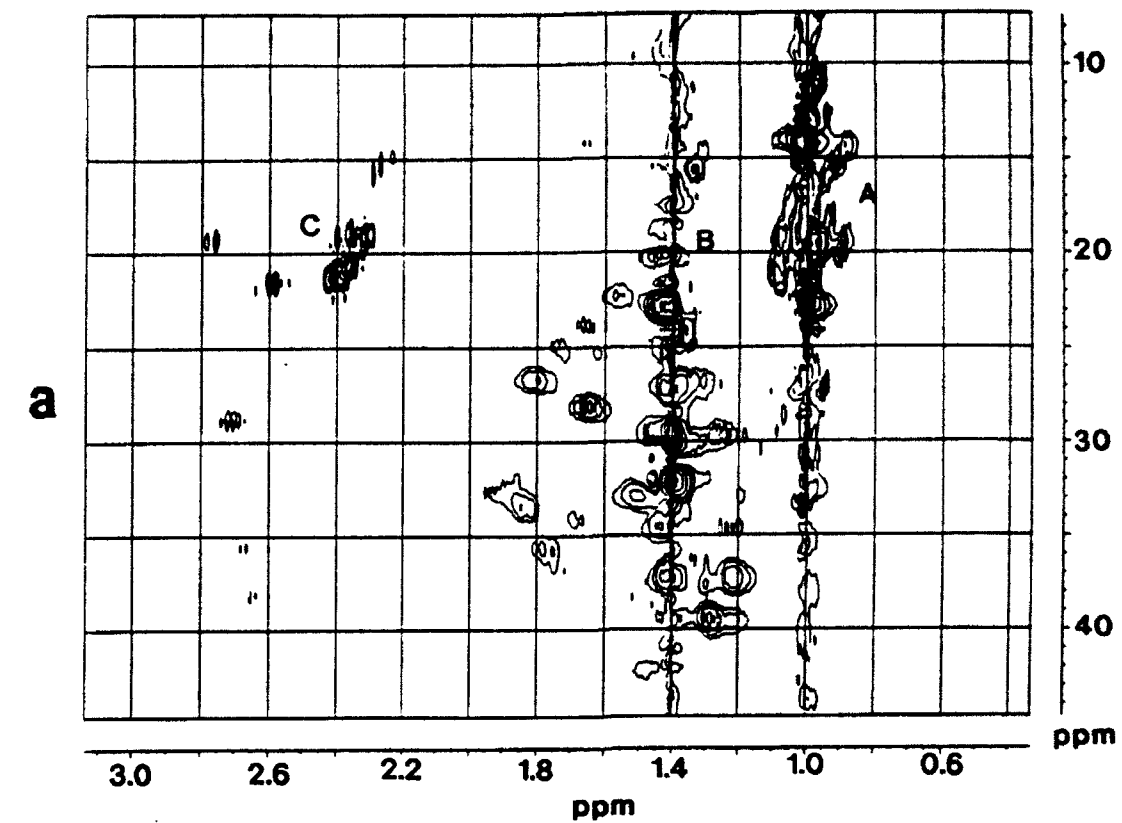


**Figure 1-10.** The heterocorrelated multiple quantum coherence (HMQC) spectrum of JP-8P (a) the aliphatic region (b) the aromatic region.

**Table 1.3** Tentative assignments of  $^1\text{H}$  NMR and  $^{13}\text{C}$  NMR spectra of jet fuels

Chemical Shift Values (ppm)		Band Assignments	
$^1\text{H}$ NMR##	$^{13}\text{C}$ NMR	Corresponding $^*\text{H}$ & $\text{C}^*$	Compounds Type
6.00-9.00	125-138	$^*\text{Ar-H}^*$	Aromatics
5.55-6.00	139-141	$\text{R-}^*\text{CH}^*=\text{CH}_2$	External Olefin
5.30-5.55	123-133	$\text{R-}^*\text{CH}^*=\text{CH}^*-\text{R}'$	Internal Olefin
5.05-5.30		$\text{R(R')-C}^*=\text{CH}^*-\text{R}'$	Internal Olefin
4.75-5.05	114-124	$\text{R-CH}^*=\text{CH}_2^*$	External Olefin
4.50-4.75		$\text{R(R')-C}^*=\text{CH}_2^*$	External Olefin
3.40-4.50	36-42	$\text{Ar-}^*\text{CH}_2^*-\text{Ar}$	Alpha Methylene
2.60-3.40	23-38	$\text{Ar-}^*\text{CH}_2^*-\text{R}$	Alpha Methylene
2.00-2.60	19-21	$\text{Ar-}^*\text{CH}_3^*$	Alpha Methyl
1.60-2.00	15-34	$\text{Ar-CH}_2^*-\text{CH}_2^*-\text{R}$	Beta Methylene <sup>b)</sup>
1.05-1.60	15-33	$\text{R-}^*\text{CH}_2^*-\text{R}$	Paraffinic Methylene
	14-23	$\text{Ar-(CH}_2)_2\text{-(CH}_2)_n^*-\text{CH}_3$	Gamma Methylene <sup>a)</sup>
	15.8-25	$\text{Ar-CH}_2\text{-CH}_3^*$	Beta Methyl <sup>a)</sup>
0.50-1.05	14-16	$\text{R-(CH}_2)_n\text{-CH}_3^*$	Paraffinic Methyl
	14-15	$\text{Ar-(CH}_2)_n\text{-CH}_3^*$	Gamma or Terminal Methyl

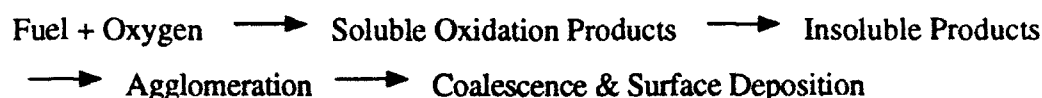
## With  $\text{Me}_4\text{Si}$  as an internal standard. The  $^1\text{H}$  NMR bands were assigned based on earlier reports: C. Song et al., *Energy & Fuels*, 1988, 2, 639-644; *Bull. Chem. Soc. Japan*, 1986, 59, 3643-3648; *PSU 1991 Jet Fuel Annual Report*, WL-TR-91-2117.

### Activity 3. Thermal Degradation of Long-Chain Paraffins

#### Introduction

The high performance aircraft of today and tomorrow requires fuels that can withstand significantly higher temperatures. The stability of aviation fuel is a critical factor to be considered in the design of aircraft fuel systems because the fuel also serves as a coolant for various surfaces of the aircraft. There have been numerous studies done relating to the thermal stability of jet fuels.<sup>1-9</sup> The thermal stability of jet fuel refers to its resistance to decomposition at elevated temperatures to form gums, sediments, or solid deposits within the fuel systems and engines.

The high temperatures encountered by the jet fuel in aircraft fuel systems stimulate oxidation reactions that lead to the formation of insoluble material or solid deposits. The deposit formation also involves the pyrolysis of hydrocarbon fuel molecules which undergo homolytic cleavage of C-C bonds to generate free radical species. These radicals can then undergo further reactions to form higher molecular weight species which ultimately lead to the formation of deposits. This degradation process is also aided by the presence of fuel impurities such as metals, sulfur, and nitrogen.<sup>7</sup> The overall reaction process for the decomposition of the jet fuel and formation of these gums and deposits is as follows<sup>10,11</sup>:



These decomposition products, gums and solid deposits, can cause inefficient operation of the aircraft by clogging filters, obstructing valves in the fuel lines, degrading performance of injector nozzles, and reducing performance of fuel/oil heat exchangers, causing a reduction in heat transfer.<sup>2,5,10</sup>

Previous studies of lower molecular weight n-alkanes than those currently being studied, n-hexane and n-heptane, in an inert atmosphere have proposed mechanisms that the initiation of cracking reactions can occur at various points along the carbon chain.<sup>12,13,14</sup> The formation of light saturates (CH<sub>4</sub>, C<sub>2</sub>H<sub>6</sub>, C<sub>3</sub>H<sub>8</sub>, n-C<sub>4</sub>H<sub>10</sub>, and n-C<sub>5</sub>H<sub>12</sub>) is the result of hydrogen transfer reactions. The light unsaturates (C<sub>2</sub>H<sub>4</sub>, C<sub>3</sub>H<sub>6</sub>, 1-C<sub>4</sub>H<sub>8</sub> and 1-C<sub>5</sub>H<sub>10</sub>) are the products of decomposition reactions that are produced by a series of chain reactions. The heavier products, > C<sub>6</sub> or C<sub>7</sub>, are the products of recombination reactions. Gas chromatographic analysis of the liquid pyrolysis products from experiments done by Domine<sup>14</sup>, shows that it contains products from n-C<sub>6</sub> to n-C<sub>12</sub> and various methyl and ethyl isoalkanes up to C<sub>12</sub>. It does not indicate formation of cycloalkanes or alkylbenzenes, which are found in the analysis of samples generated in the current work. The gas chromatogram of the gaseous products generated in the experiments from Domine shows moderate amounts of methane, ethane, propane, and butane and a very large proportion of hexane. There are also small amounts of ethylene, propylene, and 1-butene present. This analysis also shows no signs of any isoalkanes or cycloalkanes. The results from the present work differ from these results in that analysis of the headspace gas revealed large concentrations of methane, ethane + ethylene (ethane and ethylene are reported as one peak because they were not able to be separated on the column used), and propane, along with lesser amounts of higher molecular weight n-alkanes (C<sub>4</sub> to C<sub>6</sub>) cycloalkanes, and isoalkanes.

One objective of the study being done at Penn State University is to determine the high-temperature thermal stability of a suite of model compounds typical of those present in jet fuels.

The petroleum-derived jet fuel, JP-8P, is composed mainly of long-chain paraffins with a low concentration of alkylbenzenes and alkylnaphthalenes.<sup>8</sup> Coal-derived jet fuels, JP-8C, contain a higher content of aromatics, mainly cycloalkanes, and a lower concentration of long-chain paraffins. This particular study of several alkanes refers mainly to the petroleum-derived jet fuels, since JP-8P has a wide carbon-number distribution of components, ranging from C<sub>8</sub> to C<sub>17</sub>.<sup>8,9,15</sup>

## **Experimental**

### **Microautoclave Reactor (Tubing Bomb)**

The microautoclave reactors are those presently being used at Penn State University. A schematic diagram of the 25-ml tubing bomb, drawn by Dr. Semih Eser, is shown in Figure 1.11. The body of the reactor consists of 316 stainless steel tubing, 3/4-inch o.d., with Swagelock fittings at each end. A 1/4-inch stainless steel tube (stem) is connected to the upper portion of the reactor using a reducer. The top of the tubing bomb consists of a pressure gauge, needle valve, and a quick-connect stem for the input and release of gas.

### **Procedures**

A 10-ml sample was used in all experiments. The model compounds studied were straight-chain alkanes octane, dodecane, tridecane, and tetradecane. The reactor was loaded with the sample, assembled, and leak-tested by pressurizing the tubing bomb to 1000 psi (7 MPa) and submerging the reactor in water. Once the reactor is leak-free, it was repetitively pressurized to 1000 psi and purged with ultra-high purity (UHP) nitrogen. This process was repeated five times before the tubing bomb was pressurized to an operating pressure of 100 psi.

The tubing bomb, once pressurized to the operating pressure, was placed in a preheated fluidized sand bath. The temperatures of the sand bath for these experiments were set at 400°, 425°, 450°, and 475°C for times ranging from 1 to 72 hours, depending on the temperature used. The heating of the fluidized sand bath was controlled by a thermostat and three 3000-watt heating elements. The tubing bombs were attached to a post placed over the center of the sand bath. The sand bath was then raised until the top of the reactor was ~1/2-3/4 inch below the top of the sand. The microautoclave reactor reached the reaction temperature in 2-4 minutes. At the end of the reaction time the tubing bomb was removed from the sand bath and quenched in a cold water bath. Once cooled, the headspace gas was vented and collected in gas sampling bags for later gas chromatographic (GC) analysis. The liquid products were removed, the amount measured in a graduated cylinder, and stored for later analysis by gas chromatography (GC) and gas chromatography-mass spectrometry (GC-MS). The reactor was then rinsed using pentane to remove any excess liquid residue. If there was any solid formation, it was carefully scraped off the inner wall of the reactor, weighed and stored.

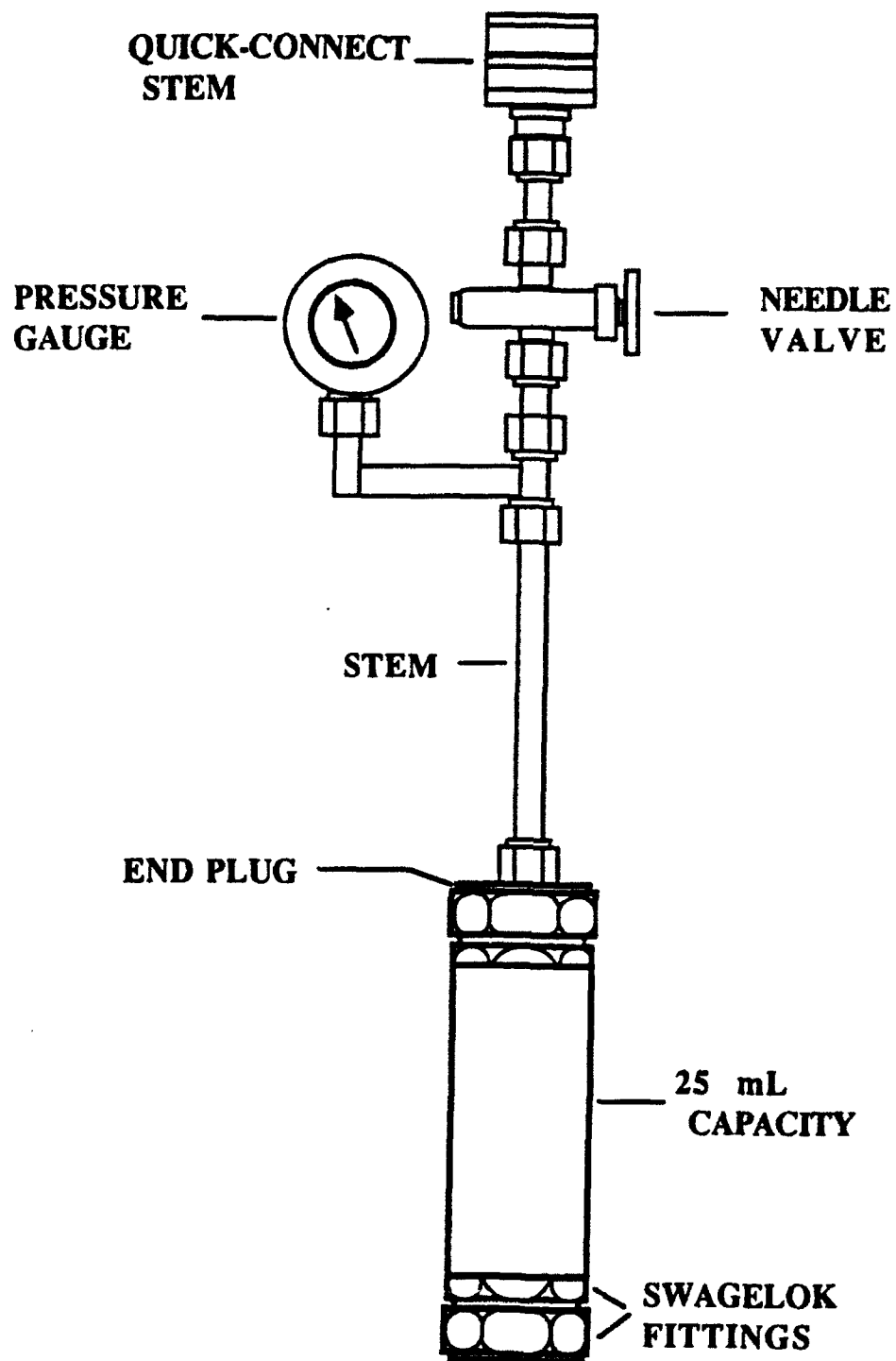


**Figure 1.11.** A schematic diagram of the 25-ml microautoclave (tubing bomb) reactor.

## **Analysis**

The headspace gas samples were analyzed on a Perkin Elmer AutoSystem GC. The analysis utilized a flame ionization detector (FID) and a program with an initial temperature of 30°C for 10 minutes and a ramp of 10°C/min to a final temperature of 200°C. The injection and detector temperature were set at 200°C and 320°C, respectively. The attenuation was set at 4 and the range was set at 20. Standard gases, purchased from Scott Specialty Gases Co., of C<sub>1</sub> to C<sub>6</sub> alkanes, C<sub>2</sub> to C<sub>6</sub> alkenes, isoalkanes, and cycloalkanes were run using the same program. The peaks were identified by comparing retention times on the chromatograms from the sample to the retention times of the standards.

The liquid samples were analyzed by GC and GC-MS. The GC is a Perkin Elmer 8500 GC. This contains a DB17 50% methyl and 50% phenyl polysiloxane, 30m x 0.25 i.d column. The GC-MS is Hewlett Packard 5890 Series II GC with a Hewlett Packard 5971A Mass Selective Detector. This utilizes the same column as the Perkin Elmer 8500 GC. The GC was programmed at an initial temperature of 40°C for 5 minutes and ramped at 4°C/min to a final temperature of 280°C for 10 minutes. The sample was injected onto the column using a split mode in a 0.1- $\mu$ l increment.

The solid deposits were analyzed on a Chemagnetics M-100 NMR using cross-polarization magic-angle-spinning (CPMAS). The conditions which the sample was analyzed were as follows:

contact time	1 msec
pulse repetition rate	1 sec
line broadening	40 MHz
sweep width	14 KHz
<sup>13</sup> C frequency	25.03 MHz
sample spin rate	3.5 KHz

## **RESULTS AND DISCUSSION**

### **Solid Formation**

Thermal stability tests of octane, dodecane, tridecane, and tetradecane have been conducted at four different temperatures: 400°, 425°, 450°, 475°C, at times ranging from 1 to 72 hours. These tests show that as chain length increases the stability of the alkane decreases. Octane, the most stable of the the four compounds, did not show excessive signs of degradation until 450°C, 6 hours, when solids began to form. Dodecane, tridecane, and tetradecane all show degradation to the point of solid formation at 400°C, 48 hours. The reaction temperature, time and amount of deposit produced from the four compounds at each temperature is tabulated in Table 1.4 along with a comparison plot of this data in Figure 1.12.

**Table 1.4.** Summary of deposits produced at specific reaction temperatures and times.

(T,t)		Octane	Dodecane	Tridecane	Tetradecane
400°C	4 hr	none	none		none
	*24 hr	none	none		none
	48 hr	none	0.0200g	0.0182g	0.0370g
	*72 hr	none	0.0850g	0.1832g	0.1634g
425°C	*6 hr	none	none	none	none
	8 hr	none	none		0.0020g
	*12 hr	none	0.0180g	0.0507g	0.0130g
	16 hr	none	0.0539g		0.1550g
	*24 hr	none	0.1943g	0.1626g	0.2360g
450°C	*3 hr	none	0.0026g	0.0123g	0.0039g
	6 hr	0.0103g	0.1229g		0.1197g
	8 hr	0.1077g	0.2627g		0.2370g
	*12 hr	0.1591g	0.3979g	0.2969g	0.3087g
	16 hr	0.2633g	0.5685g		0.4822g
	*24 hr	0.4215g	0.6760g	0.5163g	0.5754g
475°C	1 hr	0.0221g	0.0562g		0.0302g
	*2 hr	0.0879g	0.1124g	0.1538g	0.1315g
	4 hr	0.3529g	0.5574g		0.5752g
	*6 hr	0.5557g	0.7196g	0.7417g	0.5811g

\* Samples analyzed by GC-MS

Note: Selected reactions were done for tridecane at low, intermediate, and high severity thermal stressings. A blank space indicates no experiment at the indicated time.

Analysis of the solid deposits by solid-state CPMAS  $^{13}\text{C}$  NMR was somewhat limited since only samples that produced ~0.2g or greater of solid deposit could be analyzed. This amount of sample was required in order to maintain proper spinning of the sample. The results clearly show a highly aromatic nature in the solids. The intermediately stressed samples, where enough solid deposit was produced to run an NMR, have a small peak upfield from the large aromatic peak. This peak at 30 ppm,  $-\text{CH}_3$ , is most likely a terminal alkyl group attached to the large polyaromatic structure.<sup>16</sup> Figure 1.13 is a solid state  $^{13}\text{C}$  NMR spectrum of the solids produced from an intermediately stressed sample of tetradecane. The terminal methyl group is at ~30 ppm adjacent to the spinning side band. The more severely stressed samples, where significant



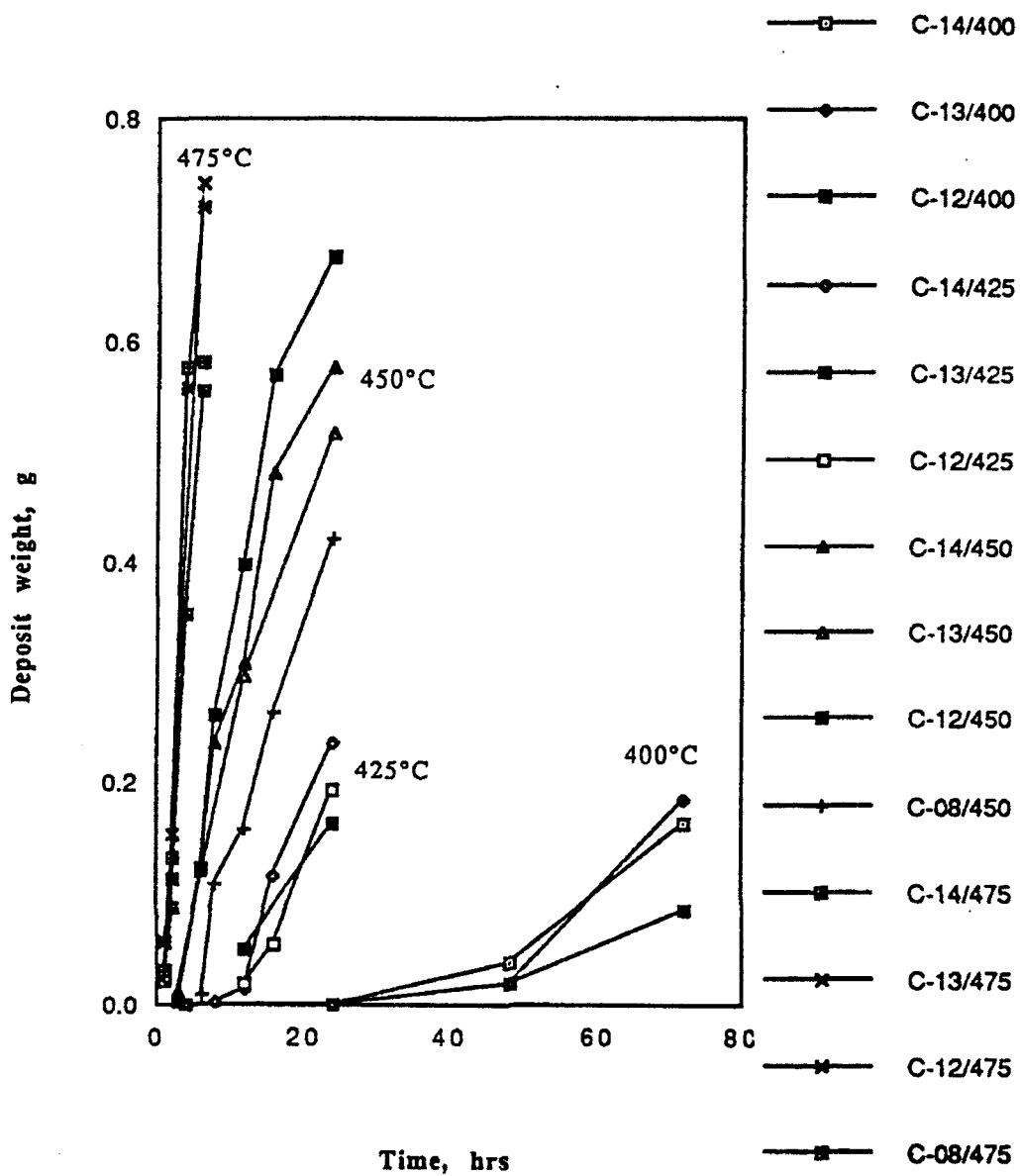


**Figure 1.12.** Rate of solid deposition for C8, C12, C13, C14 at various thermal stressing conditions.

CON, TETRADECANE 450C 8HR CPMAS 7-31-81

FNA, C1445008.M04  
 F08S, 25.035000  
 NA, 10000  
 AC, 10000  
 AL, 512  
 DL, 4096  
 TLB, 19.965  
 PV1, 8.0 us  
 CT, 1000.0 us  
 PD, 1.00 s  
 MJC, 13C  
 TAU, 1.00 s

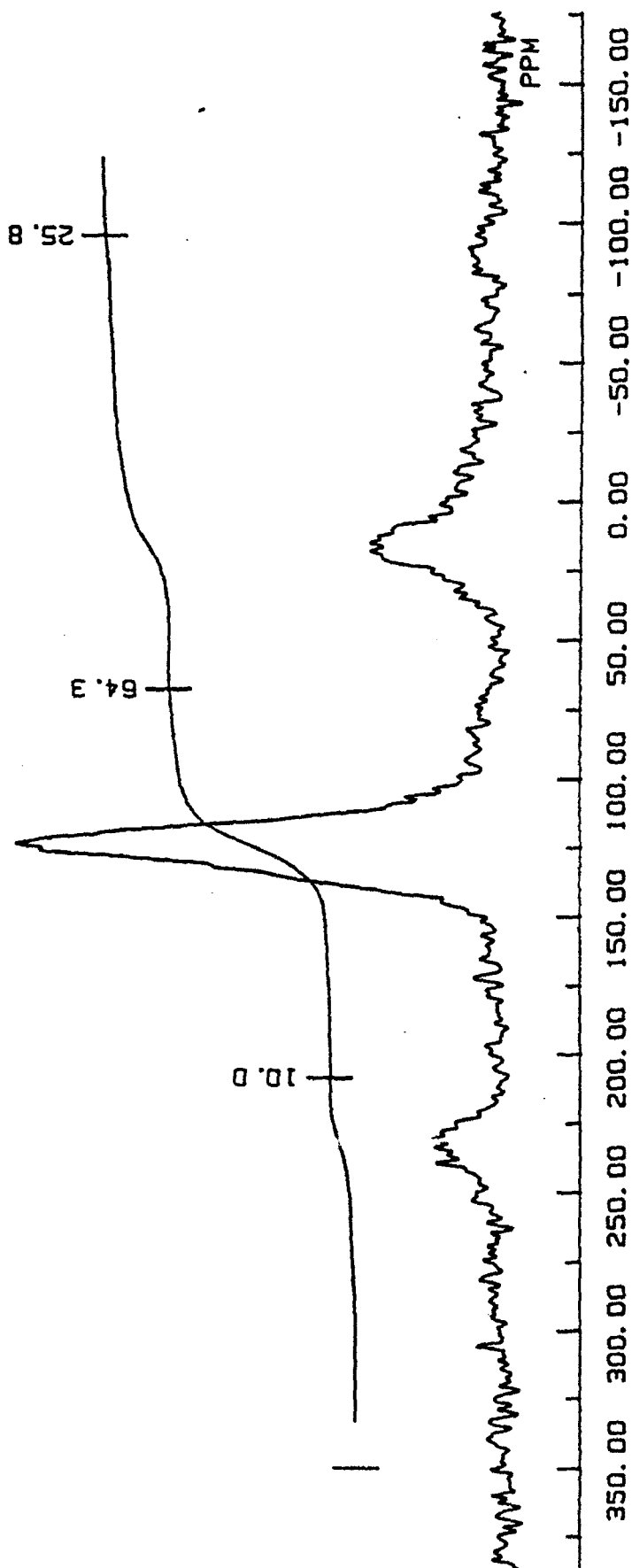
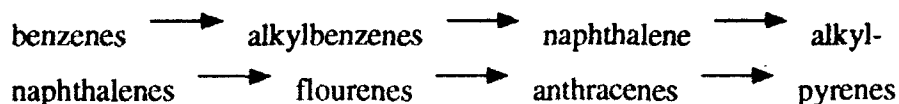


Figure 1.13. Solid State CPMAS  $^{13}\text{C}$  NMR spectrum of the solids produced from tetradecane at 450°C for 8hrs.

amounts of deposits are produced, have two smaller peaks upfield from the large aromatic peak. The aliphatic carbons present,  $-\text{CH}_2\text{CH}_3$  and  $-\text{CH}_3$ , are also most likely terminal alkyl groups attached to the large polyaromatic structures. Figure 1.14 is a solid state  $^{13}\text{C}$  NMR spectrum of the solids produced from a highly stressed sample of dodecane. The  $-\text{CH}_2\text{CH}_3$  and  $-\text{CH}_3$  groups are at  $\sim 45$  ppm and  $\sim 25$  ppm, respectively. Integration of the NMR spectra indicate that as temperature and time increases the aromaticity,  $f_a$ , also increases. These results are tabulated in Table 1.5. The increase in aromaticity is relatively constant with the exception of an octane sample at  $450^\circ\text{C}$ -12 hrs and a dodecane sample at  $475^\circ\text{C}$ -2 hrs. These samples produced less than 0.2g of solid deposit. Analysis of these samples results in a spectrum containing a significant amount of noise. The integration is affected by the noise, resulting in an exaggerated increase in aromaticity.

### **Liquid-phase chemistry**

Analysis by GC-MS of the unstressed model compounds was initially done to ensure that the compounds were in fact pure. Results of this analysis did show that only the specified n-alkane was present in the model compound. Detailed analyses by GC-MS of the liquid products, selected at short, intermediate, and long reaction times, have revealed significant changes in the composition of the liquid as the severity of the stressing increases. These changes are the result of cracking and recombination reactions that later go on to form naphthalene, alkyl naphthalenes, and multicyclic 3-4 ring compounds. The cracking reactions lead to the formation of smaller alkanes and cycloalkanes and, in the cases of the larger chain compounds, alkylbenzenes. The radicals produced are stabilized by hydrogen-abstraction reactions. Recombination reactions lead to the formation of higher molecular weight compounds, such as alkanes larger than the starting compound; other cyclic compounds, such as indenenes and naphthalenes; and multicyclic compounds. Examples of these types of reactions are illustrated in Figures 1.15-1.17. Figure 1.15 is a chromatogram of dodecane, stressed at  $425^\circ\text{C}$ -6 hrs, illustrating cracking and recombination reactions to produce both smaller and larger molecular weight n-alkanes. Figure 1.16 is a chromatogram of octane, stressed at  $450^\circ\text{C}$ -12 hrs, illustrating the production of alkylbenzenes, naphthalene, alkyl naphthalenes. Figure 1.17 is a chromatogram of tetradecane, stressed at  $450^\circ\text{C}$ -24 hrs, illustrating the production of multicyclic 3-4 ring compounds. According to the analysis, the general trend of aromatic compounds formed with increasing severity are:



It is the formation of these polynuclear aromatics (PNA's) that ultimately leads to the formation of solid deposits.<sup>15</sup>

# PENN STATE UNIVERSITY M100-0301

CON: DODECANE 475C 4HR CPMAS 8-13-91

FNA: C1247504.M18  
 F085: 25.035000  
 NA: 10000  
 AC: 10000  
 AL: 512  
 DL: 4096  
 TLB: 28.947  
 PWT: 6.0 us  
 CT: 1000.0 us  
 PD: 1.00 s  
 MJC: 13C  
 TAU: 400.00 ms

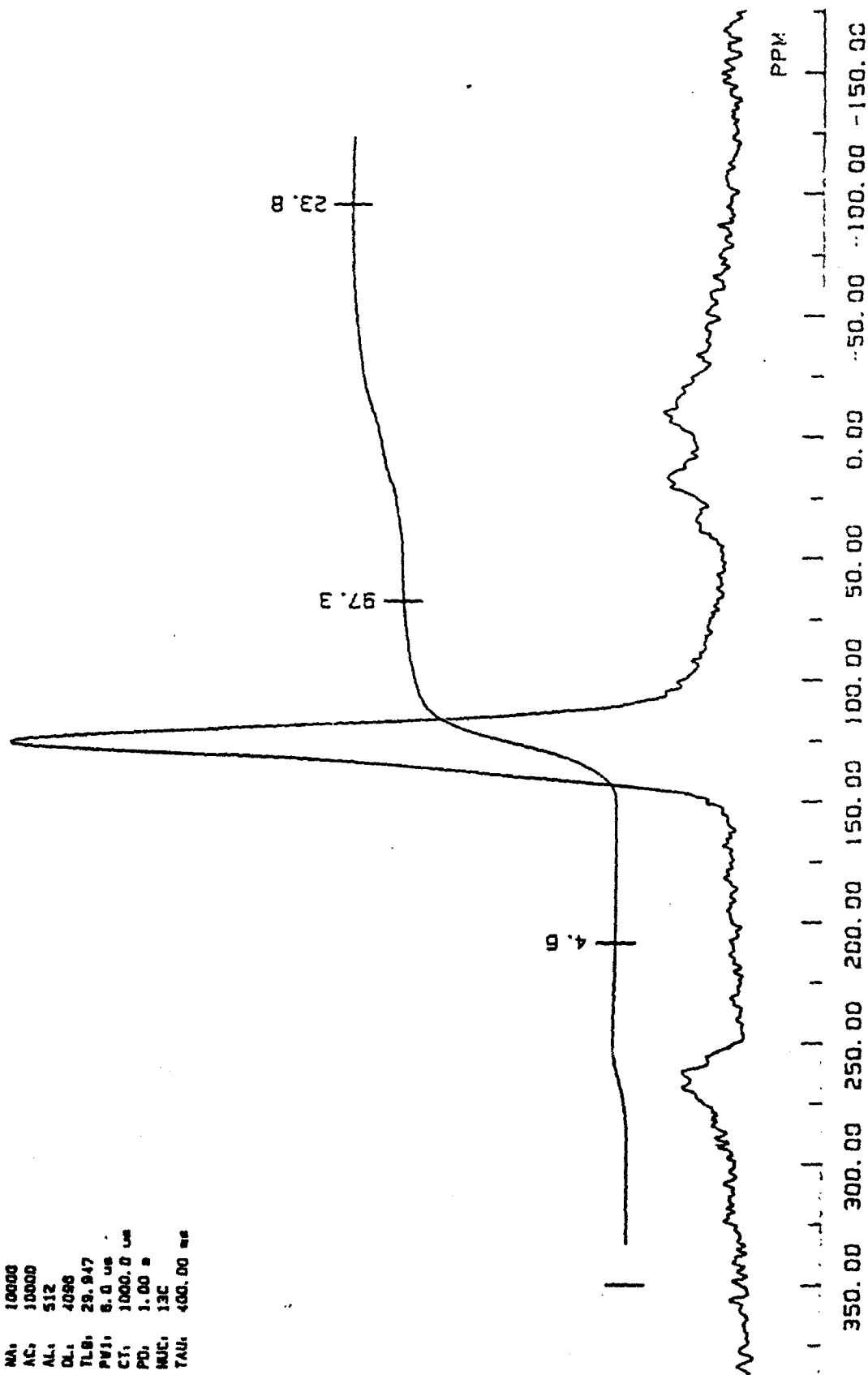


Figure 1.14. Solid State CPMAS <sup>13</sup>C NMR spectrum of the solids produced from dodecane at 475°C for 24hrs.

**Table 1.5.** Aromaticity as a function of rank.

Temp.	time	$f_a$		
		C8	C12	C14
425°C	24 hr		0.79	0.85
450°C	6 hr		0.76	0.82
	8 hr		0.82	0.84
	12 hr	0.83	0.83	0.86
	16 hr	0.81	0.87	0.88
	24 hr	0.82	0.86	0.88
475°C	2 hr		0.88	0.80
	4 hr		0.85	0.85
	6 hr		0.90	0.86

Thermal stressing of octane shows that it is stable at mild stress conditions, 400°C-24 hrs and 72 hrs, 425°C up to 12 hrs, and 450°C up to 3 hrs. At these conditions n-alkanes, specifically C8 and lower, are the major components of the system. The alkylbenzenes are beginning to form at all these conditions. At more severe thermal stressings, 425°C-24 hrs and 450°C-12 hrs, alkylbenzenes are more predominant and become the major components of the system. It is at these conditions where the formation of naphthalene and alkylnaphthalenes is beginning, and either a blackening of the reactor wall occurs or very small amounts of deposit are formed. The liquids produced at extremely severe conditions for octane, 450°C-24 hrs, and 475°C-2 and 6 hrs, contain increased amounts of alkylbenzenes and alkylnaphthalenes and are now beginning to form the multicyclic 3-4 ring compounds. Even though the abundance of the multicyclic compounds is low, it is believed that these are the precursors to solid formation. All of the aromatic compounds formed contain more carbon atoms than the starting material, suggesting that there is a considerable amount of recombination reactions occurring.

Thermal degradation experiments of decane were done by Ronald Copenhaver at Penn State University. Experiments in a nitrogen atmosphere at 400°, 425°, and 450°C for reaction times ranging from 1 to 72 hrs showed moderate degradation producing small quantities of solids. The amounts of solids produced in these experiments are indicated on a comparison plot in Figure 1.18. The amount of solids produced at 400°C and 425°C are lower than the amount of solids produced from C12, C13, and C14. This is to be expected since, as the chain length decreases,

File: D:\DATA\12M10406.D  
Operator: MIKE  
Date Acquired: 6 Aug 91 4:08 pm  
Method File: MIKE.M  
Sample Name: DODECANE 425C 6HR  
Misc Info:  
ALS vial: 1

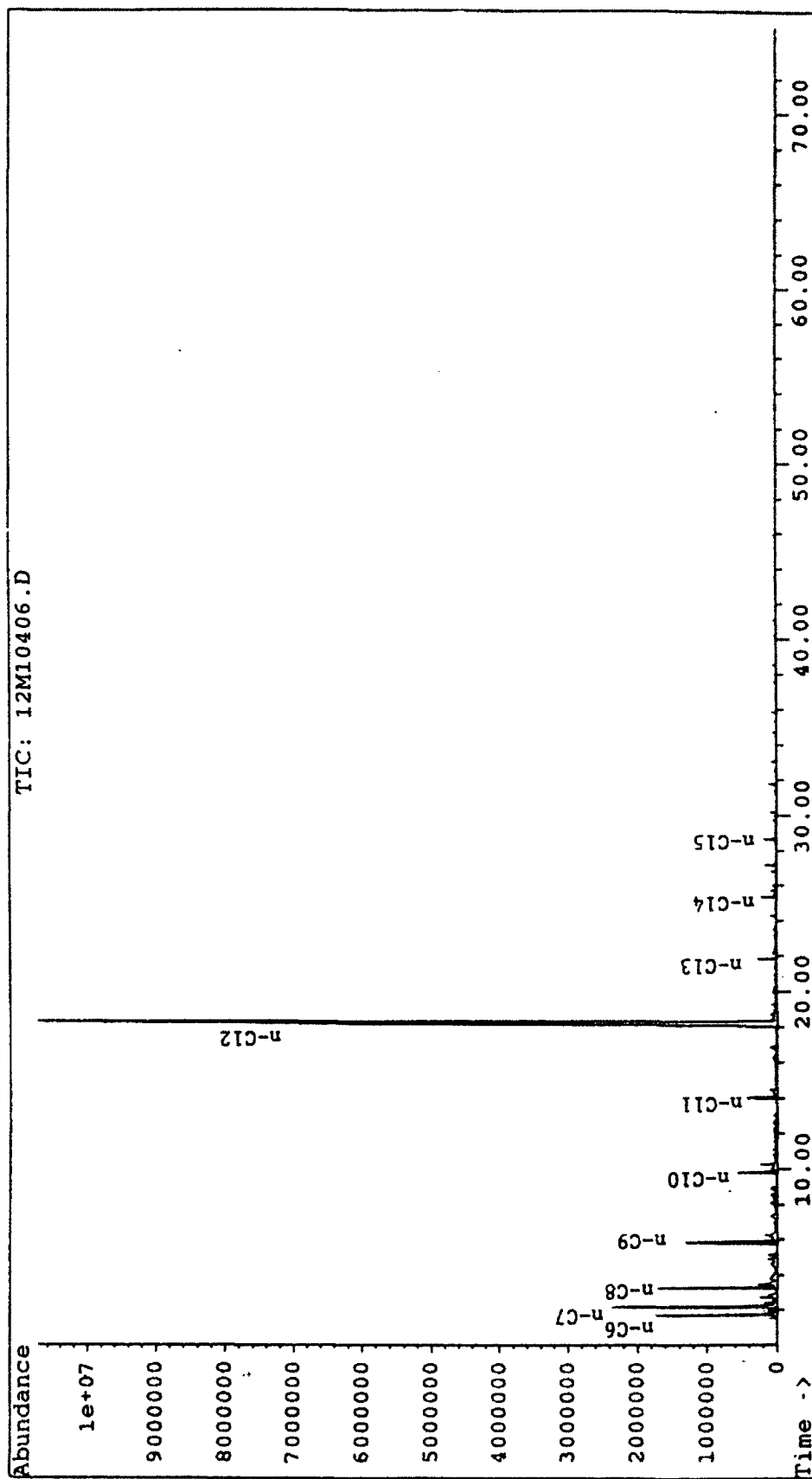


Figure 1.15. GC-MS chromatogram of dodecane stressed at 425°C for 6 hrs illustrating the production of smaller and larger molecular weight n-alkanes.

File: D:\DATA\08M11212.D  
Operator: MIKE  
Date Acquired: 8 Aug 91 7:48 pm  
Method File: MIKE.M  
Sample Name: OCTANE 450C 12HR  
Misc Info:  
ALS vial: 1

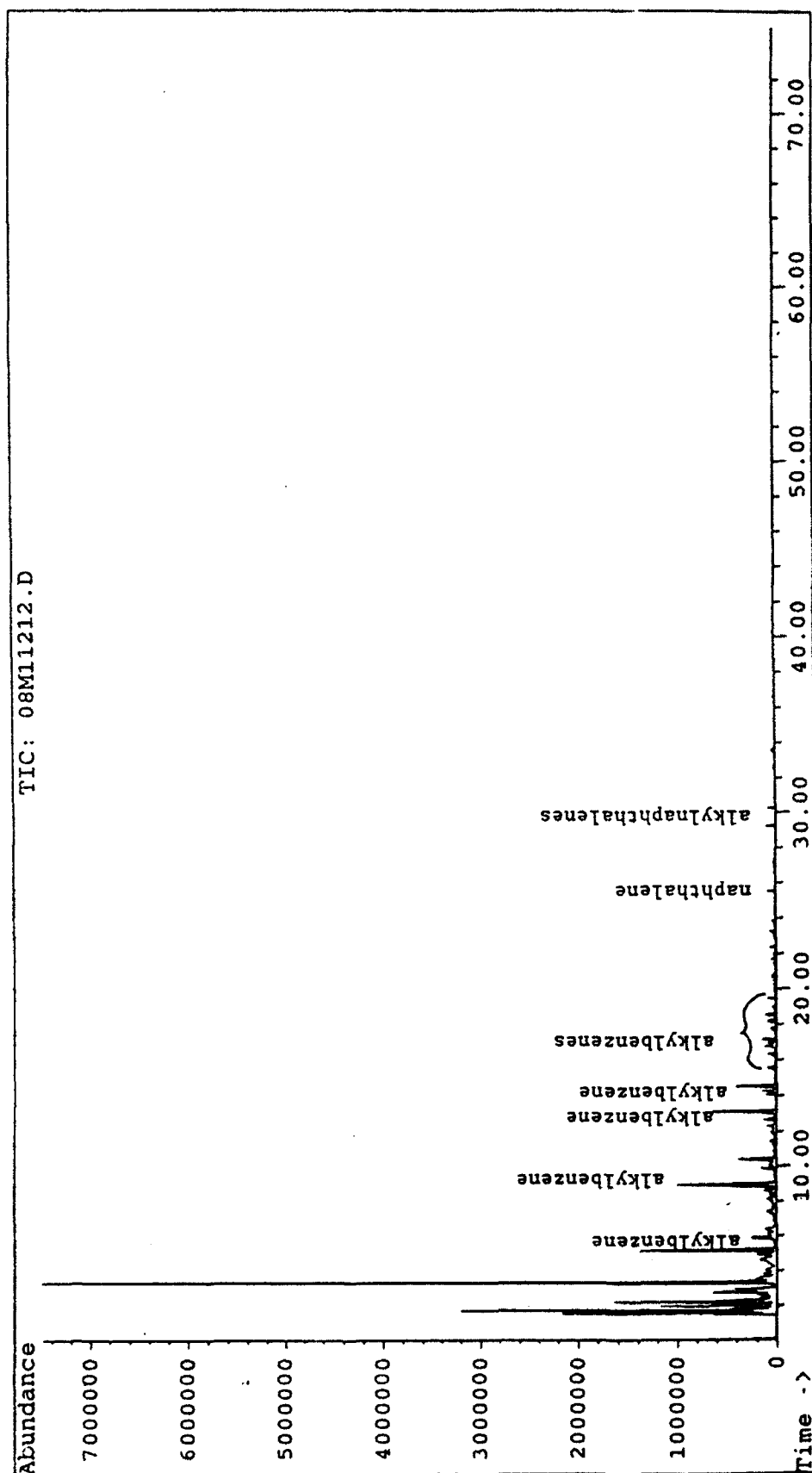


Figure 1.16. GC-MS chromatogram of octane stressed at 450°C for 6 hrs illustrating the production of alkylbenzenes, naphthalene, alkylnaphthalenes.

File: C:\CHEMPC\DATA\C1445024.D  
 Operator: MIKE  
 Date Acquired: 31 Jul 91 9:20 pm  
 Method File: MIKE.M  
 Sample Name: TETRADECANE 450C 24H  
 Misc Info:  
 ALS vial: 1

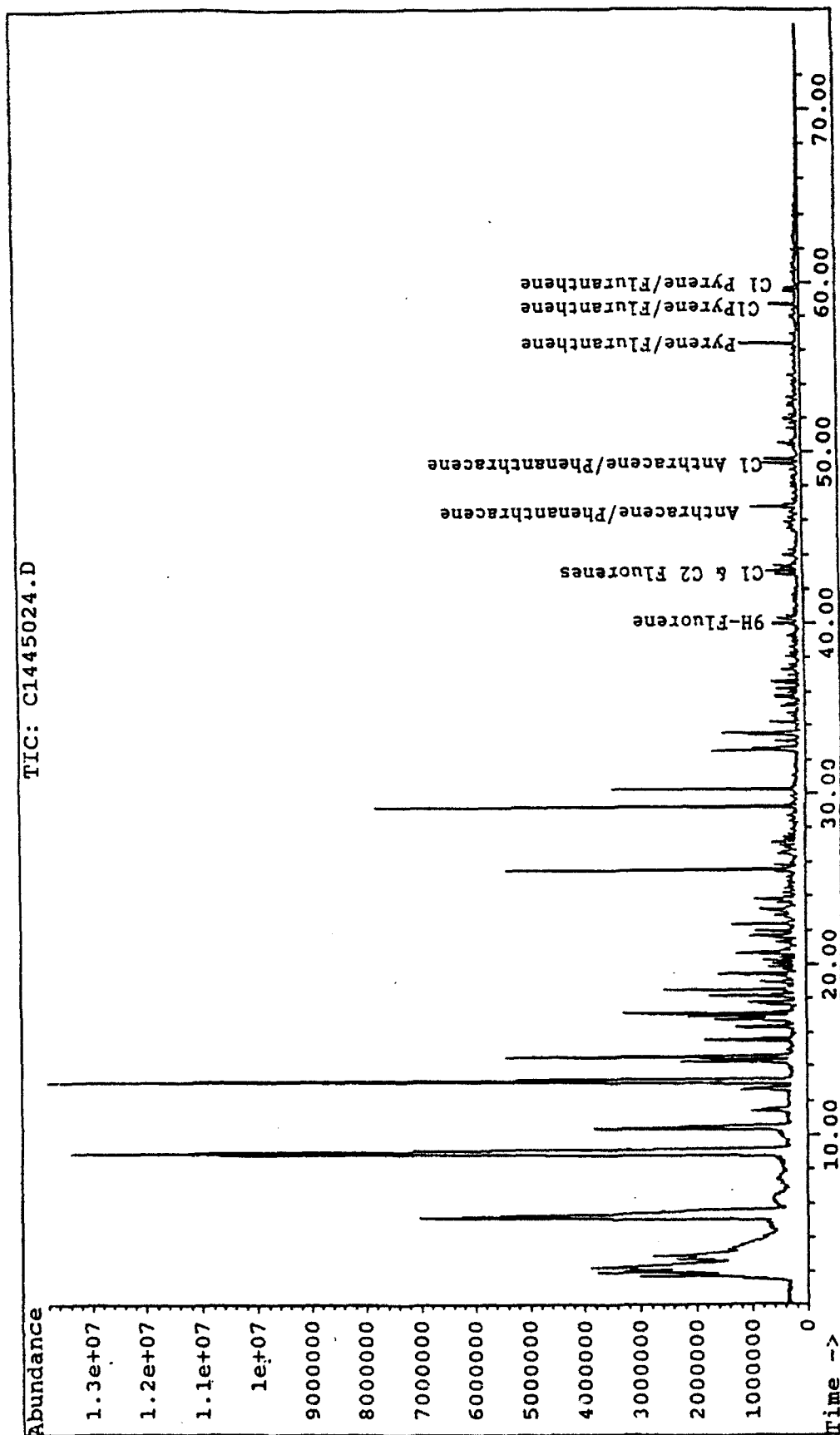


Figure 1,17. GC-MS chromatogram of tetradecane stressed at 450°C for 24 hrs illustrating the production of multicyclic 3-4 ring compounds.



File: D:\DATA\13M11806.D  
Operator: MIKE  
Date Acquired: 11 Feb 92 0:12 am  
Method File: MIKE.M  
Sample Name: TRIDECANE 475C 6HRS  
Misc Info:  
ALS vial: 1

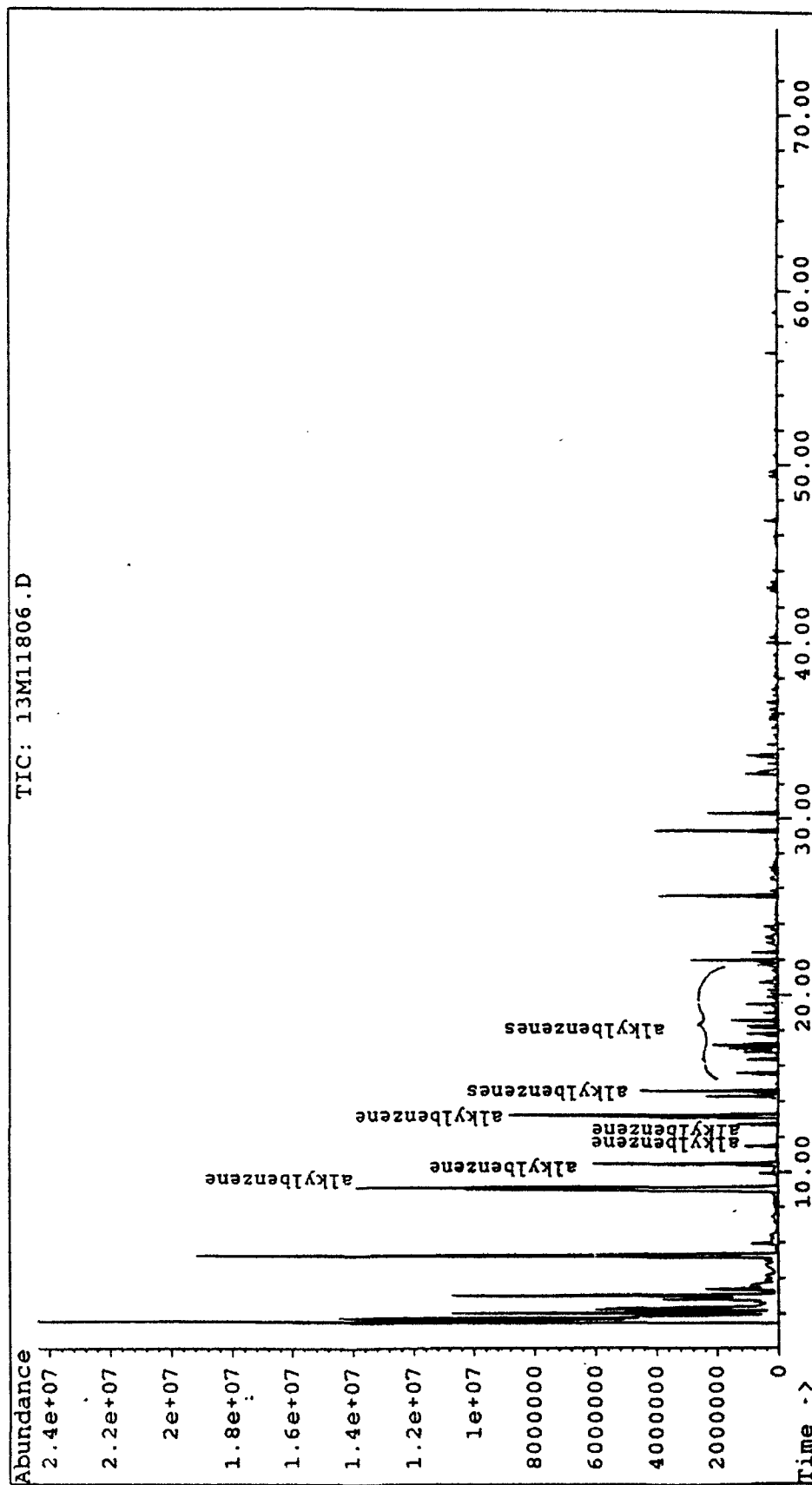


Figure 1.18. GC-MS chromatogram of tridecane stressed at 475°C for 6 hrs illustrating the large proportion of alkylbenzenes produced.

the stability of the compound increases. There is a decrease in solid production going from 24 hrs to 48 hrs at both 400°C and 425°C. This is possibly due to a higher solubility of the solids.<sup>16</sup> The yield of solids produced at 450°C is also lower than the amount of solids produced from C<sub>12</sub>, C<sub>13</sub>, and C<sub>14</sub>, but are formed at the rate at which solids are produced at 475°C. Analysis of liquid product at 450°C-6 hrs by GC-MS indicates that there are primarily alkylbenzenes and alkyl-naphthalenes produced. Analysis of the liquid product at 450°C-24 hrs indicates the presence of alkylbenzenes and alkyl-naphthalenes, and multicyclic 3-4 ring compounds.

Thermal stress tests on dodecane have shown that it is considerably less stable than octane. Dodecane is stable at 400°C up to 24 hrs and 450°C up to 8 hrs. At these conditions, there are n-alkanes, cycloalkanes, and alkylbenzenes being produced with the n-alkanes as the major components. More severe stress conditions, 400°C-72 hrs, 425°C-12 hrs, and 450°C-3 hrs, still have alkanes as the major component. The alkylbenzenes are becoming more predominant and naphthalene and alkyl-naphthalenes are beginning to appear. Deposits are just beginning to form at these conditions. The extremely severe conditions for dodecane, 425°C-24 hrs, 450°C-12 hrs and longer, and 475°C, no longer have n-alkanes but alkylbenzenes as the major component of the system. The naphthalene and alkyl-naphthalene contents continue to increase and the formation of multicyclic 3-4 ring compounds is now evident. The presence of the PNA's results in a large amount of solids being produced.

Results from the thermal stability tests on tetradecane are very similar to those of dodecane. The only condition at which tetradecane was shown to be stable was 400°C-24 hrs. Cracking of tetradecane at this temperature and time only produced smaller n-alkanes. The more severe conditions, 400°C-72 hrs, 425°C-12 hrs and longer, and 475°C-2 hrs, still have n-alkanes as the major component, but also contain alkylbenzenes, naphthalene, and alkyl-naphthalenes. Solid deposits are just beginning to form. The most severe thermal stressing, 450°C-24 hrs, and 475°C-6 hrs, results in alkylbenzenes, naphthalene, and alkyl-naphthalenes being the major components in the system. The amount of multicyclic 3-4 ring compounds present in the system is significant. These conditions yield a large amount of solid deposit.

Tridecane was included in this study to determine if an odd-number carbon compound would react differently than the even-number carbon compounds. Tridecane did not appear to be stable at any condition. At moderately severe conditions, 425°C up to 12 hrs, the lower molecular weight n-alkanes are the major components. There is also a considerable amount of alkylbenzenes present along with lesser amounts of naphthalene and alkyl-naphthalenes. There is either a blackening of the reactor wall or very small amounts of deposits produced at these conditions. At slightly more severe conditions, 400°C-72 hrs and 450°C-3 hrs, the n-alkanes are still major components, the amount of alkylbenzenes and alkyl-naphthalenes is increasing, and there are trace amounts of multi-cyclic compounds present. The deposit formation is slightly increasing. The extremely severe conditions, 425°C-24 hrs, 450°C-12 hrs and longer, and 475°C 2 and 6 hrs, now

produce both lower molecular weight n-alkanes and alkylbenzenes as major components in the system. This is illustrated in Figure 1.19. The formation of the multicyclic 3-4 ring compounds is apparent, along with a large production of solid deposits.

A comparison of the liquid degradation products for the four model compounds surprisingly shows tridecane to be the least stable. At the present we are unsure as to why such a great quantity of alkylbenzenes are produced. It is posited that when the odd carbon chain undergoes homolytic C-C bond cleavage there is an odd-number carbon chain radical produced. If this radical undergoes a recombination reaction, it may cyclize to form an alkylbenzene. These alkylbenzenes can then undergo further recombination reactions to form multicyclic compounds. The formation of these compounds is believed to be the precursors that lead to solid formation. Figure 1.20 illustrates the progression of degradation in the liquid products.

### **Gas Analysis**

The headspace gas samples from octane, dodecane, tridecane, and tetradecane were analyzed on a Perkin Elmer AutoSystem gas chromatograph. For the purpose of identifying the gases, the retention times of C<sub>1</sub> to C<sub>6</sub> alkanes, C<sub>2</sub> to C<sub>6</sub> alkenes, various isoalkanes (isobutane, 2-methyl butane, 2,2-dimethylpropane, 2,2-dimethylbutane, 2-methylpentane, and 3-methylpentane), and various cycloalkanes (cyclopentane, methylcyclopentane, cyclohexane, and methylcyclohexane) were identified from the standards purchased from Scott Specialty Gases Co. The results of the identification of the sample gases analyzed are shown in Table 1.6.

The three major components found in the gas analyses were methane, ethane/ethylene, and propane. Ethane and ethylene are reported as one peak because they were not able to be separated on the column used. The ethane/ethylene was the major component of the gas samples, followed by slightly lesser or equal concentrations of methane and propane. The high concentration of ethane/ethylene suggests that in the initial stages of cracking, beta-bond scission predominated. The gas composition remains relatively constant throughout the various thermal stressings as shown in Figure 1.21. This is a comparison of three chromatograms, octane, dodecane, and tetradecane, illustrating that the gas composition remains relatively constant. The product gases that tend to vary more than other product gases are butane (1) and hexane (2).

### **Conclusion**

It has been shown that as the chain length increases, the thermal stability of the compound decreases. Octane, the most stable of the model compounds studied, did not form deposits until 450°C. Dodecane, tridecane, and tetradecane were all considerably less stable and formed deposits at 400°C. There are several reactions that occur at different temperatures and times. Cracking reactions are predominant for the mild reaction conditions forming lower molecular weight n-alkanes. As the thermal stressing conditions became more severe, there are cyclization and dehydrogenation reactions occurring. These reactions lead to the formation of aromatic

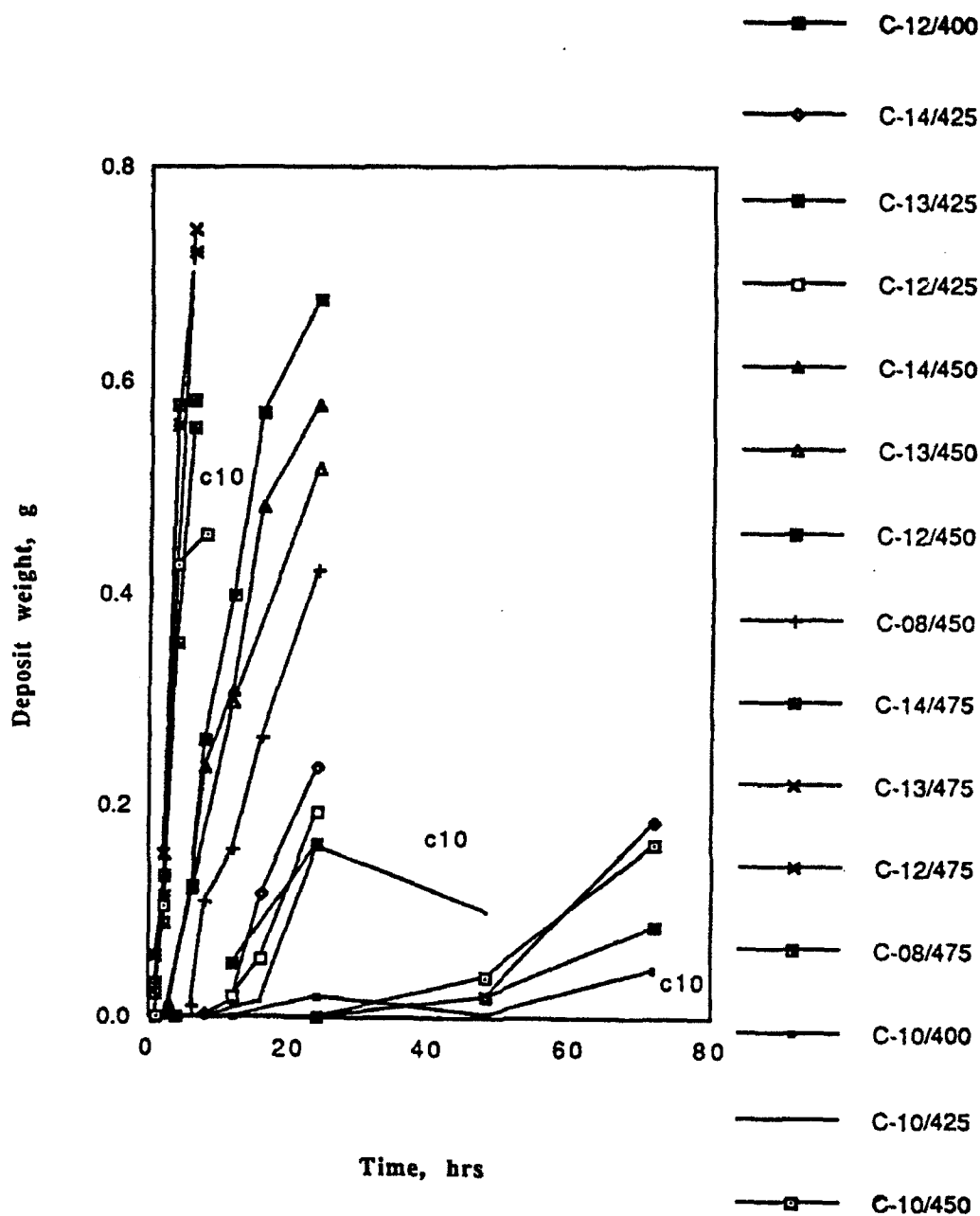


**Figure 1.19.** Comparison of the rate of solid deposition for C<sub>10</sub> to the model compounds at various thermal stressing conditions.

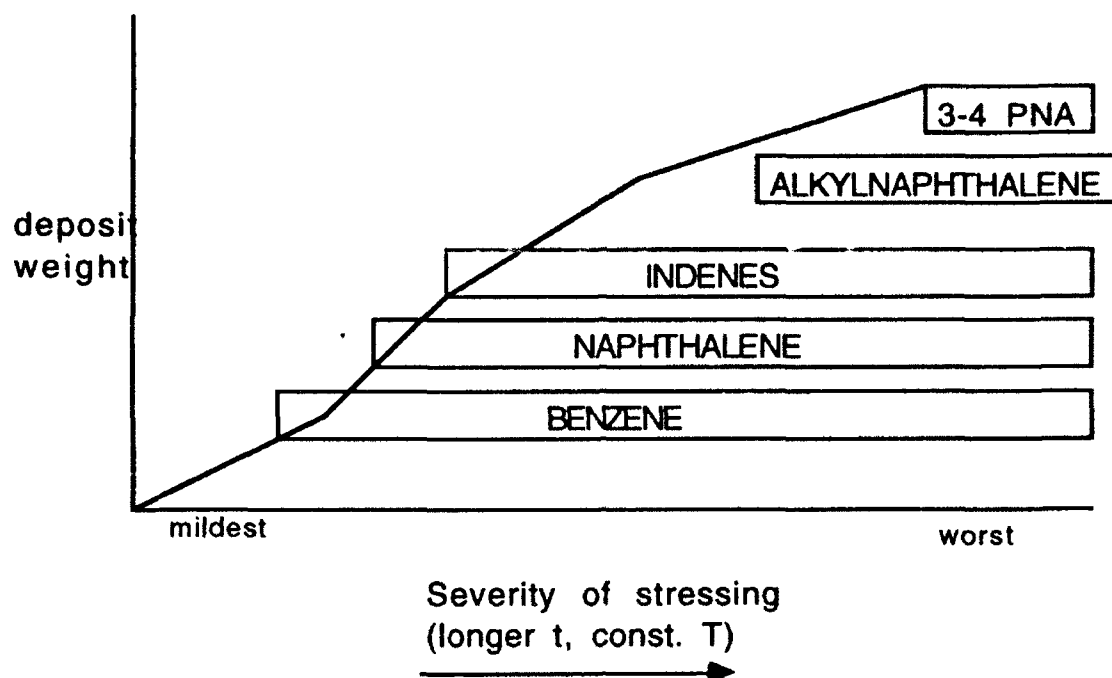


**Figure 1.20.** Progression of degradation in the liquid products.

**Table 1.6.** Gas products identified from the thermal stressing of model compounds C<sub>8</sub>, C<sub>12</sub>, C<sub>13</sub>, and C<sub>14</sub>.

Retention Time (min)	Compounds
1.4-1.6	Methane
1.7-1.9	Ethane + Ethylene
2.3-2.5	Propane
2.6-2.8	Propylene
3.1-3.3	iso-Butane
3.8-4.1	n-Butane
4.5-4.7	1-Butene
8.9-9.1	2,2-dimethylpropane.
10.8-11.0	n-Pentane
13.4-13.6	Cyclopentane
13.9-14.1	2,2-dimethylbutane
15.4-15.5	2-methylpentane
15.7-15.8	3-methylpentane
16.3-16.4	n-Hexane
16.9-1.70	Cyclohexane
19.5-19.6	Methylcyclohexane

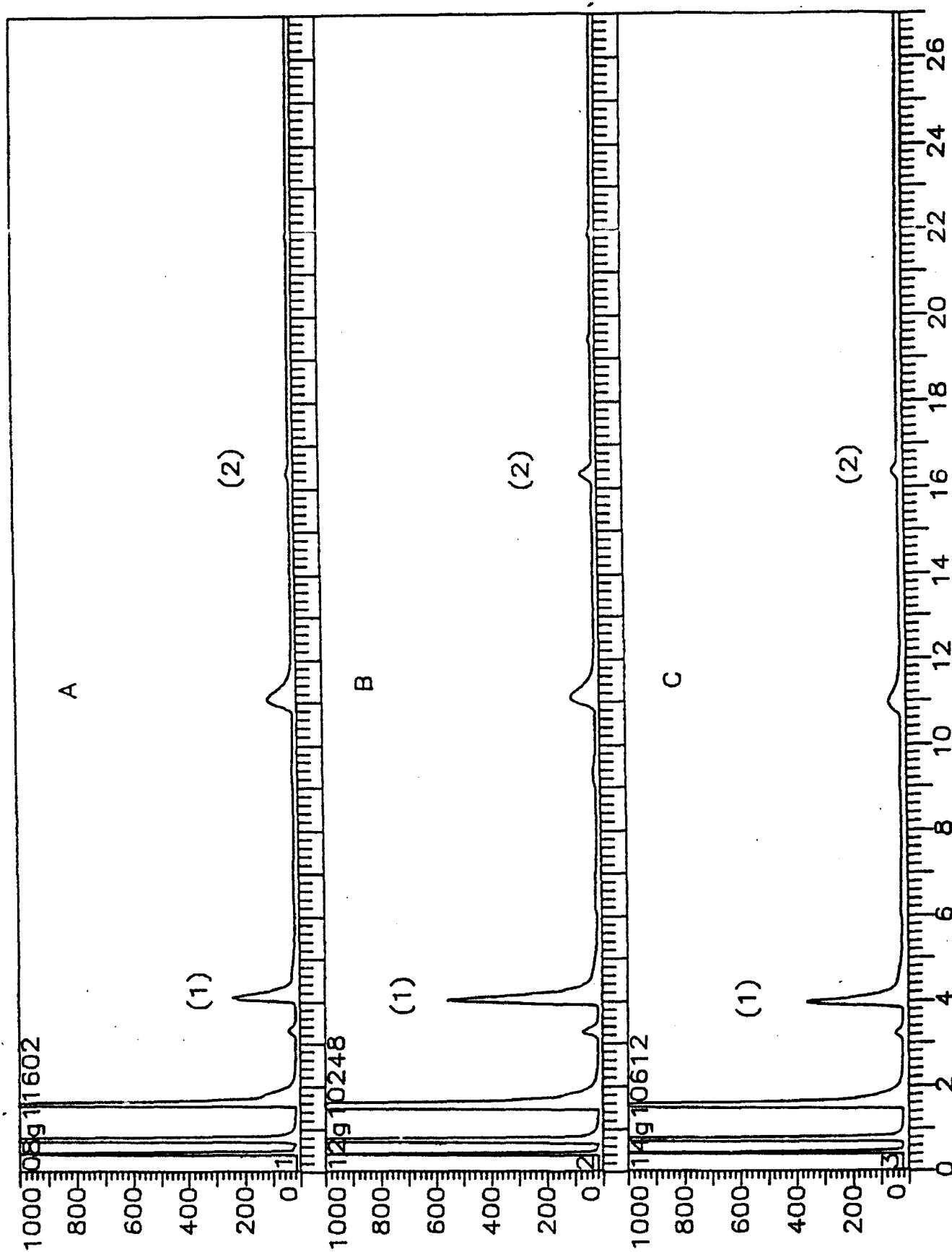


**Figure 1.21.** Comparison of chromatograms octane 450°C for 2 hrs (A), dodecane 400°C for 48 hrs (B), and tetradecane 425°C for 12 hrs (C).

compounds such as benzene and alkylbenzenes. The extremely severe conditions have a considerable amount of recombination reactions occurring to produce large aromatic products, multicyclic 3-4 ring compounds, that have a greater carbon number than the starting material. When aromatic compounds such as naphthalene and larger are not present in the sample, there is usually a blackening of the reactor wall but no deposit is obtained. To get even minimal deposit, alkylnaphthalenes must be present. In the cases where substantial deposit is obtained, multicyclic 3-4 ring compounds are identified in the sample.

## References

1. Marteney, P.J., Spadaccini, L.J. *Journal of Engineering for Gas and Turbine Power*, **108**, 648, 1986.
2. Krazinski, J.L., Vanka, S.P. Development of a Mathematical Model for the Thermal Decomposition of Aviation Fuels, Wright Research and Development Center, Final Report for period Sept. 88 - Dec. 89, WRDC-TR-89-2139.
3. Mills, J.S., Edwards, F.R. The Thermal Stability of Aviation Fuel, Shell Research Limited, Thornton Research Centre, Chester, UK.
4. TeVelde, J. Spadaccini, L.J., Szetela, E.J., Glickstein, M.R., Thermal Stability of Alternative Aircraft Fuels, AIAA-83-1143, 19th Joint Propulsion Conference, June 27-29, 1983, Seattle, Washington.
5. Roquemore, W.M., Pearce, J.A., Harrison III, W.E., Krazinski, J.L., Vanka, S.P. PREPRINTS, *Div. of Petrol. Chem., ACS*, **34**(4), 841, 1989.
6. Chen, N.Y., Garwood, W.E. *Ind. Eng. Chem. Process Des. Dev.*, **17**(4), 513, 1978.
7. Giovanetti, A.J., Szetela, E.J., Long Term Deposit Formation in Aviation Turbine Fuel at Elevated Temperature, AIAA-86-0525, 24th Aerospace Sciences Meeting, January 6-9, 1986.
8. Song, C., Eser, S., Schobert, H.H., Hatcher, P.G. *Am. Chem. Soc. Div. Pet. Chem. Prepr.*, **37**, 540, 1992.
9. Song, C., Hatcher, P.G. *Am. Chem. Soc. Div. Pet. Chem. Prepr.*, **37**, 529, 1992.
10. Reddy, K.T., Cernansky, N.P. *J. Propulsion*, **5**(1), 6, 1989.
11. Reddy, K.T., Cernansky, N.P. *Energy & Fuels*, **2**, 205, 1988.
12. Hague, E.N., Wheeler, R.V., *Fuel and Science in Practice*, **8**(12), 585, 1929.
13. Domine, F., *Energy and Fuels*, **3**, 92, 1989.
14. Appleby, W.G., Avery, W.H., Merrbott, W.K., *J. Am. Chem. Soc.*, **69**, 2783, 1947.
15. Song, C., Peng, Y., Jiang, H., Schobert, H.H. *Am. Chem. Soc. Div. Pet. Chem. Prepr.*, **37**, 484, 1992.

16. Eser, S., Jiang, H., Hatcher, P.G., Copenhaver, R.C., Schobert, H.H. Compositional Factors Affecting Thermal Degradation of Jet Fuels, Technical Progress Report 42-3462-TPR-2, The Pennsylvania State University, December 1989.
17. Eser, S., Song, C., Schobert, H.H., Hatcher, P.G., et. al. Compositional Factors Affecting Thermal Degradation of Jet Fuels, Annual Progress Report, The Pennsylvania State University, June 1990.

#### ***Activity 4. Mechanisms of PAH and Solid Formation During Thermal Degradation of Jet Fuels***

##### **Introduction**

Deposit formation during fuel degradation in a low temperature regime ( $<300^{\circ}\text{C}$ ) has been generally attributed to autoxidation, but pyrolysis predominates at high temperatures<sup>1,2</sup>. Much previous work has been done at low temperatures, but the future high-performance jet aircraft requires jet fuels thermally stable at high temperatures<sup>3,4</sup>. In a companion paper we have reported on the thermal degradation behavior of petroleum- and coal-derived jet fuels at high temperature<sup>5</sup>. There is little information on the mechanisms of solid formation from jet fuels and relevant hydrocarbons. In this report, we will focus on the mechanistic aspects of pyrolytic fuel degradation in terms of the formation of polycyclic aromatic hydrocarbons (PAH) and solid deposits. To develop a fundamental understanding, we examined the fuel degradation chemistry by using a number of model compounds. Based on the spectroscopic analyses of liquid and solid products from jet fuels and model compounds, the possible mechanisms for PAH and solid formation are proposed.

##### **Thermal Degradation and Solid Formation**

In general, hydrocarbon pyrolysis is characterized by the production of light molecules on the one hand, and the formation of heavier materials on the other hand. For evaluation of thermal stability and solid-forming tendency of hydrocarbon fuels, Figure 1.22 shows the extents of liquid depletion and formation of gas and solids from a number of model compounds as well as petroleum-derived JP-8P and coal-derived JP-8C jet fuels (5 ml sample in a 25-ml stainless steel reactor) stressed at  $450^{\circ}\text{C}$  for 4 hours under 0.7 MPa (100 psi) UHP-grade  $\text{N}_2$ . Long-chain paraffins such as n-tetradecane and n-decane, which are among the predominant components in all the petroleum-derived jet fuels<sup>5,6</sup>, underwent significant decomposition reactions, as reflected by the substantial gas formation. Considerable solid formation was observed from n-butylbenzene (n-BB), n-tetradecane (n-C<sub>14</sub>), n-decane (n-C<sub>10</sub>) and JP-8P, with the highest amount of solid produced from n-BB, as shown in Figure 1.22. In distinct contrast to this, the liquid depletion was



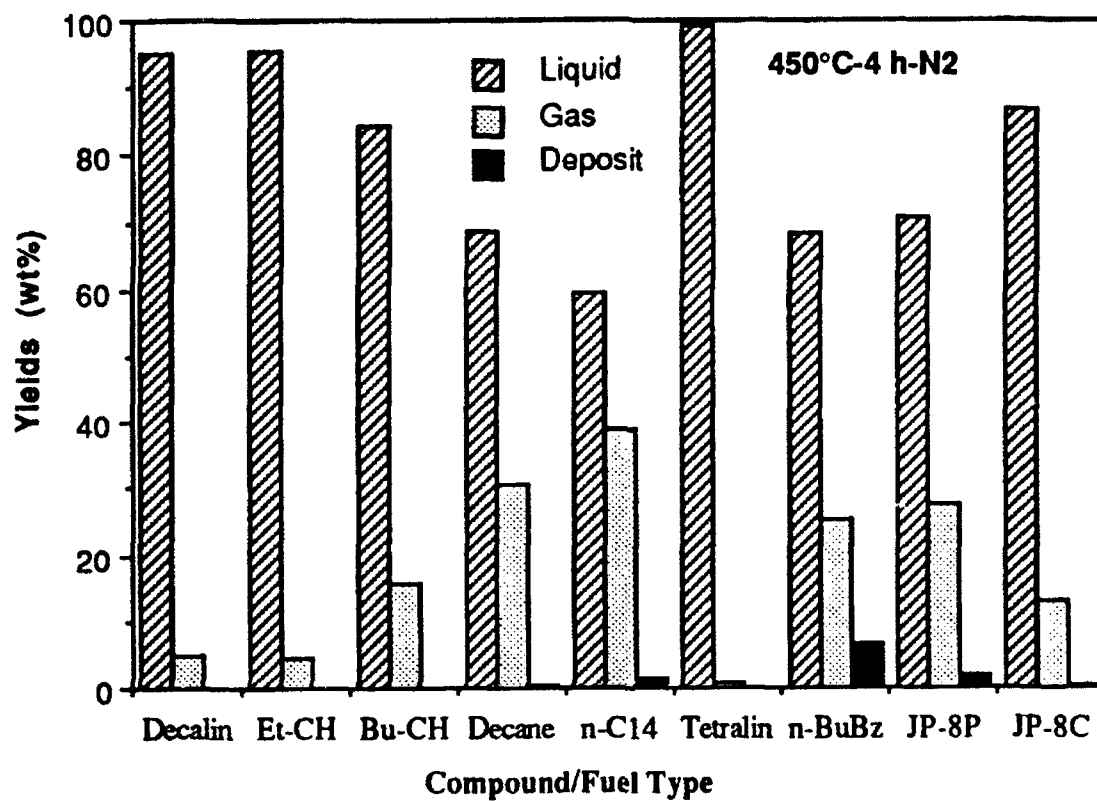


**Figure 1.22.** Decomposition of model compounds and jet fuels at 450°C for 4 h in N<sub>2</sub>

much less and there was no solid formation from tetralin and cycloalkanes including decalin, ethyl- and n-butylcyclohexane (Et-CH and Bu-CH in Figure 1.22) at 450°C for 4 hours. The cycloalkanes and tetralin are the major components of JP-8C jet fuel<sup>5-7</sup>.

As described later, reactive alkylaromatics appear to be important intermediates for solid formation from jet fuels, and n-BB is a typical model of such alkylaromatics. Figure 1.23 shows the effect of residence time at 450°C on yields of solids from JP-8P, JP-8C and n-BB. Solid formation begins to be observed or becomes measurable after 1 hour stressing of n-BB, 2.5 hours for JP-8P and 4 hours for JP-8C. This time period can be considered as an induction period, during which the precursors to solids are formed and accumulated. The longer induction period and lower solid formation from JP-8C can be attributed to its higher contents of cycloalkanes and tetralins<sup>6</sup>. The order of yields of solids produced at 450°C were n-BB >> JP-8P >> JP-8C for 1-4 hours stressing, and n-BB > JP-8P >> JP-8C for 4-8 hours stressing. Surprisingly, the solid yields from n-BB stressed for over 5 hours reached a steady state; solid yields from 8-16 hours stressing of JP-8P stressing approached to, and subsequently exceeded those from n-BB.

### Mechanisms of Solid Formation

In spite of numerous investigations, little is known about the reaction mechanisms for solid formation from jet fuels. From their pioneering work on n-dodecane stressing using flow apparatus (JFTOT), Hazlett et al.<sup>2</sup> attributed the jet fuel degradation and solid formation to different reactions in three temperature regimes: autoxidation at <260°C, decomposition of oxygenated products at intermediate temperatures between 290-480°C, and pyrolysis at > 480°C. Their results apply to the short-residence time (28 seconds) degradation. The present results, however, are pertinent to the long-duration pyrolytic degradation characteristics of fresh and stressed fuels at the "intermediate" temperatures, the study of which has become more important for developing advanced jet fuels<sup>3,4</sup>.

The following observations provided a basis for the mechanisms proposed in this work. First, there is an induction period for deposit formation from jet fuels and model compounds (Figure 1.23). The length of this period was n-BB << JP-8P < JP-8C. Second, identification of liquid products from decane and tetradecane and JP-8P stressed at 450°C for 4 hours revealed that decomposition of long-chain paraffins is accompanied by cyclization, dehydrogenation and condensation reactions to form cyclic alkanes and alkenes, alkylbenzenes and PAHs. Third, we have found from <sup>13</sup>C NMR analysis of thermally stressed jet fuels that solid deposition becomes remarkable when the content of aromatic carbon in the liquids from JP-8P increased to a certain degree, as shown in Figure 1.24. This fact in combination with GC-MS data indicates that the solids are formed from aromatic compounds. Finally, solid state CPMAS <sup>13</sup>C NMR and FT-IR of solid deposits formed from decane, n-BB and JP-8 and long-term stressing of n-butylcyclohexane

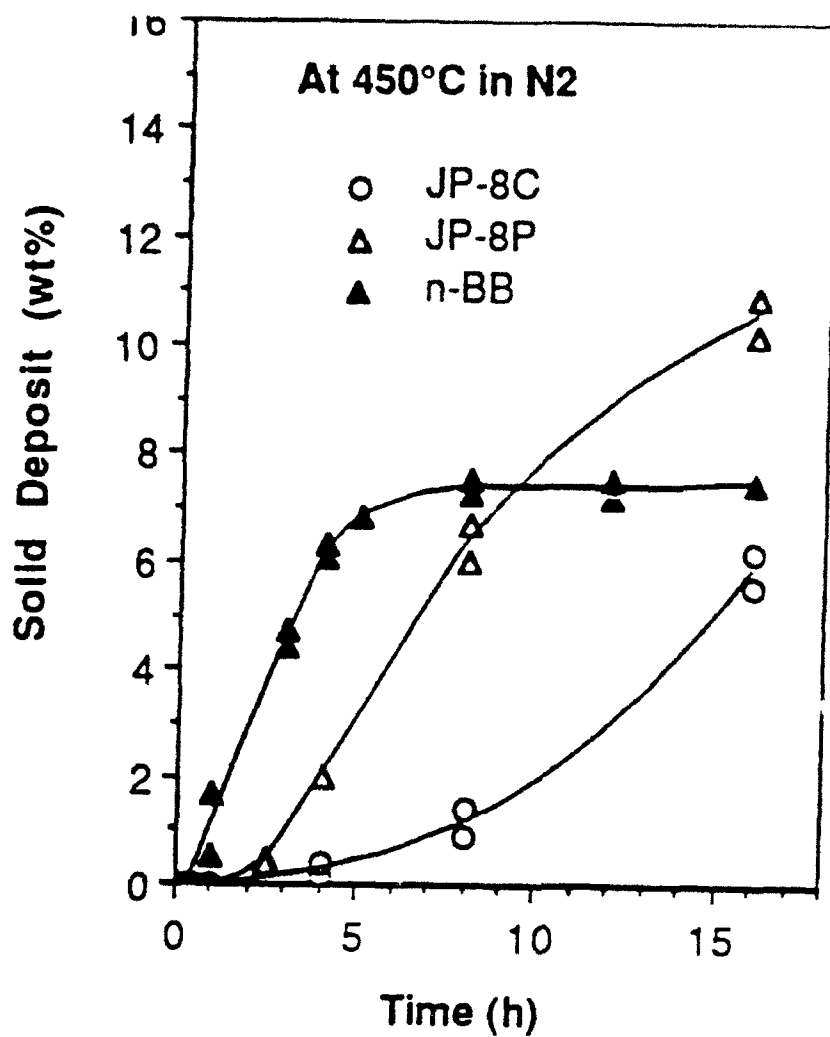


**Figure 1.23** Solid formation from n-BB, JP-8P and JP-8C at 450°C

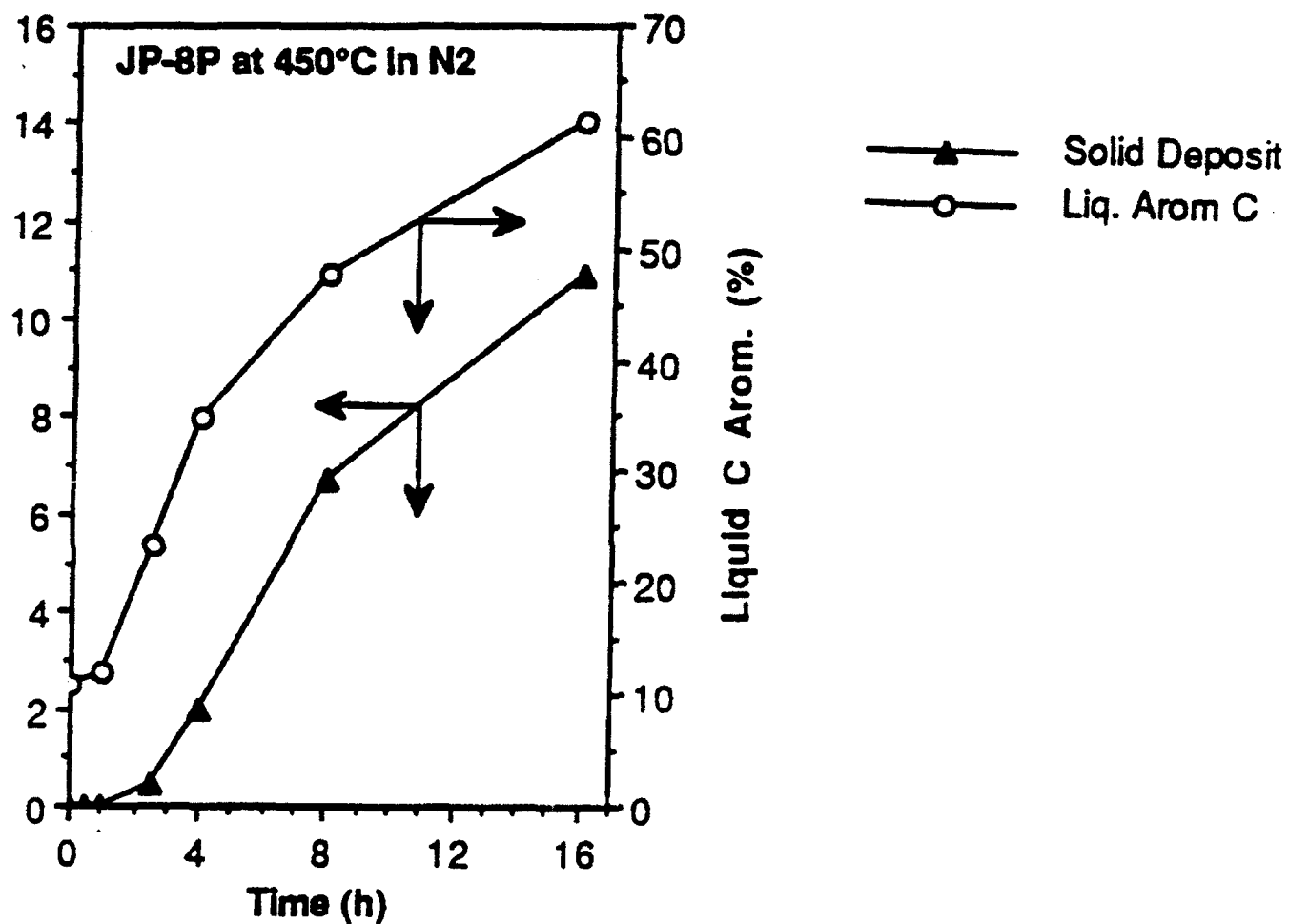


**Figure 1.24.** Relation between solid deposition and liquid aromaticity during JP-8P stressing.

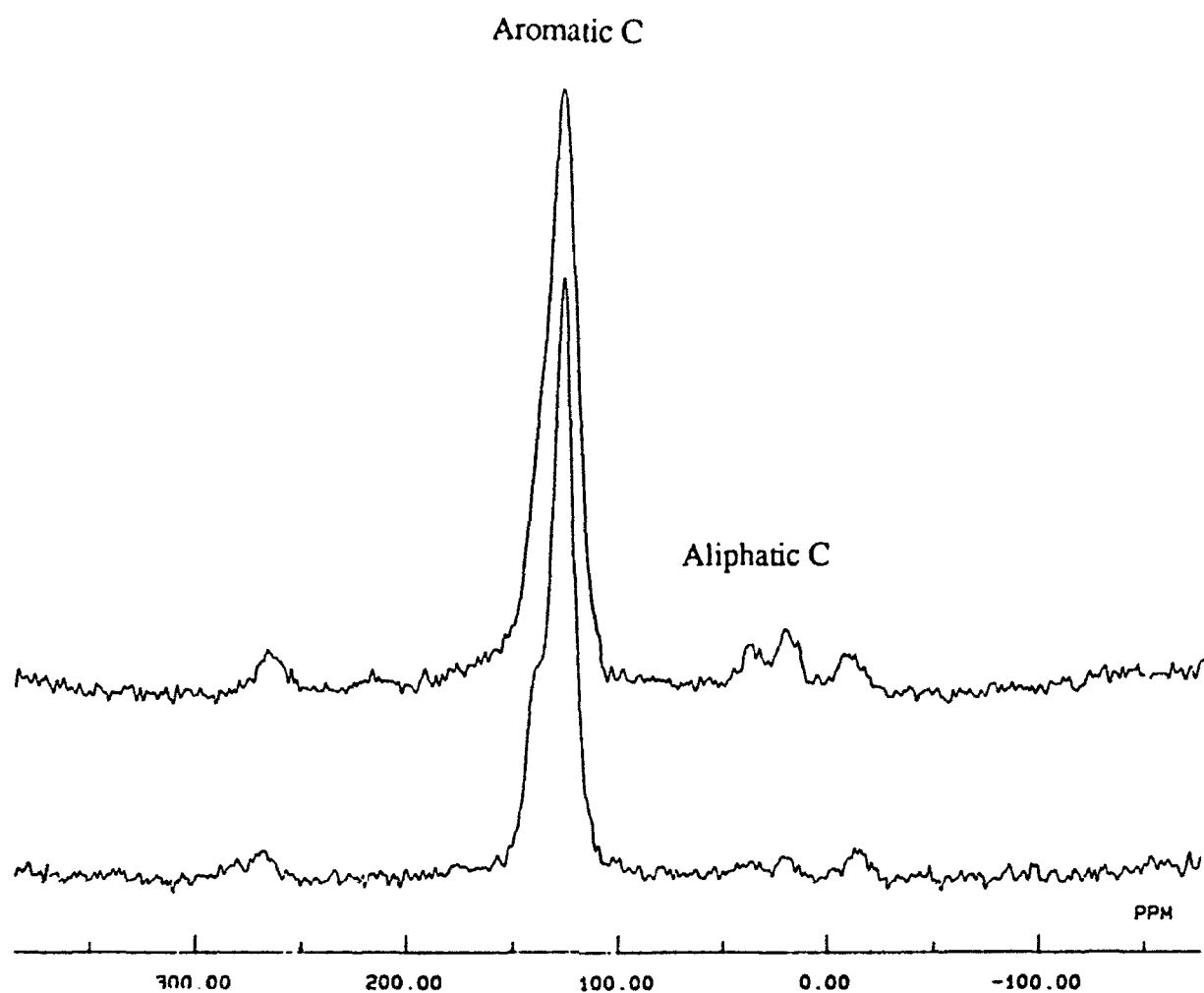
and decalin<sup>7</sup> have clearly indicated the highly aromatic nature of the deposits. As an example, Figure 1.25 shows the NMR spectra of solid deposits produced from n-BB and n-decane.

Figure 1.26 shows the proposed mechanisms for the formation and growth of solids during pyrolytic degradation of jet fuels. The mechanism 1 represents the overall reaction sequences for solid formation from long-chain paraffins. This mechanism involves as the first step cyclization to form alkylcyclohexenes, which undergo subsequent dehydrogenation to form alkylbenzenes. Some reactive alkylbenzenes then start to generate polyaromatics via ring condensation, coupling and dehydrogenation. Probably the induction period is dominated by the fuel decomposition and the reactions from step A to C, during which the precursors to the solids are formed and accumulated. Further growth by condensation, coupling or dehydrogenation of some PAHs, which are the so-called precursors, begins to create polycondensed aromatics (step C to D) which are sparingly soluble or insoluble and tend to precipitate or deposit on the wall. The precipitated or deposited species can undergo further condensation reactions, and the nucleation or agglomeration of such species will give rise to large-sized particles or deposits.

The mechanism 2 in Figure 1.26 should apply to solid-forming reactions when there are considerable amounts of aromatics formed or originally present as in the case of stressing n-BB. The data in Figure 1.24 imply that as the aromaticity of the stressed jet fuels increased above a certain extent, the solid formation becomes faster. The aromatics in Eq. 2 include not only monoaromatics but also polycyclic aromatics.  $R\cdot$  in Eq. 2 can be aliphatic or aromatic radicals. This mechanism would account for faster growth of PAHs, and consequently faster solid formation rate from highly degraded fuels. An additional mechanism for long-term stressing in the presence of formed solids is the reaction between radicals and solids, which contributes to the thickening of the deposits on the surface or to an increase in particle size, Eq.3. Optical microscopy revealed that the microstructure of the solids (from JP-8P, JP-8C, model compounds) also depends on the type of feedstock and reaction conditions, and on the relative contribution of liquid-phase and gas-phase reactions<sup>8,9</sup>.

### Mechanisms of PAH Formation

With the desire to clarify the details of the solid-forming chemical reactions of Eqs. 1-3, we now turn to discussing mechanisms for PAH formation. Numerous PAHs have been detected in liquids from jet fuels, n-decane and n-tetradecane and n-BB stressed at 450°C<sup>5-7,10</sup>. Figure 1.27 shows the GC-MS results for liquids from n-BB at 450°C for 4 hours. Most of the PAHs shown in Figure 1.27 were also found in lower concentrations in stressed n-tetradecane, n-decane and jet fuels. Figure 1.28 shows the possible mechanisms for the formation of a number of PAHs, which were proposed based on the identified products and intermediates. In general, radicals from alkylaromatics play an important role in the PAH formation. The C-C bond cleavage of



**Figure 1.25.** Cross-polarization magic angle spinning  $^{13}\text{C}$  NMR of solid deposits from n-decane (top, 450°C-6 h) and from n-butylbenzene (bottom, 450°C-4 h).

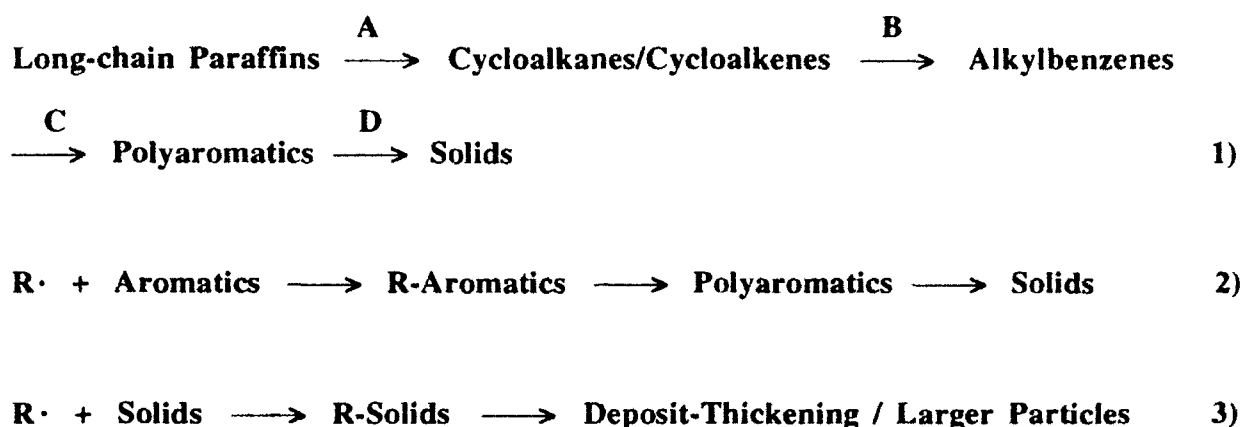


**Figure 1.26.** Possible mechanisms for solid formation from jet fuels

alkylbenzenes can occur readily to generate benzyl radical, but the route to phenyl radical remains ambiguous.

Naphthalene and alkylnaphthalene are the most abundant PAH products. These compounds can be formed by the cyclization of n-butylbenzene or similar compounds, followed by dehydrogenation, Eq. 3. They can also be formed from the Diels-Alder type reaction between butadiene and cycloalkenes, Eq. 4. Alkylcyclohexenes and trace amounts of butadiene were detected in products from JP-8P stressed at 450°C. The key intermediate for these two reaction paths is tetralin. Tetralin was found in the products of n-BB stressed at 450°C for 30-60 minutes, but disappeared after 4 hours. Tetralin can also undergo, to a small extent, ring contraction [11] to form 1-methylindan (Eq.3B). In addition, the Diels-Alder type reaction between styrene and olefin may also contribute to naphthalene formation<sup>12</sup>. Styrene is the major product of n-BB decomposition within first 30 minutes, but most styrene seems to have been converted to ethylbenzene<sup>10</sup>.

Biphenyl, methylbiphenyl and terphenyls are also abundant PAH products from n-BB. Attack of phenyl radical on benzene (Eq.5) and/or recombination of phenyl radicals can account for most of the biphenyl formed. Three terphenyl isomers, p-, o-, and m-terphenyls, have been found. They may have been formed phenylation of biphenyl (Eq.5) or by attack of biphenyl radical on benzene, resulting in terphenyls. 1- and 2-Phenylnaphthalene were formed in relatively high concentrations (Figure 1.27). Most of them could arise from phenylation of naphthalene at the 1- and 2-positions, Eq.6.

Fluorene can be formed by attack of benzyl radical on benzene to form diphenylmethane, Eq. 7, or phenylation of toluene to form o-methylbiphenyl, followed by ring closure condensation. The intermediates for these paths such as diphenylmethane and methylbiphenyls were found in the

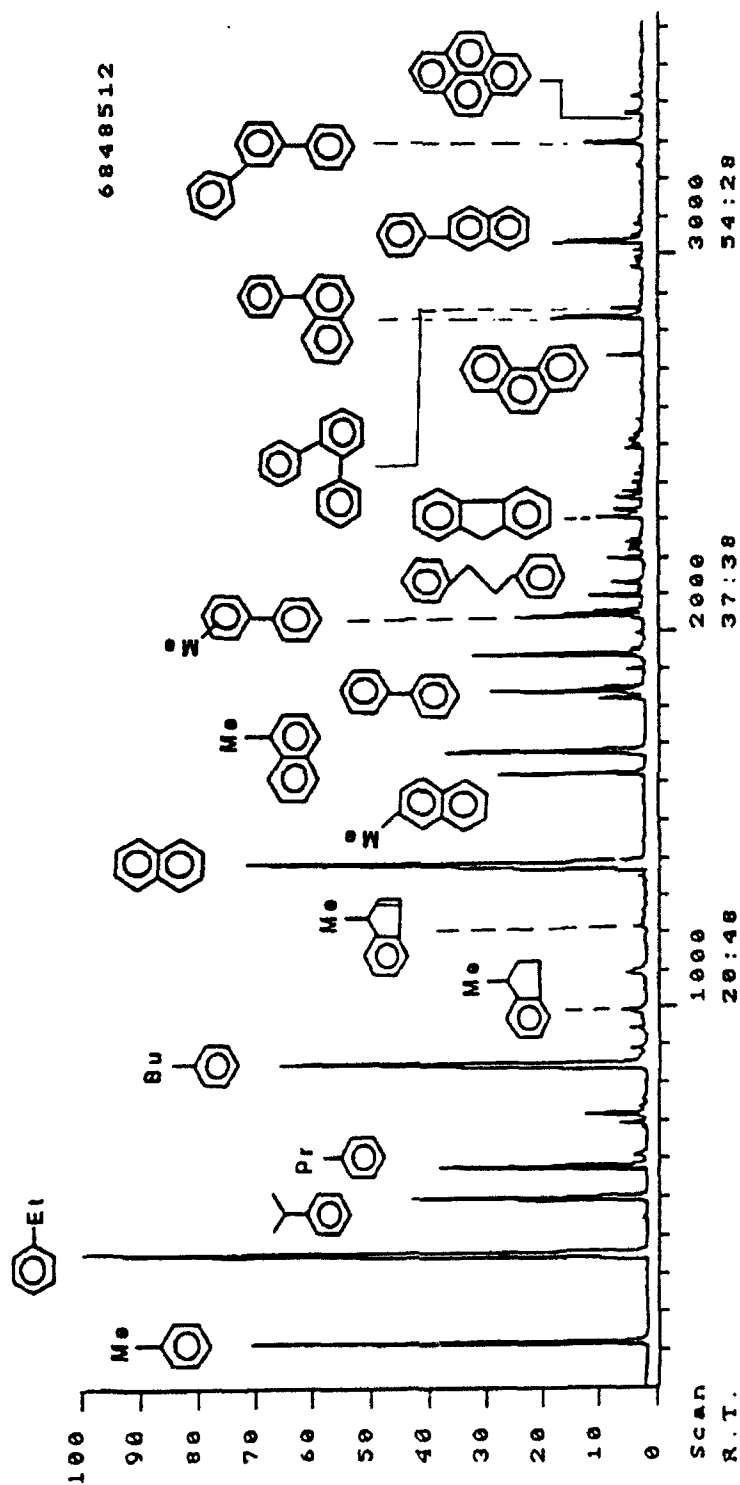


**Figure 1.27** GC-MS total ion chromatogram of liquid products from n-butylbenzene stressed at 450°C for 4 h.



**Scheme II. Possible mechanisms for the formation of PAHs**

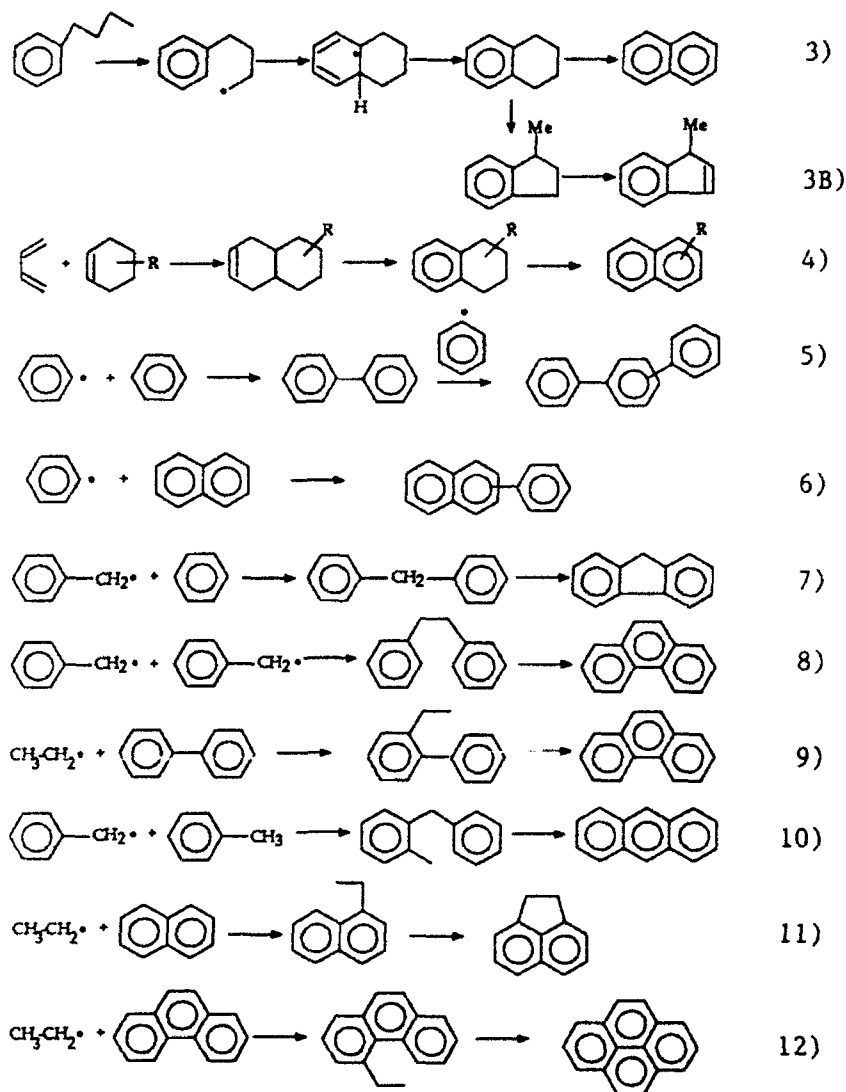


**Figure 1.28. Possible mechanisms for the formation of PAHs**

liquids from n-BB. Sweeting also reported fluorene formation from diphenylmethane at 700°C.<sup>13</sup>

Phenanthrene was formed from n-BB as early as 30 min at 450°C. Probably it was formed by coupling of two benzyl radicals to form bibenzyl, followed by condensation and dehydrogenation via 9,10-dihydrophenanthrene, Eq. 8. Both bibenzyl and 9,10-dihydrophenanthrene were detected.<sup>10</sup> In addition to bibenzyl, 1,3-diphenylpropane and 1,4-diphenylbutane were also formed from n-BB, probably by coupling of two phenylalkyl radicals. An additional minor path leading to phenanthrene may be the attack of ethyl radical on biphenyl to form 2-ethylbiphenyl, followed by condensation, Eq. 9. The Diels-Alder reaction between ethylene and 1-vinylnaphthalene, if any were formed in these reactions, also leads to phenanthrene.<sup>12</sup>

Anthracene was found in very low concentration after 4 hours reaction of n-BB. It can be formed by condensation of o-benzyltoluene, which could arise from the attack of benzyl radical on the 2-position of toluene, Eq.10. Acenaphthene was found in stressed jet fuels. It could arise from ring-closure of 1-ethylnaphthalene, Eq.11. In additions to the reactions shown by Eqs. 3-4, the addition of ethyl radical to naphthalene can also produce 1-ethylnaphthalene. Both 1- and 2-ethylnaphthalene appeared after 1 hour, but the former diminished with increasing time.

Fluoranthene and pyrene were detected in very low concentrations in n-BB products (Figure 1.27). Intramolecular condensation of 1-phenylnaphthalene (Eq.5) should lead to fluoranthene, as has been demonstrated by Stein.<sup>14</sup> It is difficult to explain the pyrene formation during the pyrolysis

of n-BB and jet fuels. Weizmann et al. suggested the union of two styrene molecules, and Badger and Spotswood proposed the coupling of two vinylcyclohexane units.<sup>15</sup> A third hypothesis involves the attack of ethyl radical on phenanthrene, followed by ring closure to form 4,5-dihdropyrene and finally pyrene, as shown by Eq. 12.

In regard to the precursors to solids, it should be noted that there are also heavier PAHs dissolved in the thermally stressed jet fuels and long-chain paraffins (after 4 hours at 450°C). They are soluble in stressed fuels but insoluble in n-pentane or fresh fuel, and are too heavy to be detected by GC-MS. Probably these heavier PAHs were formed via reactions similar to some of those in Eqs. 3-12, but with higher condensation degree or larger ring number. They may have formed from condensation and/or coupling reactions of two- to four-ring aromatics. When the reactions shown in Eqs.3 and 5-13 proceeded to certain extents, heavier PAHs can be readily formed from the radical attack of phenyl, benzyl and aliphatic radicals on the two- to four-ring PAHs. It is likely that these heavier PAHs and some of those in Eqs. 3-12, especially their alkyl-substituted homologues, are the precursors to solids. This is because the intermolecular and intramolecular condensation of larger polycyclic aromatics can readily occur at <450°C, leading to carbonaceous solids.<sup>11,14,16</sup> Naphthalene and biphenyl may have only very limited contribution to solid formation from jet fuels under the conditions used, because these two compounds have low reactivity and are quite stable when stressed alone at 450°C. A large amount of naphthalene was

formed after 4 hours stressing of JP-8C and the saturate fraction isolated from JP-8C by column chromatography, but the solid formation was still limited after 8 hours.<sup>5-6</sup> However, in the presence of reactive compounds they can undergo radical attack, such as phenylation, as observed during n-BB pyrolysis (Figure 1.28).

### Summary

The solid formation during pyrolytic degradation of jet fuels can be attributed to the formation of PAHs and subsequent condensation reactions. Reactive alkylaromatics, for which n-BB is a model, play an important role in PAH and solid formation. The combination of the proposed mechanisms shown in Scheme I and Figure 1.28 can explain the observed "induction" for production of solids and rapidly increased solid formation rate after induction period during thermal degradation of jet fuels and model compounds. The length of induction period depends mainly on fuel type, temperature, time and pressure. At a given condition it depends on the tendencies of fuel components toward the formation of PAHs. This period is longer with more stable samples and shorter with a reactive substrate. After the induction period, the amounts of solids formed in a given system are dependent on the concentrations of precursors, and on the amounts of reactive intermediates. Combination of the results with JP-8P, JP-8C and n-BB suggests that solid-forming reactions will continue in the presence of reactive intermediates and radical generators, and tend to stop when the reactive species are almost completely converted. It is expected that solid yields from JP-8P and JP-8C will also reach a steady state when the stressing time is extended long enough. Some questions remain about the effect of a stainless steel wall on solid formation. It is possible that the wall may catalyze the cleavage of some C-C and C-H bonds.<sup>17,18</sup>

### References

- (1) Frankenfeld, J.W. and Taylor, W.F., I&EC Prod. Res. Dev., **19**, 65 (1980).
- (2) Hazlett, R.N., "Free Radical Reactions Related to Fuel Research," in W.A. Pryor Ed. "Frontiers of Free Radical Chemistry," Academic Press, New York, 1980, pp.195-223.
- (3) Lee, C.M. and Niedzwiecki, R.W., PREPRINTS, Div. of Petrol. Chem., ACS, **34**, (4) 911 (1989)
- (4) Roquermore, W.M., Pearce, J.A., Harrison III, W.E., Krazinski, J.L., and Vanka, S.P., Preprints, Div. of Petrol. Chem., ACS, **34**, (4) 841 (1989).
- (5) Song, C., Eser, S., Schobert, H.H., Hatcher, P.G. et al., Advanced Thermally Stable Jet Fuels Development Program Annual Report, Volume II, Interim Report for period July 1990 to July 1991, WRDC-TR-91, Vol. II, 1991.
- (6) Song, C., Eser, S., Schobert, H.H. and Hatcher, P.G., preprint paper in this issue.

- (7) Eser, S., Song, C., Schobert, H.H., Hatcher, P.G. et al., Advanced Thermally Stable Jet Fuels Development Program Annual Report, Volume II, Interim Report for period July 1989 to June 1990, WRDC-TR-90-2079, Vol.II, September 1990.
- (8) Eser, S., Song, C., Gergova, K., Parzynski, M. and Peng, Y., Preprint paper in this issue
- (9) Song, C., Eser, S., Schobert, H.H., Hatcher, P.G. et. al., "Compositional Factors Affecting Thermal Degradation of Jet Fuels," DOE/Sandia National Laboratories, Technical Progress Report for period February to April 1991, 42-3462-TPR-3, May 1991.
- (10) Peng, Y., Schobert, H.H., Song, C. and Hatcher, P.G., Preprint paper in this issue.
- (11) Poutsma, M.L., *Energy and Fuels*, 4, 113 (1990).
- (12) March, J., "Advanced Organic Chemistry," 3d Ed., John Wiley & Sons, New York (1985).
- (13) Sweeting, J.W. and Wilshire, J.F.K., *Aust. J. Chem.*, 15, 89 (1962).
- (14) Senthilnathan, V.P. and Stein, S.E., *J. Org. Chem.*, 53, 3000 (1988).
- (15) Badger, G.M. and Spotswood, T.M., *J. Chem. Soc.*, 4420 (1960).
- (16) Stein, S.E., Griffith, L.L., Billmers, R. and Chen, R.H., *J. Org. Chem.*, 52, 1582 (1987).
- (17) Ghaly, M.A. and Crynes, B.L., *ACS Sym. Ser.*, 32, 218 (1976).
- (18) Dunkleman, J.J. and Albright, L.F., *ACS Sym. Ser.*, 32, 241 (1976).

## ***Activity 5. Thermal Degradation of Alkylbenzenes***

### **Introduction and Objectives**

Jet fuels in high-speed aircraft are in thermal stressing conditions because there exist many sources of heat, and most of these dump heat into the jet fuels.<sup>1</sup> Some of the sources, such as fuel pumps, warm the fuel because of working on the fluid. In other cases, the fuel must pass through a heated region, such as a compressor discharge, on the way to the combustor. In the systems requiring cooling (e.g., in lubricating, hydraulic, electrical and environmental systems), the fuel, having a reasonable heat capacity, serves as a coolant. The heat may result in a rise of the temperature in the jet fuels, especially in the case of the supersonic jet aircraft where severe thermal stressing is expected and the pyrolytic breakdown of the hydrocarbons of jet fuel range may take place.<sup>2</sup> As a result, carbonaceous solids are formed which can clog the fuel system, such as the fuel lines and nozzles.

The request for design and development of thermally stable jet fuels and the concerns for their deposit formation at high temperatures have stimulated a lot of research in the recent years.<sup>3-7</sup> A fundamental understanding of the degradation processes of the hydrocarbons in the jet fuel range under pyrolytic conditions is crucial. Typical petroleum-derived jet fuels consist mostly of long-chain paraffins (e.g., 85% for JP-8P) and alkylbenzenes or alkylaromatics (<10% for JP-8P).<sup>8</sup> Paraffins have been shown to be the least stable components in jet fuels.<sup>9</sup> Thermal chemistry of

long-chain paraffin has been extensively studied together with the development of petroleum industry. Two fundamental mechanisms have been proposed to account for the free radical reactions mechanism of paraffins: the Rice-Kossiakoff mechanism and the Fabuss-Smith-Satterfield mechanism.<sup>10,11</sup> When paraffins are subjected to pyrolysis, 1-alkenes, cycloalkenes/cycloalkanes and alkylaromatics are detected in the liquid products.<sup>9</sup> The formation of unsaturated rings is believed to be related to the Diels-Alder type reactions of conjugated alkenes and olefins formed initially in the system.<sup>12</sup> Upon further heating, these unsaturated rings may undergo dehydrogenation reactions to form alkylbenzenes and solid products thereafter. The overall reaction sequence for solid formation from long-chain paraffins may be expressed in Figure 1.29. From the above discussion, it is obvious that alkylbenzenes are not only a representative constituent in jet fuels, but also one of the "intermediates" between paraffins and solid deposits.

It is the objective of the present work to study the latter part of the scheme in Figure 1.29 beginning from alkylbenzenes. There has been comparatively little detailed mechanistic work on the pyrolysis of alkylbenzenes as opposed to that on straight-chain paraffins.<sup>13-31</sup> Most of the previous work focused on either primary reactions to calculate the bond dissociation energies of the corresponding initiation reactions<sup>21, 22, 25-27</sup> or low conversions of substrate to study the dominant reaction mechanisms and kinetic expressions<sup>32</sup> during the gas-phase pyrolysis. In contrast to most of the previous studies, the purpose of the present study is to explore the mechanism of pyrolytic degradation and solid formation from alkylbenzenes, mixtures of alkylbenzenes and finally jet fuels in closed vessels at relatively high temperatures and pressures. This objective ensues the following characteristics of the work:

(1) Complex phase behaviors: The temperature recorded so far in the fuel system of a jet engine is below 500°C. The situation of fuel system at this temperature range can be best simulated by static microautoclave reactors at temperatures between 400-500°C. Considering that most alkylbenzenes in jet fuels have critical temperatures less than 400°C, the initial reactions are probably in supercritical phase. The phase is expected to change as the reaction proceeds due to the formation of large amounts of high molecular weight compounds that have critical temperatures higher than the reaction temperature. As a result, there might be reactions happening in two phases, gas phase and liquid phase, if reactions within solid products are neglected.

(2) Very high conversions: Since the whole sequence of the pyrolysis from the initiation reaction to the reactions that lead to the solid product is of interest in the study, the pyrolysis reactions have to proceed to high conversions.

(3) Very complex product mixtures: The pyrolysis is governed by the nature of the starting material and operational parameters, such as temperature, pressure, atmosphere (inert or oxidative), reaction time, etc. The reactions are composed of many consecutive and parallel free radical chains. All these lead to very complex product mixtures in three phases--gaseous, liquid and solid--under typical pyrolysis conditions.

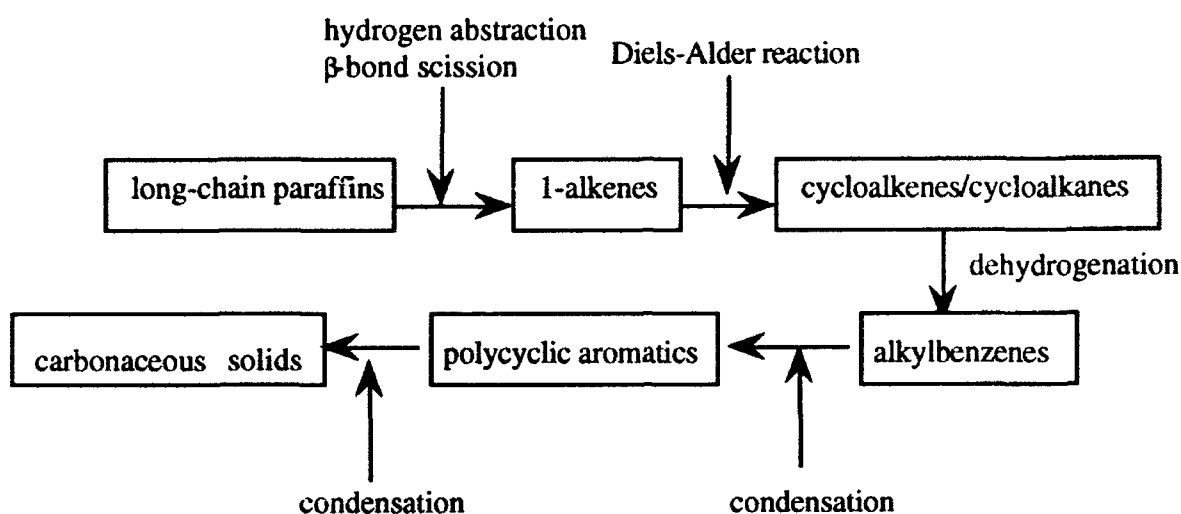


**Figure 1.29.** General reaction scheme of paraffins

## Research Approaches

On the basis of the objective of the study, a guide line that simulates the composition of jet fuels in a stepwise fashion is created and shown in Figure 1.30. Generally, all the reactions will be conducted in 25-ml microautoclave reactors (tubing bombs) under ultra-high purity (UHP) N<sub>2</sub> atmosphere at temperatures between 400-500°C. Major instruments used will be GC, GC-MS, solid state <sup>13</sup>C-NMR, liquid <sup>1</sup>H-NMR and headspace GC.

### 1. Pyrolysis of individual alkylbenzenes

Eight alkylbenzenes typically present in jet fuels, including ethylbenzene, butylbenzenes (four isomers), n-hexylbenzene, n-heptylbenzene and n-octylbenzene, will be chosen to subject to pyrolysis with the aim of investigating and examining the components or groups of components leading to the formation of undesirable solid products. Difference in substitution pattern (length and branching) on the benzene ring is expected to have a significant effect on the reactivity and solid formation tendency. In the case of n-alkylbenzene, the longer the side chain, the more reactive the alkylbenzene will be. The effect of branching of the side chain is more complex than the effect of length. t-Butylbenzene was found to be less reactive than its isomer n-butylbenzene.<sup>34</sup> The relationship between the structure of alkylbenzenes and compositions and distributions of products will be established. This can provide some fundamental understanding of pyrolytic mechanisms of individual alkylbenzenes.

### 2. Pyrolysis of mixtures of alkylbenzenes

Artificial blends of alkylbenzenes will be prepared according to the compositions of jet fuels. Since there is only about less than 10% of alkylbenzenes in real jet fuels, it is convenient to

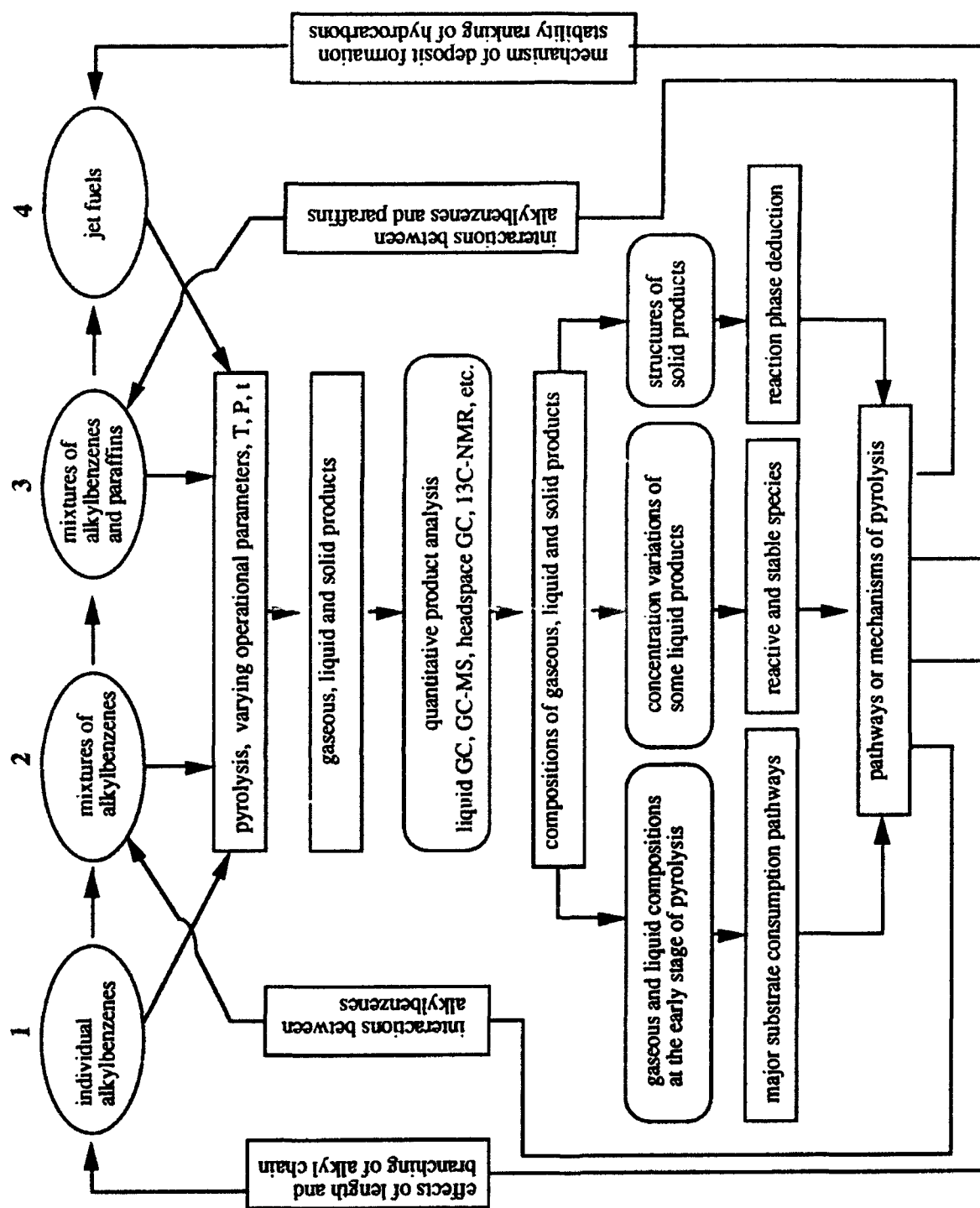


Figure 1.30. Schematic experimental design of the research work

use artificial mixtures of similar compositions. This part of work will be based on the analysis of jet fuels. Jet fuels will be separated according to procedure developed by Song et al.<sup>8</sup>, and the composition of alkylbenzene fractions will be characterized and quantified. According to the preliminary results of the pyrolysis of individual alkylbenzenes, there exist significant differences in reaction behaviors, such as induction time and solid formation tendency (see next section), due to the effect of the structures of the side chains. In comparison to this, the interactions between components in the mixture might exist and the pyrolysis reactions may be governed by the least stable one. As a result, the pyrolytic behaviors of the mixtures of alkylbenzenes would not be a simple summation of that of individual alkylbenzenes.

### **3. Pyrolysis of mixtures of alkylbenzenes and paraffins**

This is a further simulation of the composition jet fuels by model compounds. The experimental work is essentially similar to the above. It is known that paraffins are generally more reactive than alkylbenzenes. The initial stage of the pyrolysis of the mixture may be governed by the reaction of paraffins simply because paraffins are more reactive. At this stage, alkylbenzenes might show some degree of inhibition for the decomposition of paraffins.<sup>4</sup> Paraffin-induced reactions of alkylbenzenes are expected to happen shortly after the initial stage. The long time reactions of the mixture may show some similarity to the pyrolysis of mixture of alkylbenzenes.

### **4. Pyrolysis of jet fuels**

Jet fuels will be stressed at similar conditions to the model compounds and their mixtures. By comparison of the results, a detailed mechanism concerning the solid formation from jet fuels should be established. The driving force or active species leading to the instability and solid formation should be identified. The fundamental understanding of the pyrolysis behavior of the model compounds and their mixtures will provide profound knowledge for the deposit formation from jet fuels at latter stage of degradation.

## **Results and Discussion**

The major efforts made us so far were directed towards the step 1 designated in the last section. Four isomeric butylbenzenes, n-butylbenzene (n-BB), sec-butylbenzene (s-BB), iso-butylbenzene (i-BB), tert-butylbenzene (t-BB) have been studied.

### **1. General Scheme in the High Pressure Microautoclave Reactor**

Experiments were carried out in the microautoclave reactors (tubing bombs) at 450°C under 100 psi using ultra-high purity (UHP) N<sub>2</sub>. Under this condition, the pyrolysis reactions are extremely complex. In a conventional flow reactor, the dominant reactions are scission of  $\beta$ -bonds, while in microautoclave reactors, this reaction is suppressed and secondary reactions are favored. For jet fuels and related model compounds, generally, three groups of compounds are formed in the quenched tubing bomb reactors. They are: (1) low molecular weight gaseous hydrocarbons with the carbon chain length varying from C<sub>1</sub> to C<sub>4</sub>, (2) liquid products of a wide range of



molecular weight, and (3) carbonaceous solid products. As a result of thermal treatment, the reactions proceed to a thermodynamically stable state. If the treatment is severe, a three-phase thermodynamic equilibrium among gaseous, liquid and solid products can be reached. This appears to be the reason for the changes of the color of the liquid products from white to light yellow to brown to dark brown to light brown. The change of color from dark brown to light brown after long reaction times seems to be an indication of the achievement of equilibrium state.

## **2. Substrate Disappearance and Solid Product Formation**

Figures 1.31 and 1.32 show the rate of disappearance of model compounds and the yield of solid products formed, respectively. Over a time period from 15 minutes to 8 hour, n-butylbenzene is quickly converted and t-butylbenzene is the most stable isomer, as shown in Figure 1.31. As the substrate compounds disappear, carbonaceous solids have been observed to form in the reactors. It can be seen from Figure 1.32 that each compound has a different induction period for the formation of solid products. The induction period reflects the ability of the compound to resist the formation of carbonaceous solid products. The order for the induction time of the four compounds is: n-<sec-<iso-<tert-butylbenzene. The order is the same as that of the rate of their disappearance. The amount of the solids formed increases with the reaction time for sec-, iso- and t-butylbenzene. This behavior is similar to that of jet fuels, which also exhibit a monotonic increase in the amount of solid products.<sup>9</sup> Surprisingly, although solid products are quickly formed in the pyrolysis of n-butylbenzene after a short induction period, the amounts leveled off to an asymptotic value at around 5 hours. As a result, the least amounts of solids is formed from the reaction of n-butylbenzene after 8 hours at 450°C. The unique behavior of n-butylbenzene will be discussed in the following sections.

## **3. Early stage of pyrolysis**

The early stage of pyrolysis is monitored by pyrolyzing the model compounds at very short residence times where little or no solid products are formed and examining the compositions of the initial gaseous and liquid products. The results showed that all four model compounds have one common characteristic in their nature of initiation reactions during the decomposition, i.e., the free radical chains are initiated by the homolytic  $\beta$  C-C bond cleavage to form the stable benzylic or benzylic-type radicals as shown below. This step is also considered to be one of the major ways of the consumption of the individual compounds since  $\beta$ -bonds have the lowest bond dissociation energy.<sup>33</sup> From the high yields of low molecular weight compounds, such as toluene, ethylbenzene and propylbenzene, it can be inferred that the H-abstraction reactions between the benzylic and benzylic-type radicals formed and the substrate compounds that are present in overwhelming abundance could be another major way to consume the starting materials.

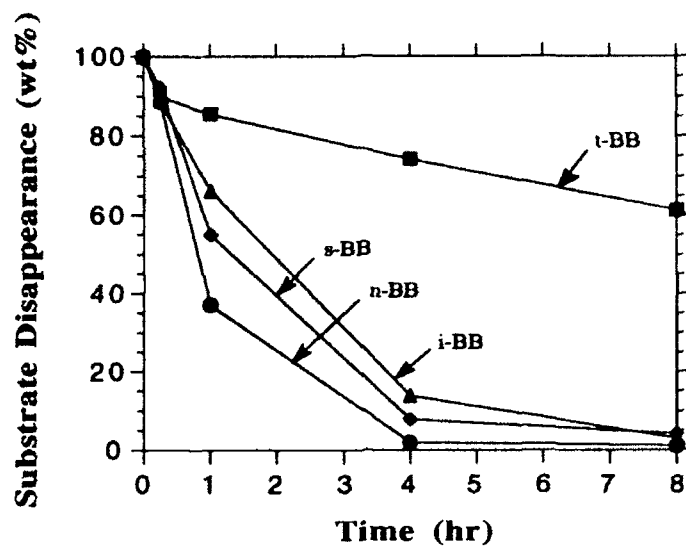


Figure 1.31. The disappearance of the substrate compounds at 450°C

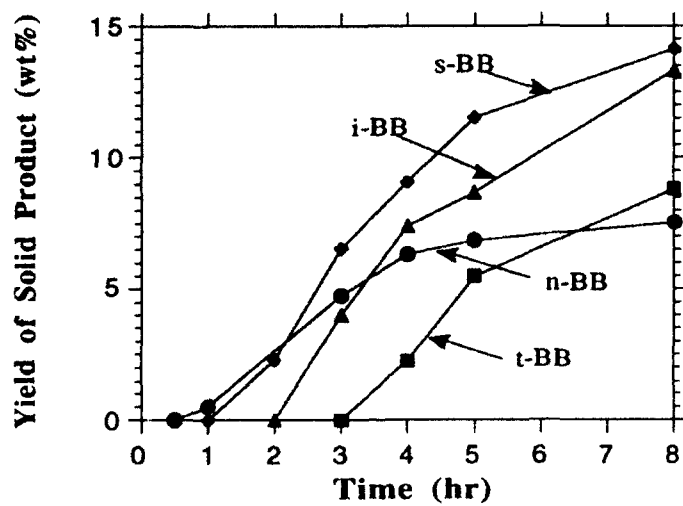
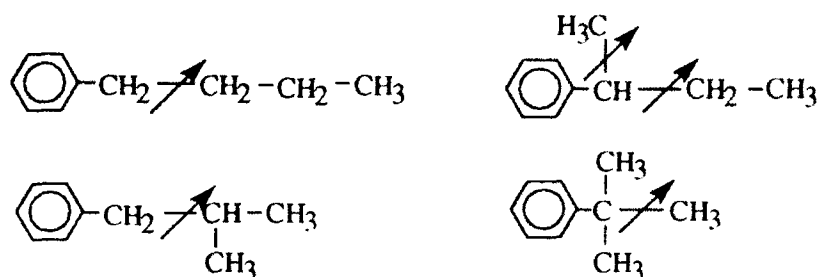


Figure 1.32. Formation of solid products at 450°C from the pyrolysis of butylbenzenes



t-Butylbenzene has the highest selectivity for benzene. This results show that  $\alpha$  bonds (alkyl-aryl bonds) in t-butylbenzene are weakened by the presence of the bulky t-butyl groups. The formation of benzene could also be due to the attack of H atom to the ipso position of t-butylbenzene.

Various styrene series compounds are formed by  $\beta$ -bond scission immediately after the H-abstraction reactions mentioned above. The concentrations of this type of compounds usually either are the highest at the beginning or go through a maximum within a few hours. Major styrene series formed from each compounds are listed as follows:

- n-BB  $\longrightarrow$  styrene;
- s-BB  $\longrightarrow$  trans- $\beta$ -methylstyrene,  $\alpha$ -methylstyrene,  $\alpha$ -ethylstyrene, dimethylstyrenes, 1-methyl-1-propenylbenzene, methylindenes;
- i-BB  $\longrightarrow$  trans- $\beta$ -methylstyrene,  $\alpha$ -methylstyrene, 2-methylstyrene, allylbenzene, 2-methyl-1-propenylbenzene, allyltoluene, styrene;
- t-BB  $\longrightarrow$  trans- $\beta$ -methylstyrene,  $\alpha$ -methylstyrene, 2-methyl-1-propenylbenzene, 2-methylstyrene.

There seems to be a qualitative relationship between the amounts of the styrene series compounds and the solid products formed. More solids are found to be produced from the pyrolysis of s-BB. This suggests that styrene series compounds could be the so-called "active intermediate" compounds during the pyrolysis of butylbenzenes at the initial stage.

#### **4. Major Substrate Consumption Pathways**

Major substrate consumption pathways are studied in this paper by pyrolyzing the model compounds at very short residence times where little or no solid products are formed, and examining the compositions of the initial gaseous and liquid products.

##### **(1) n-Butylbenzene (n-BB)**

The pyrolysis of n-BB for 15 minutes at 450°C indicates that ethane is present in the gas phase as a major product and toluene and styrene are major species present in liquid products.

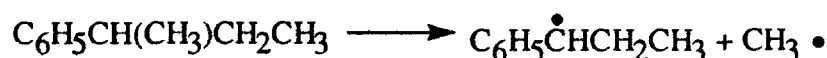
These results suggest that the major pathway of consumption n-BB is by breaking C $\alpha$ -C $\beta$  bonds in the side chain.<sup>6</sup>

### (2) t-Butylbenzene (t-BB)

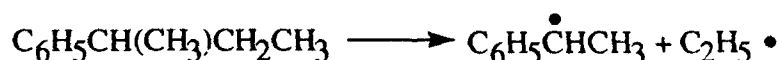
Although the initiation of t-BB is similar to that of n-BB (C $\alpha$ -C $\beta$  bond cleavage), its initiation process is significantly retarded as shown in Figure 1.31. This can be explained by the following two reasons. Firstly, the C $\alpha$ -C $\beta$  dissociation energy for t-BB is 73.7 $\pm$ 1.5 kcal/mol, which is higher than that for n-BB, 70.0 $\pm$ 1 kcal/mol.<sup>9</sup> Secondly, the H-abstraction reaction by C<sub>6</sub>H<sub>5</sub>C(CH<sub>3</sub>)<sub>2</sub> radicals formed by the homolysis of t-BB is expected to be much slower simply because of the relatively high stability of C<sub>6</sub>H<sub>5</sub>C(CH<sub>3</sub>)<sub>2</sub> radicals and the poor stability of C<sub>6</sub>H<sub>5</sub>C(CH<sub>3</sub>)<sub>2</sub>CH<sub>2</sub> radicals produced. As a result, the pyrolysis of t-BB is mainly carried out by isomerization reaction to form i-BB and s-BB.<sup>6</sup>

### (3) s-Butylbenzene (s-BB)

The composition of gaseous products for the reaction of s-BB are shown in Table 1.7. The major gaseous products after the initial period are methane, ethane and ethylene. As the reaction time increases, the concentration of ethylene decreases. Major liquid products identified include ethylbenzene (0.72 wt%), styrene (0.11 wt%),  $\alpha$ -methylstyrene (0.10 wt%), trans- $\beta$ -methylstyrene (0.70 wt%) and  $\alpha$ -ethylstyrene (0.16 wt%). According to these results, removing a CH<sub>3</sub> radical from s-BB appears to be a dominant initiation process:

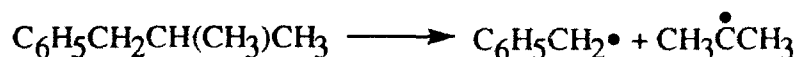


The presence of C<sub>2</sub> species in relatively high concentration in the gas phase indicates that removing a CH<sub>3</sub>CH<sub>2</sub> radical also exists as another initiation process:



### (4) i-Butylbenzene (i-BB)

The composition of gaseous products for i-BB is also shown in Table 1.7. Methane and propylene are two major gaseous products. Toluene (1.47 wt%) and trans- $\beta$ -methylstyrene (2.80 wt%) are the major liquid products in the initial period. These data suggest that the following initiation reaction exists in the pyrolysis of i-BB:



## 5. Major Liquid Product Selectivities

Liquid products consist mostly of cracking products, the molecular weights of which are less than the substrate compounds.<sup>4</sup> Cracking products include mainly benzene, toluene, ethylbenzene, i-propylbenzene and n-propylbenzene. Figures 1.33, 1.34 and 1.35 show the plot of selectivities of benzene, toluene and ethylbenzene from the pyrolysis of butylbenzenes. t-BB has the highest

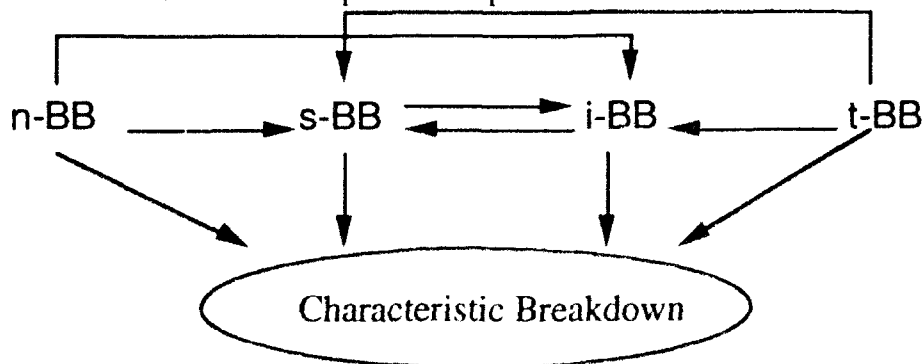
**Table 1.7.** Composition of Gaseous Products from sec- and iso-Butylbenzenes at 450°C

Time (hr)	CH <sub>4</sub> (mol%)		C <sub>2</sub> H <sub>4</sub> (mol%)		C <sub>2</sub> H <sub>6</sub> (mol%)		C <sub>3</sub> H <sub>8</sub> (mol%)		C <sub>3</sub> H <sub>6</sub> (mol%)		Volume (ml)	
	s-BB	i-BB	s-BB	i-BB	s-BB	i-BB	s-BB	i-BB	s-BB	i-BB	s-BB	i-BB
0.25	83.49	71.84	9.52	0.34	6.04	0.87	0.75	3.02	0.08	21.17	44	42
1.00	86.59	62.85	3.13	0.54	8.07	4.11	1.29	7.18	0.80	19.28	293	203
2.00	84.25	68.25	1.50	0.57	10.79	6.35	1.91	9.61	0.59	10.43	497	355
4.00	83.99	63.39	1.08	0.89	12.16	9.58	2.26	14.60	0.32	4.08	687	601
8.00	82.15	62.67	0.54	0.26	13.36	12.16	3.11	15.32	0.23	4.55	727	733

selectivity for benzene as shown in Figure 1.33. This appears to suggest that the aryl-alkyl bonds in t-BB are weakened by the presence of bulky t-butyl groups. The formation of benzene may also due to the attack of H to the ipso position of t-BB. In Figure 1.34, the concentration of toluene increases almost linearly with the increase of conversion except that the slope is lower for s-BB. Since  $\beta$ -bond scission to form benzyl radicals is the only initiation process in n-BB and it is easy for the benzyl radicals to abstract H from other species in the reaction system, n-BB has the highest selectivity to form toluene. In contrast, i-BB has two initiation pathways, only one of which forms benzyl radicals that lead to the formation of toluene. This lowers its toluene production. t-BB has been known to pyrolyze mainly by isomerization reactions to form i-BB (and s-BB to a lesser extent). The formation of toluene from t-BB might be attributed to the further dissociation of i-BB. It is obvious that direct decomposition of s-BB does not form toluene. Figure 1.35 shows the ethylbenzene selectivities. Similar behavior is observed in n-BB, s-BB and i-BB, t-BB. This could be understood from the discussion in the last section. It is possible that ethylbenzene can be formed as an initial reaction product for n-BB and s-BB, while i-BB and t-BB can only be formed between secondary reaction products.

## 6. Comparison of Solid Formation Tendencies

Compositions of liquid products seem to demonstrate that the reactivity of a model compound is governed by the initial reaction products. Generally there are two competing sets of reactions in the pyrolysis of all four model compounds at the initial stage, i.e., isomerizations and the characteristic breakdown for each specific compounds as shown below:



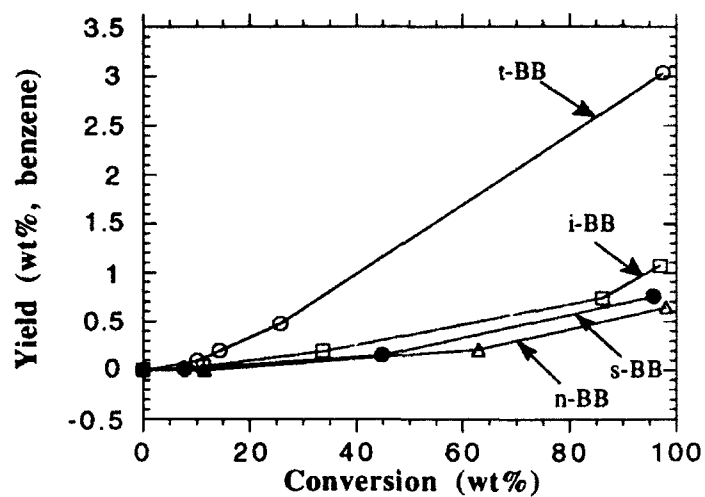


Figure 1.33. Selectivities of benzene in the pyrolysis of butylbenzenes

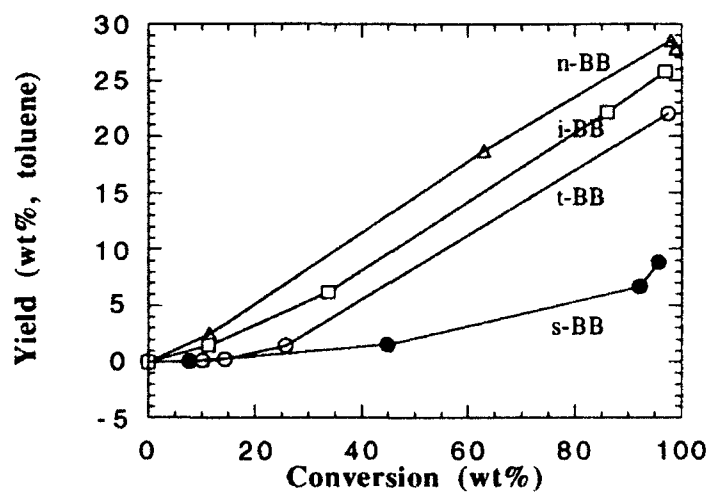
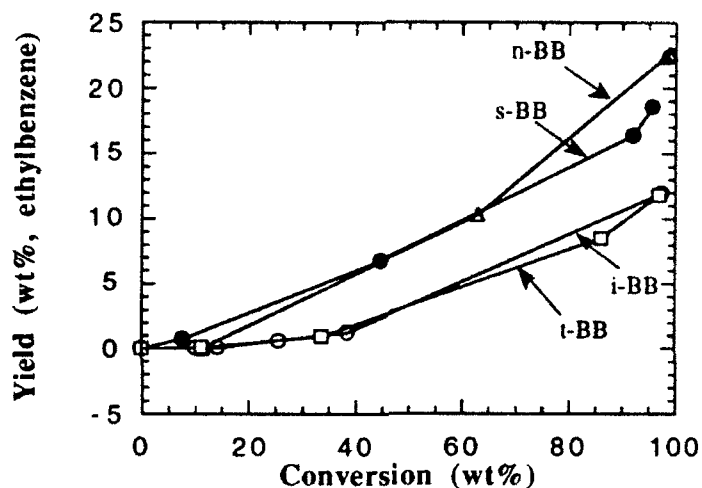


Figure 1.34. Selectivities of toluene in the pyrolysis of butylbenzenes



**Figure 1.35.** Selectivities of ethylbenzene in the pyrolysis of butylbenzenes

It is obvious from the previous discussion that for the pyrolysis of t-BB, the isomerization reaction to i-BB is more important than its characteristic breakdown. Therefore, the induction time for the solid formation from t-BB mainly depends on the isomerization reaction and the induction period of i-BB. This might account for its low reactivity and long induction period for solid formation (Figures 1.31 and 1.32). n-BB is the one that is most easily converted, but not the one that forms the highest amounts of solids. One reason for this is that it appears to be easy for n-BB to form cracking products such as toluene and ethylbenzene as shown in Figures 1.34 and 1.35, and stable high molecular weight compounds such as naphthalene as shown in Figure 1.36. The other reason is that fewer compounds of styrene-series were found in the liquid products of n-BB. In fact, only styrene is identified, and its concentration decreases rapidly as the reactions proceed. In the case of s-BB and i-BB, large amounts of compounds such as styrene, allylbenzene,  $\alpha$ -methylstyrene,  $\beta$ -methylstyrene, and ethylstyrenes were present after the initial reaction period. This may constitute the reason for the formation of large amounts of solid products from the pyrolysis of s-BB and i-BB.

## Conclusions

There is a significant effect of the structure of the side chains on the pyrolysis of alkylbenzenes. The rate of the disappearance or reactivity of an alkylbenzene depends on the ease of the dissociation energy of its initiation reactions. The order of reactivity or conversion of substrate was found to be n->sec->iso->tert-butylbenzenes. This indicates that, in general, branching seems to decrease the thermal reactivity of the alkylbenzenes. The amount of solids

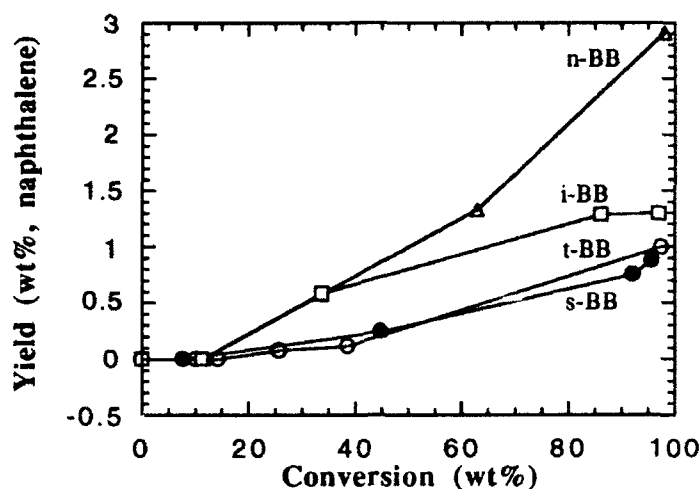


**Figure 1.36.** Selectivities of naphthalene in the pyrolysis of butylbenzenes

produced is related to the stability of the intermediate products especially at the initial stage. It seems that styrene-series compounds formed at the early stage are responsible for the formation of large amounts of solid products during the pyrolysis of sec- and iso-butylbenzenes.

## References

1. Hazlett, R.N., in *Thermal Oxidation Stability of Aviation Turbine Fuels*, ASTM, 1991.
2. Frankenfeld, J.W. and Taylor, W.F., *Ind. Eng. Chem. Prod. Res. Dev.*, 1980, **19**, 65.
3. Hazlett, R.N. and Hall, J.M., in *Chemistry of Engine Combustion Deposits*, L.B. Elbert, Editor, 1985, Plenum Press, New York.
4. Taylor, W.F., *Ind. Eng. Chem. Prod. Res. and Dev.*, 1969, **8**, 375.
5. Serio, M.A., *ACS Div. Petrol. Chem. Preprints*, 1989, **24**, 816.
6. Mushrush, G.W., Hazlett, R.N., Hardy, D.R. and Watkins, J.M., Jr., *Ind. Eng. Chem. Res.*, 1987, **26**, 662.
7. Eser, S., Song, C., Copenhaver, R. and Parzynski, M., *ACS Div. Petrol. Chem. Preprints*, 1992, **37**, 493.
8. Song, C. and Hatcher, P.G., *ACS Div. Petrol. Chem. Preprints*, 1992, **37**, 529.
9. a) Song, C., Peng, Y., Jiang, H. and Schobert, H.H., *Preprints. Div. Pet. Chem., ACS*, 37(2), 484, 1992; b) Song, C., Eser, S., Schobert, H.H., Hatcher P.G., et al., *Advanced Thermal Stable Jet Fuels Development Program Annual Report, Volume II*, 1990-1991, Fuel Science Program, Penn State University.



10. Fabuss, B.M., Smith, J.O. and Satterfield, C.N., Adv. Petrol. Chem. Refin., 1964, **9**, 158.
11. Kossiakoff, A. and Rice, F.O., J. Am. Chem. Soc., 1934, **65**, 590.
12. Nohara, D. and Sakai, T., Ind. Eng. Chem. Res., 1992, **31**, 14.
13. Savage, P.E. and Klein, M.T., Chem. Eng. Sci., 1989, **44**, 985.
14. Savage, P.E. and Klein, M.T., Ind. Eng. Chem. Res., 1987, **26**, 374.
15. Savage, P.E. and Klein, M.T., Ind. Eng. Chem. Res., 1987, **26**, 488.
16. Savage, P.E. and Klein, M.T., Ind. Eng. Chem. Res., 1988, **27**, 1348.
17. Savage, P.E. and Klein, M.T., Chem. Eng. Sci., 1989, **44**, 393.
18. Savage, P.E., Jacobs, G.E. and Javanmardian, M., Ind. Eng. Chem. Res., 1989, **28**, 654.
19. Savage, P.E. and Korotney, D.J., Ind. Eng. Chem. Res., 1990, **29**, 499.
20. Savage, P.E., Chem. Eng. Sci., 1990, **45**, 859.
21. Szwarc, M., J. Chem. Phys., 1948, **16**, 128.
22. Szwarc, M., J. Chem. Phys., 1949, **17**, 431.
23. Orchin, M. and Friedel, R.A., J. Chem. Soc., 1946, 573.
24. Orchin, M. and Regel, L., J. Chem. Soc., 1947, 505.
25. Leigh, C.H. and Szwarc, M., J. Chem. Phys., 1952, **20**, 844.
26. Leigh, C.H. and Szwarc, M., J. Chem. Phys., 1952, **20**, 407.
27. Leigh, C.H. and Szwarc, M., J. Chem. Phys., 1952, **20**, 403.
28. Freund, H., Matturro, M.G., Olmstead, W.N., Reynolds, R.P. and Upton, T.H., Energy and Fuels, 1991, **5**, 840.
29. Badger, G.M. and Spotswood, T.M., J. Chem. Soc., 1959, 1635.
30. Badger, G.M. and Spotswood, T.M., J. Chem. Soc., 1960, 4420.
31. Badger, G.M., Buttery, R.G., Kimber, R.W.L., Lewis, G.E., Moritz, A.G., et al., J. Chem. Soc., 1958, 2449.
32. Freund, H. and Olmstead, W.N., Int. J. Chem. Kinet., 1989, **21**, 561.
33. Lide, D.R., *CRC Handbook of Chemistry and Physics*, 1990-1991, CRC Press.
34. Peng, Y., Schobert, H.H., Song, C. and Hatcher, P.G., ACS Div. Petrol. Chem. Preprints, 1992, **37**, 505.

## ***Activity 6. Hydrogen-Transferring Pyrolysis of Hydrocarbons. Enhancing High Temperature Thermal Stability of Aviation Jet Fuels by H-Donors***

### **Introduction**

The present work is a fundamental study of condensed-phase pyrolysis of saturate hydrocarbons including alkylcyclohexanes, trans- and cis-steric isomers of decalin and straight-chain paraffins as well as hydroaromatics such as tetralin. This work is a part of an on-going research program for developing advanced jet fuels thermally stable at high temperatures. One of the critical problems in developing thermally stable jet fuels for high-Mach aircraft is the formation of solid from hydrocarbon fuels in pyrolytic regime.<sup>1,2</sup> In studying the pyrolytic degradation of jet fuels, it occurred to us that hydrogen-transfer from H-donors, such as those present in coal-derived JP-8C jet fuel, could play an important role in suppressing thermal decomposition and solid formation.<sup>3,4</sup> The hydrogen-transferring pyrolysis described in this report refers to the thermal decomposition of straight-chain and cyclic hydrocarbons in the presence of H-donors.

In this report we discuss 1) pyrolytic degradation of the above-mentioned cyclic and straight-chain hydrocarbons; 2) inhibiting effects of H-donors on the decomposition and solid-forming tendency of n-tetradecane (n-C<sub>14</sub>), n-butylcyclohexane (n-BCH), cis-decalin (cis-D) and n-butylbenzene (n-BB) as well as a petroleum-derived JP-8P jet fuel; and 3) the mechanisms of the pyrolysis and H-transferring pyrolysis. It should be noted that the experimental conditions used in this work are such that they are close to the high-temperature thermal environment of jet fuel in the future high-Mach aircraft under consideration. These conditions are characterized by condensed or supercritical phases, relatively high pressure, static reactor, and long residence time. Such conditions are distinctly different from those used in most previous paraffin pyrolysis work (vapor phase, low-pressure, flow reactor, short residence time).

### **Experimental**

Reagent-grade n-C<sub>14</sub>, n-BCH, ethylcyclohexane (ECH), trans-decalin (trans-D) and cis-decalin (cis-D), decalin, tetralin, n-butylbenzene (n-BB) from Aldrich and a petroleum-derived JP-8P jet fuel were used.<sup>5</sup> Several compounds including tetralin, decalin, cis-D and trans-D were also examined as H-donors. The pyrolysis was conducted at 450°C for 0-8 hours under 0.69 MPa UHP-N<sub>2</sub> (cold) in 25-mL tubing bombs using 5 mL sample. A fluidized sandbath preheated to 450°C was used as heater. The products were identified by capillary GC-MS and quantified by GC. More experimental details may be found in recent reports.<sup>5,7</sup>

## RESULTS AND DISCUSSION

### L. Pyrolysis of Cyclic and Straight-Chain Hydrocarbons

We first conducted a comparative examination of thermal stability of several cyclic and straight-chain hydrocarbons, which are representative components in coal- and petroleum-derived jet fuels, respectively. Figure 1.37 shows the time-pressure profiles for the pyrolysis of these compounds. Since static reactor was used, the sample is always confined within the reactor. Therefore, the increase of system pressure after equilibrium boiling is indicative of the extent of thermal decomposition. As shown in Figure 1.37, when tetralin was heated under 0.69 MPa N<sub>2</sub> (cold) pressure, the system pressure increased to 3.4 MPa within 10 minutes, then the pressure maintained nearly constant. All the other compounds displayed more or less pressure increase. Their t-p profile patterns provide a convenient measure for the extent and rate of their thermal decomposition to form smaller molecules. It should also be noted from Figure 1.37 that the temperature of 450°C and pressures at 450°C ( $\geq 3.5$  MPa) are higher than the critical temperatures and critical pressures of all the compounds, suggesting the occurrence of supercritical-phase pyrolysis.

Figure 1.38 shows the conversion of several compounds versus residence time at 450°C for 0-8 hours. The typical component of petroleum jet fuels, n-C<sub>14</sub>, exhibited the highest degree of decomposition, and its pyrolysis led to 50% conversion in just 30 min. For the cycloalkanes, the rate of n-BCH decomposition is faster than that of ECH, indicating that increasing the length of side chain on alkylcyclohexane decreases the thermal stability. Decalin appears to be more stable than the other saturates but it is originally a mixture of trans- and cis-D<sup>6-8</sup> (see below). Tetralin was the most stable compound when stressed alone. Combination of the data in Figures 1.38 and 1.39 indicates that cycloalkanes are much more stable than the long-chain paraffins; the increase in the length of side-chain of alkylcycloalkanes or straight-chain paraffins decreases the stability and increases the decomposition rate.

**Alkylcyclohexanes.** Figures 1.39 and 1.40 show the distribution of products from n-BCH versus residence time and conversion, respectively. At low conversion level of 11.8 mol%, the major products are cyclohexane (3.0, mol%), methylene-cyclohexane (2.3), methylcyclohexane (1.9) and cyclohexene (1.1). Figure 1.41 shows the possible reaction mechanisms proposed based on the identified products. The initiation reaction of n-butylcyclohexane is likely the homolytic cleavage of the C-C bond between the ring and the side-chain to form cyclohexyl and 1-butyl radicals. The formation of the four predominant initial products can be rationalized by the radical reaction pathways I, II, III, and IV, respectively. After 1 hour at 450°C, the yield of methylene-cyclohexane begins to decrease with further increasing residence time, presumably due to hydrogenation to form methylcyclohexane. In regard to the reaction mechanisms for alkyl-cyclohexane pyrolysis, there is little information in the literature except for the recent report of

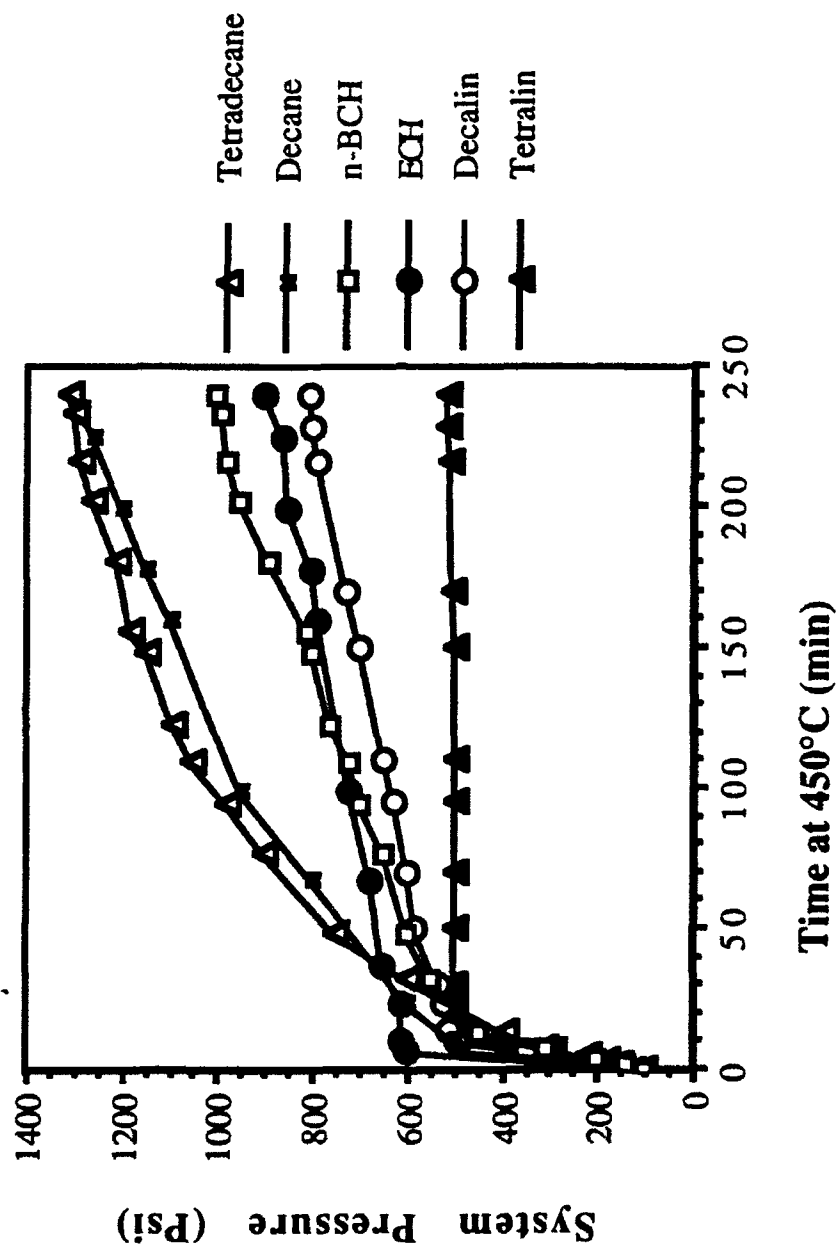


Figure 1.37. System t-p profiles for pyrolysis of model compounds.

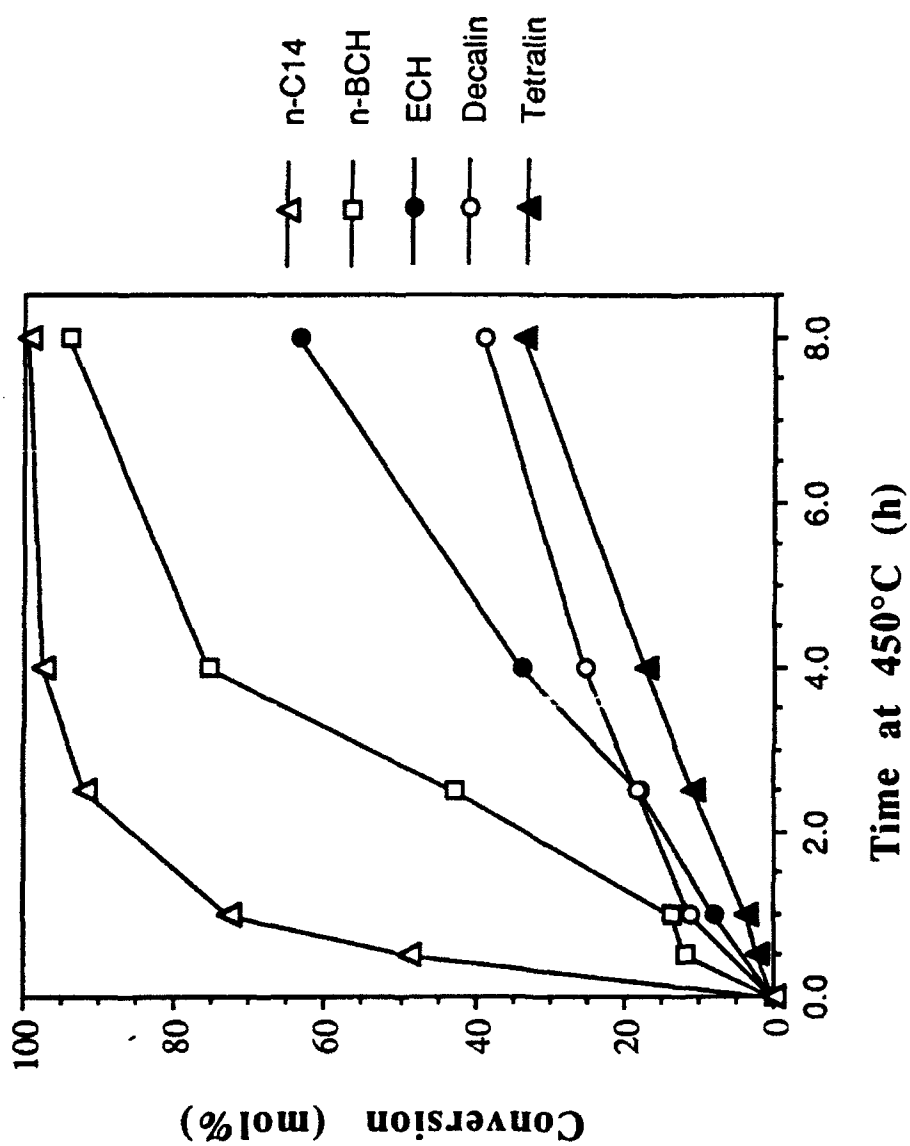
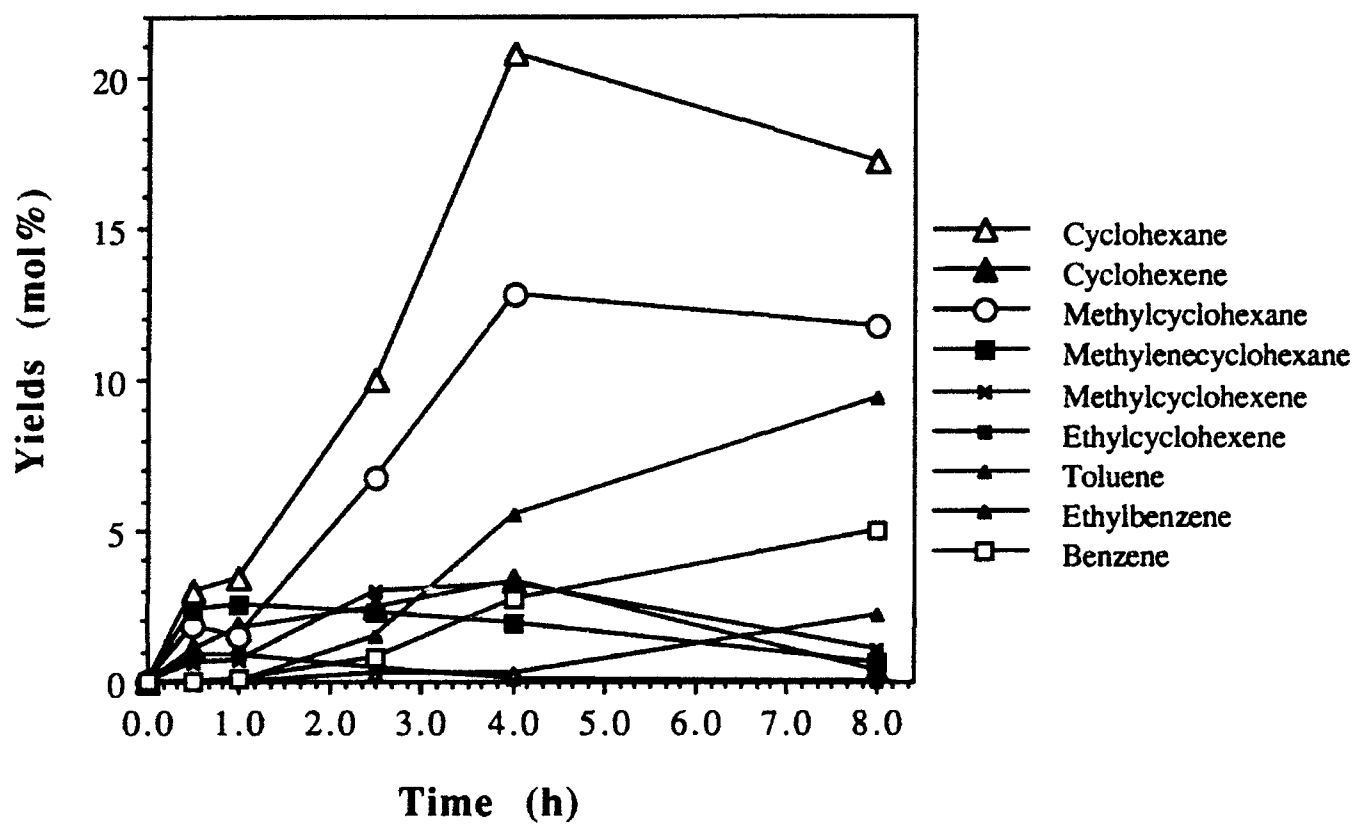


Figure 1.38. Conversion of model compounds during pyrolysis at 450°C under 0.69 MPa (cold) N<sub>2</sub>.



**Figure 1.39.** Product distribution for pyrolysis of n-butylcyclohexane (n-BCH) as a function of residence time at 450°C.

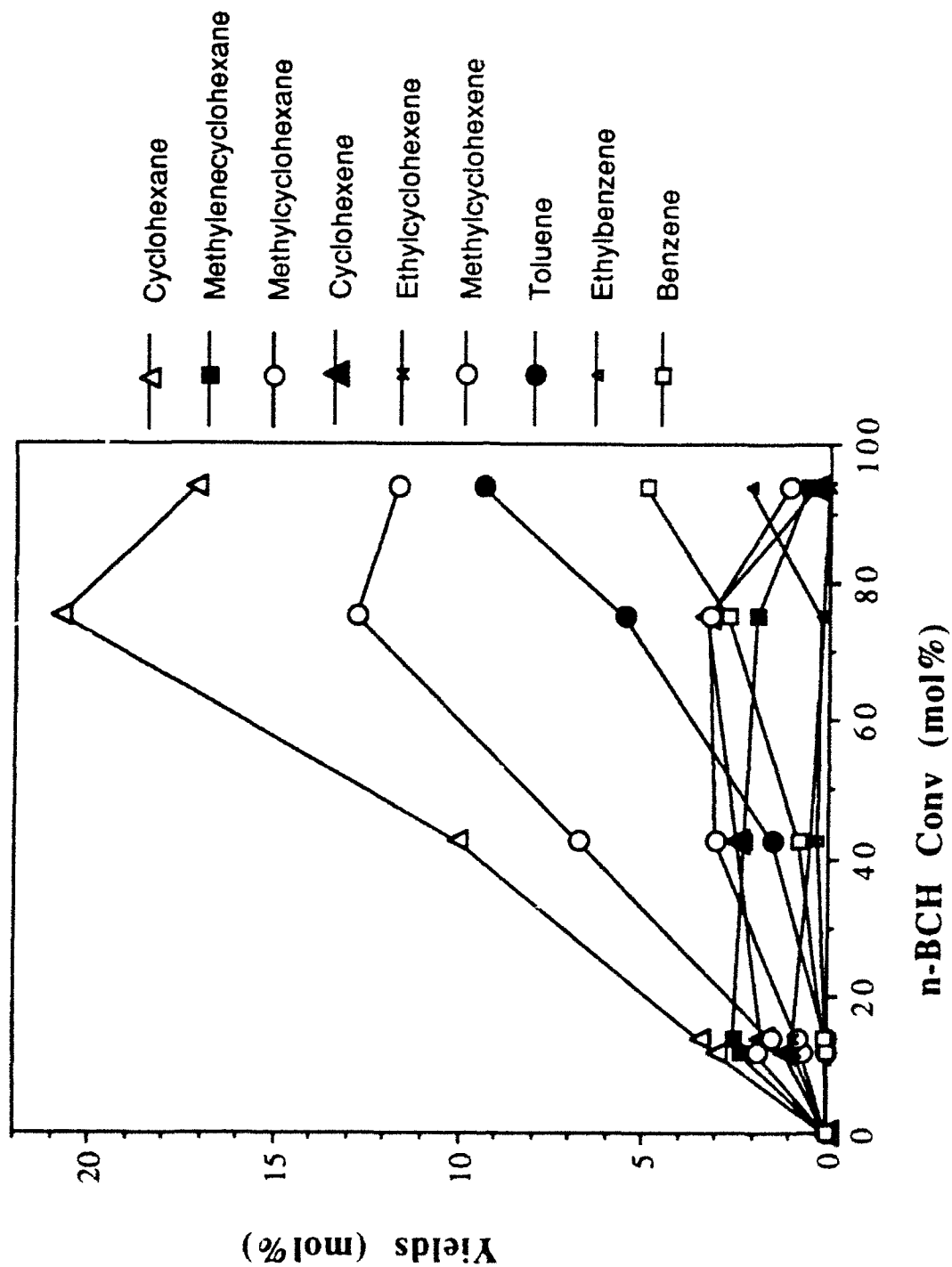
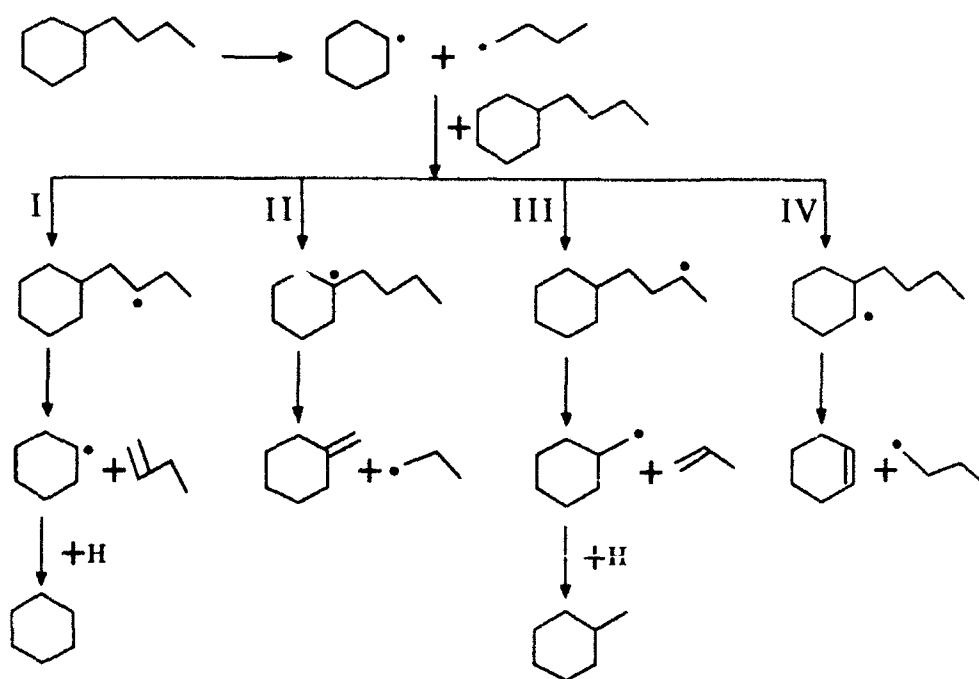


Figure 1.40. Product distribution for pyrolysis of n-butylcyclohexane (n-BCH) as a function of molar conversion of n-BCH at 450°C.



**Figure 1.41.** Possible Mechanisms for Pyrolysis of n-Butylcyclohexane

Savage and Klein, who found that there are only two major pathways for pyrolysis of n-tridecylcyclohexane.<sup>9</sup> The pathways I and II for n-BCH are also consistent with their observations. However, the present work reveals that other major pathways, III and IV, also exist for the alkylcyclohexanes with shorter side-chains, as shown in Figure 1.40. Interestingly, when the residence time was extended to 2.5 hours and longer, cyclohexane and methylcyclohexane become the two most predominant products, and their yields were several times higher than those of all the other products. These results suggest that pathways I and III dominate in long-duration n-BCH pyrolysis.

Figure 1.42 shows the distribution of products from ECH. At low conversion level (7.3 mol%), the major products from ECH are cyclohexene (1.50 mol%), methylcyclohexane (0.83 mol%), methylcyclohexene (0.87 mol%). The preference of cyclohexene formation indicates that the reaction via cyclohexyl radical is a major path, similar to path IV for n-BCH. However, methylenecyclohexane is a minor product in this case (0.17 mol%), indicating that one of the major pathways for n-BCH becomes a minor one for ECH. Another major difference between ECH and n-BCH is the higher yields of isomerization products from ECH pyrolysis, such as methylcyclopentane.



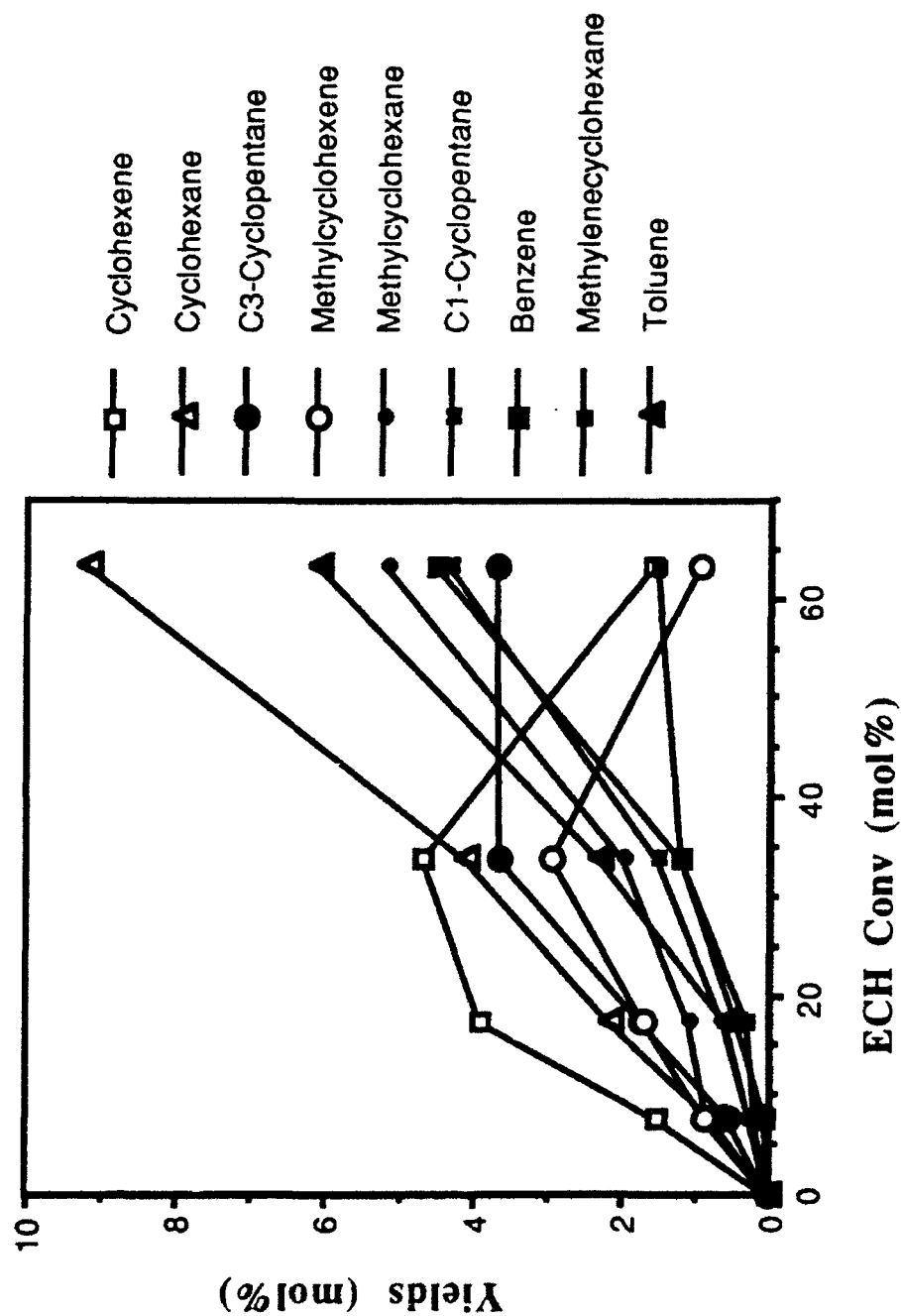


Figure 1.42. Product distribution for pyrolysis of ethylcyclohexane (ECH).

**Decalin.** Figure 1.43 shows the product distribution for pyrolysis of decalin, which was originally a mixture of nearly equivalent weights of trans- and cis-D. After decalin pyrolysis at 450°C, the yield of trans-D increased slightly and that of cis-D decreased monotonically with increasing time up to about 4 hours. There are two possible reasons for such observations: isomerization of cis- to trans-D or decomposition of cis-D. To gain further insight, we performed the runs of pure trans-D and cis-D, as shown in Figure 1.44. It was found that cis-D is not stable and tends to isomerize into trans-D as shown in Figure 1.45. Amount of trans-D formed from cis-D increased from 6% in 30 min to 41% after 4 hours at 450°C. Roberts and Madison found that di-*t*-butylperoxide can initiate such an isomerization.<sup>10</sup> Probably this is initiated via H-abstraction by a radical from 9-position. On the other hand, trans-D is much more stable than cis-D. Its isomerization to cis-D also occurred but the extent was very limited, even after 8 hours, as can be seen from Figure 1.43. In fact, trans-D was found to be one of the most stable components in coal-derived jet fuel JP-8C.<sup>5</sup>

We also observed substantially higher gas yields from cis-D (5.4 wt% in 4 hours) than from trans-D (0.8 wt% in 4h), showing higher degree of ring-opening cracking and subsequent dealkylation with cis-isomer. In the case of cis-D, 1-butylcyclohexene was also detected as a major cracking product (0.7 mol%) after 30 min at 450°C. It was formed probably via the 9-decyl radical and subsequent  $\beta$ -scission which caused the ring-opening cracking. The cracking via 9-decyl radical was also suggested for hydrolysis of decalin by Shabtai et al.<sup>11</sup> Therefore, the ring-opening cracking and isomerization of cis-decalin may share the same initiation path, because the latter also involves 9-decyl radical formation as the first step. In summary, the steric conformation of cycloalkanes also affects their thermal stability, and for decalin, trans-isomer is much more stable.

**n-Tetradecane Pyrolysis.** Pyrolysis of n-tetradecane at 450°C for 0-8 hours produced up to about 175 compounds, and the products ranged from lightest molecules such as hydrogen and methane to heavy polyaromatics such as pyrene and solid deposits. After 30 min at 450°C, 49% of n-C<sub>14</sub> has been decomposed, and the main products are C<sub>1</sub>-C<sub>13</sub> alkanes and C<sub>2</sub>-C<sub>13</sub> 1-alkenes. Figure 1.46 shows the possible reaction pathways for thermal cracking of long-chain n-alkanes such as n-tetradecane under the conditions employed. The first substrate radicals from n-C<sub>14</sub> include both sec-C<sub>14</sub>H<sub>29</sub>• (eq.2) and 1-C<sub>14</sub>H<sub>29</sub>• (eq. 3). Formation of the primary radical requires higher activation energy than that of secondary radical, but the difference is not very large in H-abstraction reaction. For example, the activation energies for H-abstraction from n-butane to form 2-C<sub>4</sub>H<sub>9</sub>• and 1-C<sub>4</sub>H<sub>9</sub>• at 427°C are 10.4 and 12.3 kcal/mol, respectively.<sup>12</sup>

There are two extremes of the same fundamental mechanism for radical reactions: the Rice-Kossiakoff mechanism and the Fabuss-Smith-Satterfield mechanism, which afford different product spectra.<sup>13,14</sup> Pyrolysis of long-chain paraffins is still the subject of many investigations.

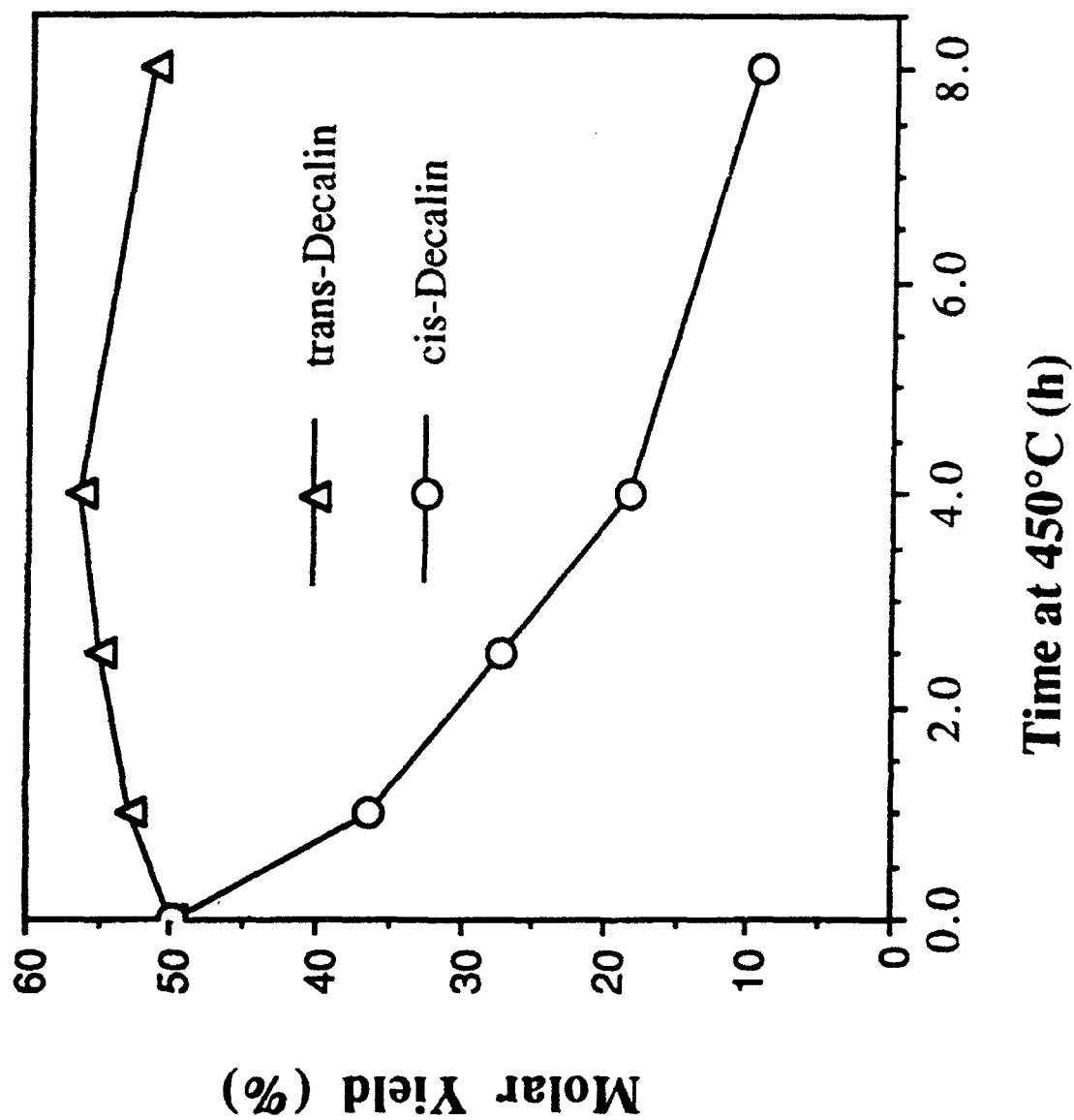


Figure 1.43. Compositional change during decalin pyrolysis.

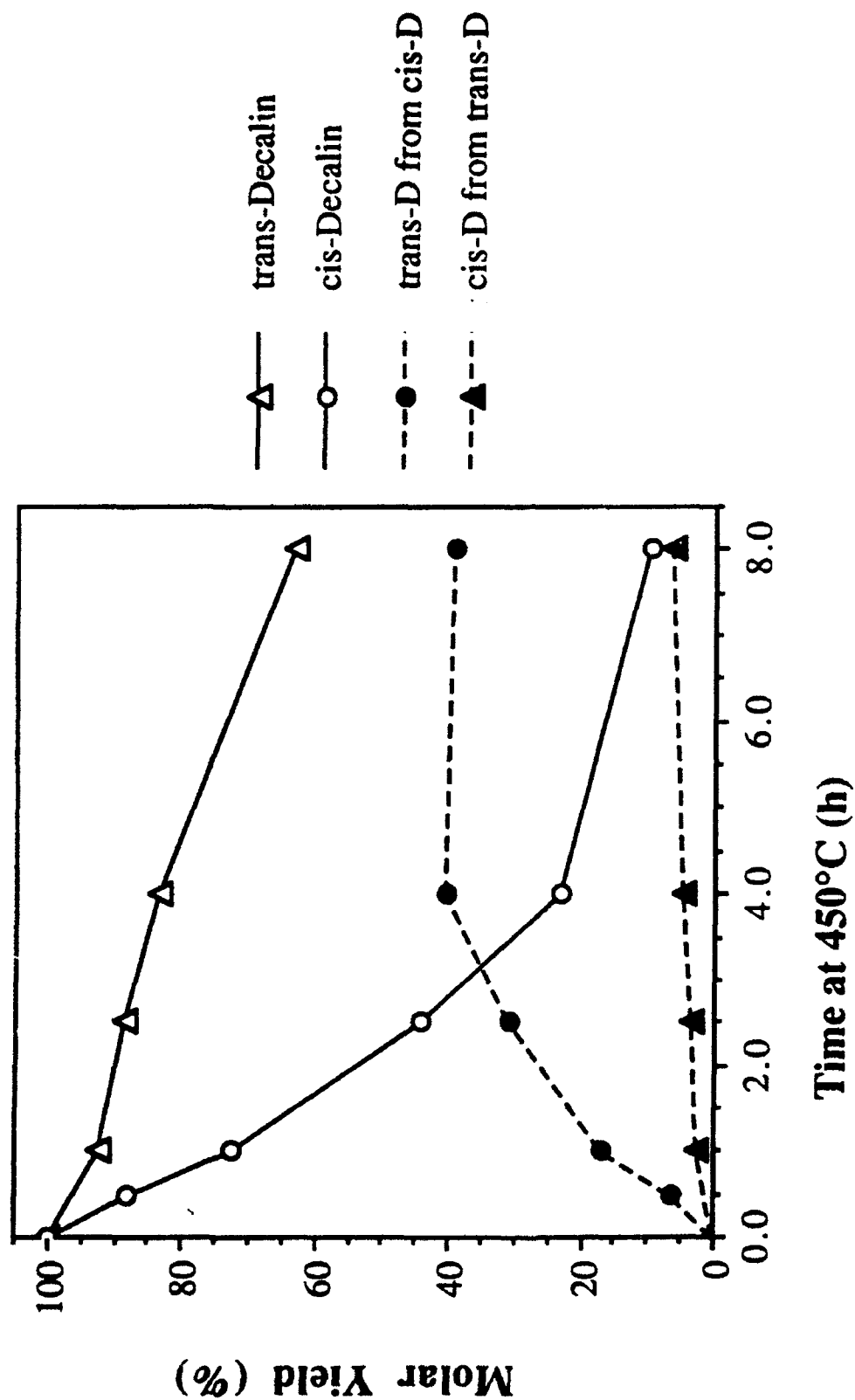
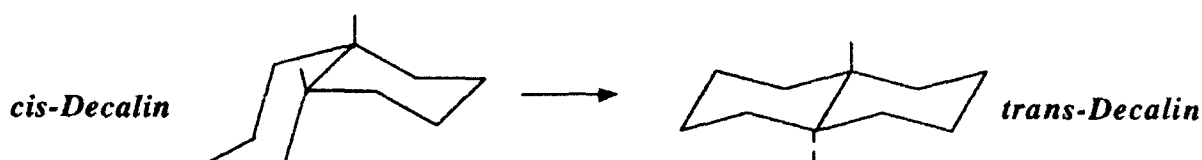
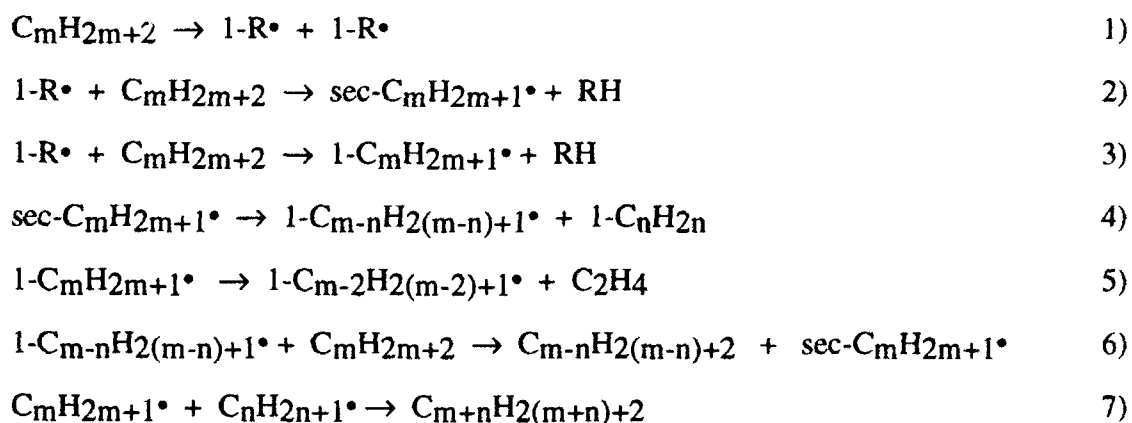


Figure 1.44 Conversion and isomerization during pyrolysis of pure cis-decalin and pure trans-decalin at 450°C.



**Figure 1.45.** Isomerization of *cis*-Decalin to *trans*-Decalin



**Figure 1.46.** Possible mechanisms for pyrolysis of *n*-alkanes  $\text{C}_m\text{H}_{2m+2}$

Several recent papers reported the preferential formation of 1-alkenes from vapor-phase pyrolysis of long-chain paraffins.<sup>15,16</sup> In the present work, significant amounts of olefins, mainly 1-alkenes, were also detected, both in liquid and gaseous products. However, unlike the literature results for high temperature and short-residence time pyrolysis, the olefins are not dominant species for most product groups with the same carbon number under the present conditions, except the  $\text{C}_{12}$  group in which 1-dodecene yield was higher than dodecane for 30 min run.

The differences between the present and literature results can be explained as follows. At high temperature ( $\geq 550^\circ\text{C}$ )-low pressure-short residence time ( $< 1$  minute) conditions, as employed in most previous pyrolysis work, radicals tend to undergo  $\beta$ -scission, which leads to products rich in 1-alkene and ethylene. Analytical data show that pyrolysis under our conditions (about 3.4-8.9 MPa system pressures at  $450^\circ\text{C}$  for 0-4 hours) leads to more alkanes, which can be rationalized based on the Fabuss-Smith-Satterfield mechanism. Under high-pressure conditions, which in

general tend to enhance bimolecular reactions,  $\beta$ -scission (eqs. 4,5) will be in competition with hydrogen abstraction (eq.6). Because C<sub>8</sub>-C<sub>12</sub> alkanes and alkenes were still the major components in liquid products after 30 min at 450°C, it is likely that the first radical formed by  $\beta$ -scission of C<sub>14</sub>H<sub>29</sub>• radicals (eqs. 4,5) will already prefer to undergo hydrogen-abstraction (eq. 6), which yield one 1-alkene molecule and one alkane molecule. The activation energy required for H-abstraction by a radical from a hydrocarbon or molecular H<sub>2</sub> is smaller than that required for  $\beta$ -scission of the same radical. For example, the energy for  $\beta$ -scission of 1-C<sub>5</sub>H<sub>11</sub>• to form 1-C<sub>3</sub>H<sub>7</sub>• plus C<sub>2</sub>H<sub>4</sub> is 29 kcal/mol, while that for its H-abstraction from another hydrocarbon or H<sub>2</sub> is about 10-12 or 15-17 kcal/mol at 427°C.<sup>12</sup>

## **II. H-Transferring Pyrolysis and Inhibition of Solid Formation**

The present work on H-transferring pyrolysis seeks to clarify whether and how the hydrogen-donors affect the pyrolytic degradation and solid-forming tendencies of jet fuel components. Figure 1.47 shows the inhibiting effect of tetralin on solid deposit formation from JP-8P fuel, n-C<sub>14</sub>, and n-BB, respectively, at 450°C for 4 hours. In the absence of H-donor, the amounts of deposits formed were n-BB (5.6 wt%) > JP-8P (3.1 wt%) ≥ n-C<sub>14</sub> (3.0 wt%). These figures are extremely large if one considers the deposit formation inside fuel lines in aircraft. It is clear from Figure 1.47 that adding a small amount of tetralin significantly reduced the deposit formation from all these compounds. As for the efficiency of H-donor, adding 10 vol% tetralin to JP-8, n-C<sub>14</sub> and n-BB reduced the formation of deposits by 90% (from 3.1 to 0.3 wt%), 77% (from 3.0 to 0.7 wt%) and 54% (from 5.6 to 2.6 wt%), respectively. These results demonstrate that by means of H-transferring pyrolysis, hydrocarbon jet fuels can be used at high operating temperatures in pyrolytic regime with little or no solid deposition.

Multi-ring cyclic alkanes such as decalin can also serve as H-donors at high temperatures, although decalin is not as active as tetralin for inhibiting solid formation.<sup>17</sup> Table 1.8 shows that decalin can also suppress the deposit formation from JP-8P jet fuel, n-C<sub>14</sub> and n-BB. In fact, adding both trans- and cis-D by 50 vol % almost eliminated solid formation from n-C<sub>14</sub>, JP-8P, and n-BB. Since decalin and n-C<sub>14</sub> are also representative components of coal- and petroleum-derived jet fuels, respectively, their mixture can also be viewed as a fuel blend. These results also account for the fact observed in previous work that the presence of significant amounts of C<sub>12</sub>-C<sub>18</sub> in coal-derived JP-8C did not cause remarkable solid formation.<sup>4,5</sup>

Based on the foregoing, the reduced solid formation and the enhanced stability of hydrocarbons in H-transferring pyrolysis can be attributed to the stabilization of the reactive radicals via hydrogen-abstraction from tetralin or decalin type compounds, which contributes mainly to inhibiting the secondary radical reactions and suppressing solid formation, as shown in Figure 1.48.

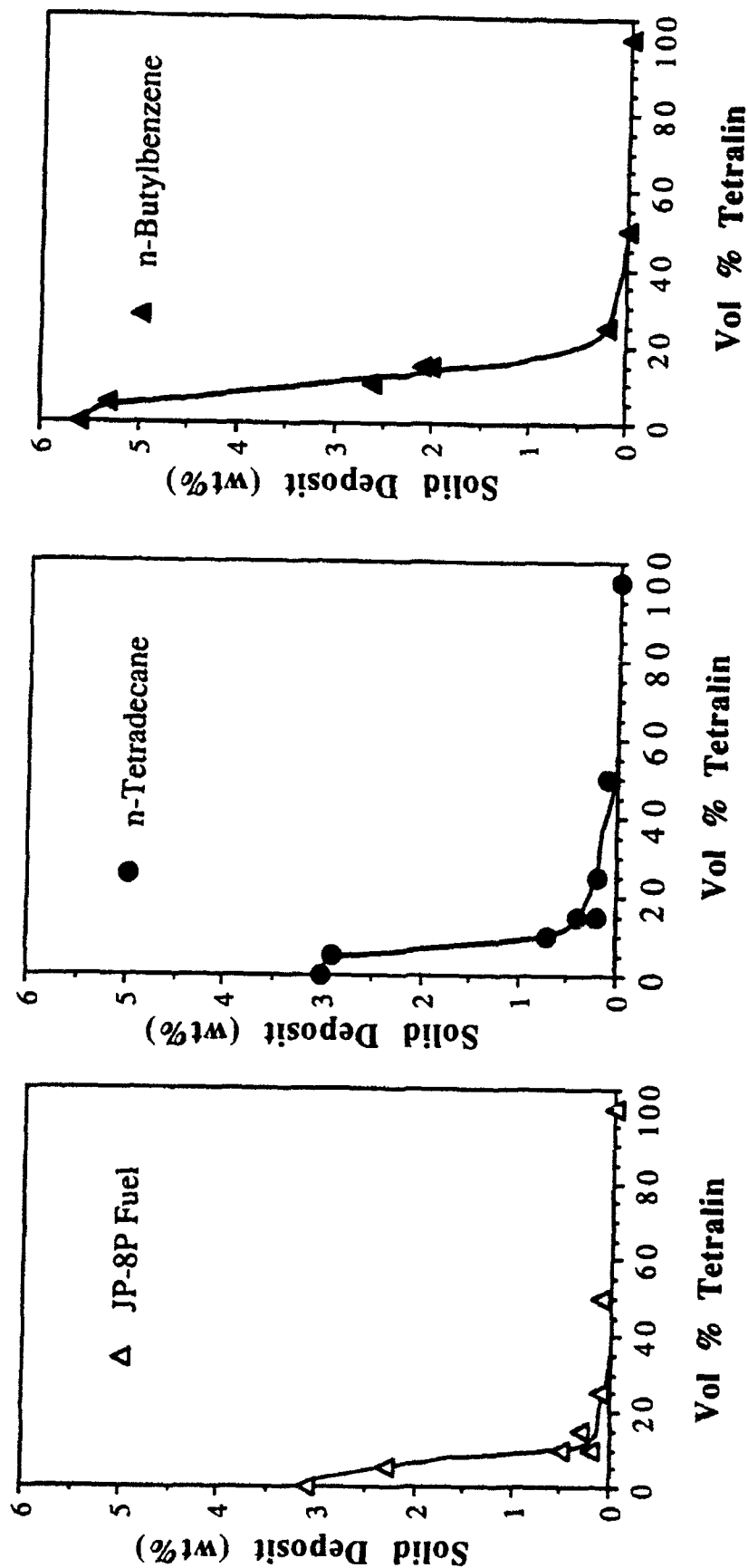


Figure 1.47. Inhibiting effect of tetralin on solid deposit formation from JP-8P fuel, n-C<sub>14</sub>, and n-BB.

**Table 1.8.** Deposit Formation and Liquid Depletion during H-Transferring Pyrolysis of Hydrocarbons and JP-8P Jet Fuel

Feedstocks		Condition		Products (wt%)			
Sample	+ vol% H-Donor	Temp, °C	Time, hs	C1-C4 Gas	≥ C5 Liquid	Solid Deposit <sup>a</sup>	Recovered Deposit <sup>b</sup>
n-Tetradecane		450°C	4.0	38.3	58.8	3.0	1.9
Tetradecane + 50% cis-Decalin		"	"	19.5	80.3	0.1	0
Tetradecane + 50% trans-Decalin		"	"	18.2	81.7	0.1	0
Tetradecane + 10% Tetralin		"	"	27.3	72.0	0.7	0.2
Tetradecane + 50% Tetralin		"	"	9.1	90.8	0.1	0
cis-Decalin		"	"	5.4	94.6	0	0
trans-Decalin		"	"	0.8	99.2	0	0
Tetralin		"	"	0.7	99.4	0	0
n-Butylbenzene (n-BB)		"	"	17.2	77.2	5.6	5.0
n-BB + 50% cis-Decalin		"	"	14.3	85.9	0	0
n-BB + 50% trans-Decalin		"	"	12.1	87.9	0	0
n-BB + 10% Tetralin		"	"	15.4	82.0	2.6	2.5
n-BB + 50% Tetralin		"	"	9.8	90.2	0	0
JP-8P Jet Fuel		"	"	26.8	70.2	3.1	1.9
JP-8P + 50% trans-Decalin		"	"	13.3	86.6	0.1	0
JP-8P + 10% Tetralin		"	"	20.0	79.7	0.3	0.1
JP-8P + 50% Tetralin		"	"	7.9	92.0	0.1	0
n-Tetradecane		450	0.5	5.9	94.1	0	0
n-Tetradecane + 10% Tetralin		"	"	2.3	97.7	0	0
n-Butylbenzene		"	"	5.1	94.9	0	0
n-BB + 10% Tetralin		"	"	5.4	94.6	0	0
n-Butylcyclohexane		"	"	1.8	98.2	0	0
n-Butylcyclohexane + 10% Tetralin		"	"	0.7	99.3	0	0
cis-Decalin		"	"	0.3	99.7	0	0
cis-Decalin + 10% Tetralin		"	"	0.2	99.8	0	0
Tetralin		"	"	0.1	99.9	0	0

a) Solid deposit on the reactor wall determined by measuring weight gain of the microreactor after the stressing, pentane washing and drying; b) Solid deposit recovered from the reactor wall.



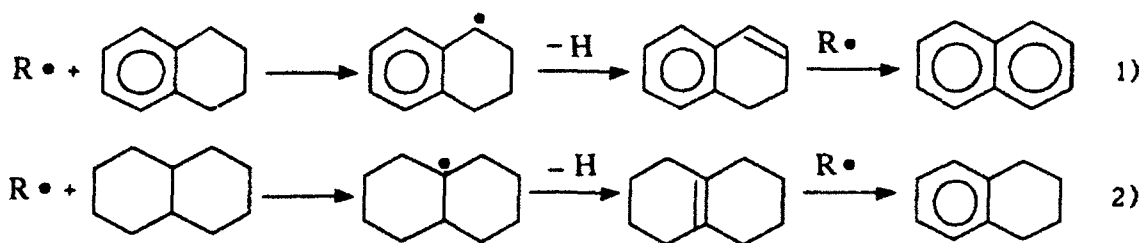


**Figure 1.48.** Radical stabilization via H-transfer from tetralin and decalin.

We further examined the effect of adding 10 vol% H-donor tetralin on pyrolysis of n-C<sub>14</sub>, n-BB, n-BCH, and cis-D at 450°C for 0.5 hours (Table 1.8). Adding tetralin significantly suppressed the n-C<sub>14</sub> decomposition, and its conversion decreased from 49 to 37 mol%. Surprisingly, it was found that the yields of lower alkanes decreased more than those of corresponding 1-alkenes upon tetralin addition. For example, the ratio of 1-dodecene to n-dodecane increased from 1.6 to 2.6, and that of 1-undecene to undecane increased from 0.5 to 0.6 upon addition of 10 vol% tetralin. In long duration runs, the effect of tetralin in suppressing n-C<sub>14</sub> decomposition becomes smaller. This is because H-donors inhibit the radical-induced reactions but do not suppress the homolytic C-C bond cleavage. After 4 hours, the major effects of H-donor appear to be the inhibition of solid and C<sub>1</sub>-C<sub>4</sub> gas formation, as can be seen from Table 1.8.

For 30-minute run of n-BCH, adding tetralin decreased its conversion from about 12 to 6 mol%. In addition to the conversion decrease, the product distribution pattern changed upon tetralin addition. It was found that the decreasing extents in yields of cyclohexane, methyl- and ethylcyclohexane were higher than those for cyclohexene, methyl- and ethylcyclohexene. For cis-D, adding 10 vol% tetralin suppressed the isomerization and decomposition of cis-decalin: the conversion decreased from 12 to 8 mol%, and the cis-D/trans-D ratio increased from 14.2 to 18.9.

### **III. Reactions of H-donors in H-Transferring Pyrolysis**

Tetralin is quite stable when stressed alone at 450°C. The major products from pyrolysis of pure tetralin are 1-methylindan and naphthalene as well as a small amount of n-butylbenzene. Even after 8 hours pyrolysis at 450°C, the total gas products were still within 1 wt%, indicating the ring-opening cracking and dealkylation reactions were very limited with tetralin. On the basis of the findings of Benjamin et al.<sup>18</sup> and Franz et al.,<sup>19</sup> the isomerization proceeds mainly through the 2-tetralyl radical to form 1-indanylmethyl radical, as shown in Figure 1.49.

In the H-transferring pyrolysis of n-C<sub>14</sub> and n-BB, the distribution of products from tetralin shows a significantly different pattern. n-BB is a reactive alkylbenzene.<sup>20</sup> As shown in Figure 1.50, in the presence of n-C<sub>14</sub> or n-BB, tetralin mainly undergoes dehydrogenation reaction to form naphthalene. For the mixtures of 10 vol% tetralin with reactive compounds such as n-C<sub>14</sub> or

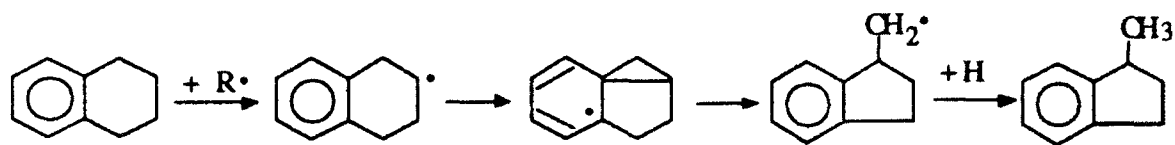


Figure 1.49. Isomerization of tetralin to 1-methylindan

n-BB, the ring-contraction isomerization was enhanced slightly at 450°C for 30 minutes but further increasing residence time increased mainly dehydrogenation. After 4 hours, more than 90% of tetralin has been dehydrogenated in the case of its mixture and its isomerization was reduced significantly as compared to the run of itself. For 30-minute runs, the radicals from n-BB were more active in dehydrogenating tetralin, although n-BB conversion was lower than that of n-C<sub>14</sub> under this condition. For the mixtures of 25 vol% tetralin with n-C<sub>14</sub>, however, the yield of 1-methylindan from tetralin increased significantly after 4-hour run, the value of which is close to that from pure tetralin.

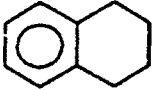
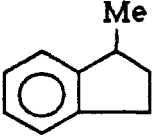
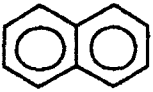
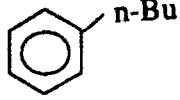
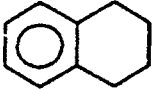
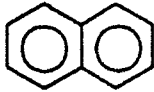
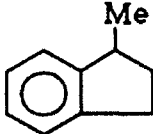
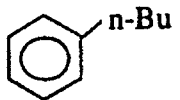
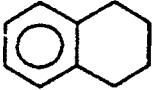
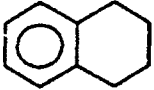
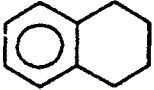
	Pure	 »  » 		
	450°C/30 min	1.7	1.3	0.2 mol%
	450°C/4 h	12.7	4.0	0.5 mol%
	With C <sub>14</sub> or n-BB	 »  » 		
	10% Tetralin-C <sub>14</sub>			
	450°C/30 min	5.9	4.5	mol%
	450°C/4 h	90.9	5.7	mol%
	10% Tetralin-BB			
	450°C/30 min	27.1	3.6	mol%
	450°C/4 h	97.0	2.3	mol%
	25% Tetralin-C <sub>14</sub>			
	450°C/4 h	64.1	12.6	mol%
	25% Tetralin-BB			
	450°C/4 h	92.3	5.6	mol%

Figure 1.50. Products formed from tetralin in pyrolysis & H-transferring pyrolysis.

Taking into account the difference in reaction mechanisms of dehydrogenation (Figure 1.48) and isomerization (Figure 1.49), our results show that when the H-donor concentration is relatively low, the radicals from n-C<sub>14</sub> and n-BB mainly abstract benzylic hydrogen to yield 1-tetralyl radical. In such case, the formation of 2-tetralyl radical is very limited and hence the isomerization is not very important. This also confirms that the reactions via 1-tetralyl radical shown in Figure 1.48 are the major reactions. When tetralin is present at high levels, however, radicals from n-C<sub>14</sub> abstract hydrogens from both 1- and 2-positions. As a result, n-C<sub>14</sub> not only promotes tetralin dehydrogenation, but also enhances its isomerization to form 1-methylindan, although the former is still the dominant reaction. It is also interesting to note that the presence of 90 vol% n-BCH caused little increase in reactions of tetralin, neither dehydrogenation nor isomerization, although tetralin suppressed the n-BCH decomposition from 12 to 6 mol% at 450°C for 0.5 hour. On the contrary, adding 10 vol% tetralin to n-BB had little impact on n-BB conversion and gas formation at 450°C for 0.5 hour, although tetralin dehydrogenation was more remarkable than in the case of n-BCH.

## Conclusions

High temperature thermal stability of hydrocarbons depends mainly on their chemical structure, carbon number, length of main-chain or alkyl side-chain, and steric conformation (cis, trans). Cycloalkanes are more stable than long-chain paraffins. The stability of straight-chain paraffins decreases with increasing carbon number. Increasing the length of side-chain of alkylcyclohexanes decreases the thermal stability. Steric conformance also affects thermal reactivity, and it was found that trans-decalin is much more stable than cis-decalin.

Pyrolysis of n-tetradecane, a JP-8P jet fuel and n-butylbenzene at 450°C can result in significant amounts of solid deposits. Adding small amounts of H-donors such as tetralin and decalins was found to be effective for inhibiting fuel decomposition and solid formation at 450°C. By taking advantage of hydrogen-transferring pyrolysis reported in this work, hydrocarbon jet fuels can be used at high temperatures in pyrolytic regime with little or no solid deposition.

## REFERENCES

1. Roquemore, W.M.; Pearce, J.A.; Harrison III, W.E.; Krazinski, J.L.; Vanka, S.P. ACS Div. Petrol. Chem. Prepr., **1989**, 34 (4), 841.
2. Hazlett, R.N., Thermal Oxidation Stability of Aviation Turbine Fuels, ASTM, 1991, and references cited therein.
3. Song et al., Compositional Factors Affecting Thermal Degradation of Jet Fuels, Technical Progress Report for Period October 1990-January 1991, Air Force Aero Propulsion Laboratory, 42-3462-TPR-2, February, **1991a**.

4. Song et al., Advanced Thermally Stable Jet Fuel Development Program Annual Report, Vol. 2, Final Report for Period July 1990-July 1991, Air Force Aero Propulsion Laboratory, WL-TR-91-2117, Vol. II, August **1991b**.
5. Song, C.; Eser, S.; Schobert, H.H.; Hatcher, P.G., ACS Div. Petrol. Chem. Prepr., **1992a**, 37 (2), 540-547.
6. Song, C.; Peng, Y.; Jiang, H.; Schobert, H.H., ACS Div. Petrol. Chem. Prepr., Vol. 37, **1992b**, 37 (2), 484-492.
7. Lai, W.-C.; Song, C.; Schobert, H.H.; Arumugam, R., Paper in this issue.
8. Eser, S.; Song, C.; Copenhaver, R.; Parzynski, M., ACS Div. Petrol. Chem. Prepr., **1992**, 37 (2), 493-504.
9. Savage, P.E.; Klein, M.T., Ind. Eng. Chem. Res., **1988**, 27, 1348-1356.
10. Roberts, R.M.; Madison, J.J., J. Am. Chem. Soc., **1959**, 81, 5839.
11. Shabtai, J.; Ramakrishnan, R.; Oblad, A.G., Adv. Chem. Ser., **1979**, 183, 297.
12. Allara, D.L.; Shaw, R. J. Phys. Chem. Ref. Data, **1980**, 9 (3), 523-559.
13. Fabuss, B. M.; Smith, J.O.; Satterfield, C.N., Adv. Petrol. Chem. Refin., **1964**, 9, 158-201.
14. Poutsma, M.L., Energy & Fuels, 1990, 4 (2), 113-131.
15. Zhou, P.; Hollis, O.L.; Crynes, B.L., Ind. Eng. Chem. Res., **1987**, 26, 846-852.
16. Fairburn, J.F.; Behie, L.A.; Svrcek, W.V., Fuel, **1990**, 69 (12), 1537-1545.
17. Song, C.; Nihonmatsu, T.; Nomura, M., Ind. Eng. Chem. Res., **1991c**, 30 (8), 1726-1734.
18. Benjamin, B.M.; Hagaman, E.W.; Raaen, V.F.; Collins, C.J. Fuel, **1979**, 58, 386.
19. Franz, J.A.; Camaioni, D.M., J. Org. Chem., **1980**, 45, 5247-5245.
20. Peng, Y.; Schobert, H.H.; Song, C.; Hatcher, P.G., Paper in this issue.

## **TASK 2. CHARACTERIZATION OF SOLID GUMS, SEDIMENTS, AND CARBONACEOUS DEPOSITS**

Carbonaceous solids examined in this work by polarized-light and scanning electron microscopy are the solid samples from an actual fuel line which feeds the burner in an aircraft engine and the solid deposits produced in microautoclaves from stressing a JP-8 Neat fuel with and without an added activated carbon.

### ***Activity 1. Characterization of Solid Deposits from Thermal Stressing of Jet Fuels and Related Compounds by Polarized-Light Microscopy***

#### **Introduction**

Thermal decomposition of jet fuels leads to the formation of solid deposits which interfere with various functions of an aircraft fuel system.<sup>1</sup> Only a limited number of many studies on autoxidative deposit formation from jet fuels were concerned with the microstructure or morphology of solid deposits.<sup>2-5</sup> Scanning electron microscopy (SEM) studies of autoxidative jet fuel deposits showed that the deposits are usually microspherical particles approximately 100 nm in diameter, although particles in the shape of plates or rods are also present.<sup>3</sup> SEM analysis of deposits obtained from pure compound blends showed that the dissolved oxygen levels had a significant influence on the morphology of deposits.<sup>2</sup> Elemental analysis of autoxidative deposits gave high concentrations of oxygen (15 to 30 wt%),<sup>6</sup> while a deoxygenated fuel produced deposits at 371-482°C with much lower oxygen contents (3 wt%).<sup>7</sup> There is not much information available on the microstructure of deposits formed by high-temperature (>350°C) stressing of jet fuels. We reported earlier that a sample of actual engine deposits from an aircraft fuel system contained deposits with distinctly different particle morphologies.<sup>8</sup> The examination of these particles by polarized-light microscopy showed that the different particle morphologies can be related to different microstructures formed separately by liquid-phase and gas-phase pyrolysis reactions.

In this report we present polarized-light microscopy studies of solid deposits produced by thermal stressing of petroleum- and coal- derived JP-8 jet fuels and some model compounds including decane, tetradecane, decalin, and n- and t-butylbenzene. The characterization of solid deposits by polarized light microscopy can provide answers to the following questions:

- Do the solids have isotropic or anisotropic microstructures ?
- Is the solid deposition catalyzed by the metal surfaces ?
- Are the solids produced by liquid-phase or gas-phase reactions ?

All of these questions are important for understanding the mechanisms of solid deposition. Studies on chemical mechanisms and kinetics of solid formation from jet fuels and model compounds are presented separately in this symposium.<sup>9-11</sup>

## **Experimental**

All thermal treatments of the model compounds and the jet fuel samples were conducted isothermally at temperatures 400-450°C in 25 cc 316 stainless steel reactors heated in a fluidized-sand bath. The experimental procedure is given elsewhere.<sup>9</sup>

For microscopic examination of the solid deposits, the samples were embedded in epoxy resin to prepare polished sections for microscopic examination by using conventional methods.<sup>12</sup> A brief description of the microscope system and the interpretation of the optical image is given below.

A Zeiss microscope (Model GFL) with a rotating stage was used to examine the polished specimens in incident plane-polarized light obtained by placing a polarizer between the light source and the specimen surface. Another polarizer was inserted in the path of the reflected light. With the incorporation of a retardation (phase-sensitive plate, red-quartz, 1/4 -wave in this case), an anisotropic coke or carbon exhibits from its surface yellow, blue and dark purple areas.<sup>13</sup> Each color, formed by wave interference of the reflected light,<sup>14</sup> represents a section of a volume element with a certain crystallite orientation. A purple color is indicative of basal planes (large sheets of polynuclear aromatic molecules) lying parallel to the surface. The surface of isotropic cokes also exhibits a purple color which is somewhat lighter in shade. Both purple colors remain unchanged upon the rotation of the specimen stage. Yellow and blue colors are seen when a prismatic edge is presented to the surface. A rotation of the specimen stage by 90° changes a yellow color into a blue color and vice versa. Therefore, the size and shape of the isochromatic areas indicate the extent of microstructural order present in the specimen. After viewing each specimen, selected areas were photographed using 400 ASA 35 mm color film and a Nikon camera attached to the microscope.

## **Results and Discussion**

### **Aircraft Fuel System Deposits**

Two different samples of solid deposits produced in aircraft fuel systems (AR and BR) were examined by polarized-light microscopy. The first sample (AR) contained two types of macroscopically different solids (the flakes and globular particles) found in the actual fuel system deposits were formed via different mechanisms. Based on their microstructure, it was concluded that the flakes were formed primarily by gas (or vapor) phase reactions leading to a pyrolytic carbon texture under severe thermal stress conditions.<sup>8</sup> On the other hand, the porous globular particles were formed in the liquid phase involving the mesophase development from an isotropic

matrix which had been formed via cracking and polymerization of fuel components.<sup>8</sup> The second sample (BR) also showed a pyrolytic carbon microstructure, but quite different from that seen in the flaky solids of sample AR. In contrast to the well-aligned extended layered structure of the flakes in AR, BR shows, in general, a more isotropic, mosaic structures of pyrolytic carbon, as shown in micrograph **a** in Figure 2.1. There are also isolated regions of more ordered structures in BR solids (Figure 2.1, micrograph **b**) similar to those seen in AR flakes. It is clear that the deposits in the sample BR were formed under quite different conditions from those that produced the AR flakes. Most likely, BR solids were formed at lower temperatures with high concentrations of solid precursors. Figure 2.2 shows scanning electron micrographs of BR solids, clearly indicating the pyrolytic carbon microstructures of these solids.

Many mechanisms have been proposed to explain the formation of pyrolytic carbons.<sup>15</sup> The proposed mechanisms differ in terms of the intermediate species and the sequences of aggregation involved in the formation of carbons from relatively small molecules. The models which involve polymerization reactions to form large molecules of carbon atoms arranged in hexagonal arrays appear to be most relevant to the formation of gas phase deposits from jet fuels. The growth cones and the overall order present in the AR flakes and BR suggest that the deposition involved large complexes formed in the gas phase before condensation on the tube surface or on the surface of the previously formed carbonaceous layer. Although the reactions in the gas phase appear to govern the formation of tube deposits, the presence of an intermediate liquid phase condensed as droplets in the gas phase or on the substrate surfaces cannot be ruled out for either sample. A common feature of both AR flakes and BR solids was that growth structures indicated "regenerative" or "continuous" nucleation, suggesting that the nucleation of the deposits took place in the gas phase or on the previously formed carbonaceous deposits.<sup>15</sup> This observation further suggests that the initial substrate surface did not play a catalytic role in the deposition of solids.

As different from AR flakes and BR solids, AR globules were clearly formed in a liquid-phase which involves carbonaceous mesophase development. Carbonaceous mesophase is a plastic, anisotropic phase which is formed during carbonization of a range of materials including petroleum feedstocks, thermoplastic polymers, and polynuclear aromatic compounds. Mesophase is considered as a unique ordered fluid consisting of essentially planar molecules of polynuclear aromatic hydrocarbons which are aligned roughly parallel to each other without any order of stacking sequence.<sup>16</sup> Some properties of carbonaceous mesophase resemble some characteristics of nematic liquid crystals. Considering that major components of jet fuels are straight-chain paraffins and that mesophase formation involves a gradual generation of large polyaromatic molecules, one can conclude that the formation of globular solids in the aircraft fuel system requires prolonged exposures (practically hours) to relatively high temperatures (400-500°C).

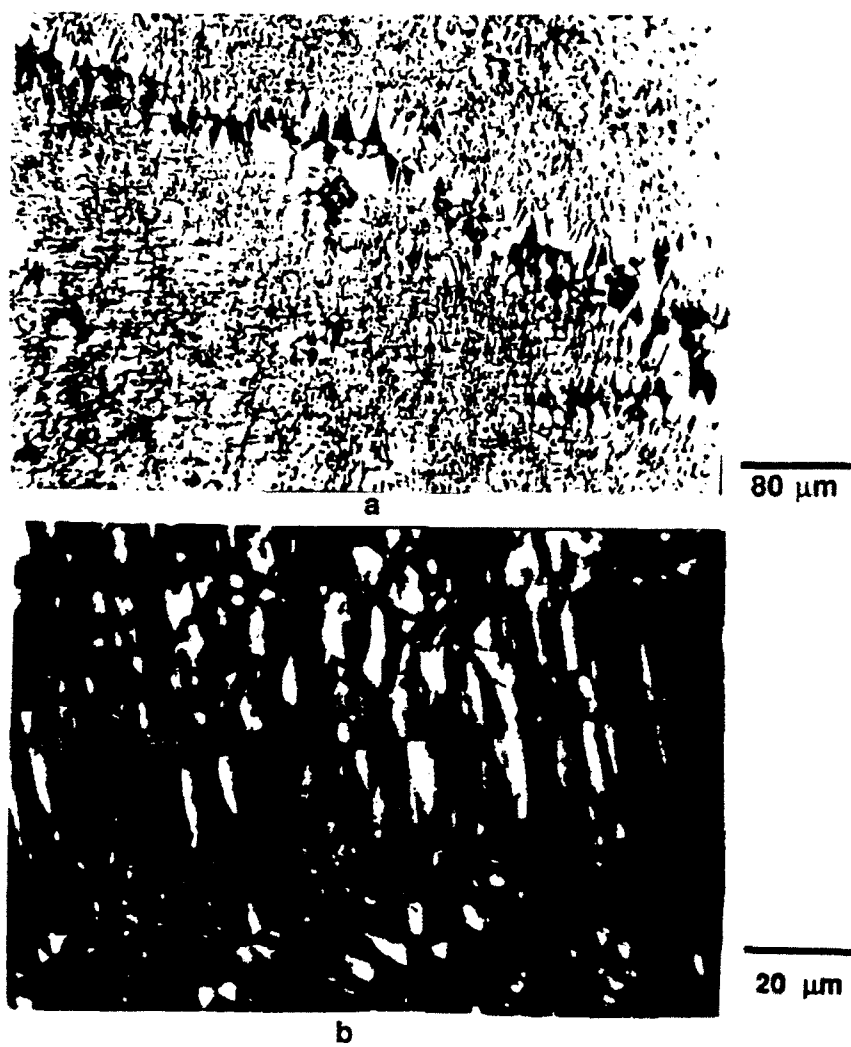


**Figure 2.1.** Polarized-light micrographs of the burner solids (BR)



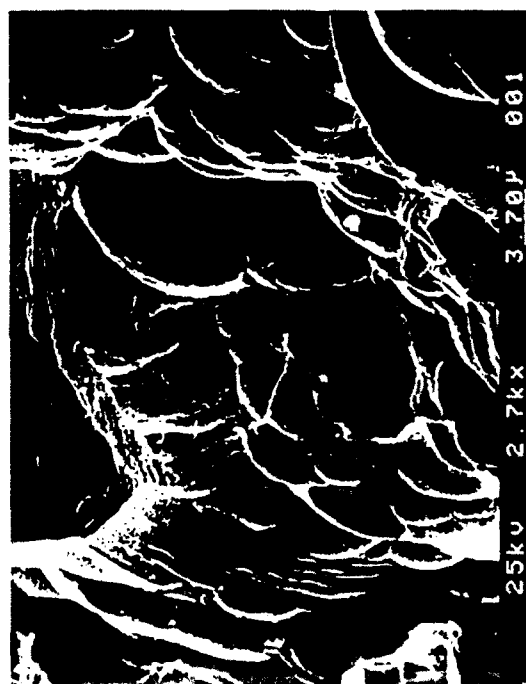
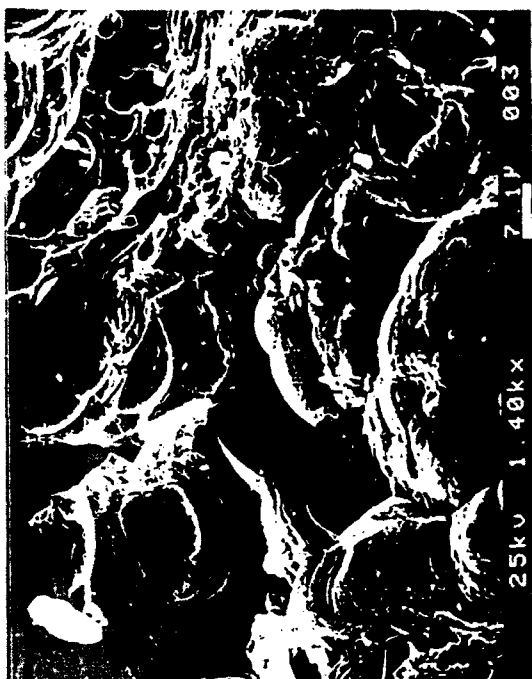


**Figure 2.2.** Scanning electron micrographs of the burner solids (BR).

This observation should be taken into consideration in designing stressing experiments to determine the thermal stability of jet fuels.

The solid deposits produced in laboratory reactors showed some similarities in structure to those produced in actual aircraft fuel systems. The microstructures of some laboratory deposits are described and discussed below.

### **Laboratory Reactor Solids**

#### ***Solids from Jet Fuels***

In both petroleum-derived JP-8 (JP-8P) and coal-derived JP-8 (JP-8C) solids produced at 450°C in stainless reactors under autogenous pressure, we observed particles showing the nucleation of mesophase spheres in an isotropic matrix, the initial stage of mesophase development.<sup>16</sup> Gas-phase deposits in the form of flakes with pyrolytic carbon microstructures were also common to the solids produced by JP-8P and JP-8C at 450°C. Figure 2.3 shows the optical textures of the solids produced from JP-8P and JP-8C at 450°C -16 hours in a nitrogen atmosphere. In Figure 2.3a, JP-8P solids show a band of pyrolytic carbon deposited on top of a particle formed by liquid-phase reactions involving mesophase development. JP-8C solids, shown in Figure 2.3b, exhibit a large particle formed via mesophase development and a thin flake of an anisotropic solid carbon produced by gas-phase reactions. These observations indicate that both gas-phase and liquid-phase reactions were involved in the formation of solid deposits from jet fuels in batch reactors. JP-8P produced more gas-phase carbons than JP-8C under comparable conditions. In general, the solids produced from JP-8C exhibit a higher degree of mesophase development preceding the formation of solids than those obtained from JP-8P. It can be inferred that the reaction intermediates, or solid precursors, produced during the thermal stressing of JP-8C are more planar and less reactive, in other words, more aromatic, than those involved in solid formation from JP-8P. Also, hydrogen transfer reactions involving hydroaromatic compounds as hydrogen donors, which are present in high concentrations in JP-8C, promote mesophase development via stabilizing the nascent free radicals.

It appears that, in addition to the temperature, the stressing pressure and/or the concentration of volatile reaction products also have a significant effect on the microstructure of the solids produced from jet fuels. For example, the doubling of the sample volume of JP-8C (from 5 to 10 ml) appears to have changed the solid formation mechanisms from predominantly liquid-phase reactions (carbonaceous mesophase) to predominantly gas-phase reactions (pyrolytic carbons). This effect can be explained by increased stressing pressure and the attendant changes in phase equilibrium and/or formation of a supercritical phase.

#### ***Solids from Model Compounds***

Rather thick flakes (80-200  $\mu\text{m}$ ) were produced upon thermal treatment of decane at 450°C. A high degree of preferred orientation was, clearly visible. In addition, more randomly ordered, large mesophase structures and finer structures in flakes were also present in decane solids.

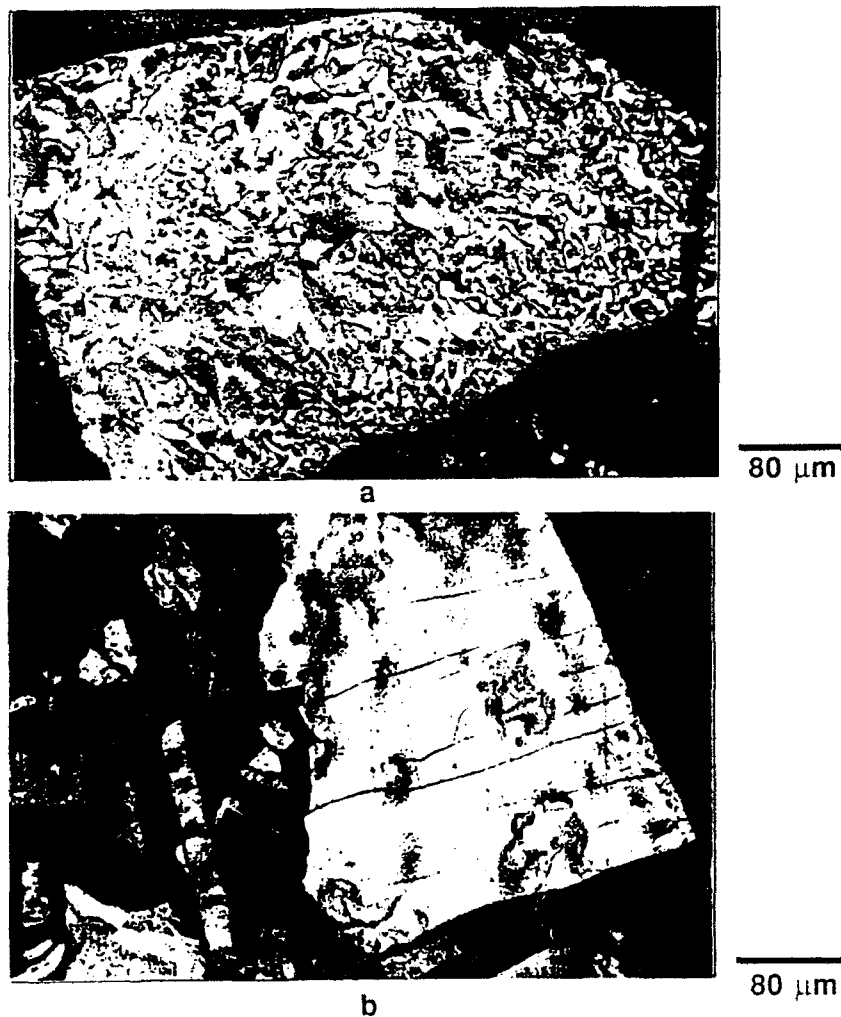


**Figure 2.3.** Polarized-light micrographs of the solids produced from JP-8P (a) and JP-8C (b) by thermal stressing at 450°C for 16 h in nitrogen.

The deposits recovered from the top of the microautoclaves after the treatment of dodecane at 475°C showed flakes with typical pyrolytic carbon texture, whereas the solids formed at the bottom of the reactors showed signs of mesophase development and porous structures. This observation, again, points out the simultaneous occurrence of gas-phase and liquid-phase reactions leading to solid formation.

Thermal stressing of n-butylbenzene at 450°C produced a range of mesophase structures (from mosaics to flow domains) in the solids, whereas t-butylbenzene produced isotropic and fine mosaic structures in the solids produced by both gas- and liquid-phase reactions. It is clear that the reaction intermediates leading to the formation of solids from these two isomers are different, in addition to the difference in relative thermal stability of these compounds.<sup>9,10</sup>

One particular feature of the flakes found in the sample AR was its layered nature, which was attributed to temperature cycles as effected by the flights of the aircraft. A series of experiments was planned to consist of multiple stressing of 10 ml of tetradecane at 450°C for 8 hours with quenching and making up the depleted liquid volume to 10 ml after each stressing. The thermal stressing was carried out three times, and the solids were recovered only after the third stressing.

A microscopic examination of the solids obtained from tetradecane by multiple stressing, indicated layered structures somewhat similar to those observed in the AR flakes with, however, a significantly lower degree of crystallite alignment. These structures indicate that principally the gas-phase reactions were responsible for the formation of solids during multiple stressing of tetradecane. The presence of layered microstructures indicates, on the other hand, that the surface of the solid deposits initially produced can act as a substrate for further solid deposition (i.e., regenerative nucleation), as was also found in the AR flakes.

## Conclusions

Polarized-light microscopy is useful for characterization of solid deposits especially in determining the microstructural isotropy or anisotropy present in the deposits. The examination of deposit samples from aircraft fuel systems and those from laboratory stressing experiments showed similarities between both sets of samples. Both liquid-phase (carbonaceous mesophase) and gas-phase (pyrolytic carbon) reactions are involved in the formation of solid deposits in aircraft fuel systems and in batch reactors. The deposition of solids in aircraft fuel systems does not appear to be catalyzed by tube surfaces, and liquid phase deposits appear to have been formed after hours of exposure to rather high temperatures (400-500°C).

## References

1. CRC Literature Survey on the Thermal Oxidation Stability of Jet Fuel, CRC Report No. 509, Coordinating Research Council, Inc., Atlanta, Georgia, 1979.

2. Frankenfeld, J. W. and Taylor, W. F., Ind. Eng. Chem. Prod. Res. Dev., 19, 65, 1980.
3. Schirmer, R. M., "Morphology of Deposits in Aircraft and Engine Fuel Systems," SAE National Air Transportation Meeting, New York, N.Y., Paper 700258, Apr. 1970.
4. Roback, R., Szetela, E. J., and Spadaccini, L. J., J. Eng. Power, 105, 59, (1983).
5. Giovanetti, A. J. and Szetela, E. J., J. Propulsion, 2, 450, (1986).
6. Nixon, A. C., in "Autoxidation and Antioxidants," Vol. II, W. O. Lundberg, Ed., Interscience, New York, N.Y., 1962.
7. Taylor, W. F., Ind. Eng. Chem. Prod. Res. Dev., 13, 133, 1974.
8. Eser, S., Song, C., Schobert, H. H., Hatcher, P. G., Extended Abstracts, 20th Biennial Conf. on Carbon, p. 440, 1991.
9. Eser, S., Song, C., Copenhaver, R., and Parzynski, M., Am. Chem. Soc. Div. Petrol. Chem. Prepr., Vol. 37, 1992, No.2, 493-504.
10. Peng, Y., Schobert, H. H., and Song, C., Am. Chem. Soc. Div. Petrol. Chem. Prepr., Vol. 37, 1992, No.2, 505-513.
11. Song, C., Peng, Y., Jiang H, and Schobert, H. H., Am. Chem. Soc. Div. Petrol. Chem. Prepr., Vol. 37, 1992, No.2, 484-492.
12. Dubois, J., Agache, C. and White, J. L., Metallography, 3, 337 (1970).
13. Smith, J. and Marsh, H. in "Analytical Methods for Coal and Coal Products," (Ed. C. Carr, Jr.), Academic Press, NY, Vol. 2, 371, 1978.
14. Forrest, R. A. and Marsh, H., Carbon, 15, 348, 1977.
15. Bokros, J. C., in "Chemistry and Physics of Carbon," (Ed. P. L. Walker, Jr.), Dekker, NY, 5, 1, 1969.
16. Brooks, J. D. and Taylor, G. H. in "Chemistry and Physics of Carbon," (Ed. P. L. Walker, Jr.), Dekker, NY, 4, 243, 1968.

## ***Activity 2. FORMATION OF SOLID DEPOSITS FROM JET FUELS IN THE PRESENCE OF DIFFERENT SOLID CARBONS***

### **Introduction**

The thermal stability of an aviation fuel is a major concern for the operation of advanced aircraft systems which are exposed to high temperatures ( $> 350^{\circ}\text{C}$ ). Thermal stressing of jet fuels at high temperatures produce carbonaceous deposits in fuel lines. Although the thermal stability of hydrocarbon fuels has been studied for a long time, an understanding of the processes involved in the formation and deposition of solids is still limited.<sup>1-4</sup>

The formation of surface deposits from the decomposition of jet fuels is governed by a number of chemical and physical processes. When dissolved oxygen is present in the fuel, the

increase of fuel temperature can result in autoxidation reactions and the formation of free radicals which can lead to the production of carbonaceous deposits on the walls.<sup>5</sup> In the absence of oxygen at high temperatures, pyrolysis reactions create the reactive free radicals which eventually lead to the formation of solid.<sup>4,5</sup>

There is not much information available on the microstructure of deposits formed by high-temperature stressing. We reported earlier that a sample of actual engine deposits from an aircraft fuel system contained deposits with different morphologies and microstructures resulting from both gas-phase and liquid-phase reactions.<sup>6,7</sup> The presence of an added solid carbon during thermal stressing appears to have a substantial influence on the amount and structure of the deposits. This information may be particularly relevant to understanding the role of initial carbonaceous deposits on further formation and deposition of solids during thermal stressing. In this study, we investigated the effects of adding activated carbons, a carbon black and a graphite on solid formation from a commercial jet fuel sample thermally stressed in a batch reactor.

## **Experimental**

Thermal stressing experiments were carried out on 10-ml samples of a commercial JP-8 jet fuel mixed with 1-g samples of two different activated carbons, a carbon black and a graphite spectroscopic powder SP-1. JP-8 jet fuel with and without the added solid carbons was heated in vertical stainless steel microautoclaves. In order to remove air, microautoclaves were pressurized five times to 1000 psi with subsequent depressurization using UHP N<sub>2</sub>. After pressurizing to 100 psi with UHP N<sub>2</sub> the reactors were immersed in a preheated fluidized-bed sand bath. Thermal stressing experiments were carried out at 450°C and 475°C for 5 and 2.5 hours, respectively. Dodecane was also stressed at 450°C in the presence of an activated carbon to compare its behavior with that of JP-8 jet fuel.

For analyzing the liquid products, a Perkin-Elmer 8500 Gas Chromatograph with a fused silica capillary column was used. In addition, the liquid products were also analyzed by GC/MS (Hewlett-Packard 5890 interfaced with a HP 5971A Mass Selective Detector) and by UV/VIS spectrophotometry (Perkin Elmer- Lambda). Gas products were analyzed using an autosystem GC Perkin-Elmer with an FID detector and Chemipack C18 columns. The solids were examined by a polarized-light microscope (Nikon-Microphot-FXA) and an ISI 6-40 Scanning Electron Microscope.

## **Results and Discussion**

### **Product Yields from Stressing of JP-8 and Dodecane with Added Solid Carbons**

A distinct difference in the appearance of the liquid products obtained at 450°C from JP-8 and dodecane was that the liquids obtained in the presence of the activated carbons were much lighter in color than those obtained in the other experiments with and without the added carbons.

The addition of carbon black also produced a lighter color liquid product but the effect was not as pronounced as that seen with the activated carbons. The SP-1 graphite addition did not produce much change in the appearance of the liquid products at 450°C. In other words, the solid carbons with the most disordered structure and highest surface reactivity (i.e., activated carbons) produced the most significant effect on thermal degradation, while the most ordered and the least reactive solid (SP-1 graphite) did not have any significant influence on thermal reactions. The presence of added carbons during thermal stressing of the jet fuel and dodecane also produced substantial changes in the yield and composition of the stressing products, especially when the activated carbons were added. Table 2.1 contains some of the results from the experiments carried out at 450 and 475°C. The reproducibility of selected data obtained from multiple duplicate experiments is also shown in Table 2.1.

Invariably, for both jet fuel and dodecane, a lower liquid yield and higher gas pressures were obtained when solid carbons were present. It should be noted that the addition of carbons, especially activated carbons, prevents the deposition of solids on the reactor walls at 450°C. Although at 475°C, some deposits were observed on reactor surfaces in the presence of the solid carbons, the amount of deposits was much less than that produced by the stressing of JP8 alone. All the solid carbons gained weight during stressing at 475°C, while only activated carbons and carbon black gained weight at 450°C without a change in the weight of SP-1 graphite. For example, the weight gain of the activated carbon-1 after stressing with JP-8 is 54% at 450°C and 71% at 475°C. Based on the microscopic examination and thermal gravimetric analysis (TGA) of the added activated carbon after stressing, we believe that a large part of the weight gain by the activated carbon at 450°C is not due to massive solid deposition on the activated carbon, but to the adsorption of the heavy, non-volatile liquid stressing products and rather thin layers of solid carbon deposits ( $<0.5\text{ }\mu\text{m}$ ) on the activated carbon surface compared to thick deposits ( $>500\text{ }\mu\text{m}$ ) formed on reactor walls. A TGA analysis of the original activated carbon-1 and the activated carbon particles after stressing with JP8 showed a 6% more weight loss from the latter when heated to 700°C in nitrogen. We don't believe that this weight loss accounts for all the adsorbed species on the carbon surface; it most probably excludes the high-molecular weight polycondensed aromatic compounds that are strongly adsorbed on the surface.

#### **Head Space Gas Composition and Yields from Stressing JP-8 with/without Added Carbons**

In addition to the varying liquid and solid product yields, the head space gas yield and composition were also different for different carbons added before stressing JP-8. Figure 2.4 shows the gas chromatograms for the head space gases obtained from stressing JP-8 with and without the added activated carbon 1 (AC-1) at 450°C and Table 2.2 shows the headspace gas

**Table 2.1.** Yields of liquids and solids products and pressure build-up from thermal stressing experiments on jet fuel and dodecane.

Sample Liquid: 10 ml Solid: 1 g	Solid on reactor wall mg $\pm$ 10 mg		Liquid yield, ml $\pm$ 0.3 ml		Final gas pressure (hot) psi $\pm$ 100 psi		Increase of weight of solid, %	
Temperature, °C	450	475	450	475	450	475	450	475
JP8 without carbon	84	187	5.2	4.0	800	1300	-	-
JP8 + Activated Carbon-1	0	71	3.5	2.5	1900	3000	54	71
JP8 + Activated Carbon-2	0	n.a.†	3.3	n.a.†	n.a.†	1750	58	n.a.†
JP8 + Carbon black	n.m.*	98	4.5	3.0	1800	3200	35	68
JP8 + Graphite	n.m.*	146	3.8	2.9	1300	3800	0	41
Dodecane	150	n.a.	5.0	n.a.	1000	n.a.	-	-
Dodecane + Activated Carbon-1	n.m.*	n.a.	4.0	n.a.	1500	n.a.	49	n.a.†

\*not measured, negligible amount

†not applicable or available

composition obtained at 450 and 475°C. Table 2.3 shows the yields of headspace gases, including a GC analysis using a TCD detector, obtained with and without the added carbons from 10 ml of JP-8 stressed at 450°C for 5 hours. In general, the addition of solid carbons produced less C<sub>1</sub> and C<sub>2</sub> and more C<sub>3</sub>, C<sub>4</sub> and C<sub>5</sub> compounds. The headspace gas obtained from stressed JP-8 mixed with carbons, especially with AC-1, contains higher concentrations of CO<sub>2</sub> gas resulting probably from the decomposition of the surface oxygen functionalities present in the solid carbons.

#### **Analysis of Liquid Products from Stressing of JP-8 and Dodecane with/without Added Carbons**

The liquids obtained from stressing of JP-8 with and without the added carbons appear to consist of similar compounds but at different concentrations. A distinct difference in the appearance of the liquid products obtained at 450°C was that the liquids obtained from stressing of JP-8 mixed with the activated carbons were much lighter in color than those obtained in the all the



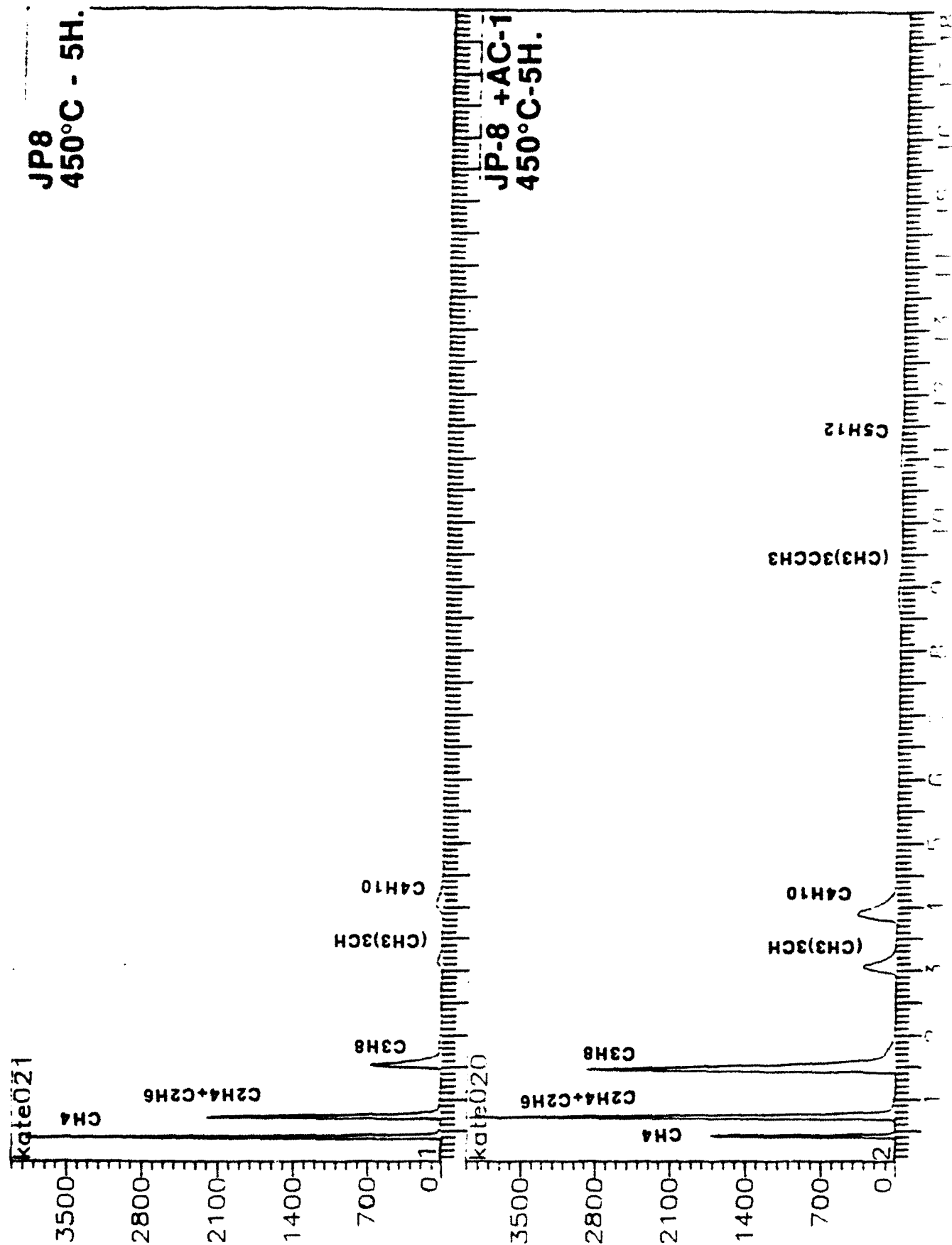


Figure 2.4. Gas chromatograms for head space gases obtained from JP-8 with and without the added activated carbon - 1 at 450°C for 5 h.

**Table 2.2.** Headspace gas composition determined by GC using a FID detector.

	CH <sub>4</sub>	C <sub>2</sub> H <sub>6</sub> + C <sub>2</sub> H <sub>4</sub>	C <sub>3</sub> H <sub>8</sub>	C <sub>3</sub> H <sub>6</sub>	i- C <sub>4</sub> H <sub>10</sub>	n- C <sub>4</sub> H <sub>10</sub>	n- C <sub>5</sub> H <sub>12</sub>	C <sub>5</sub> H <sub>10</sub>
450°C								
JP8 without carbon	38.3	32.1	18.2	0.7	2.6	4.8	0.9	1.0
JP8 + Activated Carbon-1	8.2	26.0	37.8	0.0	6.9	11.1	1.9	0.0
JP8+ Carbon black	33.4	31.0	20.4	0.9	3.5	5.8	1.4	0.0
JP8 + Graphite	19.8	29.9	28.0	1.4	4.8	8.8	1.9	0.2
475°C								
JP8 without carbon	40.7	32.0	14.3	3.6	2.8	4.3	0.3	0.0
JP8 + Activated Carbon-1	34.4	35.4	21.8	0.0	3.5	4.9	0.0	0.0
JP8 + Carbon Black	9.3	21.5	26.6	1.7	5.1	9.3	1.7	3.4
JP8+ Graphite	41.6	26.0	12.0	0.0	1.9	7.8	0.3	0.0

other experiments with or without the added carbons. A comparison of the integrated peak intensities obtained from the GC analysis showed that the concentration of paraffins in the liquid obtained from JP-8 mixed with the activated carbons was significantly higher than that in the liquid obtained from JP-8 stressed alone. At 475°C, however, the concentration of alkylbenzenes were seen to be higher in the liquid obtained from JP8 with the activated carbons. A comparison of the UV spectra of liquids obtained at 450°C showed lower concentrations of two- and three-ring

**Table 2.3.** Head space gas yields from JP-8 with and without added carbons.

Compound	JP8, ml	JP8 ml	JP8 +AC-1 ml	JP8 +AC-1 ml	JP8 +CB ml	JP8 +CB ml	JP8 +SP-1 ml	JP8 +SP-1 ml
Temperature, °C	450	475	450	475	450	475	450	475
CH <sub>4</sub>	256	359	66.0	171.0	216	64	128.0	286
C <sub>2</sub> H <sub>6</sub> + C <sub>2</sub> H <sub>4</sub>	214	212	208.0	267.4	208	148	185.6	174
C <sub>3</sub> H <sub>8</sub>	121	92.6	304.0	198.4	134	145	187.0	81
C <sub>3</sub> H <sub>6</sub>	4.8	24.6	-	-	4.2	11.4	9.6	-
i-C <sub>4</sub> H <sub>10</sub>	17.8	18.2	56.0	36.0	24.4	35.6	31.0	12.0
n-C <sub>4</sub> H <sub>10</sub>	32.3	29.0	89.5	62.9	38.9	65.3	62.3	60.2
C <sub>4</sub> H <sub>8</sub>	1.6	8.2	6.8	3.5	1.0	4.2	3.0	1.6
i-C <sub>5</sub> H <sub>12</sub>	6.1	6.8	15.6	8.0	12.5	12.8	12.7	4.1
n-C <sub>5</sub> H <sub>12</sub>	6.6	3.3	29.9	-	9.4	13.2	13.2	2.2
H <sub>2</sub>	0.3	0.2	0.3	0.3	0.2	0.3	0.4	0.2
CO	1.1	1.0	0.7	0.8	0.9	1.2	0.9	0.7
CO <sub>2</sub>	0.3	0.5	7.5	5.2	1.2	1.4	2.4	2.1
TOTAL GAS, ml	662	755	784	754	650	502	636	624

aromatic compounds in the liquid produced from stressing JP-8 mixed with the activated carbons. Most probably, the darker color of the JP8 stressed without the activated carbons is due to the increased concentrations of the alkyl substituted polynuclear aromatic hydrocarbons, which are the most likely precursors to carbonaceous solids.<sup>4</sup>

Figure 2.4 shows the selected ion chromatograms of JP8 stressed alone and with activated carbon-1 at 450°C for 5 hours using split injection of undiluted sample. Although the injection conditions were the same for both liquids, much weaker signals were obtained from the liquid produced from JP-8 alone most probably because of the heavy nature of this liquid. Figure 2.5 shows ion chromatograms for fragment ion of  $m/z$  71, which is characteristic of long chain paraffins, showing the relatively high concentrations of paraffins with 10 or more carbon atoms in the liquid produced from JP-8 in the presence of AC-1. Figure 2.6 shows the ion chromatograms for the ion of  $m/z$  91 indicating the presence of alkylbenzenes, and Figure 2.7 shows the



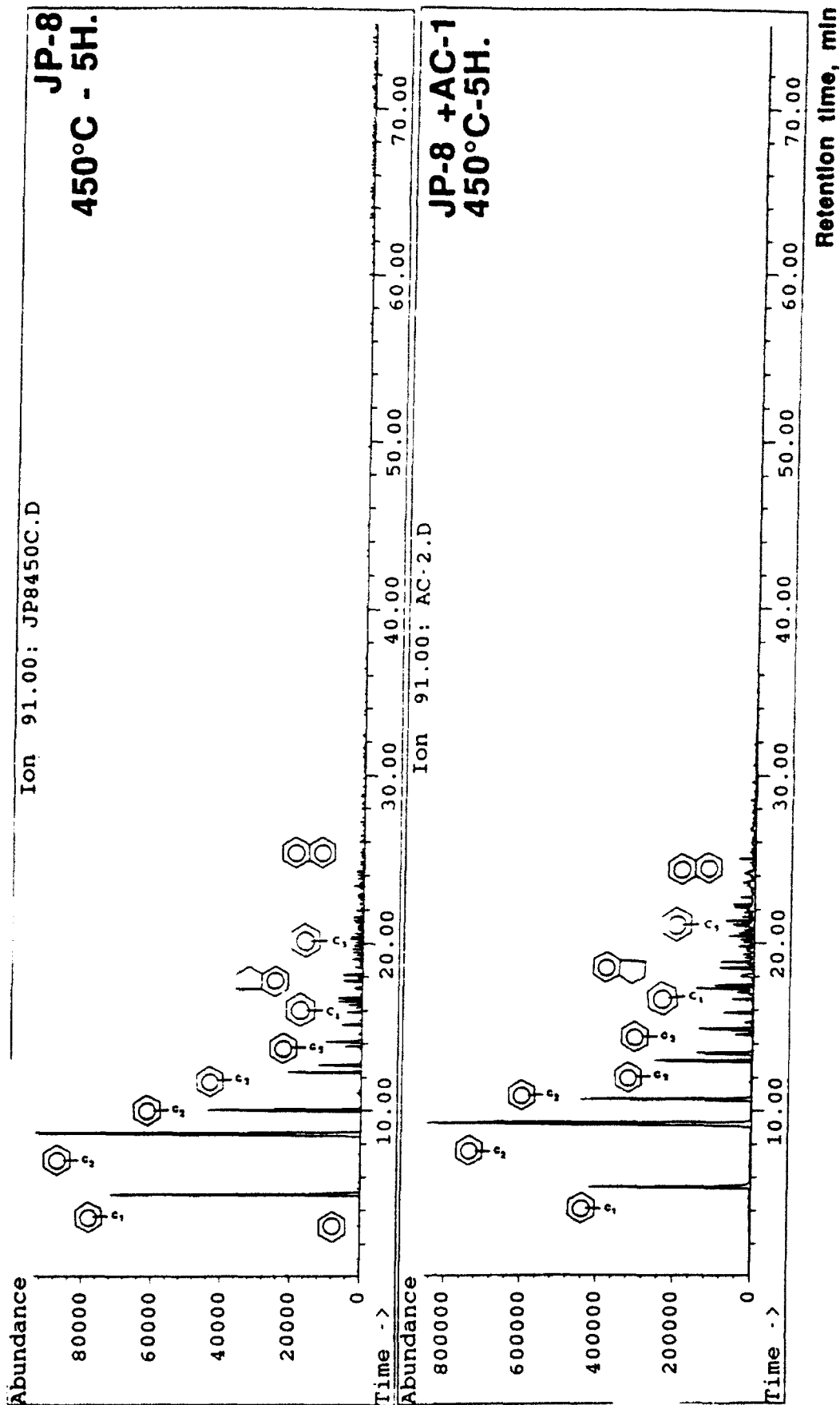


**Figure 2.6.** Specific ion chromatograms for mass 91 for the liquids obtained from JP-8 alone and JP-8 with activated carbon-1 stressed at 450°C for 5 h.

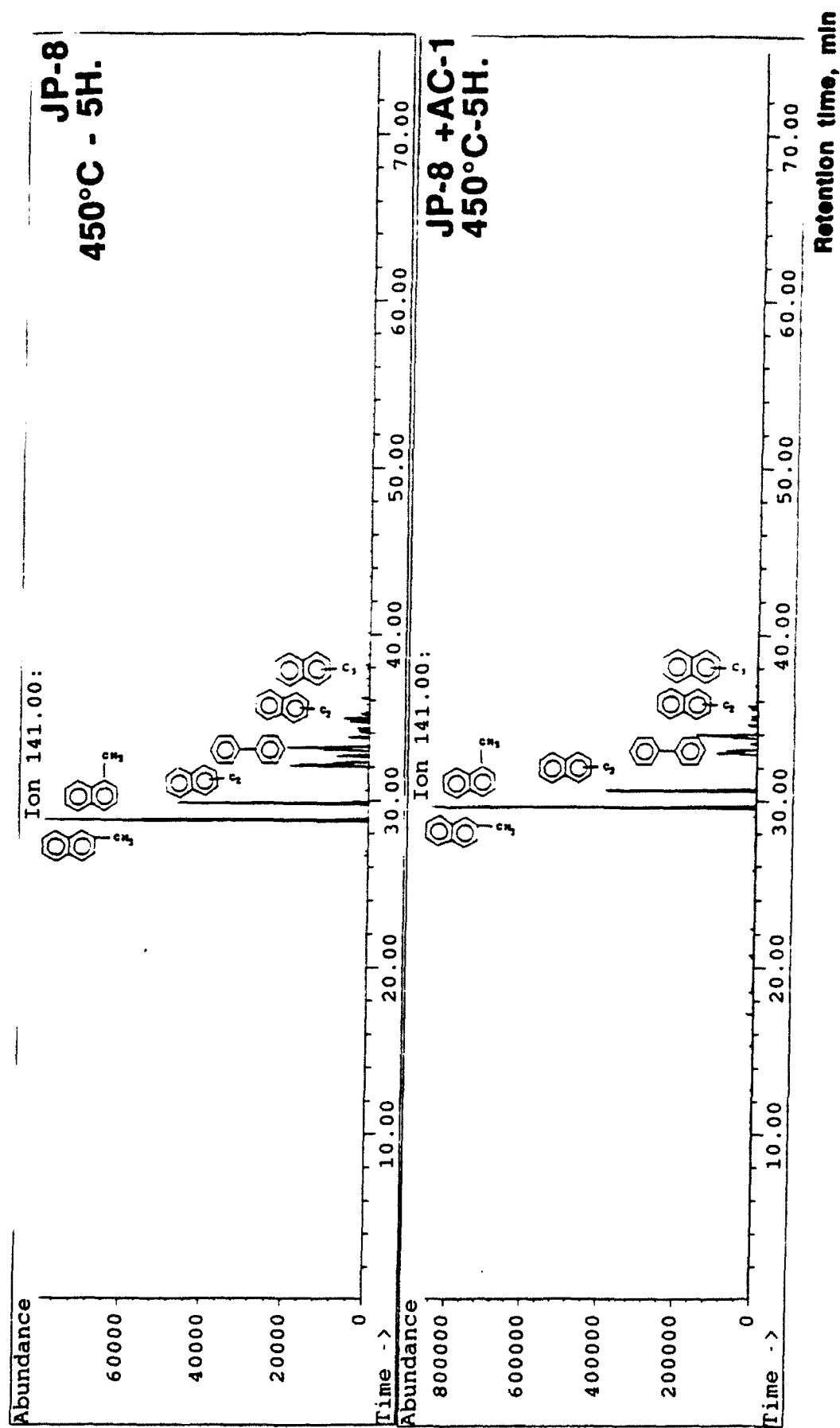


Figure 2.7. Specific ion chromatograms for masses 141 and 142 for the liquids obtained from JP-8 alone and JP-8 with activated carbon-1 stressed at 450°C for 5 h.

chromatograms for the ions of  $m/z$  141 and 142 which are characteristics of alkylnaphthalenes. Both Figure 2.6 and Figure 2.7 show higher concentrations of heavier aromatics present in the liquid product obtained from stressing JP-8 alone, compared to that obtained in the presence of the activated carbon-1. It appears that the presence of activated carbons produces a lower yield of liquids, which consists, however, of higher concentrations of paraffins and lower concentrations of polyaromatic compounds compared to the base case of JP-8 stressing alone.

Similar trends in composition were observed in the liquid obtained from the stressing of dodecane with and without the added activated carbon under the same conditions. Figure 2.8 clearly shows the differences in the concentrations of paraffins in chromatograms of dodecane stressed alone and dodecane + activated carbon-1. The presence of the added carbon again produced lower yields of liquids that are more paraffinic in nature than those produced from dodecane alone.

The yields of paraffins and aromatics from dodecane stressed at 450°C for 5 hours with and without the activated carbon were obtained from the GC analysis and are shown in Tables 2.4 and 2.5 as the volume percentages of the starting dodecane.

The concentrations of all the paraffins with 6 to 10 carbon atoms, and especially of hexane, are significantly higher in the liquid obtained from dodecane mixed with activated carbon than that obtained from dodecane stressed alone. The concentration of dodecane is slightly lower, however, in the liquid obtained with the activated carbon-1. It appears that the presence of the activated carbon gives rise to the stabilization of the free radicals after initial pyrolysis (or homolysis) to form shorter chain paraffins, such as hexane, in high yields.

Table 2.5 shows the yield of aromatics from dodecane stressed at 450°C for 5 hours with and without activated carbon. In contrast to paraffins, the concentrations of aromatics in the liquid obtained from dodecane with the activated carbon are lower than those in the liquid obtained from dodecane stressed alone.

### **Microscopic Examination of Solid Deposits on Reactor Walls and on Added Carbons**

An examination of the solid deposits by polarized-light microscopy showed that essentially all the carbonaceous solids collected on reactor surfaces or on added carbon particles had anisotropic structures. There were striking differences, however, in the morphology and optical texture of the solid deposits depending on the presence and nature of the added solid carbons.

After stressing at 450°C, very porous and isotropic structure of the original activated carbons showed some isolated regions of anisotropic microstructures of solids deposited on the surface. These anisotropic deposits appear to have nucleated in the gas phase and gone through a liquid phase before or while depositing on the activated carbons. The microstructure of the

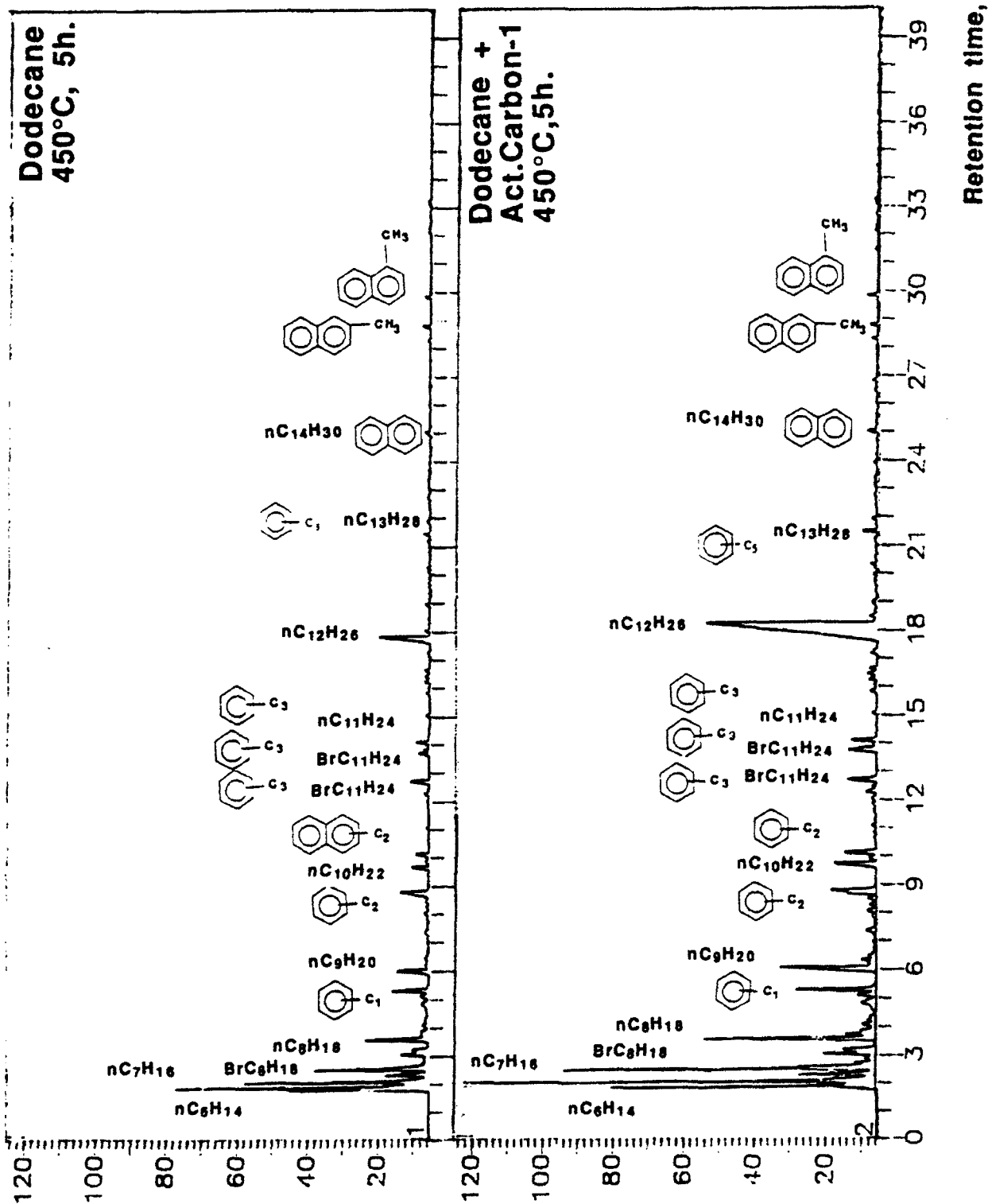


Figure 2.8. Gas chromatograms for dodecane products obtained at 450°C with and without added activated carbon-1.



**Table 2.4.** Yields of paraffins from dodecane stressed at 450°C for 5 hours with and without the activated carbon-1.

Identified Compound	Product / Dodecane %	
	Dodecane	Dodecane+ Act. Carbon-1
n-C <sub>6</sub> H <sub>14</sub>	2.96	8.80
n-C <sub>7</sub> H <sub>16</sub>	4.51	5.25
i-C <sub>8</sub> H <sub>18</sub>	3.97	3.83
n-C <sub>8</sub> H <sub>18</sub>	2.32	2.74
n-C <sub>9</sub> H <sub>20</sub>	1.68	1.98
i-C <sub>10</sub> H <sub>22</sub>	0.69	0.89
n-C <sub>10</sub> H <sub>22</sub>	0.13	0.56
n-C <sub>12</sub> H <sub>26</sub>	2.76	2.54
n-C <sub>13</sub> H <sub>28</sub>	0.17	0.18

**Table 2.5.** Yield of aromatics from dodecane stressed at 450°C for 5 hours. with and without activated carbon.

Identified Compound	Product / Dodecane, %	
	Dodecane	Dodecane+ Act. Carbon-1
Toluene + methyl-cyclohexane	1.43	1.18
Ethylbenzene	1.82	0.13
2-methylnaphthalene	0.26	0.12
1-methylnaphthalene	0.19	0.14
Ethyl-naphthalene	0.12	0.04
Fluorene	0.07	0.03
Anthracene or Phenanthrene	0.02	0.00
Ethylanthracene or Ethylphenanthrene	0.03	0.00
Pyrene	0.05	0.01

observable deposits on the activated carbon particles is quite different from those formed on the metallic surface which display a fine grained pyrolytic carbon structure.

Polarized-light micrographs of the carbon black particles obtained before and after stressing with JP8 at 450°C showed that the particles had large amounts deposits collected on their surfaces. In this case, the weight gain of the carbon black particles reported in Table 2.1 should be mostly due to the solid deposition. A TGA analysis of the original carbon black and the carbon black particles after stressing with JP8 at 450°C for 5 hours showed a difference of only 1% in weight loss when heated to 700°C in nitrogen. This is expected because of much lower adsorption capacity of the carbon black particles compared the activated carbon particles.

At 475°C, a significant amount of carbonaceous solids was deposited on activated carbon particles in addition to those on reactor walls. On polished sections, these deposits appeared to be pyrolytic layers on the external surface of the particles with no deposit formation within the pore structure. The solid deposit on the reactor walls appear to be thin flakes of gas-phase deposits. Compared to the reactor solids obtained without the added activated carbons, these deposits were much thinner with a finer grained texture. As different from the deposits on the reactor walls, solids collected on activated carbon particles showed curved boundaries suggesting the formation of an intermediate liquid phase on the surface of the carbon particles. Some solid deposition was observed even on the SP-1 graphite particles after stressing at 475°C.

Scanning electron micrographs of the activated carbons after thermal stressing with the fuel indicated carbon deposition in isolated areas. These deposits appeared to be in the form of thin uniform layers as well as discrete particles which blocked some of the pores present in the original activated carbon structure.

The differences in the microstructure of the solid deposits and the kinetics of deposition observed upon the addition of solid carbons suggest that different reactions are involved in the deposition of carbonaceous solids on reactor surfaces and on solid carbon surfaces. It is clear that activated carbon surfaces and carbon black surfaces provide more attractive surfaces for deposition of carbonaceous solids than does the surface of the stainless steel reactors. This observation further implies that the deposition of solids may be accelerated after the initial deposits are formed on the metal surfaces. The "regenerative" nucleation or "continuous" nucleation observed throughout the pyrolytic carbon deposit formed in an actual jet engine fuel line clearly shows the high reactivity of the deposit surface for further deposition of carbonaceous solids.<sup>6</sup>

#### **Surface Area Measurements on Added Solid Carbons**

Specific surface area measurements have been used to observe the changes in the structure the added solid carbons as a function of stressing. Table 2.6 shows the changes in the BET N<sub>2</sub> surface area of the two activated carbons and a carbon black, before and after thermal stressing with JP8 at 450°C for 5 hours.

**Table 2.6.** Specific area measurements on added carbons before and after thermal stressing.

Added solid carbon	BET surface area before thermal stressing m <sup>2</sup> /g	BET surface area after thermal stressing m <sup>2</sup> /g
Activated carbon-1	750	120
Activated carbon-2	1177	291
Carbon black	378	94

The dramatic decrease of the BET surface areas of both the activated carbons and carbon black shows that thermal stressing with the JP8 jet fuel changed the pore structure of the added carbons. Before stressing with JP8 both activated carbons showed typical type 1 isotherms, exhibited by microporous solids.<sup>8</sup> The carbon black sample, on the other hand, showed a type IV isotherm, associated with capillary condensation in mesopores.<sup>8</sup> After stressing with JP8 at 450°C, all three carbons showed type IV isotherms with hysteresis loops of type C, according to the classification of de Boer.<sup>9</sup> Type C hysteresis is produced by wedge shaped pores with open ends, contrary to type E hysteresis which original activated carbons showed before stressing. Type E hysteresis is attributed to ink-bottle pores. Apparently, carbon deposition selectively blocked the ink-bottle pores in the activated carbons.

### Conclusions

The presence of solid carbons, especially of activated carbons, during thermal stressing of a JP8 jet fuel and a model compound dodecane causes substantial changes in the prevailing reaction mechanisms clearly shown by the changes in the gas yields and composition. The activated carbon surfaces appear to be effective in stabilizing the free radicals or catalyzing recombination reactions to form more gases and to preserve constituent paraffins in the fuel at 450°C. A notable effect of adding activated carbons is the prevention of solid deposition on the metallic reactor surfaces even after rather severe thermal stressing of JP8 fuel at 450°C for 5 hours. This observation suggests that the surface of the initial solid deposits provides a more attractive area for further solid deposition than the relatively inert bare metal surface.

Different microstructures of the deposits observed on the added solid carbons mostly after stressing at 475°C indicate that the deposition mechanisms are also affected by the presence of different carbon surfaces during thermal stressing of the fuel.

## References

1. CRC Literature Survey on the Thermal Oxidation Stability of Jet Fuel, CRC Report No 509, Coordinating Research Council, Inc., Atlanta, Georgia, 1979.
2. Roquemore, W.M., Pearce, J.A., Harrison III, W.E., Krazinski, J.L., and Vanka, S.P., Preprints, Div. Pet. Chem., ACS, **34** (4), 841, 1989.
3. Hazlett, R.N., Thermal Oxidation Stability of Aviation Turbine Fuels, ASTM Publication Code Number (PCN) 31-001092-12, p.72, 1991.
4. Song, C., Peng, Y., Jiang, H., and Schobert, H.H. ., Preprints, Div. Pet. Chem., ACS Symposium on Structure of Jet Fuels III, San Francisco, April 5-10, 1992.
5. Hazlett, R.N., Free Radical Reactions Related to Fuel Research, Frontiers of Free Radical Chemistry, W.A.Pryor, ed., Academic Press, New York, pp. 195-223, 1980.
6. Eser, S., Song, C., Schobert, H.H., Hatcher, P.G., Extended Abstracts, 20th Biennial Conf. on Carbon, p.440, 1991.
7. Eser, S., Song, C., Gergova, K., Parzynski, M., Peng, Y., Preprints, Div. Pet. Chem., ACS Symposium on Structure of Jet Fuels III, San Francisco, April 5-10, 1992.
8. Brunauer, S., Denning, L.S., Denning, W.S., Teller, E., J. Amer.Chem.Soc. Symp. Ser. 62, 1723,1982.
9. de Boer, J.H., The Structure and Properties of Porous Materials, p.68, Butterworths, London, 1958.

## TASK 3. COAL-BASED FUEL STABILIZATION STUDIES

### *Activity 1. Stabilizers for Jet Fuels at High Temperatures*

#### Introduction

A typical jet fuel is composed of several hundred hydrocarbons and trace amounts of many other organic and inorganic compounds. Ninety-eight percent or more of a jet fuel is composed of hydrocarbons which are predominantly paraffinic and naphthenic in nature<sup>1</sup>. The trace components comprise of sulfur, nitrogen, and oxygen containing compounds. Jet fuels are not only chemically complex but they differ greatly in their composition as a result of variations in crude sources and refining processes. During the entire lifetime of the fuel, from when it is first produced in the refinery, until the moment when it is consumed by the engine, the problem of fuel

instability exists. Instability of liquid fuels is of increasing concern for both commercial and military fuel supply systems<sup>2</sup>. Fuel degradation can cause engine failure, engine malfunction, and poor engine performance. Poor stability of fuel can lead to increased maintenance problems and costs, equipment vulnerability, decreased reliability and many others which may result in profit losses.

The term "fuel stability" implies the general resistance of a fuel to change<sup>3</sup>. There are two types of stability. The first type is low-temperature storage stability, which involves a chemical change, oxidation of fuel molecules to form hydroperoxides<sup>4-6</sup>. These hydroperoxides attack elastomers in the fuel control lines<sup>7</sup>. Hydroperoxides form more readily in fuels produced by hydrocracking or by catalytic treatment followed by hydrotreatment. Refining techniques, which increase the yield of jet fuel probably remove natural inhibitors which limit hydroperoxide formation by interfering with autoxidation reactions<sup>8</sup>.

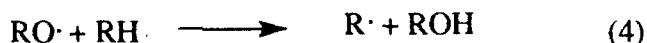
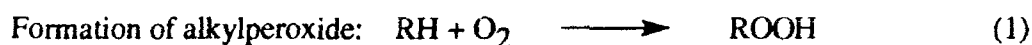
The second type of fuel stability is called the thermal oxidative fuel stability. This is the stability of the fuel exhibited on short term high temperature stress<sup>9-12</sup>. This situation is found during flight conditions, where fuel serves as a coolant on its path to the combustion chamber. Even at part per million levels, insoluble precipitates and gums can be responsible for a variety of problems which include decreased efficiency of the engine heat exchangers, seizing the fuel control valves and injector fouling<sup>7</sup>. It is known that hydroperoxides play a key role in thermal degradation of aviation fuels by initiating a variety of free radical reactions. If sufficient oxygen is present the concentration of hydroperoxides will become significant and on the other hand when the available oxygen is low, but the temperature is raised, the hydroperoxide concentration will be limited by free radical decomposition. Under these conditions fuel stability can be associated with both hydroperoxide formation and decomposition<sup>9,13</sup>. Jet fuels are also known to degrade in the absence of oxygen or in oxygen scarce atmosphere, but in general under these conditions the extent of degradation is lower than that in the presence of air<sup>11, 14</sup>.

Since many studies have shown the importance of autoxidative reactions on deposit formation, it may be expected that exclusion of molecular oxygen may suppress such reactions and result in reduction of deposit formation. But the studies performed by Taylor<sup>11</sup> show that this is not the case with all the fuels. One of the fuels studied showed heavy deposit formation with no peroxide buildup. This anomalous behavior was attributed to the presence of sizable quantities of disulfides in the fuel. Studies performed later demonstrated that the presence of a trace amount of not only disulfides but sulfides, polysulfide and thiols markedly increased the rate of deposit formation of a fuel even when it was deoxygenated<sup>27</sup>. Thus, hydrocarbon jet fuel can exhibit high deposit formation rates at low temperatures even when molecular oxygen content is greatly reduced, and hence it is also important to study the role of trace impurities such as sulfur, nitrogen and oxygen compounds on deposit formation.

## Effect of Oxygen

The detailed chemical reactions that lead to the fuel deposit formation are very complex and are poorly understood at present. However several researchers<sup>9, 15-19</sup> have reported that these reactions usually initiate with a liquid phase oxidation of the fuel, and are promoted by dissolved oxygen. It is also observed that the amount of oxygen that dissolves in the turbine fuel in equilibrium with air (50-80 mg/l), is sufficient to cause deposits which seriously degrade heat transfer<sup>20-22</sup>. At low temperatures, degradation of the fuel is predominantly autoxidation, whereas at temperature above 480°C degradation is characterized by the pyrolysis of hydrocarbon molecules and the scission of hydrogen<sup>9</sup>. The general free radical mechanism agreed upon by several researchers and outlined by Foder et al.<sup>18</sup> is given below.

In the mechanism, alkyl peroxide (ROOH) initiates the chain mechanism as shown by reactions (2) to (7). Reaction (1) is relatively slow and may consist of several unknown elementary reactions. Free radicals HO· and RO· are formed by the decomposition of ROOH in reaction (2). These radicals react rapidly to form alkyl radicals, R· as shown in reactions (3) and (4). In the presence of oxygen, the alkyl radicals are rapidly converted to alkylperoxy radicals (RO<sub>2</sub>·) as shown in reaction (5). RO<sub>2</sub>· is a relatively stable free radical as reaction (6) is slow as

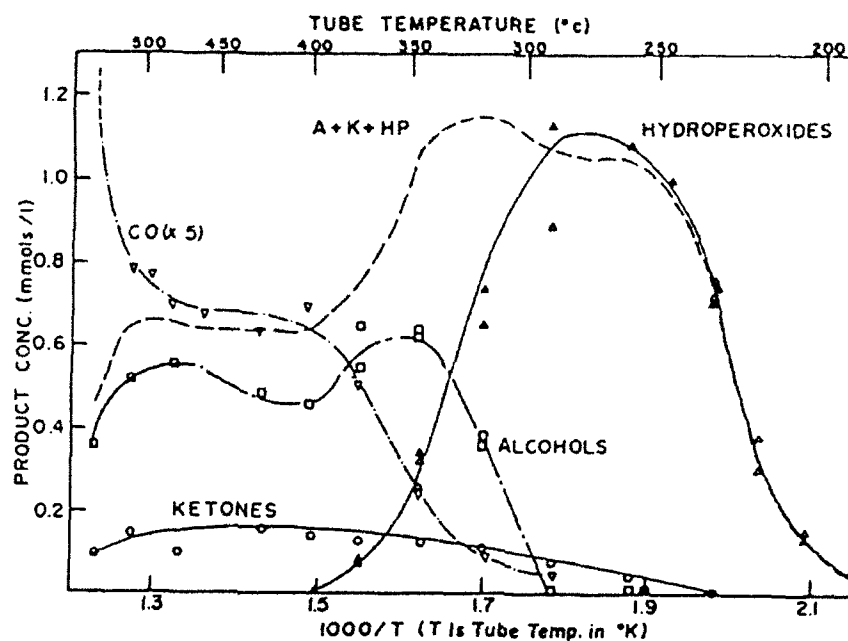


compared to reactions (3) to (5).<sup>23</sup> Since RO<sub>2</sub>· reacts slowly, its concentration is much higher than that of the other free radicals and as a result radical depletion takes place by recombination of RO<sub>2</sub>· in reaction (7). If the partial pressure of oxygen is too low<sup>24</sup> (less than about 1 psi) reaction (5) becomes the rate controlling step in the mechanism and reaction (7) would be replaced by reaction (8).

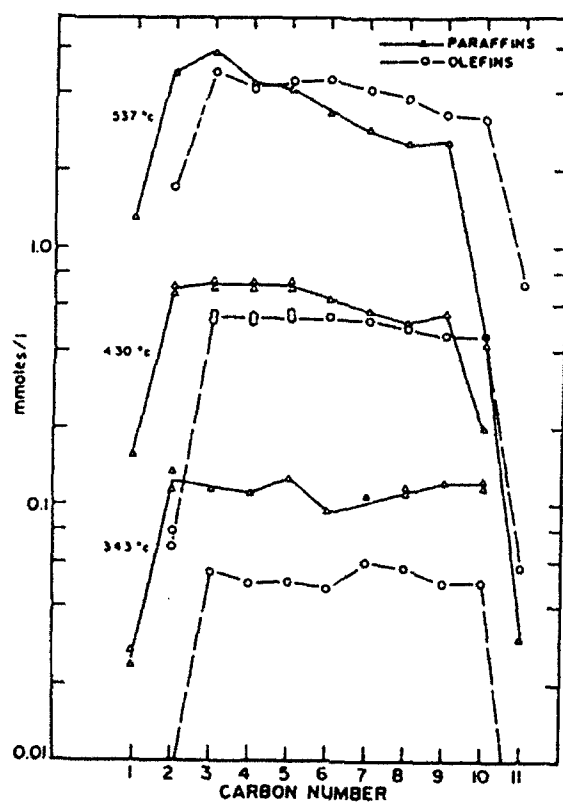
The detailed thermal degradation mechanisms of distillate fuels are not available, as the fuel composition is very complex and the resulting degradation products are many. This makes the study of multicomponent-fuel degradation and associated reaction-mechanism elucidation a very complex task. A basic approach for studying the thermal degradation problem is to understand the detailed behavior of a prototypical fuel component. Hazlett, Hall and Matson studied the liquid phase chemistry for n-dodecane<sup>25</sup> which is a significant component of the JP-5 and Jet A fuels. It was stressed in a small flow apparatus, the Jet Fuel Thermal Oxidation Tester (JFTOT)<sup>26</sup>. The chemistry of the oxygenated species formed over the temperature range 200-540°C are shown in Figure 3.1. It is observed that the major initial products are hydroperoxides. Above 300°C, hydroperoxides exhibit thermal instability and transform mainly into alcohols. Some ketones and carbon monoxide are also observed due to hydroperoxide decomposition. In addition to oxygenated species hydrocarbons smaller than n-dodecane appear as the dodecylhydroperoxides disappear. Both n-paraffins and 1-olefins are formed.

Figure 3.2 shows the distribution of n-alkanes and 1-olefins at 343, 430, and 537°C. This figure indicates that n-alkanes exceed the 1-olefins by a factor of two at 343°C but equal amounts are formed at temperatures above 430°C. These features of the reaction patterns observed in the Figures 3.1 and 3.2 can be interpreted on the basis of two processes, i. e., autoxidation and pyrolysis. The latter controls the high temperature reactions, (480°C and above), and autoxidation phenomena occur at the lower temperatures (260°C and below). In the intermediate regime, above the temperature at which oxygen is completely reacted but below pyrolysis temperatures, the reactions are more complex. In this intermediate regime between autoxidation and hydrocarbon pyrolysis reactions, oxygenated products play an important role. The decomposition of hydroperoxides via alkoxy radicals can form alcohols, ketones, carbon monoxide, n-alkanes, and 1-olefins. The importance of this path is indicated by the fact that yield patterns for CO, alkanes and alkenes exhibit a plateau above 385°C, the temperature at which ROOH is depleted. The  $\beta$ -scission of alkoxy radicals leads to alkane formation directly as well as indirectly by alkyl radical formation. The general features of these three regimes for oxygen-dodecane reactions are summarized in Table 3.1.

K. T. Reddy et al.<sup>19</sup> performed similar studies to identify and confirm the different regimes of the n-dodecane degradation mechanism proposed by Hazlett et al.<sup>25</sup>. From system verification studies,  $< C_{12}$  n-alkanes and 1-alkenes,  $C_{12}$  alcohols and ketones and ROOH product profiles agreed with Hazlett et al. data, while additional  $< C_{12}$  aldehydes, tetrahydrofurans, and  $C_{24}$  isomers were detected. At 300°C and above some alkoxy radicals decomposed by  $\beta$ -scission, forming aldehyde and a primary alkyl radical. The formation of cyclic ethers such as tetrahydrofuran was explained by the alkyl peroxy isomerization and decomposition scheme (APRID)<sup>40, 41</sup> as shown below. Consequently the existing n-dodecane degradation mechanisms were suitably modified to include these products. The modified n-dodecane oxidation mechanism



**Figure 3.1.** Oxygenated species formed by reaction between n-dodecane and air; A + K + HP = alcohols + ketones + hydroperoxides.



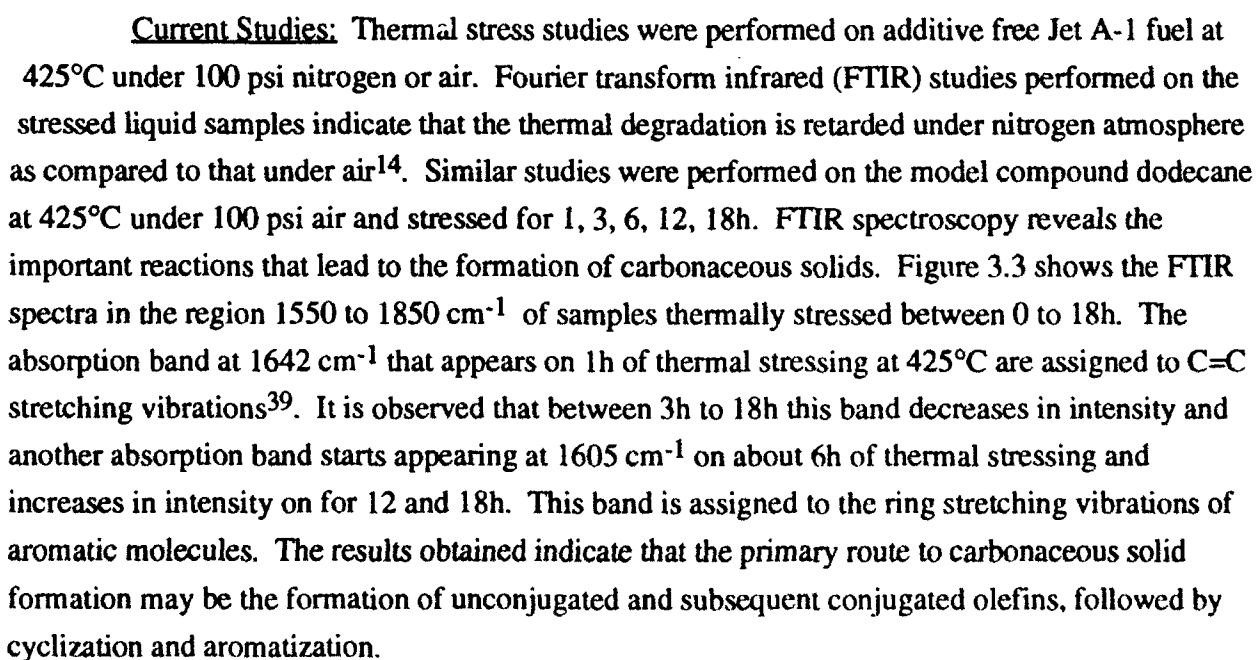
**Figure 3.2.** Distribution of n-alkanes and 1-olefins at three temperatures.

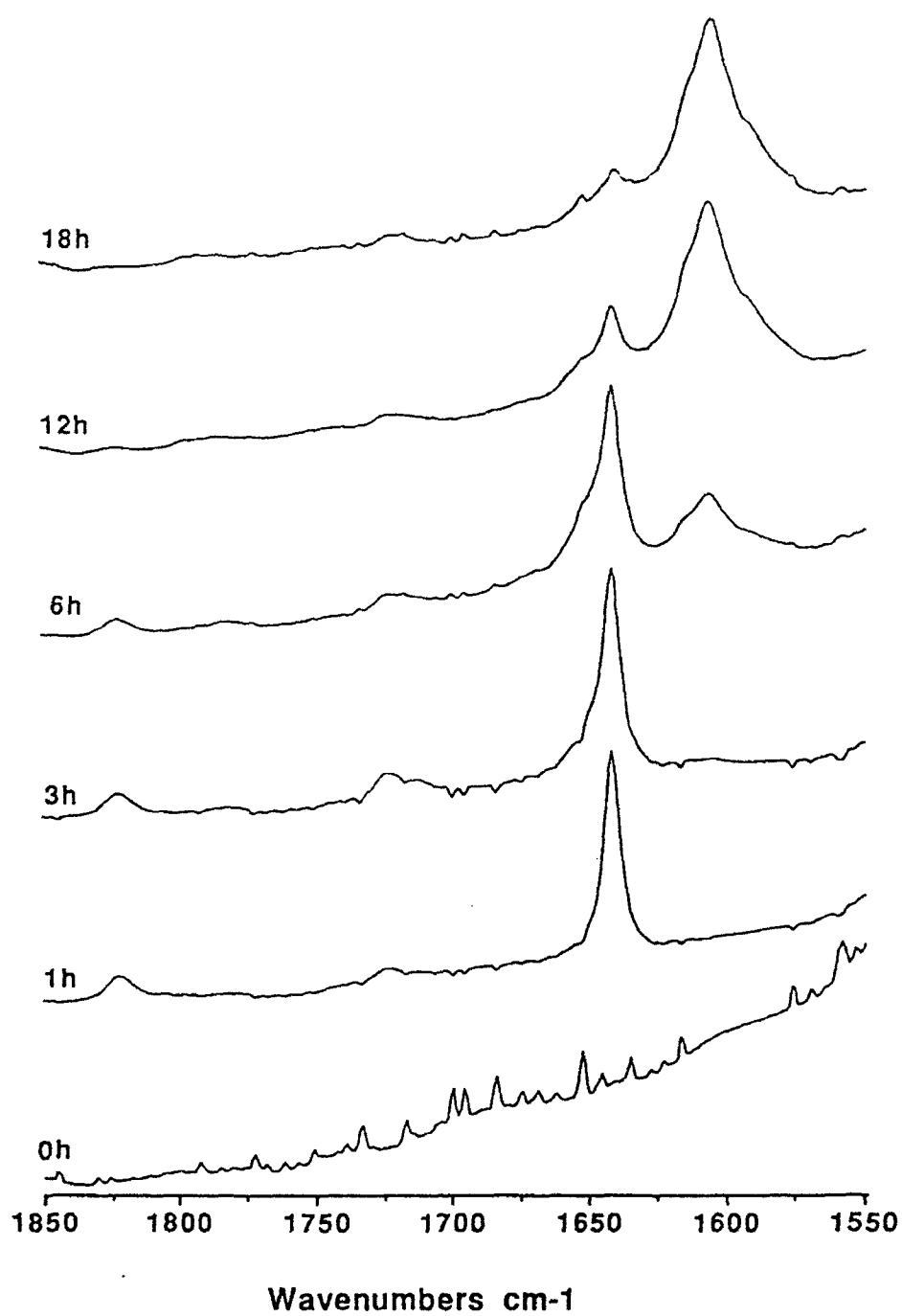


Table 3.1 General features for oxygen-dodecane reactions

Regime	Autoxidation	Intermediate	Pyrolysis
Temperature °C	260 and below	290-480	480 and above
Reactions	O <sub>2</sub> with C <sub>12</sub>	(1) ROOH decomposition (2) ROOH initiated, pyrolysis	C <sub>12</sub> cracking
Products	Hydroperoxides	(1) alcohols, ketones, CO (2) n-alkanes, 1-alkenes, H <sub>2</sub>	n-alkanes, 1-alkenes H <sub>2</sub>

hows that alkyl peroxy radical reactions dominate in the autoxidation temperature regime ( $T \leq 300^\circ\text{C}$ ). The dominant path is for alkyl peroxy radical, to react bimolecularly with fuel to yield primarily alkyl hydroperoxides. The  $\text{RO}_2\cdot$  radical also undergoes self termination and unimolecular isomerization and decomposition reactions, to yield smaller amounts of C<sub>12</sub> alcohol, ketone products and tetrahydrofuran derivatives, respectively. Thus alcohol and ketone formation in this temperature regime implies that the main termination step is via  $\text{RO}_2\cdot$  self termination reactions. In the intermediate temperature regime ( $300 \leq T \leq 400^\circ\text{C}$ ), the  $\text{R}\cdot$  radical reactions dominate over the  $\text{RO}_2$  reactions. The main supply of  $\text{R}\cdot$  radicals comes from ROOH decomposition while heterogeneous metal initiation constitutes the secondary source. The  $\text{R}\cdot$  radicals, in turn, decompose to form n-alkanes and 1-alkenes ( $< \text{C}_{12}$ ) and trace amounts of C<sub>12</sub> dimers.





**Figure 3.3.** FTIR spectra of dodecane stressed under 100 psi air at 425°C

## **Effect of trace impurities**

### **Sulfur compounds:**

Crude oil is a mixture of hydrocarbons containing varying quantities of sulfur, nitrogen and oxygen compounds. The total sulfur content varies from zero to as much as 14%. Sulfur compound classes identified in the crude oil include thiols, sulfides, and thiophenes. Generally, disulphides are rarely found in the crude oil. Sweetening processes are employed to convert the odorous thiols in a jet fuel to non odorous disulphides. Some sweetening processes employ elemental sulfur which may form polysulfides and remain in the jet fuel<sup>28, 29</sup>. Thus a jet fuel can contain sulfur compounds from the classes including thiols, sulfides, condensed thiophenes, disulphides, and polysulfides. Sulfur is the most abundant heteroatom present in military jet fuel with up to 0.4% total sulfur by weight allowed (MIT-T-5624M). For commercial jet fuel, the ASTM Standard Specification for Aviation Turbine Fuels (ASTM, 1987) permits up to 0.3% total sulfur by weight.

Taylor and Wallace<sup>30</sup> studied the influence of thiols, sulfides, disulphides, condensed thiophenes, diphenylsulfide and dibenzothiophene on the rate of deposit formation by adding them at 1000-ppm S level to essentially sulfur free air saturated hydrocarbon material at 93 to 232°C. The study indicates that thiols, sulfides, disulphides, and condensed thiophenes increased the rate of deposit formation whereas diphenylsulfide and dibenzothiophene did not increase the rate of deposit formation. Taylor<sup>27</sup> also studied the effect of trace impurity sulfur compounds on the rate of deposit formation in deoxygenated jet fuel. This study was performed by adding 3000 ppm of S to the deoxygenated jet fuel (JP-5) and its effect was determined in the advanced kinetic unit at 1014 psi with temperature zones at 371-540°C. The effect of sulfur compounds in a deoxygenated fuel was complex. In general, the addition of the polysulfide, disulfides, sulfides, and thiol all resulted in an increase in the rate of deposit formation. On the other hand the condensed thiophene compounds actually appeared to inhibit the deposit formation to some extent. This effect is observed probably due the relative strength of the aryl C-S bonds in the condensed thiophenes as compared to weaker S-S bonds and alkyl C-S bonds which presumably undergo pyrolysis and / or surface catalyzed decomposition reactions at milder conditions than the bonds present in pure hydrocarbons and whose products lead to the acceleration of deposit formation<sup>27</sup>. In contrast to the above study accelerated storage tests performed on Jet A fuel at 120-135°C suggested that while thiols promoted deposit formation sulfides and disulfides inhibited deposition by decomposing peroxides<sup>31</sup>.

In JFTOT studies performed on dodecane it was found that thiophenol inhibited autoxidation by acting as radical trap and breaking the autoxidation chains very early in the process<sup>32</sup>. When such study was performed on jet fuel it was found that the temperature over which the fuel underwent autoxidation was reduced, rather than increased as in model systems<sup>33</sup>. This is because thiols undergo oxidative addition to olefinic constituents in the fuel in a JFTOT.

Thus it is observed that the composition of the fuel, temperature, and stability of the individual sulfur compound which in turn is related to the structure of the compound, clearly governs to a great extent its influence on the rate of deposit formation.

#### **Nitrogen compounds:**

The nitrogen content of crude oil ranges from zero to a few percent<sup>34</sup>. Nitrogen compounds identified in typical jet fuel range petroleum cuts include pyrroles, indoles, carbozoles, pyridines, quinolines, tetrahydroquinolines, anilines and amides<sup>35-37</sup>. The most prevalent types are pyrroles, indoles, carbozoles, and quinolines. The effect of trace amounts of (100 ppm ) nitrogen compounds on deposit formation rate in deoxygenated JP-5 was investigated over a temperature range 371-540°C<sup>38</sup> (Table 3.2). None of the nitrogen compounds caused a significant increase in total deposits over the entire range of temperature studied. In the low temperature regimes, however the heterocyclic amines 2,5-dimethylpyrrole, indole, and carbazole promoted deposit formation to a small extent as compared to neat fuel. This suggests that the sediment formed at low temperatures either broke down to fuel soluble fragments at high temperatures or did not adhere to the surface of the walls to form deposits.

#### **Oxygen compounds:**

Oxygenated compounds are more abundant than nitrogenous species but less abundant than sulfur compounds. The oxygen compound identified in the jet fuel range petroleum fraction are carboxylic acids, phenols, furans, ketones, alcohols, esters, amides, hydroperoxides and peroxides<sup>36-37</sup>. The effects of various oxygen compounds (100 ppm ) on deposit formation rate in deoxygenated JP-5 was investigated over a temperature range 371-540°C<sup>38</sup> (Table 3.3). It is noted that compounds containing oxygen are more deleterious than those containing nitrogen. Particularly noteworthy are the peroxides although n-decanoic acid, methylbenzoate, and 5-nonanone also increased deposit formation by at least 50% over the base fuel. Aliphatic alcohols and phenols produced a moderate increase in deposit formation. On the other hand cyclic ethers, benzofuran, and dibenzofuran showed no tendency to promote deposit formation.

One of the salient features of deposit formation with air saturated fuels is the complex Arrhenius plot which results from the sharp drop in rates in the 350-430°C range. This was shown by Taylor<sup>11</sup> and is illustrated in Figure 3.4 by the typical curve for the air saturated fuel. It is seen that deposit formation rates show a sharp drop at this temperature range before continuing upward again at higher temperatures. Previous studies at sub-atmospheric pressures have shown that as a hydrocarbon jet fuel is heated, the rate of deposit formation increases until the liquid phase is lost, at which the rate of deposit formation drops sharply<sup>42</sup>. Much of this drop may be attributed to a reduction in the autoxidative reaction rate revealing the concentration of the reactive species as the system passes from the liquid phase to the vapor phase<sup>43</sup>. With increasing temperature, the autoxidative rate constants continue to increase, so that ultimately this concentration effect is

**Table 3.2** The effect of individual nitrogen compounds on total deposit formation in a deoxygenated jet fuel.

Class of added nitrogen compound <sup>a</sup>	Added compound	Oxygen content, ppm of O <sub>2</sub>	Total deposits <sup>b</sup>	
			μg of carbon	As ppm based on fuel
Pyrrole	2,5-Dimethylpyrrole	0.3	1310	0.65
	Benzo(b)pyrrole (indole)	0.2	1316	0.68
	Dibenzopyrrole (carbazole)	0.2	1028	0.54
Pyridine	2,4,6-Trimethylpyridine	0.2	1977	1.02
	Benzo(b)pyridine (quinoline)	0.2	1457	0.75
	2-Methylquinoline	0.1	1330	0.69
Primary amine	2,6-Dimethylaniline	0.2	1441	0.75
	Hexylamine	0.3	1228	0.63
	N-Methylcyclohexylamine	0.2	1411	0.73
Miscellaneous	2-Methylpiperidine	0.1	1049	0.54
	Decahydroquinoline	0.2	1360	0.71
	Hexanamide	1	1844	0.96
	Base fuel	0.4	1485	0.77

<sup>a</sup> All compounds added to the 100 ppm N level. <sup>b</sup> Cumulative deposits produced in 4 h in the Advanced Kinetic Unit. Conditions: 69 atm, zone 1, 371 °C; zone 2, 427 °C; zone 3, 482 °C, zone 4, 538 °C.

**Table 3.3** The effect of individual oxygen compounds on total deposit formation in a deoxygenated jet fuel.

Class of added oxygen compound <sup>a</sup>	Added compound	Oxygen content, ppm of O <sub>2</sub>	Total deposits <sup>b</sup>	
			μg of carbon	As ppm based on fuel
Peroxide	Di- <i>tert</i> -butylperoxide	0.2	2679	1.49
	Cumene hydroperoxide	0.1	7219	3.73
Carboxylic acid	<i>tert</i> -Butylhydroperoxide	0.2	8934	4.62
	Cyclohexanecarboxylic acid	0.1	1563	0.82
	<i>n</i> -Decanoic acid	0.1	2997	1.54
	Cyclohexanecarboxylic acid	0.2	1730	0.89
	2-Ethylbutyric acid	0.2	1291	0.67
	2,4-Dimethylbenzoic acid	0.3	1801	0.93
Phenol	2-Methylphenol	0.2	1561	0.81
	2,6-Dimethylphenol	0.1	2048	1.06
	2,4,6-Trimethylphenol	0.1	1451	0.75
Furan	Benzo(b)furan	0.2	1505	0.78
	Dibenzofuran	0.2	1410	0.73
Alcohol	<i>n</i> -Dodecyl alcohol	0.9	2046	1.06
	4-Methylcyclohexanol	0.3	1356	0.70
Ketone	5-Nonanone	0.7	2422	1.26
	4-Methylcyclohexanone	0.3	1244	0.64
Ester	Cyclohexyl formate	0.2	1318	0.68
	Methyl benzoate	0.7	2488	1.29
	Pentyl formate	0.8	1894	0.98
	Base fuel	0.4	1485	0.77

<sup>a</sup> All compounds added to the 100 ppm O level. <sup>b</sup> See Table 2 for run conditions.

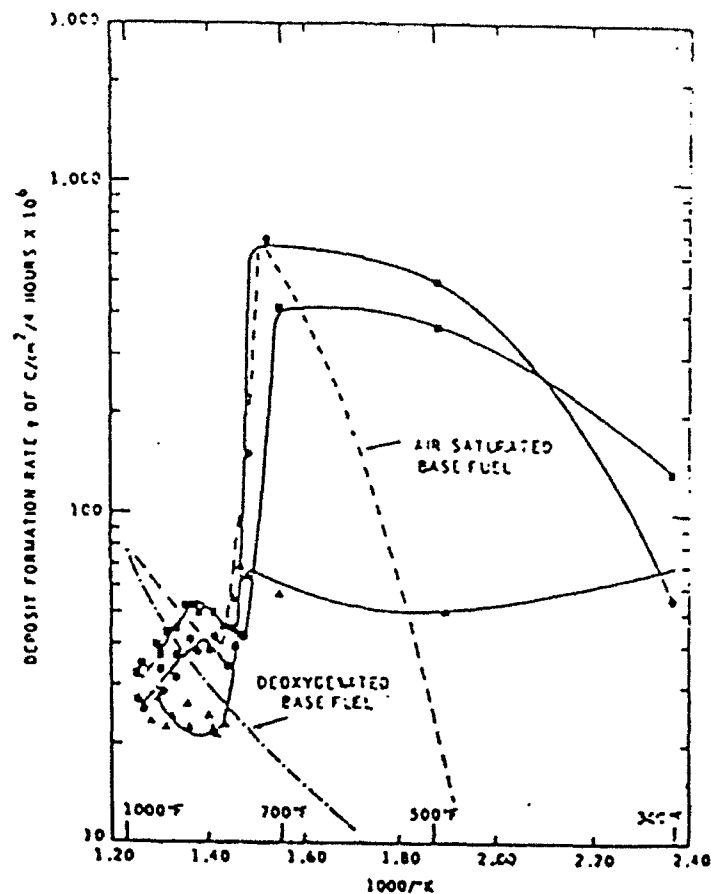


**Figure. 3.4.** Deoxygenated fuel at 1000 psi (0.1 ppm of O<sub>2</sub>): •, with added tert-butylhydroperoxide; ▲, with added cumene hydroperoxide; ▴, with added di-tert-butylperoxide. All compounds added at 100 ppm of O.

overcome and the overall rate again increases. The very similar shape of the curve is obtained when deoxygenated fuels are doped with various peroxides (Figure 3.4). This suggests that peroxides formed by autoxidation of air-saturated fuels are, indeed the reactive species, whose drop in concentration with the phase change causes this discontinuity. It is also seen that the curve for rigorously deoxygenated fuel, with no added peroxides, does not exhibit this effect.

Figure 3.4 shows that the deoxygenated fuels doped with various peroxides show an immediate increase in deposit formation in the low temperature regimes, while the air-saturated base fuel, with no added peroxides, exhibits a gradual increase in deposits. This suggests that a steady generation of peroxidic compounds is due to autoxidation of the base fuel by dissolved oxygen. These results strongly suggest that peroxides are a major cause of deposit formation in air-saturated fuel systems.

These findings suggest that trace impurities must be taken into account when assessing the thermal stability of fuel for high speed aircraft. Deoxygenation procedures will be of optimal effectiveness only when trace impurity effects are considered and eliminated or controlled.

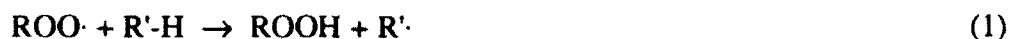
### Effect of Fuel Hydrocarbon Composition:

Jet fuels primarily consist of hydrocarbons, which are predominantly paraffinic and naphthenic in nature. Up to 5 vol.% olefins and about 20 vol.% aromatic hydrocarbons are generally allowed in many specifications. With the advent of more and more high speed aircrafts, jet fuels are exposed to very high temperature stress which leads to degradation resulting in hazardous deposit formation. Hence, it is important to know the effect of different hydrocarbon structures on deposit formation.

W. F. Taylor performed experiments to elucidate the effect of hydrocarbon fuel composition on autoxidative deposit formation tendency of various pure hydrocarbons and binary blends from 93.3 - 232.2°C.<sup>44</sup> The deposit formation rate of a series of pure paraffins typical of those found in jet fuels, n-decane, n-dodecane, n-tetradecane, and n-hexadecane were determined. It was observed that deposit formation at a given temperature decreases with increasing carbon number. Further the effect of branching in paraffins was also investigated using a binary blend containing 10 wt.% of the branched paraffin in decane and the results obtained indicate that branching increases the deposit formation rate of paraffins.

The effect of various aromatic and naphthenic compounds at low concentrations in a paraffin rich binary blend (10 wt.%) was also studied<sup>44</sup>. In general it was observed that the presence of aromatic or naphthene inhibited the rate of deposit formation at 93.3 - 176.7°C. At higher temperatures in most of the compounds inhibition becomes less pronounced. Figure 3.5 shows the activity of binary blends relative to the activity of pure n-decane at 121.1°C plotted against the number of benzylic hydrogens present in the added compound. The number of benzylic hydrogens in the structures showed a correlation with the reduction in deposition. Cycloalkanes exerted a modest inhibition on the deposit formation rate of decane but many aromatics significantly reduced deposits, particularly at lower temperatures. Fluorene and diphenylmethane reduced deposition in decane almost tenfold.

The observed inhibition in deposit formation is explained as follows. According to Ingold, a peroxy radical is a relatively unreactive radical which is selective in its hydrogen abstraction from hydrocarbons, and has preference for the most weakly bound hydrogen atom<sup>45</sup>. The hydrogen abstraction reaction, equation (i) is the limiting reaction during





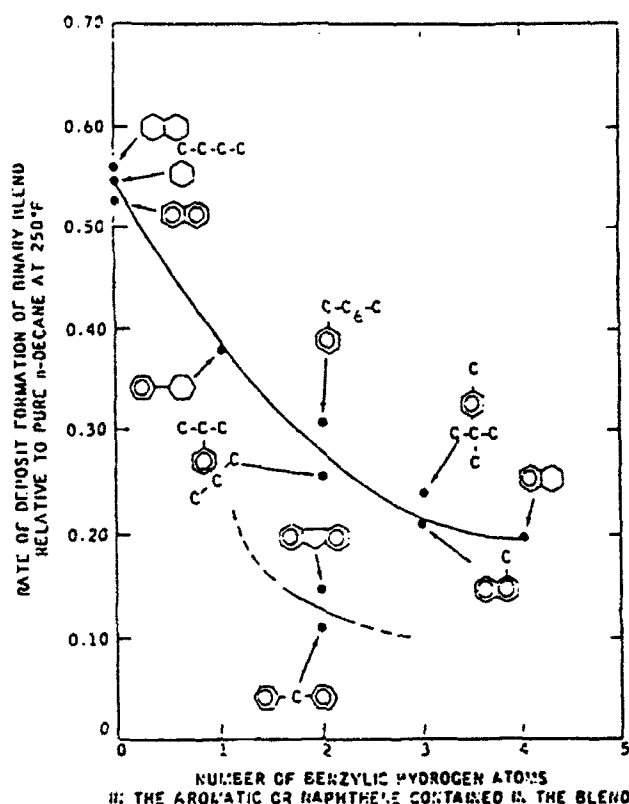


**Figure. 3.5.** Relative rate for deposit formation at 121°C of various 10/90 aromatic or naphthene in n-decane binary blends compared to pure n-decane, plotted against number of benzylic hydrogen atoms present in aromatic or naphthene. Upper. Hydrogen attached to carbon atom  $\alpha$  to a single  $\pi$  electron system. Lower. Hydrogen attached to carbon atom between two separate  $\pi$  electron systems.

chain propagation, as the reaction of hydrocarbon radical with molecular oxygen, equation (2) occurs rapidly in the presence of high concentrations of oxygen. Energetics of equation (1) indicates that the hydrogen abstraction will occur fastest when the bond that is formed is stronger than the bond that is broken. This is the case with benzylic C-H bond as the radical formed is resonance-stabilized. Thus, the correlation of the effect of the number of benzylic hydrogen atoms contained in the added compound on the reduction in deposit formation seems to reflect the bond strength during hydrogen abstraction in the cooxidation system.

Ingold also mentions that hydrogen atoms attached to a carbon atom between two separate  $\pi$  electron systems should form more stable radicals than hydrogen atoms attached to a carbon adjacent to a single  $\pi$  system. This probably explains the greater inhibition effect observed with diphenyl methane and fluorene blends with decane. R. N. Hazlett suggests that the active aromatics which have bond strengths of 82 kcal/mol or less for their weakest C-H bond, behave as traditional fuel antioxidants<sup>9</sup>. Thus the aromatic free radicals formed by hydrogen abstraction

are relatively stable at the experimentally temperatures. Reaction of oxygen with such radicals is significantly slower than with alkyl radicals. Consequently the overall rate of oxidation is reduced. It is also observed that the addition of 10 wt.% olefins in paraffin-rich blend increased the level of deposit formation. This is because olefins can either react with oxygen to form hydroperoxides initially via a hydrogen abstraction mechanism or they can undergo an addition mechanism to form polyperoxides. Both of these reactions can occur simultaneously<sup>43</sup>.

Of the three hydrocarbon basic hydrocarbon types - paraffins, naphthenes and aromatics, the naphthenes with two rings have been identified as early as in the 1960's by E. E. Donath and M. Hess to have the most desirable properties for a thermally stable jet fuel<sup>46</sup>. But the cost of manufacture of such fuels turn out to be very expensive. Thus recently a lot of research is oriented towards finding new economic routes to manufacture such fuels and to invent new additives that would efficiently stabilize the presently used petroleum derived jet fuels facing high temperatures in high Mach aircrafts.

Current studies: Our research goals are (1) to identify additives that stabilize the petroleum derived jet fuels at temperatures over 400°C and (2) to trace the major reactions involved in stabilizing the fuel with these additives. We have successfully identified a class of potential thermal stabilizers which considerably retard the decomposition of the jet fuel at 425°C under 100 psi air<sup>47</sup>. Benzyl alcohol and 1,4-benzenedimethanol are the two additives studied initially.

Th 10.0 ml of the additive free jet A-1 fuel doped with 5% of the additive was taken in a tubing bomb and flushed 5 times with 1000 psi UHP nitrogen gas to minimize the amount of dissolved oxygen and then thermally stressed at 425°C for various time durations under 100 psi UHP air in a preheated sandbath. The stressed fuel samples were then analyzed using FTIR spectroscopy. FTIR studies and visual appearance reveal that 5% benzyl alcohol retards deposit formation for 6 hours, while 1,4-benzenedimethanol retards deposit formation up to 12 hours. At present it is believed these additives act as oxygen scavengers and/or in situ hydrogenation agents at these high temperatures. Further studies are being performed to trace detailed reaction mechanism involved.

## Summary.

It is seen that free radical chemistry plays a major role in the thermal degradation reactions involved in jet fuels. In low temperature regimes, autoxidation by dissolved oxygen are important. At very high temperatures pyrolysis reactions become dominant. Deoxygenation of the fuel does retard the thermal degradation in the absence of other deleterious trace impurities. Thiols, sulfides, disulphides, and condensed thiophenes increased the rate of deposit formation whereas diphenylsulfide and dibenzothiophene did not increase the rate of deposit formation. The composition of the fuel, temperature, and stability of the individual sulfur compound which in turn is related to the structure of the compound, governs to a great extent its influence on the rate of

deposit formation. Nitrogen content in most of the fuels are very low it does not play any major role on deposit formation. Among the oxygen compounds hydroperoxides play a crucial role on deposit formation. Of the three class of hydrocarbons, paraffinic, naphthenic and aromatic two ring naphthenes are most stable and constitute an ideal high temperature stable jet fuel. Benzyl alcohol and 1,4-benzenedimethanol are found to be potential thermal stabilizers for jet fuels stressed over 400°C.

## References

1. R. N. Hazlett, "Thermal Oxidation Stability of Aviation Turbine Fuels," ASTM, 1991, 75.
2. E. W. White, ASTM STP, 1973, 531, 143.
3. J. Popsil, and P. Klemchuk, "Oxidation Inhibition in Organic Materials, vol I," CRC Press Inc., 1990, 1.
4. R. N. Hazlett, J. M. Mall, C. J. Novack, L. Craig, Proceedings of 1st International Conference on Long Term Storage Stability of liquid fuels, N. Por Ed., The Isreal Institute of petroleum and technology, Tel Aviv, Isreal, 1983, B132.
5. L. M. Turner, G. E. Speck, C. J. Nowack, Proceedings of 2nd International Conference on Long Term Storage Stability of Liquid Fuels, L. L. Stavinoha Ed., Southwest Research Institute: San Antonio, TX, 1986, 835.
6. J. M. Watkins Jr., G. W. Mushrush, R. N. Hazlett, Prepr. Am. Chem. Soc., Div. Fuel Chem., 1987, 32(1), 513.
7. R. E. Morris, R. N. Hazlett and C. L. McIlvaine III, Ind. Eng. Chem. Res., 1988, 27, 1524.
8. M. Smith, "Aviation Fuels," G. T. Foulis & Co. Ltd., Oxfordshire, Great Britain, 1970, chapter 51.
9. R. N. Hazlett, "Free Radical reactions Related to Fuel Research in Frontiers of Free Radical Chemistry," W. Pryor Ed., Academic Press, New York, 1980, 195.
10. G. Scott, "Atmospheric Oxidation and Antioxidants," Elsevier, Amsterdam, 1965, Chapter 3.
11. W. F. Taylor, Ind. Eng. Chem. Prod. Res. Dev., 1974, 13, 133.
12. W. F. Taylor, T. J. Wallace, Ind. Eng. Chem. Res., 1988, 27, 1524.
13. J. M. Watkins Jr., G. W. Mushrush, R. N. Hazlett, and E. J. Beal, Energy & Fuels, 1989, 3, 231.
14. L. Selvaraj, M. Sobkowiak, and M. M. Coleman, Prep. Am. Chem. Soc., Div. Petr. Chem., 1992, 37 (2), 451.
15. D. R. Kendall and J. S. Mills, Ind. Eng. Chem. Prod. Res. Dev., 1986, 25, 360.
16. F. R. Mayo, and B. Y. Lan, Ind. Eng. Chem. Res., 1986, 25, 333.

17. A. J. Giovannetti, and E. J. Szetela, "Long term deposit formation in aviation turbine fuel at elevated temperature," NASA Final report, Contract No. NAS3-24091, 1985.
18. G. E. Fodor, Energy and Fuels, 1988, 2, 729.
19. K. T. Reddy, N. P. Cerransky, and R. S. Cohen, Energy and Fuels, 1988, 2, 205.
20. J. J. Watt, A. Evans, and R. R. Hibbard, "Fouling charecteristics of ASTM Jet A fuel when heated to 700°F in a simulated heat exchanger Tube," NASA Technical Note D-4958, December 1968.
21. R. P. Bradley, H. R. Bankhead., and W. E. Bucher, "High temperature hydrocarbon fuels research in an advanced fuel system simulator on fuel AFFB-14-70," Air Force Aeropropulsion Lab., Rpt. No. AFAPL-TR-73-95, 1974.
22. V. A. Astaf'ev, B. D. Borisov, V. P. Logvinyuk, V. V. Malysev, and A. A. Popov, Khim. Technol. Topl. Masel, 1975, 11(7), 41.
23. A. A. Frost, R. G. Pearson, Kinetics and Mechanism, Wiley: New York, 1961, 248-251.
24. C. Walling, Free Radicals in Solution; Wiley: New York, 1957, chapter 9.
25. R. N. Hazlett, J. M. Hall, and M. Matson, Ind. Eng. Chem. Prod. Res. Dev., 1977, 16, 171.
26. "Test for thermal oxidation stability of aviation turbine fuels," ASTM Method D-3241-74, Philadelphia, Pa., 1976.
27. W. F. Taylor, Ind. Eng. Chem. Prod. Res. Dev., 1976, 15 (1), 64.
28. R. B. Thompson, L. W. Druge, and J. A. Chenicek, Ind. Eng. Chem., 1949, 41, 2715.
29. H. E. Walker, and E. B. Kenney, Pet. Process., 1956, 11, 58.
30. W. F. Taylor and T. J. Wallace, Ind. Eng. Chem. Prod. Res. Dev., 1968, 7 (3), 198.
31. S. R. Daniel and F. C. Heneman, Fuel, 1983, 62, 1265.
32. R. E. Morris and G. W. Mushrush, Fuel Sci. & Tech. Int., 1990, 8 (5), 527.
33. R. E. Morris, Fuel Sci. & Tech. Int., 1991, 9 (9), 1087.
34. J. S. Ball, Proc. Am. Pet. Inst., Sect. 8, 1962, 42, 27.
35. R. W. Sauer, et. al., Ind. Eng. Chem., 1952, 44, 2606.
36. Y. G. Hendrickson, Am. Chem. Soc., Div. Pet. Chem., Prepr., 1959, 4 (1), 55.
37. A. C. Nixon, in "Autoxidation and Antioxidants," vol. II, W. O. Lundburg, Ed., Interscience, New York, N. Y., 1962.
38. W. F. Taylor and J. W. Frankenfeld, Ind. Eng. Chem. Prod. Res. Dev., 1978, 17 (1), 86.
39. N. B. Colthup, L. H. Daly, and S. E. Wiberly, Introduction to Infrared and Raman Spectroscopy, Third edition, Academic Press, New York, 1990.
40. A. Fish, O. Rev., Chem. Soc., 1964, 18, 243.
41. A. Fish, Adv. Chem. Ser., 1968, 26, 69.

42. W. F. Taylor and T. J. Wallace, Ind. Eng. Chem. Prod. Res. Dev., **1967**, *6*, 258.
43. F. R. Mayo, Acc. Chem. Res., **1968**, *1*, 193.
44. W. F. Taylor, Ind. Eng. Chem. Prod. Res. Dev., **1969**, *8*, 375.
45. K. U. Ingold, Preprints 7th World Petroleum Congress, Mexico city, **1967**, P.D. No. 18 (2).
46. E. E. Donath and M. Hess, Chem. Engg. Prog., **1960**, *56* (4), 68.
47. M. M. Coleman, L. Selvaraj, M. Sobkowiak, and E. Yoon, Energy & Fuels, **1992**, (in press).

## ***Activity 2. Analysis of Stressed Jet Fuels with Stabilizers by NMR***

### **Introduction**

We recently reported<sup>1,2</sup> the results of Fourier transform infrared (FTIR) and visual studies of Jet A-1 samples that had been subjected to thermal stresses for varying periods of time at a temperature of 425°C. FTIR spectroscopy was shown to be an excellent experimental method that has just about the right degree of sensitivity for our purposes, as it probes at the level of the functional group and is capable of unveiling the major reactions that lead to the formation of carbonaceous solids during thermal stressing at these high temperatures. From these leads we have been successful in identifying a number of additives, specifically benzyl alcohol and 1,4-benzene dimethanol, that appear to function as hydrogen donors and which perform well as thermal stabilizers, significantly retarding the onset of carbonaceous solid formation in jet fuels at temperatures in excess of 400°C.

Evidence obtained from the infrared studies performed to date suggests that the primary route to carbonaceous deposits at temperatures above 400°C may well be the formation of olefins, followed by cyclization and aromatization, similar to the mechanism suggested for the degradation of polyacrylonitrile copolymers used in the formation of carbon fibers<sup>3</sup>. The focus of our research thus turned to studying molecules that might act as hydrogen donors in the anticipation that they might resaturate the double bonds as they are produced and ultimately retard the subsequent reactions that result in the formation of carbonaceous solids. Hydrogenation agents employed in coal liquefaction, such as tetralin or tetrahydroquinoline, do act as thermal stabilizers and significantly retard the formation of carbonaceous solids.

Surprisingly, however, the best thermal stabilizers we found were methanol derivatives, such as benzyl alcohol and 1,4-benzene dimethanol<sup>2</sup>. From infrared studies of the Jet A-1 fuels containing these two alcohols we know that methanol groups *slowly* transform over a period of hours in the jet fuel to aldehydes. A simple mass balance indicates that this is achieved with the

loss of two hydrogen atoms and this suggests that benzyl alcohol and benzene 1,4-dimethanol act as *in situ* hydrogenation agents at high temperatures, similar to coal liquefaction reagents, resaturating olefinic double bonds as they are formed and interfering with the process of aromatization and subsequent formation of carbonaceous solids.<sup>2</sup>

While the infrared studies performed to date have been rewarding, parallel NMR studies, which are the main focus of this report, were initiated to assist in the interpretation of the changes observed in the infrared spectra as a function of thermal stressing. NMR studies also provide additional information that is useful for the elucidation of the principal reaction pathways that lead to a retardation of carbonaceous solid formation.

## Experimental

Samples for these studies were prepared from an essentially additive free Jet A-1 fuel supplied by the Air Force/Wright Laboratory (No. 90-POSF-2747). Benzyl alcohol and benzene 1,4-dimethanol were purchased from Aldrich Chemical Company and used without further purification.

Thermal stressing was performed on 10 ml samples at 425°C in 15 ml type 316 stainless steel micro reactors<sup>2</sup> under 100 psi of air. The micro reactor containing the sample was purged with UHP-grade N<sub>2</sub> five times at 1000 psi to minimize the presence of dissolved oxygen and finally pressurized with 100 psi of air. It was then placed in a preheated sand bath at 425°C for the required reaction time, followed by quenching into cold water and depressurization to remove head space gases.

Samples for NMR analyses were prepared as 15 wt % solutions in deuterated chloroform. The spectra were recorded on a Bruker WP200 instrument at a field strength of 200 MHz.

## Results and Discussion

### Thermal Stressing of Neat Jet A-1 Fuel at 425°C.

The physical appearance of the neat Jet A-1 fuel after thermal stressing at 425°C under 100 psi of air, changes from a clear, colorless, transparent liquid to a transparent, light yellow liquid after 1h, a slightly turbid, light brown liquid after 3h and a black liquid after 6h. Between 6 and 24h the black liquid becomes progressively more turbid and there is an obvious increasing presence of black carbonaceous solids (color pictures are shown in ref. 2). Changes observed in the infrared spectra of neat Jet A-1 fuel as a function of thermal stressing time led us to consider hydrogen donors as potential stabilizers. Prominent bands at approximately 1642 / 1652 and 890 / 910 cm<sup>-1</sup> in the spectra were assigned to C=C stretching vibrations resulting from the formation of olefins during thermal stressing. Between 6 and 18h these bands decrease in intensity and are barely detected after 12h in air at 425°C. Other relatively broad bands are observed at approximately 880 and 675 cm<sup>-1</sup> and these become increasingly prominent in spectra of the

samples after reaction times exceed 6h. These bands were attributed to substituted aromatics and their presence correlates well with the observation of the black carbonaceous material in the thermally stressed fuel at long reaction times.

Figure 3.6 shows  $^1\text{H}$  NMR spectra (0-10 ppm) recorded at room temperature of Jet A-1 fuel samples thermally stressed under air after time periods of 0, 1, 3, 6, 12, 18 and 24h at 425°C. The NMR spectrum of the neat unstressed fuel is representative of a typical complex hydrocarbon mixture<sup>4</sup> with prominent lines attributed to paraffinic methyl and  $\gamma$ -methyl protons (0.5-1.05 ppm); paraffinic methylene,  $\gamma$ -methylene,  $\beta$ -methyl and  $\beta$ -methylene protons (1.05-2.0 ppm);  $\alpha$ -methyl protons ( $\text{Ar-CH}_3^*$ ; 2.0-2.6 ppm);  $\alpha$ -methylene protons ( $\text{Ar-CH}_2^*\text{-R}$ ; 2.6-3.4 ppm);  $\alpha$ -methylene protons ( $\text{Ar-CH}_2^*\text{-Ar}$ ; 3.4-4.5 ppm) and aromatic protons (6.0-9.0 ppm). For completeness, olefinic protons, which are not detected at this scale expansion, resonate between 4.5-6.0 ppm. Upon thermal stressing at 425°C the distribution of aliphatic to aromatic moieties changes in favor of the latter. Systematic increases in the intensity of  $\alpha$ -methyl,  $\alpha$ -methylene and aromatic protons with corresponding decreases in the intensity of paraffinic methyl and methylene groups are observed. Figure 3.7 shows  $^1\text{H}$  NMR spectra of the same samples scale expanded in the olefinic proton region (4.5-6.0 ppm). In the unstressed Jet A-1 fuel olefinic protons are not detected. However, in the spectra obtained after the sample had been thermally stressed for 1 and 3h there is the obvious presence of NMR resonances that may be attributed to internal and external olefins. In common with the infrared results<sup>2</sup>, the concentration of olefins appears to maximize between 3 and 6h. Thus the NMR results obtained on the thermally stressed neat Jet A-1 corroborate the infrared spectroscopic findings.

#### **Thermal Stressing of Jet A-1 Fuel Containing 5% Benzyl Alcohol at 425°C.**

As we have demonstrated previously<sup>2</sup> the addition of 5% benzyl alcohol to Jet A-1 fuel results in a significant improvement in the thermal stability at 425°C, as confirmed by the retardation of carbonaceous solids formation by some 3h. Infrared spectroscopic analysis was informative. A band at  $1720\text{ cm}^{-1}$ , assigned to the carbonyl stretching vibration of benzaldehyde was observed to increase in intensity to a maximum after approximately 3h of thermal stressing, decrease somewhat at 6h and was essentially absent at 12h of thermal stressing. Concomitant with these observations bands assigned to  $\text{C}=\text{C}$  stretching vibrations are detected at 1h, rise to a maximum at about 6h and are barely detected at 12h of thermal stressing. Significantly, after 12h of thermal stressing bands assigned to substituted aromatics are present and this again correlates well with the observation of the black carbonaceous material in the thermally stressed fuel. The interpretation of these results was as follows. Benzyl alcohol and similar molecules *slowly* transform over a period of hours in the jet fuel to aldehydes with the loss of 2 hydrogen atoms. We believe that they act as *in situ* hydrogenation agents at high temperatures, similar to coal

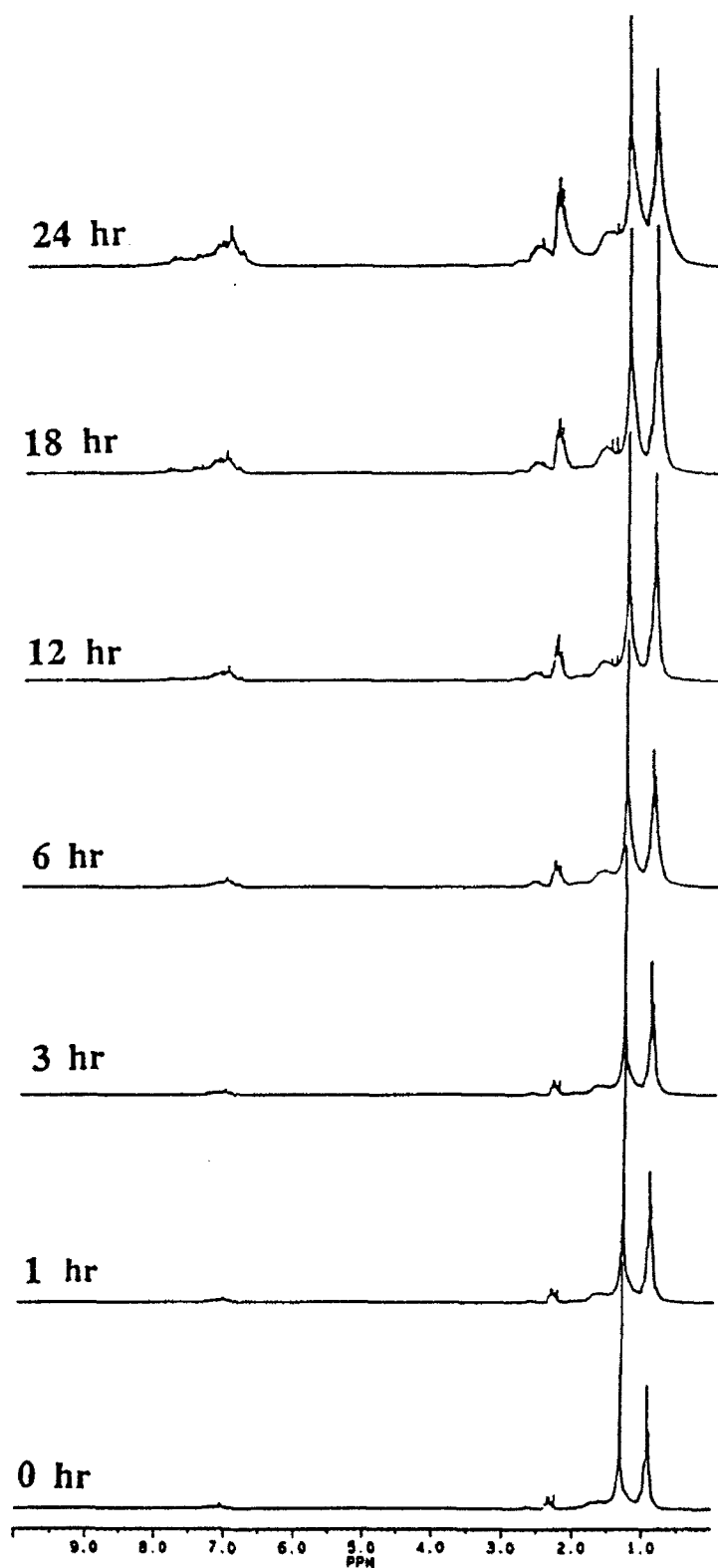
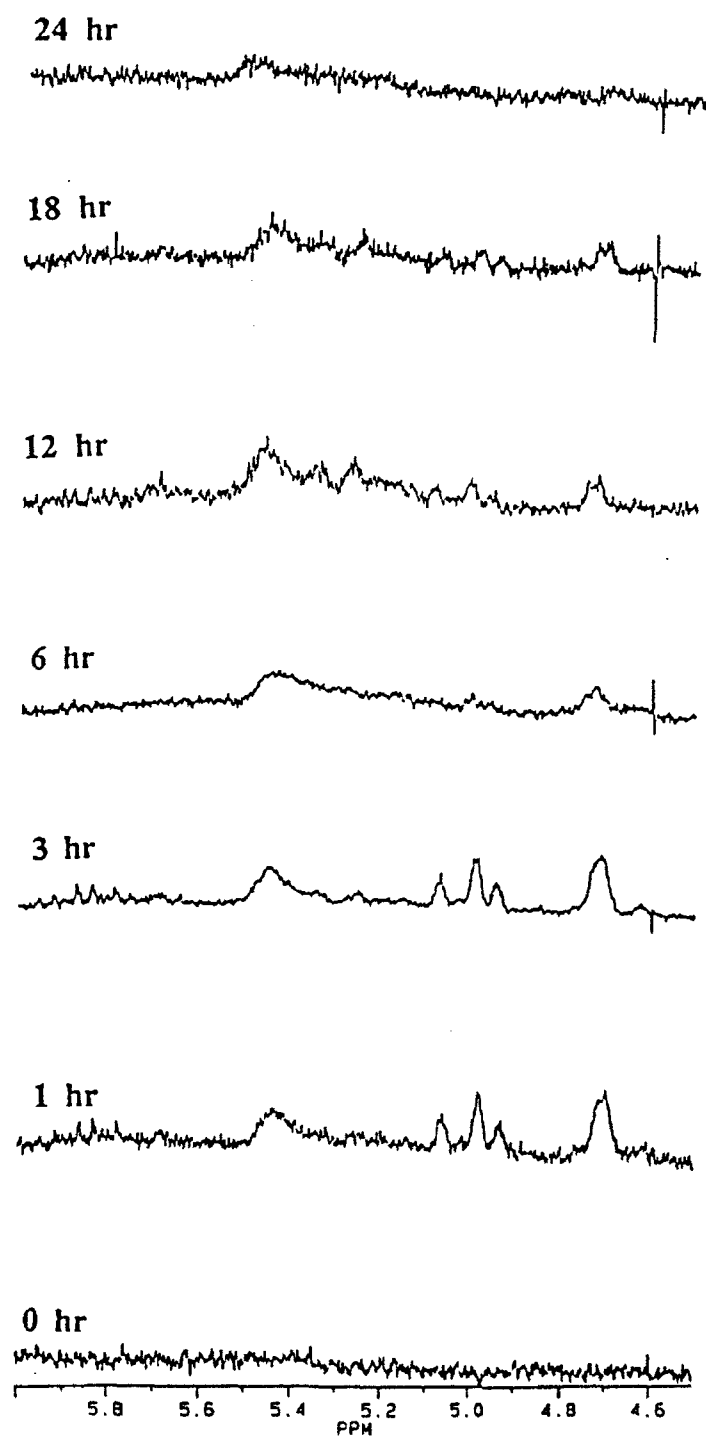


Figure 3.6.  $^1\text{H}$  NMR spectra of neat Jet A-1 fuel thermally stressed for the times indicated over air at  $425^\circ\text{C}$ .





**Figure 3.7** Scale expanded  $^1\text{H}$  NMR spectra in the olefinic region of neat Jet A-1 fuel thermally stressed for the times indicated over air at  $425^\circ\text{C}$ .

liquefaction reagents, resaturating olefinic double bonds as they are formed and interfering with the process of aromatization and subsequent formation of carbonaceous solids.

Figure 3.8 shows  $^1\text{H}$  NMR spectra (0-10 ppm) recorded at room temperature of Jet A-1 fuel samples containing 5% benzyl alcohol and thermally stressed under air after time periods of 0, 10, 60, 180, 360, and 720 minutes at 425°C. A comparison of the spectra of the unstressed Jet A-1 fuel with (Figure 3.8) and without (Figure 3.6) the additive, reveals that benzyl alcohol has a convenient characteristic resonance at 4.74 ppm attributable to the hydroxyl proton of the methanol group. Figure 3.9 shows  $^1\text{H}$  NMR spectra of the same samples (Figure 3.8) scale expanded in the olefinic proton region (4.5-6.0 ppm). In the unstressed sample there is no evidence of resonances attributable to olefinic protons and the spectrum is dominated by the intense line associated with the methanol group of benzyl alcohol at 4.74 ppm. It is significant that the intensity of this line at 4.74 ppm decreases as a function of thermal stressing, but is still present in the spectrum recorded after 6h at 425°C. This implies that benzyl alcohol gradually transforms to benzaldehyde (see infrared results<sup>2</sup>) in the Jet A-1 fuel over a period in excess of 6h under air at 425°C. At the same time, the olefinic resonances are clearly observed in the sample thermally stressed for 6h which is consistent with the infrared results and lends support for the *in situ* hydrogenation hypothesis.

## References

- (1) Selvaraj, L., Sobkowiak, M. and Coleman, M. M., *ACS Division of Petroleum Chemistry Preprints*, **37(2)**, 451 (1992).
- (2) Coleman, M.M., Selvaraj, L., Sobkowiak, M. and Yoon, E., *Energy and Fuels*, submitted.
- (3) Sivy, G.T., Gordon, B. and Coleman, M.M., *Carbon*, **21**, 573 (1983).
- (4) Song, C. et al., Compositional Factors Affecting Thermal Degradation of Jet Fuels Annual Report, Report for period July 1990 to July 1991, The Pennsylvania State University.

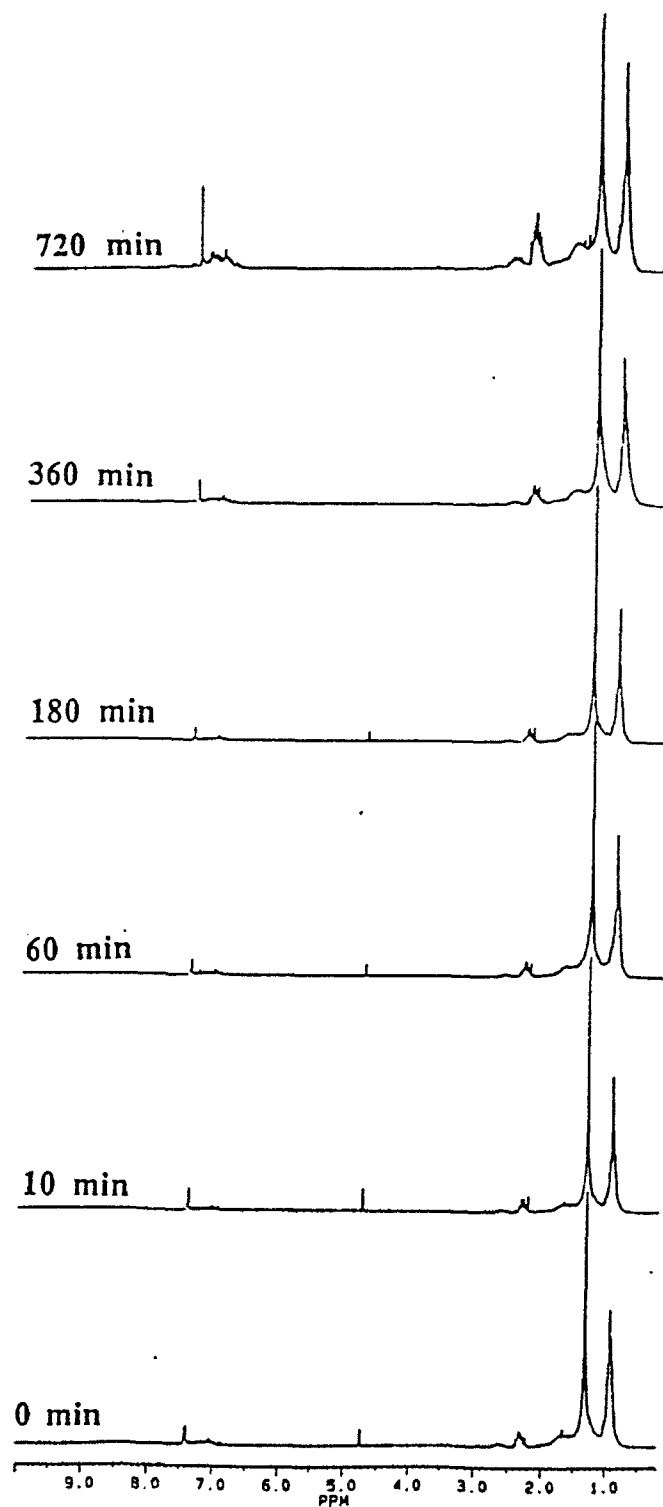


**Figure 3.8**  $^1\text{H}$  NMR spectra of Jet A-1 fuel containing 5% benzyl alcohol thermally stressed for the times indicated over air at  $425^\circ\text{C}$ .

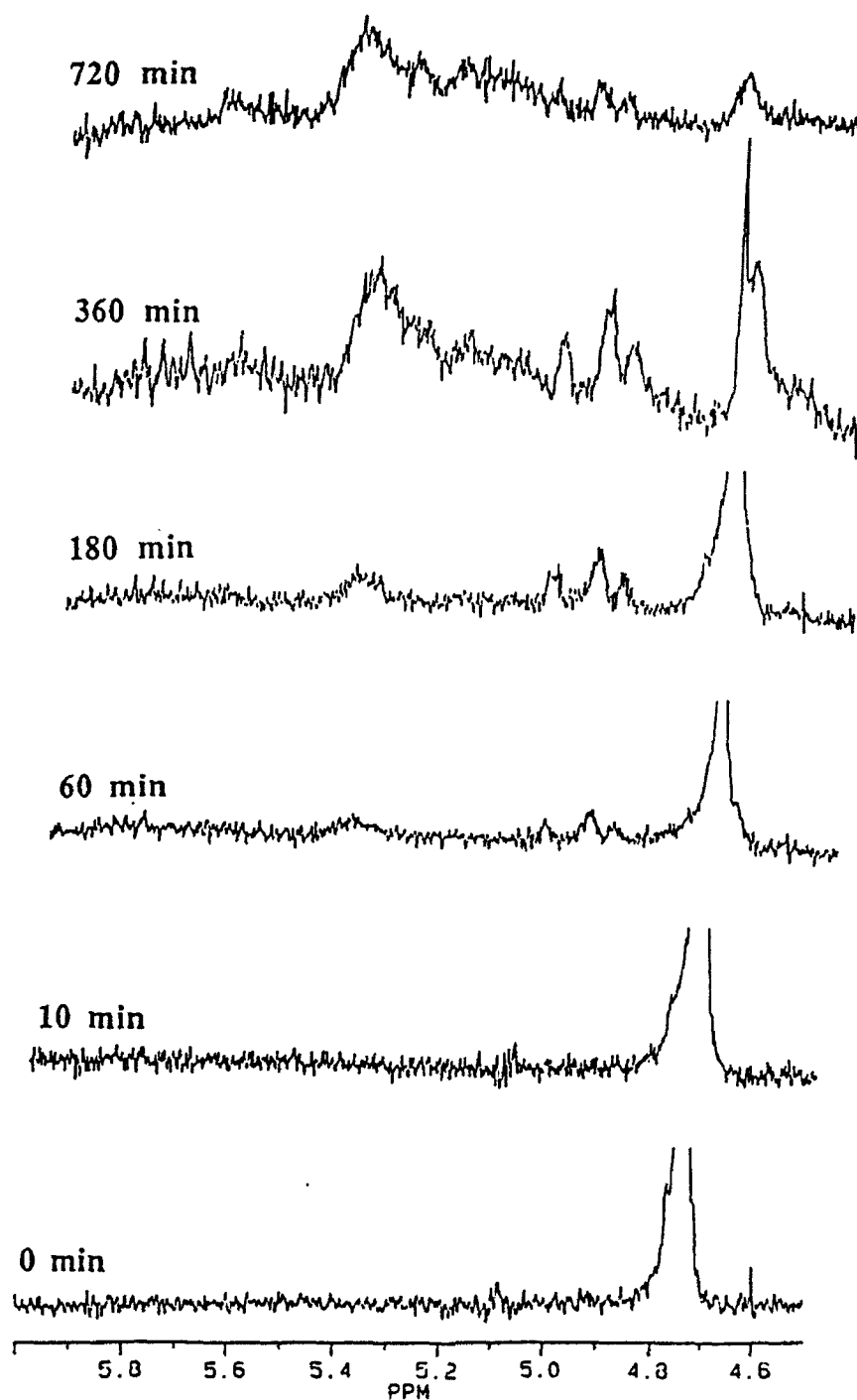


**Figure 3.9** Scale expanded  $^1\text{H}$  NMR spectra in the olefinic region of Jet A-1 fuel containing 5% benzyl alcohol thermally stressed for the times indicated over air at  $425^\circ\text{C}$ .

## **TASK 4. EXPLORATORY CONVERSION OF COAL TO HIGH THERMAL STABILITY JET FUEL**

Our previous work has clearly demonstrated that for advanced jet fuels, cycloalkanes are highly desirable components because of their higher thermal stability than the long-chain paraffins. The objective of Task 4 is to assess the potential of production of high yields of cycloalkanes by direct liquefaction, reducing the need for downstream hydroprocessing.

### ***Activity 1: Computer-Assisted Structural Elucidation of Vitrinite from High Volatile Bituminous Coal***

#### **Introduction**

In recent years, several models have been proposed for the chemical structure of coal.<sup>1-4</sup> Some of these models have been visualized in three dimensions by use of computer graphics.<sup>5</sup> The models have been constructed by considering elemental, spectroscopic, and pyrolysis/gas chromatography/mass spectrometry data. While the models have provided a visual framework for evaluating the kinds of structural elements that are contained in coal macromolecules, they fail to depict the chemical heterogeneity that exists in coal due to the many varied macerals. Developing structural models for individual macerals such as vitrinite would limit some of the heterogeneity, but vitrinite, a petrographically defined component, can also have a heterogeneous composition. There are numerous petrographic forms of vitrinite.

The approach towards defining a more homogeneous maceral component of coal used in our laboratory is one which has focused on coalified wood as a representative for vitrinite derived from xylem in ancient trees.<sup>6-9</sup> Structural models were developed from a lignin template, because lignin has been determined to be the major source of chemical structures in coalified wood. By examining the chemistry of a series of woods from peat to coalified woods from ancient rocks and seams, we have been able to discern changes in the lignin framework induced by coalification to the rank of subbituminous coal. The models were then developed by applying the observed changes to the lignin template. The model for lignin was that proposed by Adler.<sup>10</sup>

Detailed examination of coalified wood samples of higher rank, high-volatile bituminous coal, have allowed us to extend the model to this rank range. This report presents the data and the model for vitrinite from coalified wood of high volatile C bituminous coal rank. The model is constructed from elemental, solid-state  $^{13}\text{C}$  NMR, and flash pyrolysis/gas chromatography/mass spectrometric data.

## Methodology

The sample is a fossil stem which was recovered from a lacustrine shale from the Midland Formation (Triassic) near Culpeper, Virginia. Elemental and  $^{13}\text{C}$  NMR data for this sample have been previously published, but are here reevaluated for purposes of developing a structural model. Flash pyrolysis/gas chromatography/mass spectrometry was employed in a manner analogous to that described previously.<sup>6</sup> Pyrolysis products were quantified by integrating the total ion chromatogram (TIC), assuming equivalent response factors for individual components, and normalizing the concentrations to the total peak area for all peaks in the pyrogram.

The solid-state  $^{13}\text{C}$  NMR data were obtained by both the method of cross polarization with magic angle spinning (CPMAS) and by a Bloch decay. The CPMAS conditions were similar to those described previously.<sup>7</sup> The cycle time for the Bloch decay was 45 seconds. Both NMR data sets were transferred to a PC computer format and the peaks were deconvoluted by Lab Calc software available from Galactica Industries, Inc.

## Results

The elemental and NMR data for the coalified wood sample are shown in Table 4.1. The carbon content of 85.5% and a vitrinite reflectance value of 0.6 (N. Bostick, personal communication) indicate that the rank of this sample is equivalent to high volatile C bituminous coal. The oxygen content of 5.9%, measured by direct analysis, is significantly lower than oxygen contents (13.9%) of coalified logs of subbituminous rank.<sup>7</sup> A significant amount of nitrogen, 2.2%, is also observed.

Comparison of the NMR data obtained by CPMAS and by Bloch decay indicates that the two methods yield virtually identical spectra (Figure 4.1). The Bloch decay does show greater aromaticity and possibly a higher yield of phenolic carbon (Table 4.1). In both spectra the broad peaks for aromatic (100 - 160 ppm) and aliphatic (0-60 ppm) carbons dominate. Discernible shoulders at 140 and 153 ppm are observed in the aromatic carbon region, and these can be assigned to aromatic bridgehead or nonprotonated aromatic carbons and phenolic carbons, respectively. With a ratio of aryl-O to total aromatic carbon of about 0.12, it appears that nearly all aromatic rings have at least one phenolic OH or aryl ether carbon. The aliphatic carbon region also exhibits fine structure with a distinct peak at 17 ppm which can be assigned to methyl carbons. Dipolar dephasing studies confirm that this peak is that of methyl carbons.<sup>7</sup> Deconvolution of the aliphatic region shows that approximately one third of the aliphatic carbons are methyl carbons. Due to insufficient spinning speeds of the sample rotor, spinning sidebands are observed at 260 and 0 ppm.

Flash pyrolysis data for the coalified wood sample are shown in Figure 4.2 and the peaks are identified and quantified in Table 4.2. Phenol and alkylphenols are the most readily visible

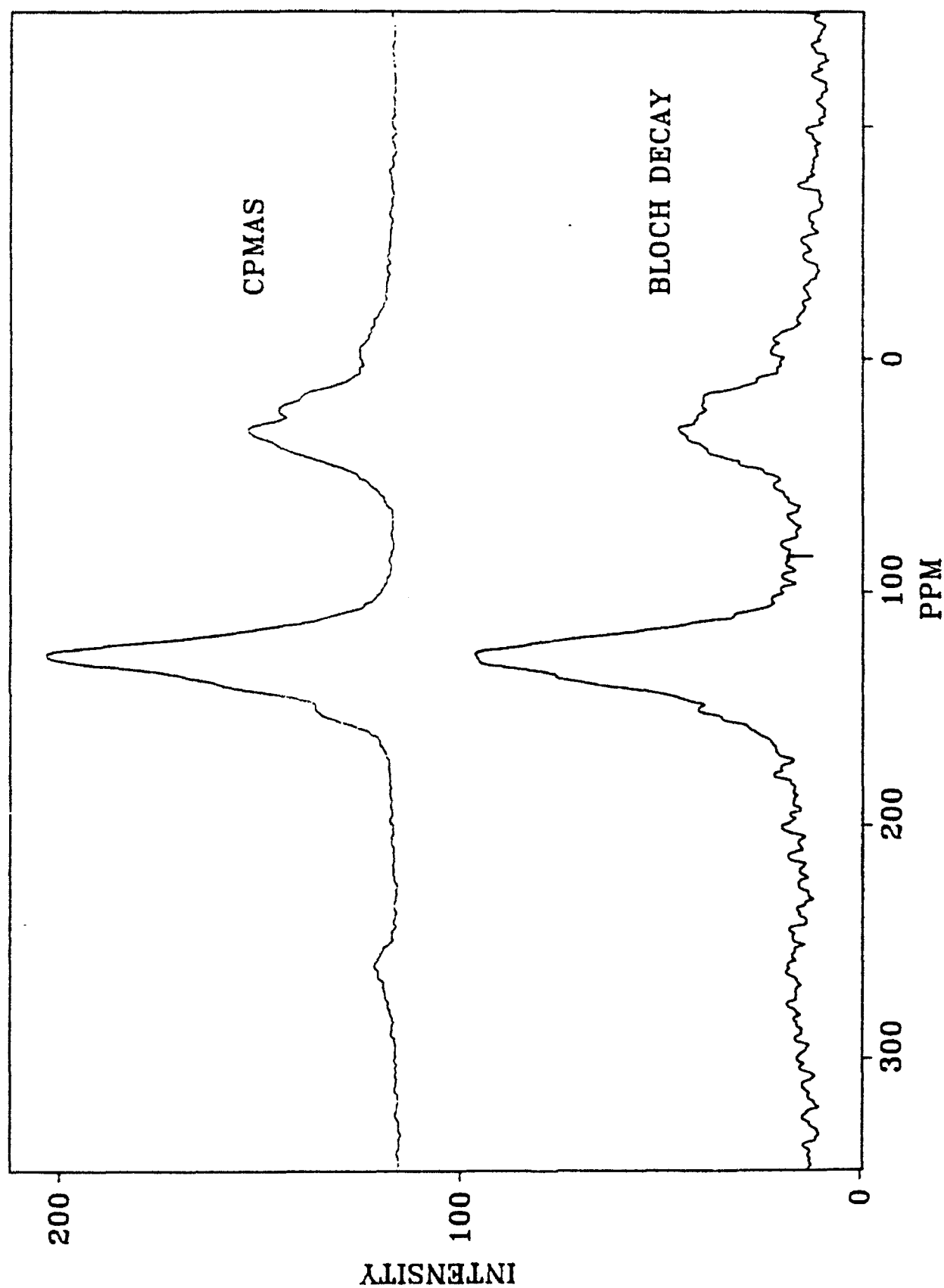


**Figure 4.1.** Solid-state  $^{13}\text{C}$  NMR data for the high volatile C bituminous coalified wood obtained by the CPMAS and Bloch decay methods

**Table 4.1.** Solid-state  $^{13}\text{C}$  NMR data for coalified wood samples.

Parameter	Hv Bituminous coal		Subbituminous coal
% carbon *	85.8		77.5
% hydrogen *	6.5		5.28
% oxygen *	5.9		13.9
% nitrogen	2.2		1.0
carbon aromaticity	0.64	(0.61)	0.59
aryl-O/aryl	0.11	(0.13)	0.22
methyl/total aliphatic	0.33	(0.28)	
aryl-H/aryl	0.44		0.40

\* - moisture and ash-free

values in ( ) are for Bloch decay data

pyrolysis products. Of these, the three cresol isomers, 4-ethylphenol, and 2,4 dimethylphenol predominate. Other isomers of C<sub>2</sub>-phenols are apparently minor or trace components. Only 4 isomers of C<sub>3</sub>-phenols predominate, trimethyl phenol, 2 isomers of ethyl, methyl phenols, and propylphenol. The specific substitution sites have yet to be discerned. As a whole, the phenols account for approximately 60% of the aromatic pyrolysis products and 40% of the total pyrolyzates. Benzene and alkylbenzenes are the second most prominent components, accounting for about 11% of the pyrolyzates. C<sub>1</sub>, C<sub>2</sub>, and C<sub>3</sub> benzenes with undetermined substitution patterns comprise the prominent components eluting in the 0-10 minute retention time window.

Other pyrolysis products which account for numerous other peaks in the pyrogram are naphthalenes, alkyl dibenzofurans, and n-alkane/n-alkene pairs. C<sub>1</sub>, C<sub>2</sub>, and C<sub>3</sub> alkynaphthalenes are present as various, as yet undetermined isomers. The n-alkane/n-alkene pairs show a range of carbon numbers ranging from C<sub>6</sub> to C<sub>22</sub>. The lower molecular weight homologs predominate and the distribution tapers off with increasing carbon number. Quantitatively, the n-alkanes/n-alkenes contribute to 33% of the pyrolyzate, a rather large percentage as a whole. At higher retention times in the pyrogram, peaks for alkyl dibenzofurans are found. These contribute to only 3.5% of the pyrolyzate and 5.2% of the aromatic products.

## Discussion

The quantitative information on carbon types afforded by the NMR data and the molecular-level information supplied by the flash pyrolysis data provide sufficient detail to allow construction of a molecular model from a lignin template. It is clear that the original lignin structures have been





**Table 4.2.** Flash pyrolysis data for Hv C bituminous coalified wood

compound	peak designation in Figure 4.2	weight %	weight % normalized to aromatics
benzene	B	2.2	3.3
toluene	B1	3.2	4.8
C-2 benzenes	B2	3.4	5.2
C-3 benzenes	B3	2.6	3.9
Total benzenes		11	17
phenol	P	2.3	3.6
<i>o</i> -cresol	P1	3.7	5.7
<i>m</i> + <i>p</i> -cresol	P1	8.9	13
2,4 dimethylphenol	P2	8.2	12
other C-2 phenols	P2	6.8	11
C-3 phenols	P3	7.2	11
C-4 phenols	P4	3.2	4.8
Total phenols		40	61
alkylnaphthalenes	N1, N2, N3	11	17
alkyldibenzofurans	F1, F2, F3	3.4	5.2
C4 - C22			
n-alkane/alkenes	4- 22	33	

modified by coalification because the coalified wood does not show any characteristics of the lignin-derived methoxy phenol structures. Previous studies<sup>8,9</sup> have suggested that lignin undergoes a series of coalification reactions that include 1)  $\beta$ -O-4 aryl-ether cleavage, 2) demethylation to form catechol-like structures, 3) dehydroxylation of the 3-carbon side chain, and 4) dehydroxylation of catechols to form phenols. In this previous study, a structural model was developed for ranks of brown coal, lignite, and subbituminous coal, using the lignin template published by Adler<sup>10</sup> and modifying the aromatic structures according to the coalification reactions observed for each rank level.

It is a logical progression to take the model developed in this prior study for subbituminous coal and to alter it in a way which would reflect the changes in chemistry observed between the high volatile C coal in the present study and the subbituminous coal in the previous study whose elemental and NMR data are shown in Table 4.1. The major changes between the two coalified

woods in going towards higher rank include 1) a decrease in oxygen content from 13.9% to 5.9% with a corresponding increase in carbon content and 2) a significant increase in benzene and alkylbenzenes in pyrolyzates. Interestingly, the carbon aromaticity does not change greatly, but the fraction of aryl-O carbon to total aromatic carbon decreases by about half. This and the significant loss of oxygen from the elemental data would imply that the primary transformation of the catechol and alkylphenolic structures in subbituminous coal is a loss of aryl-O -containing structures and a condensation of the phenols to diaryl ethers.

While tracing a template through coalification is certainly a valid approach, we have begun to investigate other approaches to molecular modeling, using primarily computer methods that have recently been described.<sup>11,12</sup> Using a molecular modeling software similar to the one developed by Faulon et al.<sup>12</sup>, we have generated two models, one which will be described in this report and the other to be described by Faulon et al.<sup>13</sup>. The model generated here provides a three dimensional graphical display of a structure constructed from a lignin framework. Briefly, the input to the model is the quantitative NMR information and the elemental data. The pyrolysis data are not used in a quantitative sense but rather a qualitative sense to input structures found that relate to lignin structural units. The lignin skeletons and inferred bonding sites are deduced from the pyrolysis data and from the previous studies on the coalification of wood showing the reactions of the various functional groups associated with lignin. For example, it is clear that the presence of 2,4 dimethylphenol in pyrolyzates indicates a lignin-derived phenol where the attachments to other structural entities are at the 2 and 4 positions. Indeed, the three-carbon side chain of lignin is in the C-4 position and a significant number of lignin units are also linked at C-2. From previous studies of coalified woods of low rank, we have deduced that the methoxy group is lost and that the three-carbon side chain is reduced to a propanyl group.

From a practical point of view, to verify the correlation between the lignin and our structure, three molecular fragments were introduced in the computerized model : propylbenzene, 4-propylphenol, and dipropylnaphthol. These fragments were built and stored in a library using the molecular modeling software PCMODEL (Serena software). Then, our program was asked to generate a structure containing these fragments by taking account of all analytical data. This operation was realized in two steps. First, the program computed the correct amount of fragments and connections between fragments to obtain a structure consistent with <sup>13</sup>C NMR and elemental analysis. The model of lignin used as template in our previous publication<sup>9</sup> contains 115 carbon atoms, therefore we asked the program to find all the solutions between 95 and 135 carbon atoms. The best solution found is C<sub>113</sub>H<sub>105</sub>O<sub>5</sub> and is composed of 3 propylbenzenes, 2 propylphenols, and 2 dipropylnaphthols. The connections between these fragments are the following: 4 biphenyl bonds, 5 benzylphenyl ether bonds, 8 bibenzyl bonds, 3 biphenylpropane bonds, and one biphenylethane bond. In a second step, from the previous list of fragments and bonds, the program was run to generate automatically a 3D structure. The program estimated first the number of

structures which can be generated. The number found was too big to build all of them, therefore one structure was chosen randomly and constructed in 3D space.

Figure 4.3 shows a two-dimensional projection of the 3D model built by the program. There are some important features of this model that need explanation. It is important to highlight the fact that this displayed model is only one of numerous possible models that the program has calculated, and as such should be viewed as only an example whose chemistry is consistent with the chemical information provided to the program. Note that all aryl-O carbons are phenolic ethers and that the structure is composed of principally one- and two-ring aromatic systems. Also, the presence of dibenzofurans is a characteristic feature that is consistent with the pyrolysis data. In fact, the entire structure can be visualized as providing pyrolysis fragments which match rather well with the distribution of aromatic pyrolysis products. What is conspicuously absent is the presence of long-chain aliphatic structures which could give rise to the n-alkane/n-alkene pairs observed in pyrolysis. We feel that these components are minor components of the coalified wood and are not derived from lignin structural units. It is likely that they were incorporated into the coal from either external materials migrating into the sample or from microbial remains present within the wood as it decomposed and was later coalified. It is also likely that the flash pyrolysis accentuates these substances because they are more readily pyrolysed in comparison with the lignin-derived materials. Also absent are the nitrogen-containing structures. Elemental data for this sample shows about 2% nitrogen.<sup>8</sup> We do not have any data concerning the types of nitrogen-containing structures that might be present in this sample. Thus, we choose to omit these structures until which time we might have enough information to include them.

The three dimensional display is not readily visualized in two dimensions, but examination of the structure in Figure 4.3 shows the connecting points which imply that the structure is three-dimensional. The visualization of the structure in three dimensions is important from the standpoint that we must visualize coal reactivity as a three dimensional phenomenon. The ability to utilize sophisticated computer graphics displays adds to our ability to eventually utilize such structures for the prediction of coal reactivity.

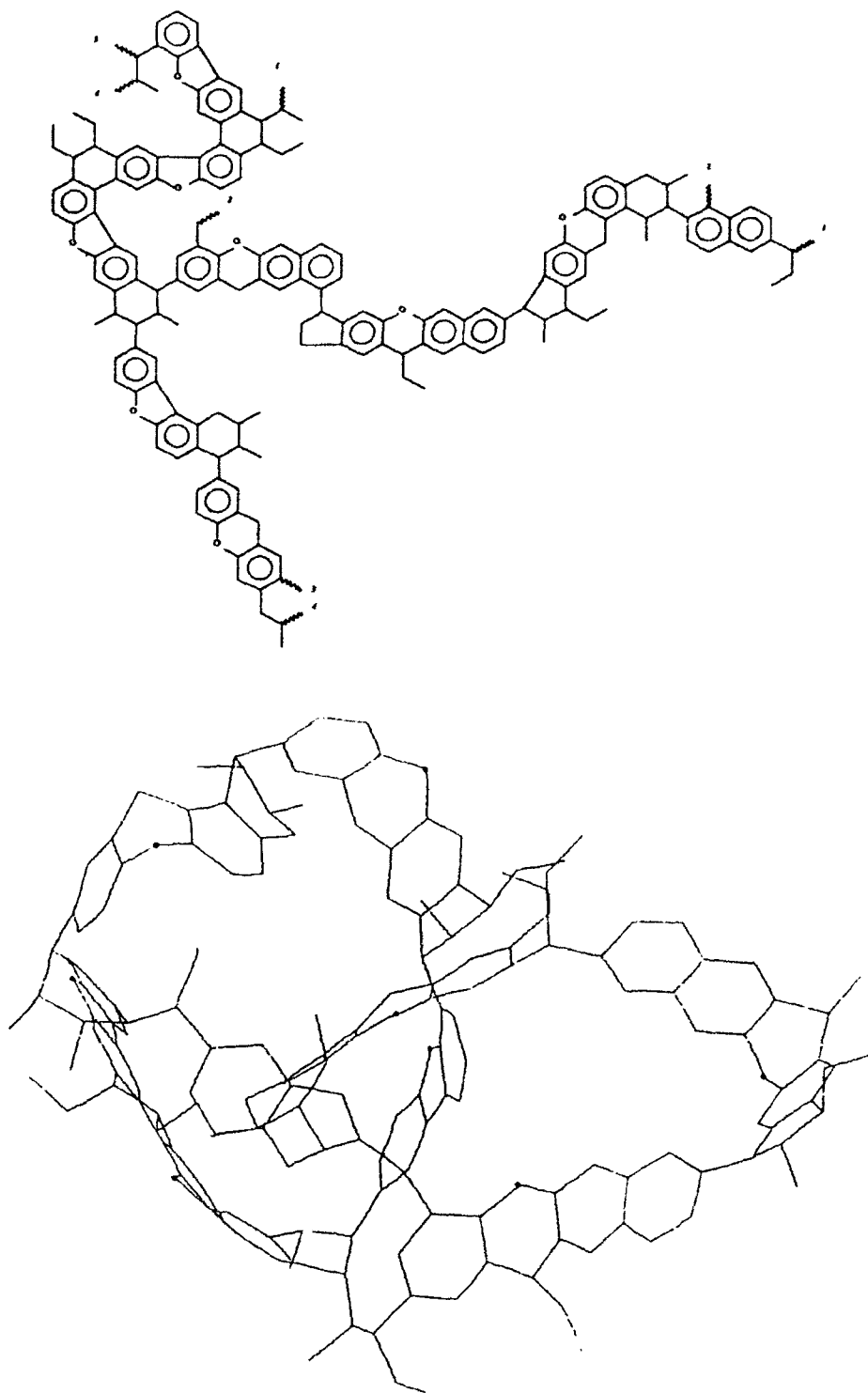


**Figure 4.3.** The two-dimensional display of the three-dimensional structural model for high volatile bituminous coalified wood.

## References

1. Given, P. H., *Fuel*, **39**, 147, 1960.
2. Wiser, W. H., *Proc. of the Electric Power Research Institute Conf. on Coal Catalysis*, 1973.
3. Solomon, P.R., in *New Approaches in Coal Chemistry*, Am. Chem. Soc. Symp. Series No. **169**, 61, 1981.
4. Shinn, J. H., *Fuel*, **63**, 1187, 1981.
5. Carlson, G. A., and Granoff, B., in *Coal Science II*, Advances in Coal Sciences series **461**, 159, 1990.
6. Hatcher, P.G., Lerch, H.E., III, Kotra, R.K., and Verheyen, T.V., *Fuel*, **67**, 1069, 1988.
7. Hatcher, P.G., *Energy and Fuels*, **2**, 48, 1988.
8. Hatcher, P.G., Lerch, H.E., III, and Verheyen, T.V., *Int. J. Coal Geol.*, **13**, 65, 1989.
9. Hatcher, P. G., *Organic Geochemistry*, **16**, 959, 1990.
10. Adler, E., *Wood Sci. Technol.* **11**, 69, 1977.
11. Faulon, J. L., *Prediction Elucidation and molecular modeling : Algorithm and Application in Organic Geochemistry*, PhD Thesis, Ecole des Mines, Paris, 1991.
12. Faulon, J. L., Vandenbroucke, M., Drappier, J. M., Behar, F., and Romero, M., *Advances in Org. Geochem.*, **16**, 981, 1990.
13. Faulon, J. L., Hatcher, P. G., and Wenzel, K. A., *Fuel Div. ACS, Preprints*, this volume, 1992.

## Activity 2. Liquefaction of Coals to Produce Jet Fuels

### Introduction

Fuels generated from coal liquefaction, in principle, are a viable alternative to fuels processed from petroleum. However, the chemical character of the fuels may not be of the optimum composition to satisfy fuel requirements, and therefore, the coal generated fuel will have to be processed further.<sup>1</sup> If it is considered that the expense of the "crude" coal-derived oil is more than that of the petroleum crude before processing, and that the "crude" coal-derived oil must be processed even further generating even more expense, it seems that the economic viability of coal liquefaction is even farther down the road. It is then important to explore either a method of generating coal liquids that reduces the necessity of downstream processing or uses for coal liquids that are inherent to its chemical characteristics. Much effort has been done at Penn State to explore both of these avenues.<sup>2,3</sup>

Not only can chemical products be produced more easily and in more abundance from coal liquids as discussed by Song and Schobert,<sup>2</sup> but certain fuels, such as jet fuel, are in fact more thermally stable than jet fuel produced from petroleum.<sup>2-8</sup> Jet fuels produced from coal are higher in density and have a higher energy content per unit volume.<sup>9</sup> The use of a high density jet fuel could increase the range of current military aircraft by 10-15%.<sup>9</sup> It is, therefore, worth exploring methods to obtain high yields of jet fuels from coal that are more thermally stable and have a higher energy content.

Here we will discuss the chemical characteristics that are desirable in a jet fuel, the desirable structural characteristics of the feed coal, and how the characteristics are to be determined. We will also discuss the method of production of the jet fuels to provide the most optimum yield by comparing various liquefaction methods, catalysts, and solvents.

### **Optimum Jet Fuel Properties**

It has been shown that jet fuel generated from coal has some superior characteristics to jet fuels generated from petroleum.<sup>3,4,6</sup> Jet fuels that come from coal tend to contain two- and three-ring aromatics and cycloparaffins. These structures, especially the cycloparaffins, are more thermally stable and have less tendency to form solids at high temperatures than jet fuels from petroleum that contain primarily straight chain paraffinic structures.<sup>3,4,6</sup> However, it must be considered that large amounts of aromatic groups in fuels decrease combustion performance and increase the likelihood of soot formation.<sup>1,9</sup>

### **Structural Characteristics of Optimum Coal Structure to Produce Jet Fuel**

It seems logical to deduce, if the most stable structures are two- and three-ring aromatics and cycloparaffins, that coals containing primarily these types of structures in the macromolecular structure would be the best coals to liquefy. It is also desirable to choose coals that do not have high heteroatom content, for oxygen, sulfur, and nitrogen are also undesirable in jet fuels.<sup>10-14</sup> However, it is difficult to find both these characteristics in one coal, as well as finding a coal that is amenable to liquefaction. This is because high-rank coals contain fewer heteroatoms but larger aromatic ring clusters (6-30 rings) and are not amenable to liquefaction, while low-rank coals contain smaller ring clusters (1-2 rings) but large quantities of oxygen.<sup>15-17</sup> The chosen coals should satisfy both requirements, and therefore, certain structural parameters must be taken into consideration when selecting the coals.

### **Problem Statement**

The goal of this project is to test one (or more) hypotheses concerning the prospects for making naphthenes via direct hydrogenation of coal. In order to accomplish this, there are three areas of concern that must be addressed because of the lack of attention given these areas in previous liquefaction research:

**A.** Little consideration has been given about specific structural information of coals for liquefaction. The structure of coal is especially important in this project in order to produce high quantities of jet fuel that contain 2- and 3-ring naphthenes. Coals must be chosen that are of low heteroatom content and that contain clusters of 2- and 3-ring aromatics and naphthenes.

**B.** Little consideration has been given about the specific structural information of the liquids produced. Typically the products of reaction are separated into fractions by solvents of various polarities. However, the fractions are not typically chemically characterized. Therefore, the coal liquid product must be analyzed by GC/MS and NMR in order to compare the liquid products of each coal with the structural composition of the coal.

**C.** Usually various catalysts have been chosen without attention being given to A and B. Only after the first two areas are considered will catalysts be chosen to enhance the production of a jet fuel with predominantly naphthenic structures.

**Hypothesis 1.** The structure of the coal will determine the percentage of 2- and 3-ring aromatics and naphthenes in the liquefaction product. Incorporation of distillation and GC/MS and NMR will provide a means to analyze the coal and liquefaction products more effectively than has been done previously.

**Hypothesis 2.** Catalysts and reaction conditions can be varied in order to optimize the production of jet fuel.

### **Structural Analysis of Coal**

Several coals have been chosen as candidates for production of a jet fuel. These coals are included in Table 4.3. These coals were chosen from the Penn State Coal Sample Bank based on rank, on elemental analysis for C, H, N, S, and O, and on mineral matter content. These coals range in rank from subbituminous C to high volatile A bituminous coals, and these coals contain less than 11% mineral matter. It is important to have low levels of mineral matter in order to minimize possible inherent catalytic effects that could interfere with external catalysts. According to Van Krevelen<sup>15</sup> and Hirsch,<sup>16</sup> coals of this rank contain aromatic clusters of one to four rings. It is most important to choose coals that contain the smaller aromatic ring clusters that can be hydrogenated; but also it is important to have reduced levels of oxygen.



**Table 4.3. Data for Coal Samples.**

<b>Penn State Sample Bank No.</b>	<b>PSOC- 487</b>	<b>PSOC- 831</b>	<b>PSOC- 1216</b>	<b>PSOC- 1379</b>	<b>PSOC- 1488</b>
Seam	Bed # 53	Brazil Block	L. Kittaning	Colorado F	Deitz
State	Wyoming	Indiana	Penn	Colorado	Montana
Country	USA	USA	USA	USA	USA
ASTM Rank	Sub A	h <sub>v</sub> C b	h <sub>v</sub> A b L	h <sub>v</sub> C b	Sub B
Moisture (as received, wt%)	11.55	13.02	1.94	11.99	23.66
Mineral Matter (dry, wt%)	6.89	4.16	4.99	5.09	6.05
<b>Elemental Composition</b>					
Carbon	75.91	83.28	83.3	76.74	76.57
Hydrogen	4.78	4.97	5.26	4.97	5.20
Nitrogen	1.21	1.61	1.63	1.69	0.95
Sulfur (organic)	0.42	0.94	0.97	0.63	0.51
Oxygen (by difference)	17.67	8.64	8.84	15.96	16.78
<b>Petrographic Composition</b>					
Vitrinite	89.60	79.20	91.1	92.20	88.60
Exinite	2.50	4.90	4.0	0.60	3.50
Inertinite	7.90	15.90	4.9	7.20	7.90

Table 4.3: cont'd.

<b>Penn State Sample Bank No.</b>	<b>PSOC- 1503</b>	<b>DECS-5</b>	<b>DECS-6</b>	<b>DECS-7</b>	<b>DECS- 12</b>
Seam	Blind Canyon	Hiawatha	Blind Canyon	Adaville #1	Pitt #8
State	Utah	Utah	Utah	Wyoming	Penn
Country	USA	USA	USA	USA	USA
ASTM Rank	hVC b	hVC b	hVA b	hVC b	hVA b
Moisture (as received, wt%)	10.35	7.54	4.70	17.34	2.40
Mineral Matter (dry, wt%)	4.46	9.80	6.67	4.79	11.88
<b>Elemental Composition</b>					
Carbon	80.8	80.27	81.72	77.45	84.75
Hydrogen	6.12	5.37	6.22	5.51	5.66
Nitrogen	1.55	1.26	1.56	1.04	1.39
Sulfur (organic)	0.54	0.31	0.40	0.91	0.83
Oxygen (by difference)	10.98	12.78	10.10	15.09	7.37
<b>Petrographic Composition</b>					
Vitrinite	91.1	65.5	69.10	n.d. *	83.00
Exinite	1.2	13.9	17.00	n.d.	8.10
Inertinite	7.7	19.8	13.60	n.d.	8.90

\* n.d. = not determined.

There are several methods available to characterize coals. In order to determine the crosslink density, the coals were swollen in pyridine according to the procedure of Joseph.<sup>18,19</sup> The  $Q$  ( $Q=h_2/h_1$ , where  $h_2$  is the height after swelling and  $h_1$  is the height before swelling) determined by this method for these coals ranged from 1.3 to 1.7, which is not a large variation in  $Q$ . The coals are of similar solvent swelling indices because they are of similar rank.<sup>20</sup>  $^{13}\text{C}$ -NMR has been done to determine the aromaticity and general structural features of the coals, and future work will be done with dipolar dephasing and flash pyrolysis/GC/MS in order to estimate the average ring size of each coal. Preliminary liquefaction experiments have been completed with each of the coals with and without a molybdenum sulfide catalyst in order to determine the reactivity of the coals. The experiments were conducted at low severity reaction conditions and in the presence of a hydrogen shuttler. These data are shown in Table 4.4. The most reactive of these coals are DECS-6, DECS-12, and PSOC-1379. PSOC-1503 and DECS-5 also show high conversion in the presence of catalyst, but the selectivity to oil yield is not as high as PSOC-1379, DECS-6, and DECS-12. The least reactive coals are the subbituminous coals PSOC-1488 and PSOC-487.

The catalyst for these liquefaction experiments is  $\text{MoS}_2$ , which is introduced into the reaction as ammonium tetrathiomolybdate. Ammonium tetrathiomolybdate is believed to decompose to the amorphous catalyst,  $\text{MoS}_2$ , during the liquefaction reaction.<sup>21-23</sup> It has also been suggested that the role of the  $\text{MoS}_2$  is predominantly the breaking of crosslinks in the coal, especially at low severity reaction conditions, but the actual mechanism is not yet clear.<sup>24</sup> Figure 4.4 is a representation of the possible reaction paths for coal liquefaction, and it is obvious that analysis of the coal liquefaction mechanism is quite complex. These data also show at  $360^\circ\text{C}$  that the predominant action of the catalyst is the breaking of crosslinks, because the predominant increase in conversion is in the production of preasphaltenes and asphaltenes. For some of the coals, hydrogenation or hydrocracking to oils also occurs when catalyst is used.

### **Optimum Coal Liquefaction to Produce a Jet Fuel**

Not only is it important to choose a coal of certain structural characteristics, but it is also important to choose optimum reaction conditions based on the structural information for the coals. It was established in the previous section that two- and three-ring cycloparaffins are thermally very stable components of jet fuels. It was also established that the middle rank of coals tend to contain two- and three-ring aromatic groups.<sup>15-17</sup> To obtain large quantities of two- and three-ring cycloparaffins, two primary steps must occur during the liquefaction procedure. First, the aromatic groups must be separated. The assumption is that the aromatic groups are connected by crosslinks which tend to consist of heteroatoms and aliphatic groups.<sup>15-17</sup> It is believed that the

**Table 4.4. Data for Solvent Swelling, Aromaticity, and Liquefaction Conversion for Single Stage Reactions.**

Coal	Rank	Reaction	Tot Conv	Oils + Gas	Asph	Preasp h	L/H <sup>a</sup>
		Conditions	wt %	wt %	wt %	wt %	
<b>PSOC-487</b>	Sub A	360°C, phen <sup>b</sup>	20.4	0.8	7.3	12.2	0.04
		360°C, phen, cat <sup>c</sup>	54.5	-4.8	18.6	40.8	-0.08
<b>PSOC-831</b>	hvC b	360°C, phen	29.0	0.1	7.0	21.9	0.00
		360°C, phen, cat	43.2	4.1	8.9	30.2	0.10
<b>PSOC-1216</b>	hvA b	360°C, phen	34.2	4.0	11.7	18.4	0.13
		360°C, phen, cat	57.4	-3.2	18.8	41.8	-0.05
<b>PSOC-1379</b>	hvC b	360°C, phen	18.1	3.5	5.4	9.3	0.24
		360°C, phen, cat	65.8	16.2	19.7	29.9	0.32
<b>PSOC-1488</b>	Sub B	350°C, naph <sup>d</sup>	18.3	11.2	7.1		1.58
		350°C, naph, cat	47.8	14.0	33.9		0.40
<b>PSOC-1503</b>	hvC b	360°C, phen	39.1	11.3	10.9	16.9	0.41
		360°C, phen, cat	74.4	8.0	19.9	46.5	0.12
<b>DECS-5</b>	hvC b	360°C, phen	30.8	-3.4	7.8	26.3	-0.10
		360°C, phen, cat	69.8	5.02	18.4	46.3	0.08
<b>DECS-6</b>	hvA b	360°C, phen	46.6	10.1	11.4	25.2	0.28
		360°C, phen, cat	83.4	18.1	19.1	46.2	0.28
<b>DECS-12</b>	hvA b	360°C, phen	38.1	-0.2	23.2	15.3	-0.01
		360°C, phen, cat	70.6	8.1	18.0	44.5	0.13

<sup>a</sup> L/H = Light-to-heavy ratio.

<sup>b</sup> phen = phenanthrene

<sup>c</sup> cat = catalyst

<sup>d</sup> naph = naphthalene

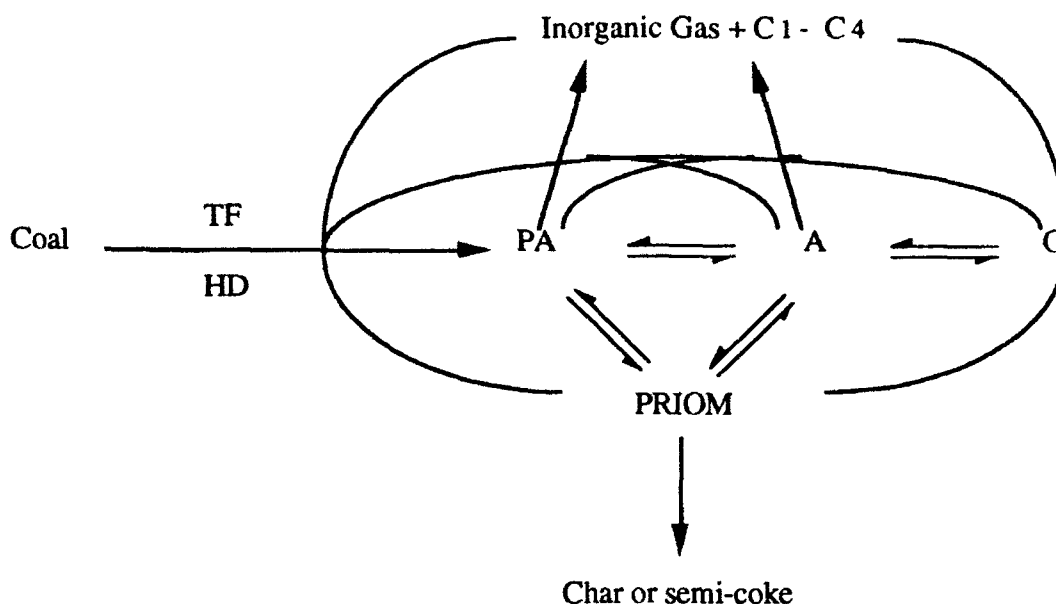


**Figure 4.4.** A Reaction Model for Coal Liquefaction (TF: Thermal Fragmentation; HD: Hydrogen Donation by H in coal, vehicle, and gas; PRIOM: Promptly Repolymerized or Re-crosslinked Insoluble Organic Materials; A: Asphaltene, PA: Preasphaltene; O: Oils).<sup>29-30</sup>

crosslinks typically begin to break apart at  $\sim 350^{\circ}\text{C}$ .<sup>25</sup> There is evidence to support that molybdenum sulfide catalyst promotes the breaking of these crosslinks.<sup>21,22,24,26</sup> Once these aromatic groups are separated, it is important to hydrogenate the aromatic groups to cycloparaffins without destroying the ring structure. There are many known hydrogenation catalysts that are used in petroleum refining, including molybdenum sulfide, but most are high activity catalysts (e.g., platinum or palladium) that tend to be poisoned either by sulfur or highly aromatic feedstocks.<sup>1,27</sup> Those that have been considered for upgrading coal liquids are typically supported Ni-Mo or Ni-Co catalysts.<sup>28</sup> Other candidate catalysts are Lewis acid complexes (e.g.  $\text{MoCl}_3\text{-LiCl-KCl}$ ,  $\text{NiCl}_2\text{-LiCl-KCl}$ ) because according to Song et al., these catalysts may selectively hydrogenate aromatic groups without destroying the ring structure.<sup>29,30</sup> It has also been suggested that *in situ* unsupported molybdenum sulfide plays a role in hydrogenation/hydrocracking of the heavier products (preasphaltenes and asphaltenes) [24].

It has been recently shown that temperature-programmed liquefaction (TPL) is an excellent liquefaction method for thermal production of high liquid yields, especially the desirable oil yields.<sup>31</sup> A solvent should also be present in the reaction system because the use of a solvent usually increases the yield and the selectivity to oils.<sup>32</sup>

There are two main considerations for the choices of solvents. First, it is believed that hydrogen donors (H-donors), which are usually hydrogenated polyaromatic hydrocarbons (PAH), donate hydrogen radicals to cap coal fragments during reaction.<sup>34</sup> PAH's also participate in the transfer of hydrogen.<sup>34</sup> These solvents are known as hydrogen shuttlers. The other consideration for choosing a solvent is the separation of the solvent from the desired products. In commercial and pilot plant work, a process solvent produced from the reaction is hydrogenated and recycled to mix with the coal. Most bench-scale work uses model compounds in order to deconvolute the role of the solvent in coal liquefaction, but usually this compound is extracted into the hexane-soluble oil yield and must be separated from the oils generated from coal (it is expected that the oils will be two- and three-ring PAH's and cycloparaffins). Getting a clean separation when there is 5 g of solvent and less than 0.5 g of oil yield has not been an easy task in previous experimentation.<sup>19,35</sup> It is, therefore, important to choose a good solvent (H-donor) that can be easily separated, so it may be best to choose a solvent, such as a hydrogenated pyrene.

Based on this information, it should be possible to choose one of the following scenarios in order to produce the optimum level of jet fuel (all will use a H-donor as a solvent):

1. TPL with a hydrogenation catalyst.
2. TPL or Temperature-Stage Liquefaction (TSL), using a single catalyst that is known to *disrupt crosslinks as well as hydrogenate*.
3. TSL using a catalyst to cut crosslinks in the first stage and a different catalyst to hydrogenate in the second stage.
4. TSL using both catalysts in both stages.

### **Analysis of Jet Fuel Produced**

Separation of the desirable jet fuel from the other products, as well as analysis of the products, will also constitute a major portion of the work for this project. The current liquefaction methods used in the laboratory may interfere with the analysis of the products; therefore, some of the workup procedures may have to be changed. Typically the contents of the reactor are removed with one of the fractionation solvents: hexane, toluene, or THF. However, since many pilot plants distill products, distillation may be incorporated into the workup procedure. It is also difficult to produce large quantities of sample in the 25-ml microautoclave, a device that is also quite different from pilot plant reactors.

Once the jet fuel has been separated, it will be important to analyze it according to the procedure developed by Song et al.<sup>3,4</sup> They separated both petroleum- and coal- derived jet fuels by liquid chromatography, and analyzed the separated components by GC/MS.<sup>3,4,6</sup> Jet fuels must adhere to standardized refinery guidelines for fuels,<sup>9,36</sup> such as the smoke point and the freeze point, so these tests will be performed as well. Song et al. and others also used <sup>1</sup>H-NMR, UV

spectra, FTIR, and optical microscopy to follow the thermal decomposition of the jet fuels and model compounds after thermally stressing the liquids.<sup>3-6,10,11</sup> All these factors must be considered in the production of jet fuel.

### Conclusions to Date

The production of jet fuel from coal in order to optimize the incorporation of two- and three-ring cycloparaffins is an extensive research project. Preliminary experiments determining the best coals for liquefaction have been completed, and the coals chosen for further structural experiments are PSOC-1379, PSOC-1488, DECS-6, and DECS-12. Although PSOC-1488 is quite unreactive during low severity liquefaction conditions, structural data determined for this coal may provide fundamental understanding of its unreactivity. Choice of the liquefaction procedure to be used will be the next step.

### References

1. Schobert, H.H. *Chemistry of Hydrocarbon Fuels*, Butterworths, London, Ch. 5, 8, and 9, 1990.
2. Song, C. and Schobert, H.H. "Specialty Chemicals and Advanced Materials From Coals: Research Needs and Opportunities," *ACS Preprints, Div. of Fuel Chemistry*, in press, 1992.
3. Song, C., Eser, S., Schobert, H.H., Hatcher, P.G. Advanced Thermally Stable Jet Fuels Development Program Annual Report, Volume II, Interim Report for Period July 1990 to July 1991, WRDC-TR-91, Vol. II, 1991.
4. Song, C. and Hatcher, P.G. "Compositional Differences Between Coal- and Petroleum-Derived Jet Fuels," *ACS Preprints, Div. of Petrol. Chemistry*, in press, 1992.
5. Song, C., Peng, Y., Jiang, H., and Schobert, H.H. "On The Mechanisms of PAH and Solid Formation During Thermal Degradation of Jet Fuels," *ACS Preprints, Div. of Petrol. Chemistry*, in press, 1992.
6. Song, C., Eser, S., Schobert, H.H., and Hatcher, P.G. "Thermal Stability of Petroleum- and Coal-Derived Jet Fuels at High Temperatures," *ACS Preprints, Div. of Petrol. Chemistry*, in press, 1992.
7. Frankenfeld, H.W. and Taylor, W.F. *Ind. Eng. Chem. Prod. Res. Dev.*, **19**, 65, 1980.
8. Taylor, W.F. *Ind. Eng. Chem. Prod. Res. Dev.*, **13**, 133, 1974.
9. Frazier, M.D. Proceedings of Third Annual Pittsburgh Coal Conference, September 1986, Pittsburgh Coal Conference, MEMS, Greensburg, PA, 608, 1986.
10. Eser, S., Perison, J., Copenhaver, R.M., Shiea, J., and Schobert, H.H. "Thermal Degradation of Alkylated Phenols," *ACS Preprints, Div. of Petrol. Chemistry*, in press, 1992.

11. Selvaraj, L., Sobkowiak, M., and Coleman, M.M. "Infrared Studies of Thermally Stressed Jet Fuels," *ACS Preprints, Div. of Petrol. Chemistry*, in press, 1992.
12. Mayo, F.R. *Acc. Chem. Res.*, **1**, 193, 1968.
13. Boss, B.D. and Hazlett, R.N. *Can. J. Chem.*, **47**, 4175, 1969.
14. Taylor, W.F. *Ind. Eng. Chem. Prod. Res. Dev.*, **8**, 375, 1969.
15. Van Krevelen, D.W. *Coal: Typology-Chemistry-Physics-Constitution*, Elsevier Scientific Publishing Co., The Netherlands, 336, 1981.
16. Hirsch, P.B. *Phil. Trans. R. Soc. Lond.*, **A226**, 142, 1954.
17. Berkowitz, N. *The Chemistry of Coal, Coal Science and Technology*, Elsevier Scientific Publishing Co., The Netherlands, 49, 1985.
18. Joseph, J.T., *Fuel*, **70**, 139, 1991.
19. Artok, L., Davis, A., Mitchell, G.D., and Schobert, H.H. *Fuel*, in press, 1992.
20. Cody, G. Private communication, 1992.
21. Derbyshire, F.J. "Catalysis in Coal Liquefaction," IEA CR/08, IEA Coal Research, London, 1988.
22. Davis, A., Schobert, H.H., Mitchell, G.D., and Artok, L. "Catalyst Dispersion and Activity Under Conditions of Temperature-Staged Liquefaction," DOE-PC-89877-1,2,3 Progress Reports, 1989-1990.
23. Naumann, A.W., Behan, A.S., and Thorsteinson, E.M. in "Proceedings of the Fourth International Conference on the Chemistry and Uses of Molybdenum," (H.F. Barry, P.C.H. Mitchell, Eds.), Climax Molybdenum Co., Ann Arbor, MI, 313, 1982.
24. Burgess, C.E., Artok, L., and Schobert, H.H. *ACS Preprints, Div. of Fuel Chem.*, **36** (2), 462, 1991.
25. Scaroni, A.W., Khan, M.R., Eser, S., and Radovic, L.R. *Ullmann's Encyclopedia of Industrial Chemistry*, VCH, Germany, Vol. A7, 245, 1986.
26. Cebolla, V.L., Diack, M., Oberson, M., Bacaud, R., Cagniant, D., and Nickel-Pepin-Donat *Fuel Proc. Tech.*, **28**, 183, 1991.
27. Solar, J.M. *PhD Dissertation*, The Pennsylvania State University, 1991.
28. Song, C., Hanaoka, K., and Nomura, M. "Effects of Pore Structure and Support Type of Catalysts in Hydroprocessing of Heavy Coal Liquids," *ACS Preprints, Div. of Fuel Chem.*, in press, 1992.
29. Song, C., Hanaoka, K., and Nomura, M. *Fuel*, **68**, 287, 1989.
30. Song, C., Nomura, M., and Ono, T. *ACS Preprints, Div. of Fuel Chem.*, **36** (2), 586, 1991.
31. Huang, L., Song, C., and Schobert, H.H. "Temperature-Programmed Catalytic Liquefaction of Low Rank Coal Using Dispersed Mo Catalyst," *ACS Preprints, Div. of Fuel Chem.*, in press, 1992.



32. Stock, L.M. in *The Chemistry of Coal Conversion* (Ed. R.H. Schlosberg), Plenum Press, New York, Ch. 6, 1985.
33. Neavel, R.C. *Fuel*, **55**, 237, 1976.
34. McMillen, D., Malhotra, R., Hum, G.P., and Chang, S-J. *Energy & Fuels*, **1**, 193, 1987.
35. Burgess, C.E. *M.S. Thesis*, The Pennsylvania State University, 1991.
36. "Standard Specification for Aviation Turbine Fuels," ASTM D1655-83a, Jan. 1984.

### ***Activity 3. Bimetallic Dispersed Catalysts for Coal Liquefaction***

#### **Introduction**

Coals can be liquefied and upgraded into transportation fuels including gasoline, jet fuels, and diesel fuels. Catalysts have been used in coal liquefaction to increase the production of oils (hexane-solubles) and the total conversion in less severe conditions than in non-catalytic conditions. One of the most promising approaches to more efficient liquefaction is the development of novel multi-component dispersed catalysts.<sup>1</sup> Earlier work on multicomponent catalysts in coal liquefaction has included the use of two inorganic salts and multicomponent Lewis acid catalysts as dispersed catalysts.<sup>1-5</sup> However, the present work is concerned with organometallic compounds as precursors for dispersed metal sulfide catalysts. Active metal sulfide catalysts are insoluble and so to get dispersion we use soluble compounds that decompose to active catalysts at, or below, reaction temperatures. There are several reasons why bimetallic organometallic compounds are good candidates as highly dispersed catalytic precursors.

1) Promotion Effect: Organometallic bimetallic compounds have been shown to have promoter effects in hydrogenation and hydrotreating reactions. Some molybdenum-cobalt thiocubane compounds have activities two to three times greater than homometallic molybdenum compounds in the hydrogenation of biphenyl and the hydrodesulphurization of dibenzothiophene.<sup>6-8</sup> Promoters have also been used in supported catalysts.

2) Good Dispersion: Compared to supported catalysts, such as CoMo/Al<sub>2</sub>O<sub>3</sub>, which have poor contact between coal and catalyst, organometallic compounds are soluble in organic solvents that can penetrate the surface of the coal structure into the inner pores, thereby giving good interaction between coal and catalyst at very low metal concentrations (<1 weight %). Some single metal organometallic compounds have been examined as dispersed catalysts in coal liquefaction, including Fe(CO)<sub>5</sub>, Mo(CO)<sub>6</sub>, and Sn(Bu)<sub>4</sub>.<sup>9-11</sup>

3) Interaction on the Atomic Scale: Two different metals bound together in a single compound should have a more systematic spatial arrangement in the catalytic phase than if two separate compounds were used to introduce the two different metals to a catalytic system.

In the present work, bimetallic thiocubanes were chosen as highly dispersed bimetallic catalytic precursors due to their elemental makeup of active metals and sulfur and their solubility in organic solvents. These bimetallic thiocubanes will be compared with respect to ligand effects in both the liquefaction of a Pittsburgh #8 bituminous coal and a Montana subbituminous coal under different temperatures and reaction conditions.

## Experimental

The two coal samples were obtained from the Penn State Coal Sample Bank. The Pittsburgh #8 bituminous coal (DECS-12, PSOC-1546, <60 mesh) had the following composition: 2.4% moisture, 10.0% ash, 35.2% volatile matter, and 52.4% fixed carbon on an as-received basis; 84.8% carbon, 5.7% hydrogen, 1.4% nitrogen, 0.7% organic sulfur, and 6.5% oxygen on a dmmf basis. The Montana subbituminous coal (DECS-9, PSOC-1506, <60 mesh) had the following composition: 24.7% moisture, 4.8% ash, 33.5% volatile matter, and 37.1% fixed carbon on an as-received basis; 76.1% carbon, 5.1% hydrogen, 0.9% nitrogen, 0.3% organic sulfur, and 17.5% oxygen on a dmmf basis. The coals were dried for two hours at 100°C under vacuum before use. Three bimetallic thiocubane compounds were used as catalytic precursors:  $\text{Mo}_2\text{Co}_2\text{S}_4(\text{S}_2\text{CNEt}_2)_2(\text{CH}_3\text{CN})_2(\text{CO})_2$  [MoCo-TC1],  $\text{Mo}_2\text{Co}_2\text{S}_4\text{Cp}_2(\text{CO})_2$  [MoCo-TC2], and  $\text{Mo}_2\text{Co}_2\text{S}_4(\text{Cp}')_2(\text{CO})_2$  [MoCo-TC3]. The three thiocubanes were synthesized in our laboratory based on the procedures by Brunner<sup>12,13</sup> and Halbert.<sup>14</sup>

The catalytic precursors were dispersed on the coal by the incipient wetness impregnation method.<sup>15</sup> The loading for the bimetallic thiocubanes was 0.5-0.6% of molybdenum on the basis of dmmf coal. Toluene or tetrahydrofuran (THF) were used to impregnate the bimetallic thiocubanes into the coal. The coal sample was dried in vacuum for 2 hours at 100°C after the loading of the catalytic precursor. All reactions were carried out in microautoclaves (tubing bombs) in a temperature-controlled fluidized sandbath. Each reaction used approximately 3 g coal and 3 g 1-methylnaphthalene as the reaction solvent. The  $\text{H}_2$  pressure was 7 MPa at room temperature.

Single-stage liquefaction (SSL) had the tubing bomb rapidly heated to the prescribed temperatures for 30 minutes (plus a 3-minute warming up period) followed by a rapid quench in cold water. Temperature-programmed liquefaction (TPL) had the tubing bomb rapidly heated up to a low temperature (200°C-275°C) and soaked at that temperature for 15 or 30 minutes before the temperature was gradually increased (4-5°C/min) to a higher temperature (400°C-425°C) and held there for 30 minutes before rapid quenching with cold water.<sup>15,16</sup>

The gaseous product was vented after the reaction was complete and the liquid and solid products were washed into a ceramic thimble with hexane. The products were separated under a  $\text{N}_2$  atmosphere by Soxhlet extraction using hexane, toluene, and THF in succession. Solvents were removed by rotary evaporation and the products were dried in vacuum at 100°C for 6 hours

except for the hexane-solubles. The asphaltene (toluene soluble, but hexane insoluble), preasphaltene (THF solubles, but toluene insoluble), and residue were weighed and the conversion and product distribution were calculated based on dmmf coal.

## Results and Discussion

Table 4.5 shows the results of liquefaction of the Montana subbituminous coal at 400°C. MoCo-TC1 did not have any perceptible catalytic activity under SSL conditions. The nitrogen present in the acetonitrile and dithiocarbamate ligands seem to be poisoning the catalyst. It was expected that the bimetallic thiocubane MoCo-TC2 would have greater yields when THF was used as the impregnating solvent since THF was considered to be better able to swell and penetrate the coal structure. Surprisingly, MoCo-TC2 catalyzed liquefaction gave both higher oil yields and total conversion when toluene was used rather than THF. There was a small increase in the oil yield coupled with a decrease in preasphaltene yield when MoCo-TC3 was used in temperature-programmed liquefaction. An increase in oil yields under temperature-programmed conditions has been observed in previous liquefaction studies with and without catalysts.<sup>15,16</sup>

Table 4.6 shows the results of liquefaction of Montana subbituminous coal at 425°C under SSL conditions. MoCo-TC2 gave better oil yields when impregnated with toluene rather than with THF, although the conversion with THF as the impregnating solvent is greater. Liquefaction runs with MoCo-TC3 had a large increase in oil yields under TPL conditions. The larger difference in oil yields between TPL and SSL conditions at 425°C than at 400°C is probably due to the greater hydrogenating ability of the bimetallic catalyst at the higher temperature. The nitrogen-containing catalytic precursor, MoCo-TC1, again had much lower yields than the other bimetallic thiocubanes.

Table 4.7 shows the effect of using various catalytic precursors on liquefaction yields on a Pittsburgh #8 bituminous coal at 400°C. As with the Montana subbituminous coal, bimetallic thiocubanes were compared to liquefaction runs where no catalysts were used. MoCo-TC2, under SSL conditions, gave a small increase in the gas and oil yield, but the conversion was much higher due to concomitant increases in asphaltenes and preasphaltenes. The increases in the gas and oil yield and total conversion for MoCo-TC2 with temperature programming as opposed to single-stage liquefaction were small, as would be expected at this lower temperature.

Table 4.8 shows the results of liquefaction of the Pittsburgh #8 coal at 425°C. At this temperature both the oil yield and the conversion for all of the catalytic runs were greater than those of the non-catalytic runs. These increases were probably due to the greater hydrogenating ability of the bimetallic catalytic phase at this higher temperature. Previous work with hydrogenation catalysts has shown that there are threshold temperatures that must be reached for catalytic coal hydrogenation to occur.<sup>1</sup> Temperature-programmed liquefaction with MoCo-TC2 gave very large increases in gas and oil yields and conversion compared with all other catalysts under SSL or TPL conditions.

**Table 4.5** Liquefaction of Montana Subbituminous Coal at 400°C

<u>catalyst</u>	<u>condition</u>	<u>solvent</u>	<u>oil &amp; gas</u>	<u>asphalt.</u>	<u>preasph.</u>	<u>conver.</u>
none	SSL	none	22.3	4.5	4.2	31.0
MoCo-TC1	SSL	THF	22.8	4.8	5.2	32.8
MoCo-TC2	SSL	Toluene	32.4	18.0	24.2	74.6
MoCo-TC2	SSL	THF	25.8	17.9	23.7	67.4
MoCo-TC3	TPL	Toluene	33.8	17.8	19.9	71.5

**Table 4.6.** Liquefaction of Montana Subbituminous Coal at 425°C

<u>catalyst</u>	<u>condition</u>	<u>solvent</u>	<u>oil &amp; gas</u>	<u>asphalt.</u>	<u>preasph.</u>	<u>conver.</u>
MoCo-TC1	SSL	THF	20.3	9.9	5.7	35.9
MoCo-TC2	SSL	Toluene	42.0	13.9	12.5	68.4
MoCo-TC2	SSL	THF	36.5	15.5	18.1	72.7
MoCo-TC3	SSL	Toluene	36.7	11.9	13.2	61.4
MoCo-TC3	TPL	Toluene	46.3	17.5	12.9	76.6

**Table 4.7.** Liquefaction of Pittsburgh #8 Bituminous Coal at 400°C

<u>catalyst</u>	<u>condition</u>	<u>solvent</u>	<u>oil &amp; gas</u>	<u>asphalt.</u>	<u>preasph.</u>	<u>overall</u>
none	SSL	none	13.7	20.4	26.8	60.9
MoCo- TC2	SSL	Toluene	14.5	27.8	34.3	76.6
MoCo- TC2	TPL	Toluene	15.8	28.7	35.4	79.9
MoCo- TC1	TPL	THF	9.8	28.7	35.4	65.7

**Table 4.8.** Liquefaction of Pittsburgh #8 Bituminous Coal at 425 C

<u>catalyst</u>	<u>condition</u>	<u>solvent</u>	<u>oil &amp; gas</u>	<u>asphalt.</u>	<u>preasph.</u>	<u>overall</u>
none	SSL	none	16.3	17.6	16.1	51.4
MoCoTC- 2	SSL	Toluene	21.8	27.6	23.9	73.3
MoCo- TC2	TPL	Toluene	33.1	31.4	23.4	87.8
MoCo- TC1	TPL	THF	21.8	25.5	18.4	65.7

A summary of the effects of ligands, reaction conditions and temperature, and coal rank on liquefaction with bimetallic catalysts will be offered. Ligands bound to the metals present in the catalytic precursor had a very noticeable effect on the catalytic activity under liquefaction conditions. The cyclopentadiene and pentamethylcyclopentadiene ligands contained in MoCo-TC2 and MoCo-TC3, respectively, were cleaved from the metals under liquefaction conditions and, as would be expected for hydrocarbons, did not have any noticeable adverse effect during catalysis. The nitrogen present in the acetonitrile and dithiocarbamate ligands for MoCo-TC1 rendered the catalyst inactive under almost all conditions (except 425°C with Pittsburgh #8 bituminous coal). Therefore, reaction temperature influenced the ligand effect.

An increase in reaction temperature from 400°C to 425°C led to an increase in the oil yield. The higher temperature leads to further cracking of asphaltenes and preasphaltenes. These smaller radical fragments are then capped by hydrogen by the active bimetallic catalyst at a greater rate than would occur without the catalyst being present.

Temperature-programmed liquefaction (TPL) gave higher oil yields under all conditions as compared to single-stage liquefaction (SSL). Sometimes the increases were very dramatic: MoCo-TC2 with Pittsburgh #8 bituminous coal at 425°C. Subtle changes in coal structure during the low temperature soaking stage coupled with the greater dispersion of the bimetallic catalytic precursor as it seeps into smaller pores as it decomposes, leading to greater activity, could be responsible for increasing yields. These subtle changes in coal structure were dependent on the rank of coal being studied.

The observation that a bituminous coal gave higher conversions, but lower gas and oil yields, than a subbituminous coal during catalytic liquefaction could be due to: 1) differences in the chemical composition of the different rank coals, or 2) physical differences in the pore structure of these two different coals, or both.

Catalytic coal liquefaction using the single-metal compound,  $(\text{NH}_4)_2\text{MoS}_4$ , and small bimetallic organometallic compounds as precursors are now in progress.

## Conclusions

The present work on bimetallic thiocubanes as catalytic precursors provided some insight on the effects of ligands, temperature, reaction conditions, and coal rank on the catalytic liquefaction of coal.

--Ligands containing nitrogen had a negative effect on catalysts, rendering them inactive, except for Pittsburgh #8 bituminous at 425°C.

--An increase in temperature always gave an increase in the gas and oil yield; the conversion usually increased at a higher temperature.

--Temperature-programmed liquefaction (TPL) gave higher oil yields, sometimes very dramatically, compared to single-stage liquefaction (SSL).

--The Pittsburgh #8 bituminous coal gave higher conversions, but lower gas and oil yields than the Montana subbituminous coal.

## References

1. Derbyshire, F., *Energy & Fuels* 1989, 273-277, and references cited therein.
2. Song, C.; Nomura, M.; Ono, T., *Am. Chem. Soc. Div. Fuel. Chem. Prepr.* 1991, 36(2), 586-596.
3. Song, C.; Nomura, M., *Bull. Chem. Soc. Jpn.* 1986, 59, 3643-3648.
4. Song, C.; Nomura, M.; Hanaoka, K., *Energy & Fuels* 1988, 2, 639-644.
5. Song, C.; Nomura, M.; Miyake, M., *Fuel* 1986, 85, 922-926.
6. Halbert, T.R.; Ho, T. C. Stieffel, E. I.; Chianelli, R. R., Daage, M., *J. Catal.* 1991, 130, 116-119.
7. Stieffel, E. I.; Halbert, T. R.; Coyle, C. L.; Wei, L.; Pan, W.-H.; Ho, T. C.; Chianelli, R. R.; Daage, M., *Polyhedron* 1989, 8, 1625-1629.
8. Curtis, M. D.; Pehher-Hahn, J. E.; Schwank, J.; Baralt, O.; McCabe, D. J.; Thompson, L.; Waldo, G., *Polyhedron* 1988, 7, 2411-2420.
9. Suzuki, T.; Ando, T.; Watanabe, Y., *Energy & Fuels* 1987, 1, 299-300.
10. Watanabe, Y.; Yamado, O.; Fujita, K.; Yoshinoba, T.; Suzuki, T., *Fuel* 1984, 63, 752-755.
11. Herrick, D. E.; Tierney, J. W.; Wender, I.; Huffamn, G. P.; Huggins, F. E., *Energy & Fuels* 1990, 4, 231-236.
12. Brunner, H.; Wachter, J., *J. Organomet. Chem.* 1982, 240, C41-44.
13. Brunner, H.; Kauermann, H.; Wachter, J., *Angew. Chem. Intl. Ed. Engl.* 1983, 22, 549-550.
14. Halbert, T. R.; Cohen, S. A.; Stieffel, E. I., *Organometallics* 1985, 4, 1689-1690.
15. Huang, L.; Song, C.; Schobert, H. H., *Am. Chem. Soc. Div. Fuel Chem. Prepr.*, 1992, 37(1), 223-227.
16. Song, C.; Schobert, H. H.; Hatcher, P. G., *Energy & Fuels* 1992, 6, 326-328.

## Appendix

### List of Relevant Papers on Coal- and Petroleum-Derived Jet Fuels and on Coal Structure and Liquefaction from Penn State Team

(List in the Order of Date and Time of Presentation)

#### 20th Biennial Conference on Carbon, American Carbon Society, June 23-28, Santa Barbara, California, 1991

1. Eser, S.; Song, C.; Schobert, H.H.; Hatcher, P.G.  
"Formation of Solid Deposits during Thermal Stressing of Jet Fuels, Extended Abstracts."  
20th Biennial Conference on Carbon, June 23-28, Am. Carbon Soc., pp. 440-441, 1991.

#### ACS National Meeting in San Francisco, California, April 5-10, 1992

2. Selvaraj L.; Sobokowiak, M.; Coleman, M., "Infrared Studies of Thermally Stressed Jet Fuels," Am. Chem. Soc. Div. Petrol. Chem. Prepr., Vol. 37, No.2, 451-455, 1992.
3. Eser, S.; Song, C.; Gergova, K.; Parzynski, M.; Peng, Y., "Characterization of Solid Deposits from Thermal Stressing of Jet Fuels and Related Compounds by Polarized-Light Microscopy," Am. Chem. Soc. Div. Petrol. Chem. Prepr., Vol. 37, 1992, No.2, 463-468.
4. Song, C.; Peng, Y.; Jiang, H.; Schobert, H.H., "On the Mechanisms of PAH and Solid Formation during Thermal Degradation of Jet Fuels," Am. Chem. Soc. Div. Petrol. Chem. Prepr., Vol. 37, 1992, No.2, 484-492.
5. Eser, S.; Song, C.; Copenhaver, R.; Parzynski, M., "Kinetics of Thermal Degradation and Solid Formation during High-Temperature Stressing of Jet Fuels and Related Model Compounds," Am. Chem. Soc. Div. Petrol. Chem. Prepr., Vol. 37, 1992, No.2, 493-504.
6. Peng, Y.; Schobert, H.H.; Song, C.; Hatcher, P.G., "Thermal Decomposition Studies of Jet Fuel Components: n-Butylbenzene and t-Butylbenzene," Am. Chem. Soc. Div. Petrol. Chem. Prepr., Vol. 37, 1992, No.2, 505-513.



7. Eser, S.; Perison, J.; Copenhaver, R.; Shiea, J.; Schobert, H.H., "Thermal Degradation of Alkylated Phenol," Am. Chem. Soc. Div. Petrol. Chem. Prepr., Vol. 37, No.2, 514-523, **1992**.
8. Song, C.; Hatcher, P.G., "Compositional Differences between Coal- and Petroleum-Derived Jet Fuels," Am. Chem. Soc. Div. Petrol. Chem. Prepr., Vol. 37, No.2, 529-539, **1992**.
9. Song, C.; Eser, S.; Schobert, H.H.; Hatcher, P.G., "Thermal Stability of Petroleum- and Coal-Derived Jet Fuels at High Temperatures," Am. Chem. Soc. Div. Petrol. Chem. Prepr., Vol. 37, No.2, 540-547, **1992**.
10. Burgess, C.; Schobert, H.H., "Relationship of Coal Structure and Donor Solvent Quality to Catalyst Action in Liquefaction," Am. Chem. Soc. Div. Fuel Chem. Prepr., Vol. 37, No.1, 200-206, **1992**.
11. Song, C.; Hanaoka, K.; Nomura, M., "Effects of Pore Structure and Support Type of Catalysts in Hydroprocessing of Heavy Coal Liquids," Am. Chem. Soc. Div. Fuel Chem. Prepr., Vol. 37, No.1, 215-222, **1992**.
12. Huang, L.; Song, C.; Schobert, H.H., "Temperature-Programmed Catalytic Liquefaction of Low-Rank Coal Using Dispersed Mo Catalyst," Am. Chem. Soc. Div. Fuel Chem. Prepr., Vol. 37, No.1, 223-227, **1992**.
13. Song, C.; Schobert, H.H.; Hatcher, P.G., "Solid State  $^{13}\text{C}$  NMR and Pyrolysis-GC-MS Studies of Coal Structure and Liquefaction Reactions," Am. Chem. Soc. Div. Fuel Chem. Prepr., Vol. 37, No.2, 638-645, **1992**.
14. Tomic, J.; Schobert, H.H., "Reactivity of Coal under Coprocessing Conditions," Am. Chem. Soc. Div. Fuel Chem. Prepr., Vol. 37, No.2, 770-777, **1992**.
15. Faulon, J.-L.; Hatcher, P.G.; Wenzel, K.A., "A Computer Assisted Structural Elucidation for Coal Macromolecules," Am. Chem. Soc. Div. Fuel Chem. Prepr., Vol. 37, No.2, 900-907, **1992**.
16. Hatcher, P.G.; Faulon, J.-L.; Wenzel, K.A.; Cody, G.D., "A Three Dimensional Structural Model for Vitrinite from High Volatile Bituminous Coal," Am. Chem. Soc. Div. Fuel Chem. Prepr., Vol. 37, No.2, 886-892, **1992**.

17. Song, C.; Schobert, H.H., "Specialty Chemicals and Advanced Materials from Coals: Research Needs and Opportunities," Am. Chem. Soc. Div. Fuel Chem. Prepr., Vol. 37, No.2, 524-532, 1992.
18. Song, C.; Schobert, H.H., "Temperature-Programmed Liquefaction of Low-Rank Coals in H-donor and Non-donor Solvents," Am. Chem. Soc. Div. Fuel Chem. Prepr., Vol. 37, No.2, 976-983, 1992.

**Carbon '92 - Inter. Carbon Conf., Essen, Germany, June 22-26, 1992**

19. Eser, S.; Gergova, K.; Arumugam, R.; Schobert, H.H.,  
"Formation of Solid Deposits from Jet Fuels in the Presence of Different Solid Carbons."

**ACS National Meeting in Washington, D.C., August 23-28, 1992**

20. Saini, A. K.; Song, C.; Schobert, H.H.; Hatcher, P.G., "Characterization of Coal Structure and Low-Temperature Liquefaction Reactions by Pyrolysis-GC-MS in Combination with Solid-State NMR and FT-IR," Am. Chem. Soc. Div. Fuel Chem. Prepr., Vol. 37, No.3, pp.1235-1242, 1992.
21. Song, C.; Lai, W.-C.; Schobert, H.H., "Hydrogen-Transferring Pyrolysis of Cyclic and Straight-Chain Hydrocarbons. Enhancing High Temperature Thermal Stability of Aviation Jet Fuels by H-Donors," Am. Chem. Soc. Div. Fuel Chem. Prepr., Vol. 37, No.4, pp. 1655-1663, 1992.
22. W.-C.; Song, C.; Schobert, H.H.; Arumugam, R., "Pyrolytic Degradation of Coal- and Petroleum-Derived Aviation Jet Fuels and Middle Distillates," Am. Chem. Soc. Div. Fuel Chem. Prepr., Vol. 37, No.4, pp. 1671-1680, 1992.
23. Peng, Y.; Schobert, H.H.; Song, C.; Hatcher, P.G., "Effects of the Structure of the Side Chain on the Pyrolysis of Alkylbenzenes," Am. Chem. Soc. Div. Fuel Chem. Prepr., Vol. 37, No.4, pp. 1733-1739, 1992.

24. Greenwood, P.F.; Zhang, E.; Hatcher, P.G.; Vastola, F.; Davis, A., "Laser Micropyrolysis/Gas Chromatography Mass Spectrometry: A Useful Technique for the Study of Coal Macerals," Am. Chem. Soc. Div. Fuel Chem. Prepr., Vol. 37, No.4, pp.1548-1554, 1992.

**The 9th Ann. Pittsburgh International Coal Conference,  
October 12-16, 1992, Pittsburgh, Pennsylvania**

25. Parfitt, D.S.; Song, C.; Schobert, H.H., "The Use of Bimetallic Organometallic Compounds as Precursors of Dispersed Catalysts for Coal Liquefaction," Proceedings of 9th Ann. Internat. Pittsburgh Coal Conference, October 12-16, University of Pittsburgh, Pittsburgh, PA, pp. 503-508, 1992.

**Papers Published in Journal Energy & Fuels**

26. Song, C.; Schobert, H.H.; Hatcher, P.G., "Temperature-Programmed Liquefaction of a Low Rank Coal," Energy & Fuels, Vol. 6, No. 3, pp. 326-328, 1992.
27. Coleman, M.M.; Selvaraj, L.; Sobkowiak, M.; Yoon, E., "Potential Stabilizers for Jet Fuels Subjected to Thermal Stress above 400°C," Energy & Fuels, Vol. 6, No. 5, pp. 535-539, 1992.
28. Song, C., Eser, S.; Schobert, H.H.; Hatcher, P.G., "Pyrolytic Degradation Studies of a Coal- and a Petroleum-Derived Aviation Jet Fuel," Energy & Fuels, to be published, 1993.